AFWL-TR-82-92

AFWL-TR-
82-92

EXPERIMENTAL STRESS-STRAIN BEHAVIOR OF A LOW STRENGTH CONCRETE UNDER MULTIAXIAL STATES OF STRESS

L. A. Traina

New Mexico Engineering Research Institute
University of New Mexico
Albuquerque, NM 87131

January 1983

Final Report

Approved for public release; distribution unlimited.

AIR FORCE WEAPONS LABORATORY
Air Force Systems Command
Kirtland Air Force Base, NM 87117

This final report was prepared by the New Mexico Engineering Research Institute, University of New Mexico, Albuquerque, New Mexico, under Contract F29601-81-C-0013, Job Order 88091347 with the Air Force Weapons Laboratory, Kirtland Air Force Base, New Mexico. Mr. Douglas R. Seemann (NTES) was the Laboratory Project Officer-in-Charge.

When Government drawings, specifications, or other data are used for any purpose other than in connection with a definitely Government-related procurement, the United States Government incurs no responsibility or any obligation whatsoever. The fact that the Government may have formulated or in any way supplied the said drawings, specifications, or other data, is not to be regarded by implication, or otherwise in any manner construed, as licensing the holder, or any other person or corporation; or as conveying any rights or permission to manufacture, use, or sell any patented invention that may in any way be related thereto.

This report has been authored by a contractor of the United States Government. Accordingly, the United States Government retains a nonexclusive, royalty-free license to publish or reproduce the material contained herein, or allow others to do so, for the United States Government purposes.

This report has been reviewed by the Public Affairs Office and is releasable to the National Technical Information Service (NTIS). At NTIS, it will be available to the general public, including foreign nations.

If your address has changed, if you wish to be removed from our mailing list, or if your organization no longer employs the addressee, please notify AFWL/NTES, Kirtland AFB, NM 87117 to help us maintain a current mailing list.

This technical report has been reviewed and is approved for publication.

Douglas R. Seemann

DOUGLAS R. SEEMANN
Project Officer

FOR THE COMMANDER

Richard H. Jolley

RICHARD H. JOLLEY
Major, USAF
Chief, Technology Applications Br

John H. Storm

JOHN H. STORM
Colonel, USAF
Chief, Civil Engineering Rsch Div

DO NOT RETURN COPIES OF THIS REPORT UNLESS CONTRACTUAL OBLIGATIONS OR NOTICE ON A SPECIFIC DOCUMENT REQUIRES THAT IT BE RETURNED.

UNCLASSIFIED

SECURITY CLASSIFICATION OF THIS PAGE (When Data Entered)

REPORT DOCUMENTATION PAGE		READ INSTRUCTIONS BEFORE COMPLETING FORM
1. REPORT NUMBER AFWL-TR-82-92	2. GOVT ACCESSION NO. AD-A124	3. RECIPIENT'S CATALOG NUMBER 062
4. TITLE (and Subtitle) EXPERIMENTAL STRESS-STRAIN BEHAVIOR OF A LOW STRENGTH CONCRETE UNDER MULTIAXIAL STATES OF STRESS		5. TYPE OF REPORT & PERIOD COVERED Final Report 6. PERFORMING ORG. REPORT NUMBER
7. AUTHOR(s) L. A. Traina		8. CONTRACT OR GRANT NUMBER(s) F29601-81-C-0013
9. PERFORMING ORGANIZATION NAME AND ADDRESS New Mexico Engineering Research Institute University of New Mexico Albuquerque, NM 87131		10. PROGRAM ELEMENT, PROJECT, TASK AREA & WORK UNIT NUMBERS 62601F/88091347
11. CONTROLLING OFFICE NAME AND ADDRESS Air Force Weapons Laboratory (NTES) Kirtland Air Force Base, NM 87117		12. REPORT DATE January 1983 13. NUMBER OF PAGES 158
14. MONITORING AGENCY NAME & ADDRESS(if different from Controlling Office)		15. SECURITY CLASS. (of this report) Unclassified 15a. DECLASSIFICATION/DOWNGRADING SCHEDULE

16. DISTRIBUTION STATEMENT (of this Report)

Approved for public release; distribution unlimited.

17. DISTRIBUTION STATEMENT (of the abstract entered in Block 20, if different from Report)

18. SUPPLEMENTARY NOTES

Subcontractor: New Mexico State University, Las Cruces, NM 88003

19. KEY WORDS (Continue on reverse side if necessary and identify by block number)

Concrete Testing
Stress-Strain Behavior
Triaxial Response
Path Dependence
Failure

20. ABSTRACT (Continue on reverse side if necessary and identify by block number)

This report presents the results of a multiaxial experimental investigation using plain concrete cubes subjected to prescribed stress histories and static loading. The results of 81 tests along 27 different load paths are presented as stress-strain plots for each of the three principal directions. Included are load paths with all principal stresses in compression; load paths with one principal stress in tension; and tests to investigate the path dependence of the limit surface for concrete.

DD FORM 1 JAN 73 1473 EDITION OF 1 NOV 65 IS OBSOLETE

UNCLASSIFIED

SECURITY CLASSIFICATION OF THIS PAGE (When Data Entered)

PREFACE

The author is indebted to many individuals for the success of this project. The author wishes to thank Howard Schreyer and James Jeter of the New Mexico Engineering Research Institute (NMERI) for their effort and cooperation throughout the project. The author is also grateful to Douglas Seemann and Capt. Terry Hinnerichs of the Air Force Weapons Laboratory (AFWL) for their support and input to the study.

William Kingsley of New Mexico State University (NMSU) deserves a great deal of credit for his assistance during the testing and for his effort in the modifications of the testing apparatus. The author also appreciates the assistance with the testing and data reduction provided by Amin Aklan of New Mexico State University.

The final typing of the report was done in the Engineering Experiment Station at New Mexico State University. The author is indebted to Pam Archuleta for her effort and patience at that time.

CONTENTS

ILLUSTRATIONS

TABLES

I. INTRODUCTION

The objective of this effort was to provide static triaxial test data on plain concrete for validating concrete constitutive relations. The effort was a part of an investigation performed by the New Mexico Engineering Research Institute (NMERI) for the Air Force Weapons Laboratory (AFWL). The purpose of the investigation was to evaluate the capabilities and limitations of existing constitutive models for concrete and reinforced concrete. The models were to be compared to existing concrete test data in the literature and further checked against triaxial test data developed as a part of this effort. The triaxial test data presented in this report are the data which were developed for this aspect of the investigation. The data were developed by New Mexico State University (NMSU) under subcontract to NMERI. Additional data on the response of standard cylindrical specimens were provided by San Diego State University.

The static triaxial data was to be developed for plain concrete subjected to prescribed loading paths that included tensile stress components. New Mexico State University was awarded the contract to develop the data because of its existing unique testing capability. The test matrix was to consist of 64 primary and 12 control tests. The control tests were to follow load paths which had been previously studied in order to verify the testing procedure. The primary emphasis of the effort was on "nonstandard" load paths for tests with all principal stresses in compression and on load paths with one principal stress in tension. The static triaxial tests were to be conducted to follow load paths specified by NMERI and agreed upon by NMSU subject to the capabilities of the testing equipment.

This report contains a description of the test program, the test apparatus and the testing procedures used. A total of 81 tests utilizing 76.2-mm (3-in) cubical test specimens for all tests were conducted as a part of this effort. The results of 79 of these tests have been documented by graphs of stress versus strain along the three principal axes used for each test. Two of these tests were preliminary uniaxial tension tests conducted to evaluate the adequacy of the tension loading system and only the tensile strength of the specimen was recorded.

II. TEST DESCRIPTION

TYPES OF LOADING PATHS

In order to develop the required data, the test apparatus was required to have a unique testing capability. It was necessary that the equipment have the capability to apply loads to the specimen along various diverse load paths. The stress states involved included various combinations of compression for all principal stresses. It was also necessary to develop stress states with one principal stress in tension and various combinations of compression for the two other principal stresses. The other critical requirement was that the test apparatus be capable of monitoring the resulting deformations in the three orthogonal directions, for each test, so that strain data could also be developed.

TEST APPARATUS

The triaxial testing machine used in this effort was designed and constructed at New Mexico State University as a part of a previous research program (Ref. 1). The testing machine design was based upon the following criteria:

a. Loads could be applied in three orthogonal directions.
b. The loading in each direction would be independently controlled.
c. The testing machine would be capable of applying a maximum stress of 206.8 MPa (30 kip/in^2) triaxially to a 76.2-mm (3-in) cube.
d. The measurement of the applied load and the accompanying deformations would be possible.
e. The restraint of the lateral deformations at the surface of the cube would be minimized.
f. The loads could be applied in tension or compression.
g. The load frame would deform symmetrically under an applied load.

---

1. Endebrock, E. G. and Traina, L. A., Static Concrete Constitutive Relations Based on Cubical Specimens, Vols. I and II, AFWL-TR-72-59, Air Force Weapons Laboratory, Kirtland Air Force Base, NM, December 1972.

Load frame--The frame of the testing machine was dimensioned such that there was sufficient space for the hardware such as the jacks, compression platens, load cells, and extensometers. The main members of the testing frame consisted of wide-flange steel sections. The sections were selected according to AISC specifications and were rolled from A36 steel. A load factor of 2 was applied in the design. All connections on the load frame were welded. The spans were short and the shear stress levels high; hence; a large number of shear stiffener plates were required. Web stiffeners were also used beneath the jacks and the bearing plates to prevent crippling of the webs.

The testing machine is composed of two frames, one suspended horizontally within the other. The horizontal frame is suspended within the vertical frame. Two jacks are attached to the horizontal frame and one to the vertical frame. The horizontal frame was constructed such that it was adjustable in both the horizontal and vertical directions to facilitate alignment of the load axes.

The loads were applied by means of manually operated hydraulic jacks with capacities of 1,334 kN (300 kip) each. The jacks were equipped with spherical heads which were self-aligning and double-acting so tensile loads could be applied and the ram easily withdrawn for the placement of specimens into the machine for each test.

Compression platens--The compression platens were machined from high strength steel with a yield point of 517 MPa (75 kip/in^2). The bearing surface dimensions were 69.9 mm by 69.9 mm (2.75 in by 2.75 in). The platen areas were necessarily smaller than the test specimen areas in order to prevent the platens from coming in contact with each other as a result of the deformations during a test. A special feature of the compression platens was a slot milled in the center to accommodate the extensometer used for deformation measurements. A hole was drilled into the center of the bearing surface to accommodate a small flanged pin (Fig. 1). An extensometer arm was placed in the slot and on one end of the pin. The purpose of the pin was to isolate deformations resulting from the use of friction-reduction pads so that the deformation detected by the extensometer was the deformation of the test cube only. To prevent the friction-reducing pads from interfering with the displacement measurements, a hole was formed in these pads, which was slightly larger in diameter than the diameter of the pin flange. This allowed the pin flange to pass through the pads and to directly contact the surface of the test cube and transfer the displacement of the center of the cube along that axis directly to the extensometer arms.

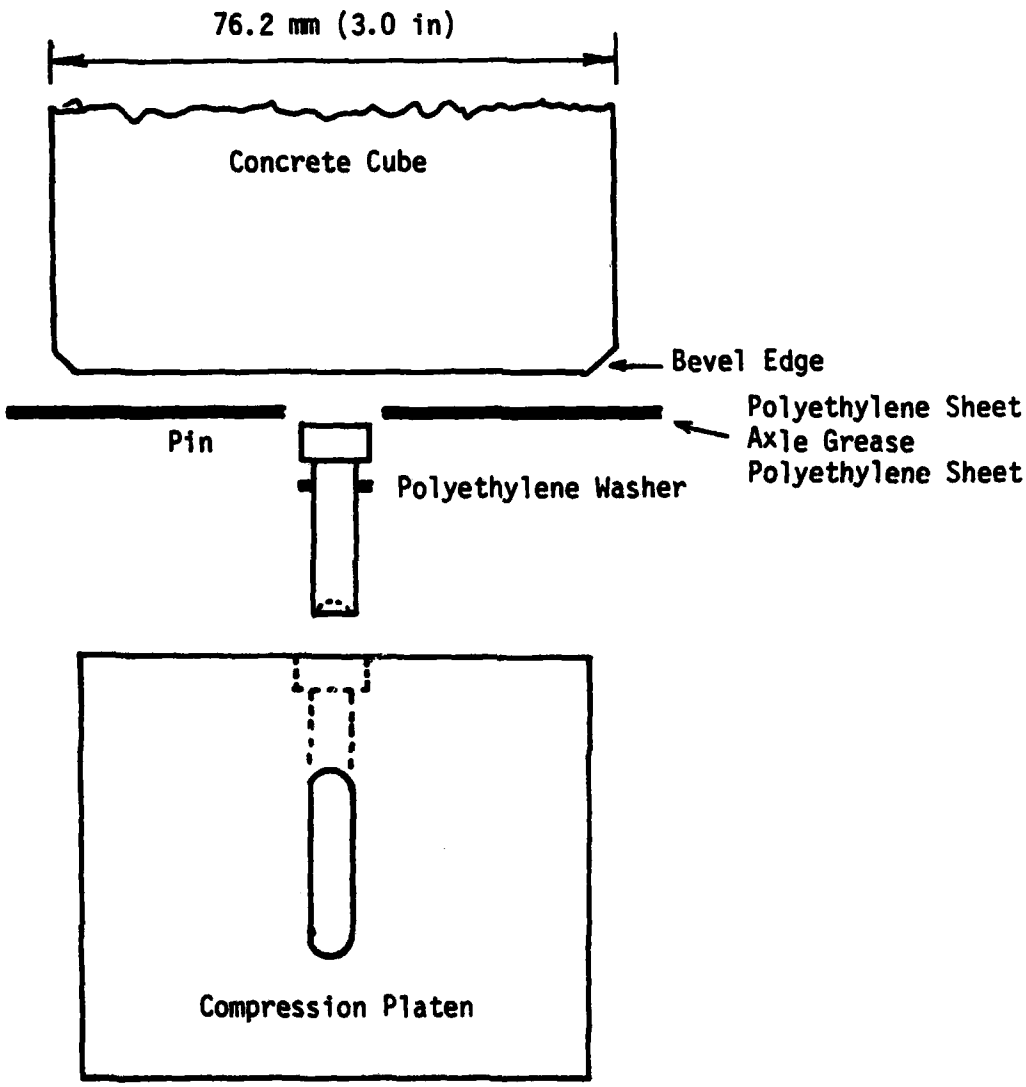

Figure 1. Arrangement of platen, pin, polyethylene sheets, and specimen for a compression test.

Polyethylene washers of the same thickness as the friction-reducing pads were placed between the flange of the pins and the bearing surface in the platen to accommodate the added dimension caused by the presence of the friction-reduction pads.

In order to approximate an unconfined state of stress when using a cubical test specimen, it is necessary to minimize the restraint of the lateral deformations at the surface of the cubes. This can be accomplished by minimizing the friction between the concrete cube and the steel loading platen at the point of interface. A solution to the problem which has proven to be quite effective with a minimum cost was suggested by Mills (Ref. 2). Friction-reduction pads consisting of two polyethylene sheets 0.1 mm (4 mils) thick with a layer of bearing grease between the sheets were used in each test to satisfy this requirement. The placement of the pads during a test is shown in Figure 1.

Tension platens--The platens used for tests involving a principal tensile stress are shown in Figure 2. The loading surface dimensions for the tension platens were 76.2 mm by 76.2 mm (3.00 in by 3.00 in). A 6.4-mm (0.25-in)-diameter hole was drilled at their center to accommodate a steel pin. During a test, one end of the pin was in direct contact with the concrete test specimen. The extensometer arm was placed on the other end of the pin. The purpose of the pin was to isolate deformations resulting from the use of an approximately 3.2-mm (1/8-in)-thick epoxy resin layer used to attach a cube to the tension platen. In this manner, the deformation detected by the extensometer was the deformation at the center of the test cube in the direction of the principal tensile stress. Loads were applied to the tension platens through ball joints in order to obtain a uniform stress distribution in the test cube.

In order to approximate an unconfined state of stress during a test involving a tension stress component, it is necessary to minimize the restraint between the concrete cube and the steel loading platen. This was accomplished by using a 3.2-mm (1/8-in)-thick epoxy resin layer at the point of interface.

---

2. Mills, L. L., "A Study of the Strength of Concrete Under Combined Compression Loads," Ph.D. Dissertation, New Mexico State University, Las Cruces, NM, December 1967.

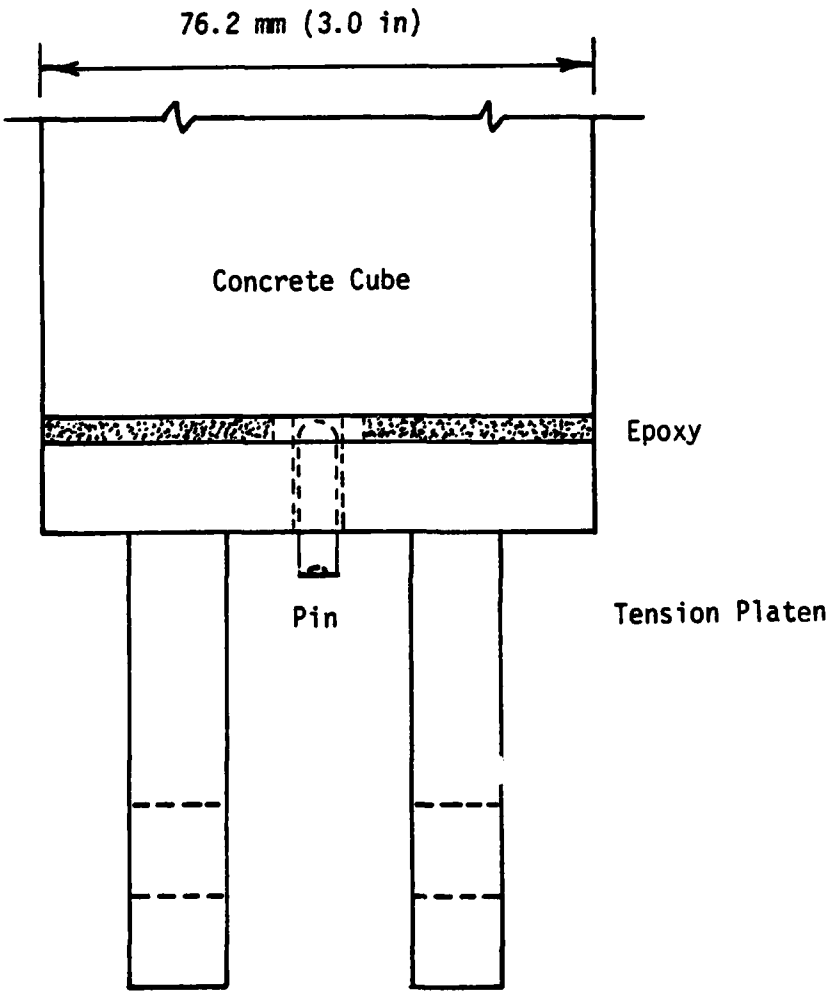

Figure 2. A tension specimen.

Although the tensile strength of the epoxy resin was much higher than the tensile strength of the concrete, its modulus of elasticity was much lower. The modulus of elasticity of most unfilled epoxies ranges from 345 MPa to 3,450 MPa as compared to a modulus of 20,700 - 41,400 MPa for concrete. It was assumed that the low modulus of elasticity of the epoxy coupled with the 3.2-mm (1/8-in) layer, would provide a negligible amount of restraint at the tension platens.

Recording equipment--The load and deformation data were recorded simultaneously for each of the three principal axes as direct analog plots on X-Y recorders. The deformations were measured at the center of the concrete cube by means of extensometer output signals. The loads were measured by means of output signals from load cells. It was necessary to amplify the load and deformation signals in order to obtain satisfactory output signals. The deformation and load output signals were recorded on the X-axis and Y-axis respectively and were scaled so that the recorded information approximated the desired stress-strain for the given test condition.

A point in time correlation was insured for each data point in the following manner. Using a separate voltage source, a voltage signal was superimposed on the data voltage signal of either the X or Y axis depending on the type of test being conducted. The signal was input to each of the three recorders simultaneously by means of a spring load gang switch. To record a data point, the switch was depressed; and this caused an instantaneous deflection of the recorder pen on each recorder at the same instant. The pen would return to the proper stress-strain output position on the recorder chart as soon as the switch was released.

This recording system has been found to have several advantages. The most important is that an experienced investigator has a graphic display of the data during a test. If there are any problems in the loading or recording systems, they are immediately evident. This allows time to stop the test and correct the problem in the case of problems occurring at the beginning of a test. Few test specimens are wasted. The investigator is immediately aware of the replication of data from test to test. The other main advantage is that the data are being recorded instantaneously on all three axes. This is extremely beneficial toward the end of a test where the strain rate is increasing rapidly. Point in time data may be obtained even though the specimen is creeping at a high rate.

Load cells--The load cells used in the testing program were constructed and calibrated at NMSU. They consisted of columns 127 mm (5 in) in length, made of steel or aluminum. Four electrical resistance strain gauges were mounted at mid-height of the columns. The strain gauges were arranged and wired in a manner such that only axial strains were detected. Three different types of load cells were used for the entire testing program. Two types were used for compression testing and a third type was used in tension testing.

One type of compression load cell had circular cross sections and was made of aluminum. Its capacity was 534 kN (120 kip). The second type of compression load cell had 69.9-mm (2.75-in)-square cross sections and was made of high-strength steel. Its capacity was 1334 kN (300 kip). The two types of load cells were interchanged at various times for different types of tests as required based on the load cell capacity. When appropriate, based on their capacity, the aluminum load cells were used since they were more sensitive and their output was linear relative to the load being measured. The steel load cells had to be used for tests where a higher load capacity was required. Since the load-output relationship was not linear, this created minor difficulties during testing and during data reduction.

The tension load cells had circular cross sections and were made of steel. Their capacity was controlled by the 12.7-mm (0.5-in) mounting bolts whose capacity was approximately 22 kN (5 kip). The tension load cells could be easily removed from the load frame for calibration checks. Several tension load cells were available for use. Only one was needed for this test program. It was calibrated in a universal testing machine located in the Materials Testing Laboratory at NMSU. The cell was loaded incrementally in tension with strain readings taken for each load increment. The strain output was recorded by means of a Budd digital strain recorder. The load cell was unloaded and reloaded several times to check the replication of the procedure. The average of all load and strain readings was used to obtain the find calibration curve.

A different calibration procedure was used for the compression load cells. Whenever a compression load cell was placed in the load frame, it required a tedious alignment procedure. Therefore, calibration checks on the compression load cells were performed in place in the load frame. The same calibration procedure was followed for all compression load cells.

A calibration load cell was constructed. It was made of steel, had 50.8-mm (2-in)-square cross sections and was 76.2 mm (3 in) long. A calibration curve was obtained for this load cell using a universal testing machine located in the Materials Testing Laboratory at NMSU. It was loaded incrementally in compression with strain readings taken for each load increment. The averages of all load and strain readings for several loading cycles were used to develop a calibration curve for this load cell. The strain output was recorded using a Budd digital strain recorder. To calibrate the compression load cells, the calibration load cell was placed in the load frame in line with the load cell which was being calibrated. A load was then applied simultaneously and incrementally to both load cells by the jacks for that load axis. The output signal for the compression load cell was compared to the strain output of the Budd digital strain recorder. The output signal for the compression load cell was recorded directly on the Y-axis of an X-Y recorder to an appropriate scale. The load signal was adjusted on the recorder to represent the stress in the concrete cube during a test.

The calibration load cell was somewhat sensitive to end restraint conditions due to its length to lateral dimension ratio. It was therefore necessary to provide similar end conditions for the calibration load cell in the universal testing machine to those that were present in the load frame when those load cells were being calibrated. This was easily accomplished. In the load frame the load was applied to the calibration load cell at each end by a compression platen. To replicate this end condition in the universal testing machine, a pair of compression platens were removed from the load frame and used to apply the load to each end of the calibration load cell. In this manner identical end conditions were established for both phases of the compression load cell calibration procedure.

Extensometers--The extensometers consisted of an aluminum bar rigidly attached to two steel clamps. The clamps were constructed with elbows in them so that the ends could be placed in the loading platens, and the remainder of the extensometer would not interfere with the other extensometers and platens. The aluminum bar served as a flexural member to measure the extensometer deformations. Four electrical resistance strain gauges were attached to the bar and used to measure the deformations.

Calibration of the extensometers was achieved with the aid of a hexagonal-shaped aluminum bar. The bar was 76.2 mm (3 in) in length and had two electrical resistance strain gauges mounted at mid-height. The strain gauges were wired to detect the axial strains in the bar. The aluminum bar was placed in the testing machine between the two compression platens of a particular axis. The strain gauges were wired into a Budd digital strain recorder. The extensometer was placed in the compression platens in the same position as used during a test. The strain gauges were wired to detect flexural strains only. The extensometer strain gauges output was wired to the X-axis of the X-Y recorder. A load was then applied to the aluminum bar. The strain in the aluminum bar was read on the Budd recorder and compared to the output of the extensometer on the X-Y recorder.

To develop the calibration curve for the extensometer, a load was applied to the hexagonal bar to produce a 2,000 microstrain readout on the Budd recorder. The corresponding output signal from the extensometer was then amplified so that a 4-cm deflection of the X-Y recorder arm was produced along the X-axis. This resulted in an average strain calibration setting of 1 cm equal to 500 microstrain. The hexagonal bar was then unloaded and reloaded in 500 microstrain increments. The resulting X-Y recorder deflections were marked and this record was retained as the calibration curve for the subsequent series of tests. The preceding calibration procedure was used for all tests with all principal stresses in compresssion. The resulting calibration curve was found to be approximately linear over the 2000 microstrain calibration range.

For tests involving one principal tension stress it was necessary to record much smaller strain resultants. A slightly different calibration procedure was used. The hexagonal bar was loaded to produce strain increments of 100 microstrain. The resulting extensometer output was marked on the X-Y recorder for each increment. The procedure was repeated several times for each axis and the average of all readings were used to determine a strain calibration function for those tests.

TEST SPECIMENS

Six batches containing 25 cubes each were cast for use in the test program. The cubes were cast using four identical molds with 6 cubes being cast in each mold. Of the 144 cubes cast, 3 from each batch were kept by NMERI. The remaining 126 cubes were shipped to New Mexico State University by automobile for use in the test program. Of the specimens shipped to NMSU, 81 were used in the

present test program and the remaining 45 are being stored in the laboratory. A summary of the specimens tested and not used are shown below:

BATCH NUMBER	SPECIMENS TESTED	SPECIMENS NOT USED
1	2	19
2	14	7
3	19	2
4	12	9
5	16	5
6	18	3

Concrete properties--The concrete mix used for the specimens was designed at the New Mexico Engineering Research Institute. The test specimens were cast there in molds which were also designed and fabricated there. The aggregates used in the mix conformed with the grading requirements of ASTM C33 specifications for concrete aggregates. The course aggregate was crushed and had a maximum size of 11 mm. The fineness modulus of the sand varied from 2.6 to 3.1. The concrete mix is shown below:

Portland Cement, Type I/II	289 kg	(16.25 percent by weight)
Fine Aggregate	739 kg	(41.54 " " ")
Coarse Aggregate	576 kg	(32.38 " " ")
Water	175 kg	(9.84 " " ")

Admixture (Master Builders Pozzolith 300 N) 59 ml.

The concrete was mixed in a Daffin mobile concrete mixer which produces concrete by a continuous mixing process. The 76.2-mm (3-in) cubes and 162 by 305-mm (6 by 12-in) control cylinders were cast in six batches. The cubes were compacted by vibration while the cylinders were compacted by rodding. All cylinders were cured at NMERI. Strength tests were performed at NMERI and deformation characteristics were developed at San Diego State University. The cubes and cylinders were moist, cured for 28 days and then stored at ambient conditions until the time of testing. The cylinders were tested for compressive strength at 7 days and at 28 days. The results of these tests are shown in Table 1. A comparison of the 28-day cylinder strength and the uniaxial cube strengths is shown in Table 2. The mean cube strength shown is the average of two tests. The mean cylinder strength is the average of three tests. The maximum difference between the mean value and an individual test is also shown to give an indication of the scatter of the results. As noted in the

TABLE 1. CYLINDER STRENGTHS

Batch	Date Cast	Strength (MPa)	
		7-day	28-day
		14.71	26.12
1	3-26-81	13.39	25.10
		15.11	25.97
		13.98	25.54
2	3-27-81	16.53	26.21
		16.17	24.88
		13.31	25.61
3	3-30-81	13.53	25.10
		13.94	26.03
		12.36	24.07
4	3-31-81	12.66	24.37
		11.74	23.64
		11.78	23.92
5	4-1-81	13.24	23.64
		13.28	23.84
		14.96	26.12
6	4-2-81	14.74	24.15
		13.36	26.12

TABLE 2. UNIAXIAL TEST RESULTS

Batch	28-Day Cylinder Strength		Cube Strength	
	Mean (MPa)	Difference From Mean (MPa)	Mean (MPa)	Difference From Mean (MPa)
1	25.73	0.63 (2.5%)	*	*
2	25.54	0.67 (2.6%)	20.00	0.40 (2.0%)
3	25.12	0.49 (1.9%)	20.14	0 (0%)
4	24.02	0.39 (1.6%)	*	*
5	23.80	0.17 (0.7%)	20.15	0.09 (0.4%)
6	25.46	1.32 (5.2%)	*	*
All	24.67	1.54 (6.3%)	20.10	0.50 (2.5%)

* No tests conducted for these batches.

tables, uniaxial cube tests were conducted for only three of the six batches. Since the scatter from batch to batch was very small, it would seem reasonable to use the mean of all tests conducted as a representative value for the other batches. This value was calculated and is also shown in Table 2.

Preparation--The cubical test specimens were cast in molds which were 76.2 by 76.2 by 78.2-mm (3 by 3 by 3 3/32-in) in size. Before the specimens were tested, the top face was milled to 76.2 mm (3 in) using a surface grinder with a diamond-tipped grinding wheel. For the specimens used in tension testing, no further machining was needed. The specimens used in tests involving standard and "nonstandard" compression load paths were machined further. These specimens were milled to form a 3.2-mm (1/8-in) bevel along each edge. This resulted in a 69.9 by 69.9-mm (2.75 by 2.75-in) bearing surface for each face of the test specimen. After the milling procedure, the specimens were washed in clear water, surface dried and stored for testing.

Epoxy--As indicated previously, the tension test specimens were attached to the tension loading platens by means of an epoxy resin layer. The epoxy used was unfilled and a 3.2-mm (1/8-in)-thick layer was used. A special fixture was designed and fabricated to hold the concrete cube and tension platens

and to aid in their alignment so that the face of the specimen and the platen were parallel. The specimens were aligned and clamped in the desired orientation. Duct tape was then used to form a closure around three sides of the 76.2 by 76.2 by 3.2-mm (3 by 3 by 1/8-in)-space between the cube and the steel platen. The epoxy was then mixed using standard procedures for mixing the two parts and poured into the cavity between the cube and platen. The epoxy had to cure overnight before it was rigid enough to remove the test specimen from the fixture. The duct tape was removed prior to testing and any excess epoxy was removed by sanding on a belt sander. The three specimens to be used for a given load path were prepared and tested at the same time. Thus the epoxy was the same age at the time of test.

The epoxy resin used was manufactured by Celanese Plastics & Specialties Company, Louisville, Kentucky. The composition used was 100 parts by weight of Epi-Rez 510 to 35 parts by weight of Epi-Cure 872. In accordance with the manufacturer's literature, this epoxy resin composition would provide an ultimate tensile strength of 61 MPa (8.9 kip/in^2) when cured for 2 weeks at room temperature. The flexural modulus at that time was listed as 3,309 MPa (480 kip/in^2). Since the listed tensile strength was much higher than needed to test the concrete cubes to failure in tension, a supplemental investigation was initiated to determine the strength of the epoxy at various ages. The investigation was designed so that adequacy of preparation of the steel loading surface, to assure proper bonding, could be determined at the same time. Tensile specimens consisting of two 15.9-mm (5/8-in)-square bars joined together by a 3.2-mm (1/8-in) layer of epoxy, were prepared. The loading surfaces were cleaned using the same procedures and materials to be used for the concrete tensile specimens. A minimum epoxy tensile strength of approximately twice the expected concrete uniaxial tensile strength of 2.1 MPa (0.30 kip/in^2) was considered to be desirable. It was felt that this would insure a failure in the concrete for all tests.

Three sets of five specimens each were prepared and tested to obtain the required data. The first set was statically tested at epoxy age of 23 to 24 hours with the following results:

SPECIMENS TESTED	STRESS (MPa)	NUMBER FAILED
5	4.41	1
4	4.64	None
4	4.89	None
4	5.14	None

The second set was tested in the following manner. Four specimens were tested statically with the following results:

SPECIMEN	AGE (Hours)	STRENGTH (MPa)
No. 1	4.75	0.11
No. 2	6.00	3.18
No. 3	6.25	3.87
No. 4	6.42	4.40

Based on the results of the four specimens listed above, it was noted that a very rapid strength gain occurred after the 6-h age. It was also noted that all failures had occurred in the epoxy, but that the epoxy behavior was very viscoelastic at this age. The fifth specimen was loaded 5 min after the fourth specimen at a 6.50-h age at a stress of 4.40 MPa. It was able to sustain this load for 24 s.

The third set was tested to determine the time that the epoxy could sustain a minimum prescribed stress before failure. The first specimen in this set was tested statically at the age of 5.75 h and developed a strength of 1.94 MPa. This was consistent with the strength versus age values determined in the previous tests. A previously determined strength of 3.87 MPa at a 6.25-h age was selected as the loading for the subsequent tests with the following results:

STRESS (MPa)	AGE (Hours)	TIME TO FAILURE (s)
4.49	6.25	8
4.49	6.50	60
4.49	6.75	64

For all of the above tests to failure, there were no bond failures at the steel loading surface. This indicated that the surface cleaning procedures were adequate. The tests resulted in consistent strength data at all test ages for the epoxy resin. Prior to beginning the required tension tests, two tensile specimens were prepared and tested uniaxially in a universal testing machine in the Materials Testing Laboratory. Two concrete specimens were selected from batch number 1 and were tested with the following results:

SPECIMEN	EPOXY AGE (Hours)	STRENGTH (MPa)
A6	16	2.00
C2	20	2.35

For both of the above specimens, the failure initiated in the concrete, but the failure surface extended into the epoxy. This appeared to be undesirable and it was decided to specify a minimum epoxy age of 24 h at the time of testing. Most tests were conducted at an epoxy age of 48 h since this fit best with the testing and test specimen preparation schedule which was established based on the availability of personnel.

TEST PROCEDURES

In addition to the 7-day and 28-day cylinder tests reported in Table 1 and Table 2, one cylinder was also tested at approximately 45 days for each batch. A comparison between these test results and the average of the 28-day cylinder strengths is shown below:

BATCH	28-DAYS (MPa)	45-DAYS (MPa)
1	25.73	29.27
2	25.55	31.61
3	25.12	31.83
4	24.02	29.92
5	23.80	33.87
6	25.46	31.54

There was a differential strength increase greater in some batches than in others relative to time. It was also assumed that some additional strength gain would occur with time. In order to have the concrete with the highest possible strength available for each test, test specimens were selected for testing in order of the highest cylinder strengths at the 45-day age. Since there would be a time lap of several weeks from the start to the end of the testing, it was also felt that this procedure would minimize the strength differential between cubes at the time of testing.

It also seemed to be desirable to try to minimize cross batch strength differentials as much as possible relative to each test series, particularly in individual replication tests for the same load path. To accomplish this, specimens for a given load path were always selected from the same batch. For a given test series, specimens were always selected as much as possible from the same batch. A summary of the selection of specimens from each batch relative to type of test and load path follows:

TEST TYPE	LOAD PATHS	BATCH
Standard Compression	1 - 8	5
Nonstandard Compression	1 - 5	3
" "	6 - 9	2
Tension	1 - 6	6
"	7 - 10	4

In addition to the 73 tests conducted for the 27 specified load paths, some additional uniaxial and biaxial tests were conducted as control test for basic batch strengths for some of the batches used.

Uniaxial compression tests--When conducting uniaxial tests in the triaxial testing frame, care was taken to ensure that no lateral confinement would occur until after the maximum stress had been obtained. The slightest lateral pressure would greatly affect the test results. During a test the compression platens of the two unloaded axes were in close proximity to those faces of the cube. This was necessary in order to mount the extensometers to measure the lateral strains. A thin metal sheet was used as a spacer to separate those platens from the specimen initially. Prior to testing, the spacer was removed and the load cells on those axes were activated. During a test it was possible to detect a pressure in those directions which would be an indication of premature lateral confinement of the specimen.

Biaxial compression tests--Biaxial tests were also greatly affected by the presence of a slight lateral pressure on the unconfined axis. Therefore, a small space was left between the cube and the compression platens on the unloaded axis as in the uniaxial tests. The load cell on that axis was activated as before, so that any lateral confinement of the specimen could be detected. This serves as a verification of possible confinement in these tests; since, as indicated above, slight confinements would produce large increases in the apparent biaxial strength and would be very noticeable.

Triaxial compression tests--Triaxial tests were performed in a manner similar to that of the biaxial tests. Since all sides were confined, the consideration of preventing confinement was not present as in the case of the uniaxial and biaxial tests. The specimen was placed in the testing machine and all of the loading platens were brought into contact with the test specimen. The extensometers were then set in place.

Tension testing--For any test involving a principal tension stress, the tension platens which had been previously glued to the test specimen were connected to the load cell and the loading ram of the jack by means of ball joints. This allowed the cube to align itself as the tensile load was applied and minimize the effect of eccentric loading. Special hardware was required to protect the extensometer used on the tension axis when separation of the cubes occurred at the time of failure.

The lateral strains which occurred in these tests were very much smaller than those in a compression test; and, in general, the face of the cube would move away from the adjacent face of the compression platen. Thus, the concern relative to lateral confinement during a compression test in general was not present for the tension tests. For tests involving combinations of tension and compression, the compression loads were applied in the same manner as for any other compression test. For those tests, a closer alignment of the specimen and load axes was necessary than for the other types of tests conducted.

III. EXPERIMENTAL RESULTS

As indicated previously, the primary requirement of this effort was to perform tests along various load paths specified by the New Mexico Engineering Research Institute. The purpose of the testing was to generate static triaxial constitutive data for specified load path. The results of those tests were to be documented by graphs of stress versus strain along the three principal axes used for each test. In this section a description of the various specified load paths will be presented along with the data reduction procedures used. The stress versus strain plots will be presented in the appendixes to this report.

THE TRIAXIAL TESTING PROGRAM

The objectives of the triaxial testing program defined by NMERI are listed below:

a. Determine the initial inelastic surface.
b. Determine the inelastic surface subsequent to inelastic deformation. (Evidence of kinematic hardening).
c. Determine the limit surface for a "standard" set of tests.
d. Determine the limit surface for an alternate set of tests to indicate the effect of inelastic deformation on the limit surface location. (Path dependence of limit surface).
e. Illustrate the nature of inelastic deformation prior to reaching the limit stress and after reaching the limit stress. (Stress-strain relation).

The purpose of the NMSU Testing Program was to meet the above objectives to the greatest extent possible, with the primary emphasis on "nonstandard" stress paths for all principal stresses in compression and on stress paths with one principal stress in tension. For the stress paths in compression or in tension, the above objectives were to be met by the following testing sequence:

a. Stress Paths in Compression (All Principal Stresses Negative)
   (1) Verification and Initialization Tests

   Perform a set of standard tests to obtain an initial definition for the inelastic and limit surfaces. Since such paths have previously been studied, these tests also serve to verify the testing procedure. Monitor stress-strain curves to meet objective e.

(2) Path Dependence Tests

Select points in stress space on the paths used in part A. Choose alternate paths involving inelastic deformation that reach these same points to meet objectives b and d.

b. Stress Paths in Tension (One Principal Stress Positive)

(1) Initialization Tests

Perform a set of standard tests to obtain an initial definition for the inelastic and limit surfaces. Use these tests to obtain stress-strain curves, also.

(2) Path Dependence Tests

Choose alternate paths involving inelastic deformation to monitor the effect on the location of the inelastic surfaces, the limit surface and stress-strain curves.

A total of 73 tests along 27 specified load paths were prescribed for the NMSU Testing Program. The tests were subdivided into three test series with a total of 73 specified tests as shown below:

	LOAD PATHS	TEST PER PATH
Standard Compression Tests	8	2
Nonstandard Compression Tests	9	3
Tension Tests	10	3

Due to the expected anisotropic behavior of the concrete, each load path was carefully defined relative to the direction of casting of the test cubes. The principal stresses σ_1 or σ_2 were always defined as the direction parallel to the direction of casting of the cube (the sides of the cube as cast). The principal stress σ_3 was always defined as the direction perpendicular to the casting direction (the top of the cube as cast). A description of all of the load paths is given below:

A. Standard Stress Paths in Compression Zone

(1) Uniaxial stress to failure

$\Delta\sigma_1 = \Delta\sigma_2 = 0$; $\Delta\sigma_3 = -\Delta s$

(2) Uniaxial stress to failure

$\Delta\sigma_1 = -\Delta s$; $\Delta\sigma_2 = \Delta\sigma_3 = 0$ (Denote maximum value of σ_1 as f'_c)

(3) Biaxial stress to failure with $\sigma_2/\sigma_1 = 1.0$; $\sigma_3 = 0$

$\Delta\sigma_1 = \Delta\sigma_2 = -\Delta s$; $\Delta\sigma_3 = 0$ (Denote maximum value of σ_1 and σ_2 as f'_b)

(4) Hydrostatic loading to $\sigma_1 = \sigma_2 = \sigma_3 = -f'_b/3$

$\Delta\sigma_1 = \Delta\sigma_2 = \Delta\sigma_3 = \Delta s$

Uniaxial loading to failure

$\Delta\sigma_1 = -\Delta s$; $\Delta\sigma_2 = \Delta\sigma_3 = 0$

(5) Hydrostatic loading to $\sigma_1 = \sigma_2 = \sigma_3 = -2/3\ f'_b$

$\Delta\sigma_1 = \Delta\sigma_2 = \Delta\sigma_3 = \Delta s$

Shear loading to failure

$\Delta\sigma_1 = -\Delta s$; $\Delta\sigma_2 = \Delta s$; $\Delta\sigma_3 = 0$

(6) Triaxial stress to failure with $\sigma_2/\sigma_1 = 1.0$; $\sigma_3/\sigma_1 = 0.1$

$\Delta\sigma_1 = \Delta\sigma_2 = -\Delta s$; $\Delta\sigma_3 = -0.1\Delta s$

(7) Biaxial stress to failure with $\sigma_2/\sigma_1 = 0.5$; $\sigma_3 = 0$

$\Delta\sigma_1 = -\Delta s$; $\Delta\sigma_2 = -0.5\Delta s$; $\Delta\sigma_3 = 0$

(8) Triaxial stress to failure with $\sigma_2/\sigma_1 = 0.5$; $\sigma_3/\sigma_1 = 0.1$

$\Delta\sigma_1 = -\Delta s$; $\Delta\sigma_2 = -0.5\Delta s$; $\Delta\sigma_3 = -0.1\Delta s$

B. Nonstandard Stress Paths in Compression

(1) Load hydrostatically to $\sigma_1 = \sigma_2 = \sigma_3 = -0.1f'_c$

$\Delta\sigma_1 = \Delta\sigma_2 = \Delta\sigma_3 = \Delta s$

Load uniaxially to $\sigma_1 = 0.85\ f'_c$; $\sigma_2 = \sigma_3 = -0.1\ f'_c$

$\Delta\sigma_1 = -\Delta s$; $\Delta\sigma_2 = \Delta\sigma_3 = 0$

Unload to $\sigma_1 = \sigma_2 = \sigma_3 = -0.1f'_c$

$\Delta\sigma_1 = \Delta s$; $\Delta\sigma_2 = \Delta\sigma_3 = 0$

Load biaxially to failure with $\sigma_2/\sigma_1 = 1.0$; $\sigma_3 = -0.1\ f'_c$

$\Delta\sigma_1 = \Delta\sigma_2 = -\Delta s$; $\Delta\sigma_3 = 0$

(2) Load hydrostatically to $\sigma_1 = \sigma_2 = \sigma_3 = -0.1\ f'_c$

$\Delta\sigma_1 = \Delta\sigma_2 = \Delta\sigma_3 = -\Delta s$

Load biaxially to failure with $\sigma_2/\sigma_1 = 1.0$; $\sigma_3 = -0.1\ f'_c$

$\Delta\sigma_1 = \Delta\sigma_2 = -\Delta s$; $\Delta\sigma_3 = 0$

(3) Load hydrostatically to $\sigma_1 = \sigma_2 = \sigma_3 = -0.1\ f'_c$

$\Delta\sigma_1 = \Delta\sigma_2 = \Delta\sigma_3 = -\Delta s$

Load biaxially to $\sigma_1 = \sigma_2 = -0.85\ f'_b$; $\sigma_3 = -0.1\ f'_c$

$\Delta\sigma_1 = \Delta\sigma_2 = -\Delta s$; $\Delta\sigma_3 = 0$

Unload to $\sigma_1 = \sigma_2 = \sigma_3 = -0.1\ f'_c$

$\Delta\sigma_1 = \Delta\sigma_2 = \Delta s$; $\Delta\sigma_3 = 0$

Load uniaxially to failure

$\Delta\sigma_1 = -\Delta s$; $\Delta\sigma_2 = \Delta\sigma_3 = 0$

(4) Load hydrostatically to $\sigma_1 = \sigma_2 = \sigma_3 = -0.1\ f_c'$

$\Delta\sigma_1 = \Delta\sigma_2 = \Delta\sigma_3 = -\Delta s$

Load uniaxially to failure

$\Delta\sigma_1 = -\Delta s;\ \Delta\sigma_2 = \Delta\sigma_3 = 0$

(5) Load hydrostatically to $\sigma_1 = \sigma_2 = \sigma_3 = -f_b'$

$\Delta\sigma_1 = \Delta\sigma_2 = \Delta\sigma_3 = -\Delta s$

Unload hydrostatically to $\sigma_1 = \sigma_2 = \sigma_3 = -2/3\ f_b'$

$\Delta\sigma_1 = \Delta\sigma_2 = \Delta\sigma_3 = \Delta s$

Load in shear to failure

$\Delta\sigma_1 = -\Delta s;\ \Delta\sigma_2 = \Delta s;\ \Delta\sigma_3 = 0$

(6) Load hydrostatically to $\sigma_1 = \sigma_2 = \sigma_3 = -2\ f_c'$

$\Delta\sigma_1 = \Delta\sigma_2 = \Delta\sigma_3 = -\Delta s$

Unload hydrostatically to $\sigma_1 = \sigma_2 = \sigma_3 = -0.1\ f_c'$

$\Delta\sigma_1 = \Delta\sigma_2 = \Delta\sigma_3 = \Delta s$

Load biaxially to failure

$\Delta\sigma_1 = \Delta\sigma_2 = -\Delta s;\ \Delta\sigma_3 = 0$

(7) Load uniaxially to $\sigma_1 = -0.75\ f_c';\ \sigma_2 = \sigma_3 = 0$

$\Delta\sigma_1 = -\Delta s;\ \Delta\sigma_2 = \Delta\sigma_3 = 0$

Load biaxially to $\sigma_1 = \sigma_2 = -0.75\ f_c';\ \sigma_3 = 0$

$\Delta\sigma_1 = \Delta\sigma_3 = 0;\ \Delta\sigma_2 = -\Delta s$

Load biaxially to failure

$\Delta\sigma_1 = \Delta\sigma_2 = -\Delta s;\ \Delta\sigma_3 = 0$

(8) Load hydrostatically to $\sigma_1 = \sigma_2 = \sigma_3 = -0.1\ f_c'$

$\Delta\sigma_1 = \Delta\sigma_2 = \Delta\sigma_3 = -\Delta s$

Load uniaxially to $\sigma_1 = -0.85\ f_c'$

$\Delta\sigma_1 = -\Delta s;\ \Delta\sigma_2 = \Delta\sigma_3 = 0$

Trace a path to $\sigma_1 = -0.1\ f_c';\ \sigma_2 = -0.85\ f_c';\ \sigma_3 = -0.1\ f_c'$

$\Delta\sigma_1 = \Delta s;\ \Delta\sigma_2 = -\Delta s;\ \Delta\sigma_3 = 0$

Load uniaxially to failure

$\Delta\sigma_1 = \Delta\sigma_3 = 0;\ \Delta\sigma_2 = -\Delta s$

(9) Load hydrostatically to $\sigma_1 = \sigma_2 = \sigma_3 = -2\ f_c'$

$\Delta\sigma_1 = \Delta\sigma_2 = \Delta\sigma_3 = -\Delta s$

Load in shear to $\sigma_1 = -f_c';\ \sigma_2 = -3f_c';\ \sigma_3 = -2\ f_c'$

$\Delta\sigma_1 = \Delta s;\ \Delta\sigma_2 = -\Delta s;\ \Delta\sigma_3 = 0$

Unload in shear to $\sigma_1 = \sigma_2 = \sigma_3 = -2\ f_c'$

$\Delta\sigma_1 = -\Delta s;\ \Delta\sigma_2 = \Delta s;\ \Delta\sigma_3 = 0$

Unload hydrostatically to $\sigma_1 = \sigma_2 = \sigma_3 = -0.1\ f_c'$

$\Delta\sigma_1 = \Delta\sigma_2 = \Delta\sigma_3 = \Delta s$

Load biaxially to failure

$\Delta\sigma_1 = \Delta\sigma_2 = -\Delta s;\ \Delta\sigma_3 = 0$

C. Stress Paths Involving Tension

(1) Uniaxial stress to failure

$\Delta\sigma_1 = \Delta s;\ \Delta\sigma_2 = \Delta\sigma_3 = 0$ (Denote maximum value of σ_1 as f_t')

(2) Uniaxial stress to failure (Check on anisotropy)

$\Delta\sigma_1 = \Delta\sigma_2 = 0;\ \Delta\sigma_3 = \Delta s$ (Denote maximum value of σ_3 as f_t')

(3) Biaxial stress to failure with $\sigma_2/\sigma_1 = -0.5$

$\Delta\sigma_1 = \Delta s;\ \Delta\sigma_2 = -0.5\Delta s;\ \Delta\sigma_3 = 0$

(4) Shear to failure

$\Delta\sigma_1 = \Delta s,\ \Delta\sigma_2 = -\Delta s,\ \Delta\sigma_3 = 0$ (Denote maximum value of σ_1 as f_s')

(5) Load uniaxially to $\sigma_1 = 0.5\ f_t';\ \sigma_2 = \sigma_3 = 0$

$\Delta\sigma_1 = \Delta s;\ \Delta\sigma_2 = \Delta\sigma_3 = 0$

Load in shear to failure

$\Delta\sigma_1 = \Delta s;\ \Delta\sigma_2 = -\Delta s;\ \Delta\sigma_3 = 0$

(6) Load in shear to $\sigma_1 = 0.5\ f_s';\ \sigma_2 = -0.5\ f_s';\ \sigma_3 = 0$

$\Delta\sigma_1 = \Delta s;\ \Delta\sigma_2 = -\Delta s;\ \Delta\sigma_3 = 0$

Load uniaxially to failure

$\Delta\sigma_1 = \Delta s;\ \Delta\sigma_2 = \Delta\sigma_3 = 0$

(7) Load biaxially to $\sigma_1 = 0.5\ f_t';\ \sigma_2 = 0.1\ f_t';\ \sigma_3 = 0$

$\Delta\sigma_1 = \Delta s;\ \Delta\sigma_2 = -0.2\Delta s;\ \Delta\sigma_3 = 0$

Load biaxially to failure

$\Delta\sigma_1 = \Delta s;\ \Delta\sigma_2 = -0.4\Delta s;\ \Delta\sigma_3 = 0$

(8) Load biaxially to $\sigma_1 = 0.5\ f_s';\ \sigma_2 = -0.4\ f_s';\ \sigma_3 = 0$

$\Delta\sigma_1 = \Delta s;\ \Delta\sigma_2 = -0.8\Delta s;\ \Delta\sigma_3 = 0$

Load biaxially to failure

$\Delta\sigma_1 = \Delta s;\ \Delta\sigma_2 = -0.6\Delta s;\ \Delta\sigma_3 = 0$

(9) Load in biaxial compression to $\sigma_1 = 0;\ \sigma_2 = \sigma_3 = -f_t'$

$\Delta\sigma_1 = 0;\ \Delta\sigma_2 = \Delta\sigma_3 = -\Delta s$

Load in uniaxial tension to failure

$\Delta\sigma_1 = \Delta s;\ \Delta\sigma_2 = \Delta\sigma_3 = 0$

(10) Load in uniaxial compression to $\sigma_1 = \sigma_2 = 0;\ \sigma_3 = -f_t'$

$\Delta\sigma_1 = \Delta\sigma_2 = 0;\ \Delta\sigma_3 = -\Delta s$

Load in shear to failure

$\Delta\sigma_1 = \Delta s;\ \Delta\sigma_2 = -\Delta s;\ \Delta\sigma_3 = 0$

STRESS-STRAIN DATA

As indicated previously, the test data from the test program were to be documented by graphs of stress versus strain for each test. The stress-strain plots for each of the 73 specified tests are presented in the appendixes. The total test program was subdivided into three test series. The test data for each test series are presented respectively in Appendix A, B and C for the standard compression, nonstandard compression, and tension test series.

In Appendix A the test data for the eight load paths included in the standard compression tests are shown in Figures A1 through A8 respectively. Each figure contains the stress-strain plots for the two specimens tested for each load path.

In Appendix B the test data for the nine load paths included in the nonstandard compression test series are shown in Figures B1 through B9 respectively. In this appendix, each figure includes the stress-strain data for the three specimens tested for each load path.

Appendix C contains the test data for the 10 load paths included in the tension test series. The test data for load paths 1 through 10 are presented in Figures C1 through C10 respectively. Each figure contains the stress-strain plots for the three specimens tested for each load path in this test series.

In addition to the 73 specified tests, stress-strain data were obtained for six additional control tests. These tests were conducted to check the batch-to-batch consistency of the concrete material. These six tests consisted of two uniaxial tests and two biaxial tests using specimens from batch 3 and two uniaxial tests on specimens from batch 2.

The uniaxial tests were the same as the load path 2 tests in the standard compression test series (A2) which were conducted using specimens from batch 5. A comparison of the strength variation obtained for these tests is shown in Table 2. Based on a total of six tests using cubes from three different batches, the maximum variation from the mean of all tests was only 2.5%. This indicated an excellent batch-to-batch replication of the basic unconfined uniaxial cube strength.

The two biaxial strength control tests conducted using specimens from batch 3 were the same as the load path B3 in the standard compression test series which used specimens from batch 5. A comparison of the strength variation obtained from these four tests follows:

Batch	Specimen	Biaxial Strength (MPa)	Difference From Mean
5	C3	25.37	1.6%
5	B3	24.56	1.6%
3	D6	26.63	1.4%
3	B6	25.83	1.4%

The batch 5 mean strength was 24.97 MPa with a difference from the mean for each test of only 1.6%. The batch 3 mean strength was 26.24 MPa with a difference from the mean of only 1.4%. A comparison of the strength variation between the two batches was made based on a mean strength of 25.61 MPa for all four tests. The maximum difference between the mean strength and a given test was only 4.1%, indicating a good batch-to-batch replication of the unconfined biaxial cube strength.

The stress-strain results of the six uniaxial and biaxial replication tests are shown in Figures 3 through 8. In each figure the batch number and specimen used for the given test are shown. Figures 3 and 4 show the uniaxial results for batch 2; Figures 5 and 6 show the uniaxial results for batch 3; and Figures 7 and 8 show the results of the biaxial tests for batch 3.

The format used for these six graphs of stress versus strain is the same as that used for all of the stress-strain plots shown in the appendixes. For each test, the stress and strain results are presented simultaneously for each of the three principal axes. For a loaded axis the stress-strain plot is designated as σ_1, ε_1 or σ_2, ε_2, etc. For an axis which is not loaded, the strains along this axis are plotted against the stress on one of the loaded axis and are designated as σ_1, ε_2, or σ_1, ε_3, etc. All compressive stresses are designated as negative and all tensile stresses are designated as positive. Similarly, all compressive strains are designated to be negative and all tensile strains are designated as positive. To further emphasize the difference between positive and negative strains, all positive strains are graphed using a solid line and all negative strains are graphed using a dashed line. To identify stess and strain data points occurring at the same point in time, the corresponding data points are labeled with the same numeral, 1, 2, 3, etc., when needed to help identify individual data points on any of the three plots.

To assist in correlating these data with conventional stress-strain curves based on cylindrical specimens, an additional experimental program was performed at San Diego State University. These results are presented in Appendix D.

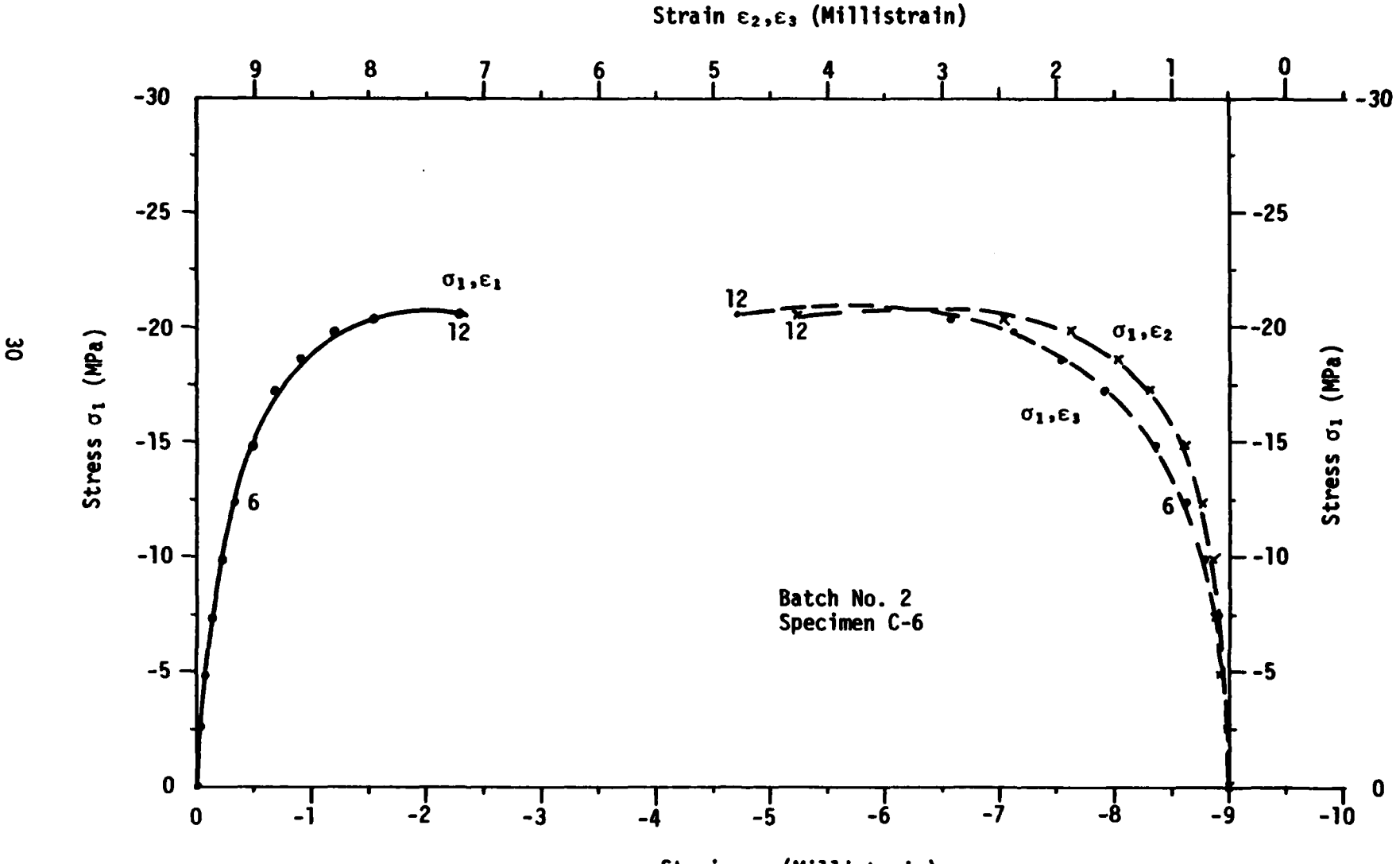

Figure 3. Uniaxial stress path in compression for Batch 2 (Test 1).

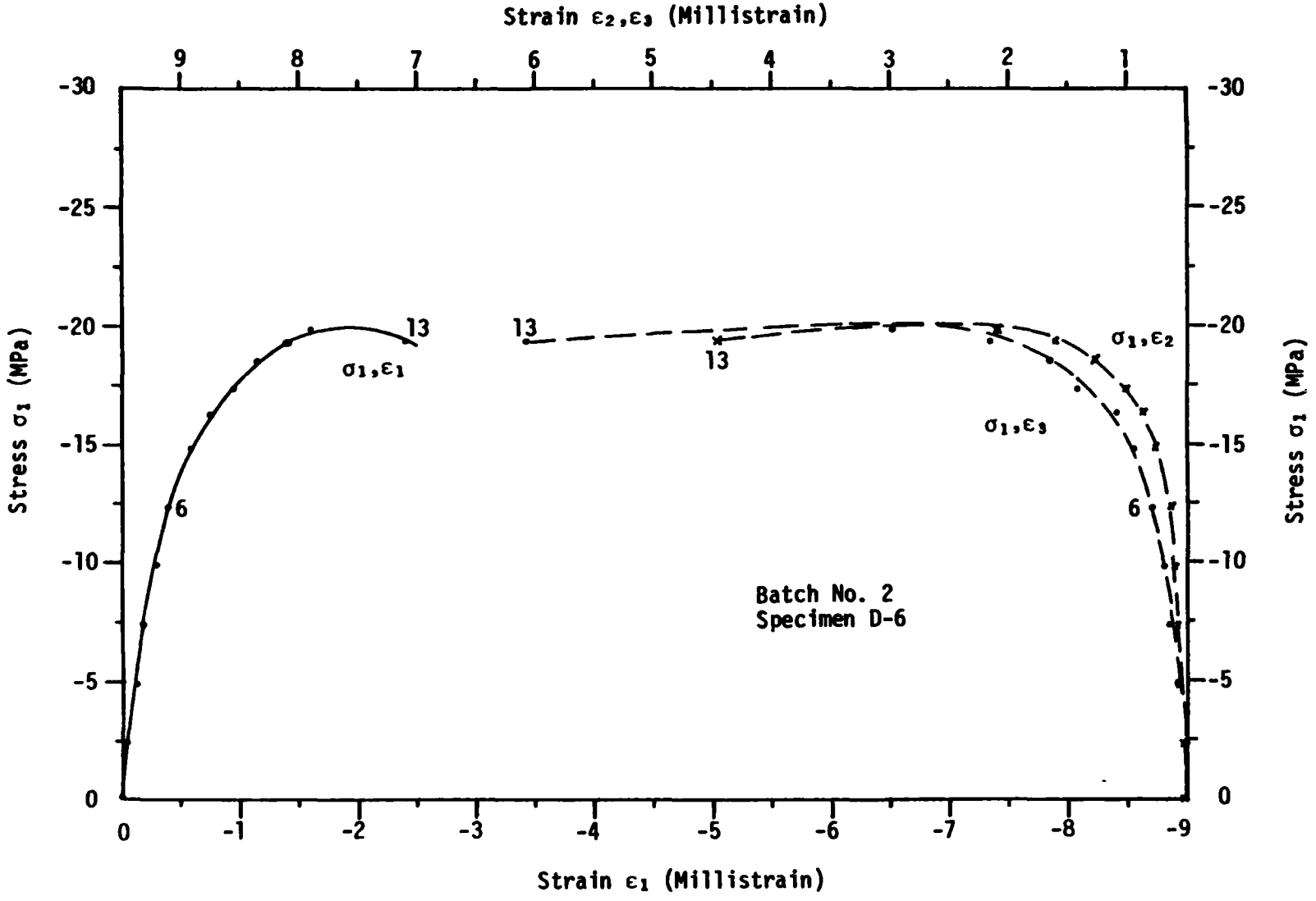

Figure 4. Uniaxial stress path in compression for Batch 2 (Test 2).

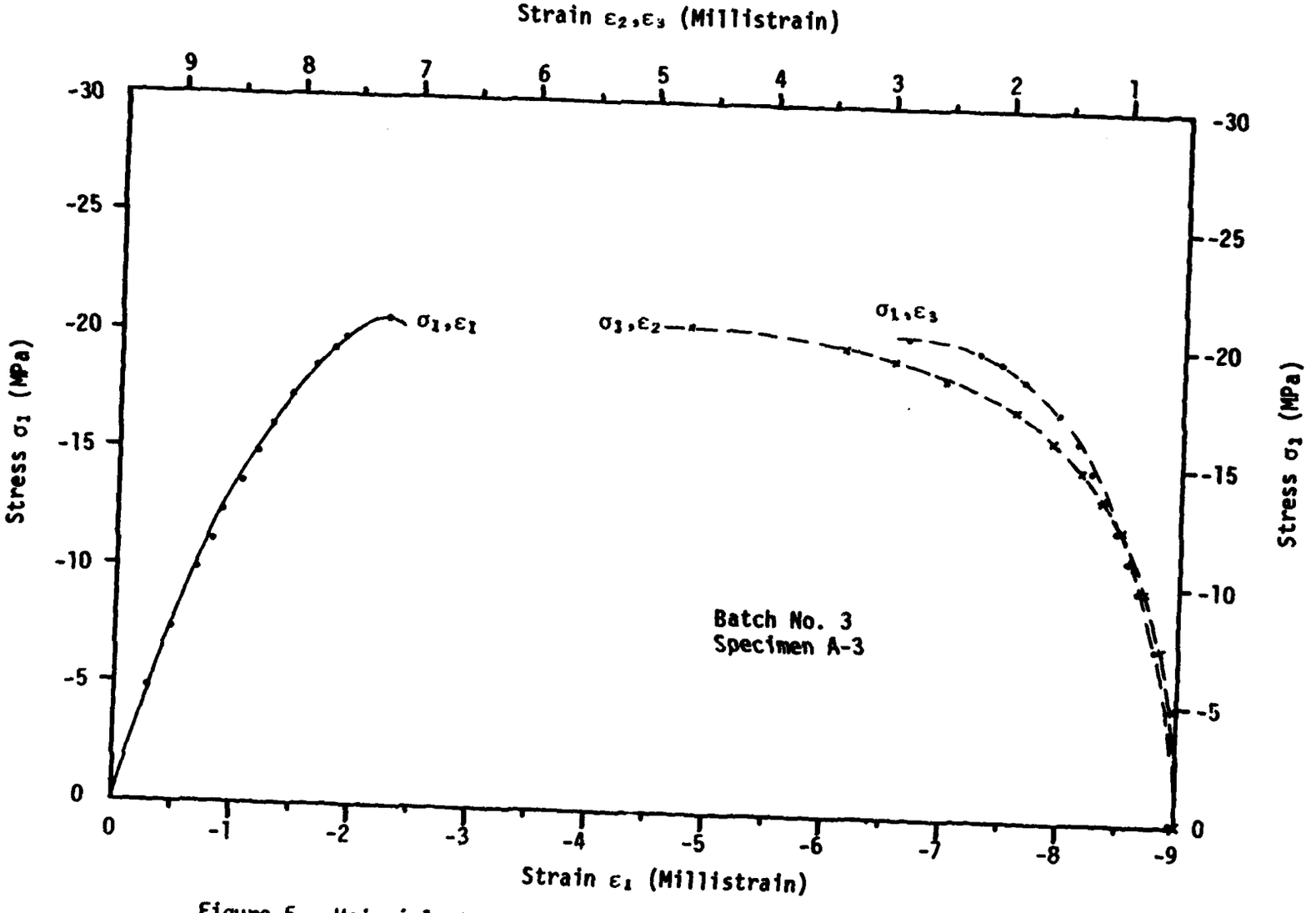

Figure 5. Uniaxial stress path in compression for Batch 3 (Test 1).

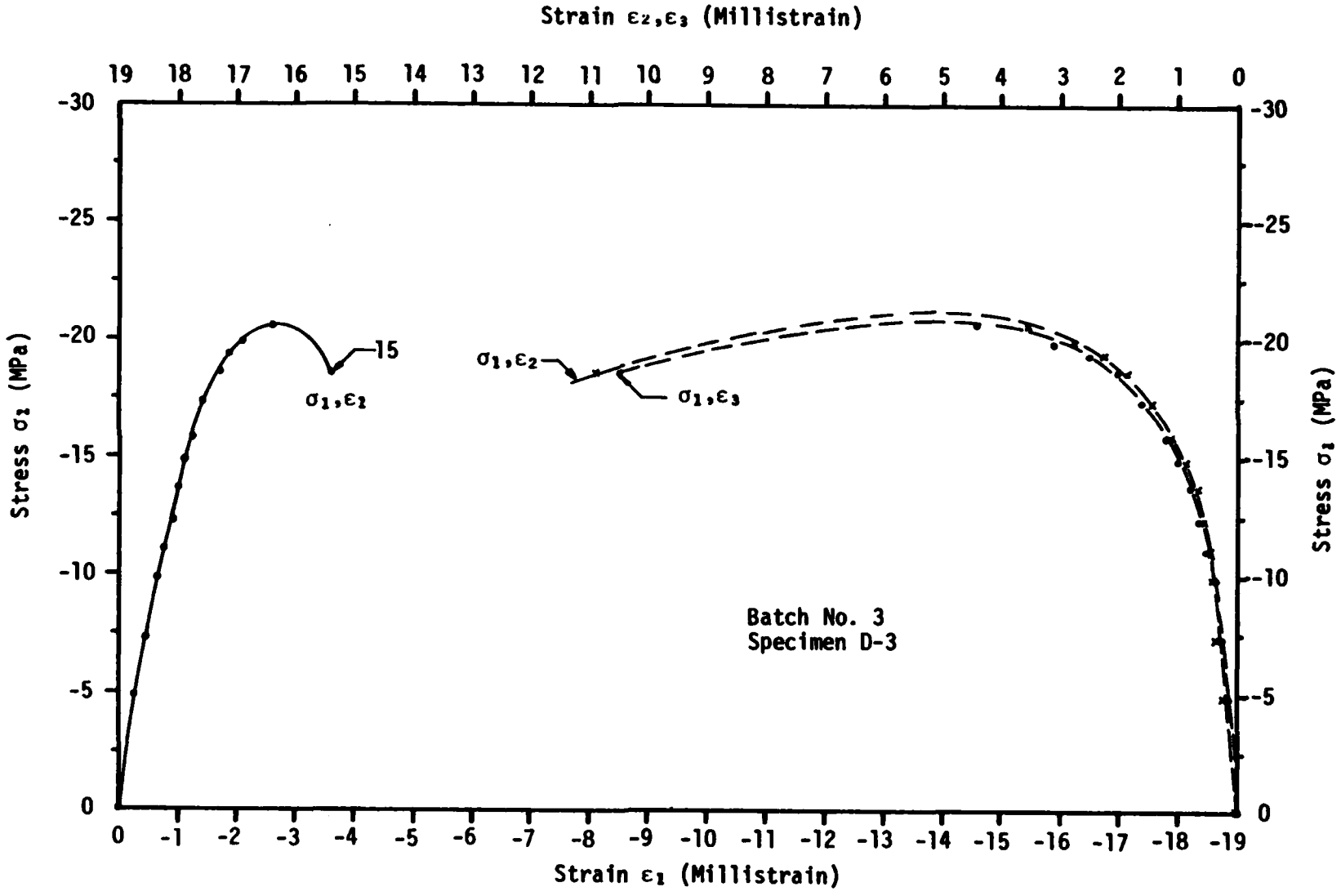

Figure 6. Uniaxial stress path in compression for Batch 3 (Test 2).

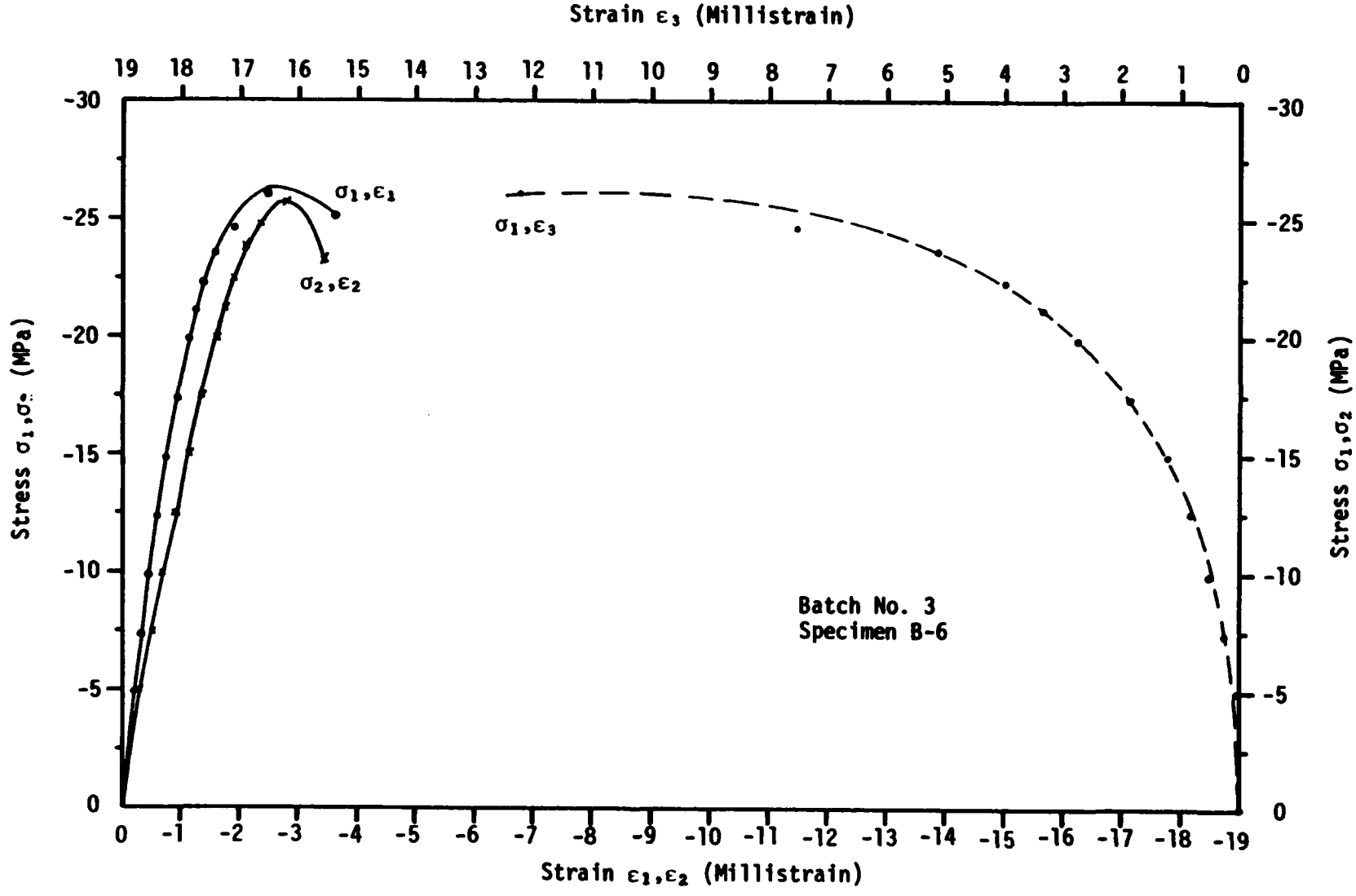

Figure 7. Biaxial stress path in compression for Batch 3 (Test 1).

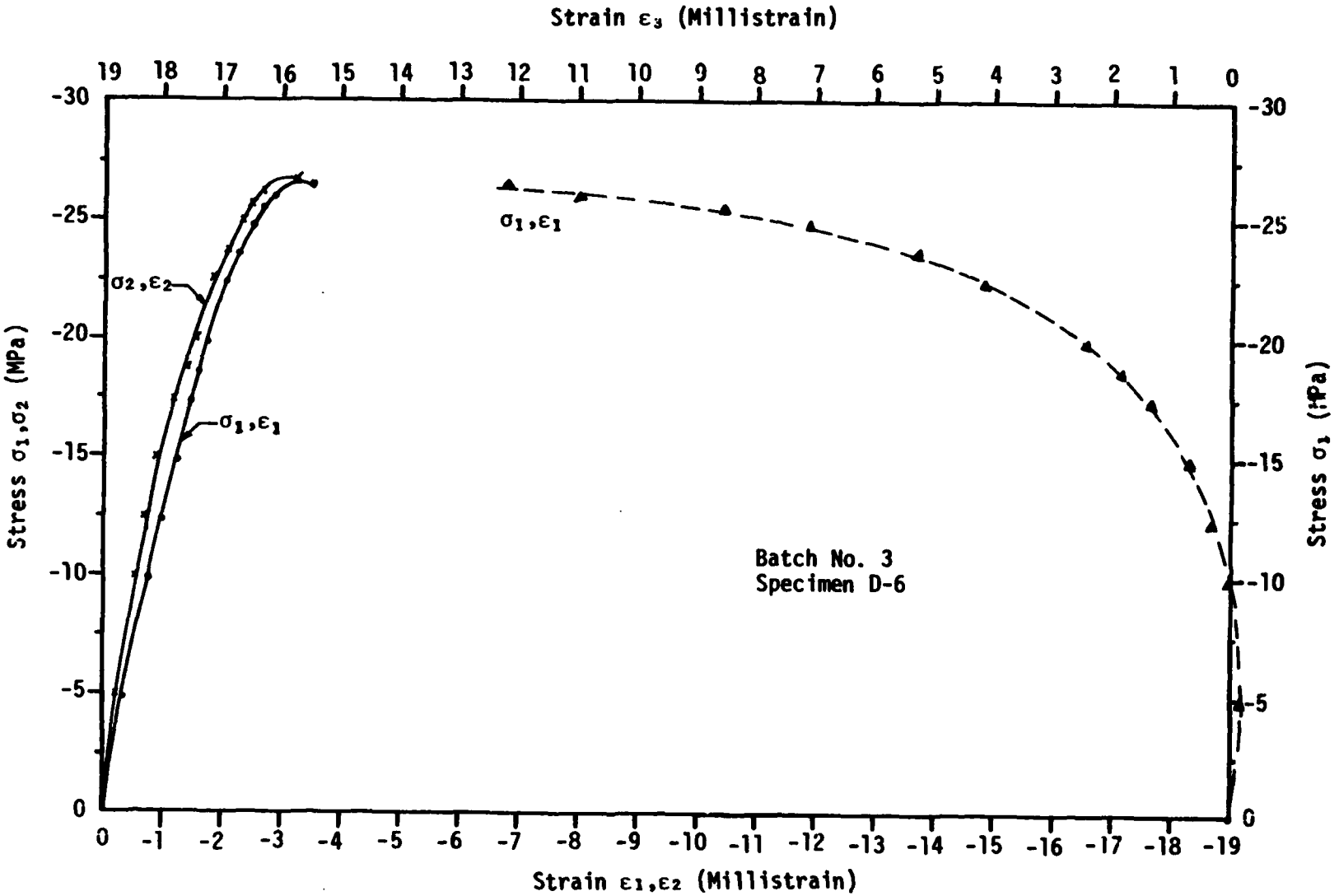

Figure 8. Biaxial stress path in compression for Batch 3 (Test 2).

IV. CONCLUSIONS AND RECOMMENDATIONS

BACKGROUND

This effort was undertaken as part of a study to determine the behavior of plain concrete subjected to various multiaxial load paths. The loading combinations included uniaxial, biaxial and triaxial states of stress with various combinations of compressive and tensile stresses. The purpose of this effort was to generate triaxial constitutive data for specified load paths based on static loadings. A total of 81 tests were conducted using 27 different load paths. The test data were reported in the form of stress-strain records for 79 of the tests. Only strength data were recorded for the other two tests.

The test specimens were 76.2-mm (3-in) concrete cubes. These specimens were cast at NMERI and transported to NMSU for testing. The cubical specimens made it possible to obtain different stresses in the three orthogonal principal directions simultaneously. The effect of friction at the interface of these specimens and the loading platens would noticeably alter the desired unconfined stress states. To overcome this difficulty, special friction reduction methods were incorporated in the loading system.

The loading apparatus used in this study was a three-dimensional manually loaded hydraulic ram system. Stresses were calculated from strain measurements on load cells in series with the ram and placed on the opposite side of the specimen from the ram. Specimen strains were calculated based on the relative displacements of opposite faces of the specimens along the centroidal axis. These displacements were determined from strain output of extensometers which were specifically designed for this purpose.

The loading frame used in the test apparatus is quite stiff. As a result, very little displacement is required to unload the stored energy in the frame during a test, and specimen failure is not explosive. For almost every test, the specimen can be removed from the test apparatus in one piece. The failure mode of the cubes and the orientation of fracture planes is quite apparant. This serves as a visual check on the effectiveness of the friction reduction methods used.

At this time the analysis of the data is in progress at NMERI. The data are being used to evaluate the capabilities and limitations of existing constitutive models for concrete. Those results will be presented separately.

CONCLUSIONS

Since the analysis of the data from this test program has not been completed at this time, this discussion will be primarily related to the testing program. Some general observations relative to the resulting data were also made.

The testing procedures used for all tests in the test program were found to be quite satisfactory. The loading system is very versatile and it was possible to develop the specified states of stress including a triaxial stress state with one tension stress component. This was in spite of the fact that some of the load paths included in the test program were fairly complex relative to previous testing conducted at NMSU or reported in the literature. The modifications made in the load frame were found to be quite helpful for alignment of the three loading axes for the various tests.

Dimensional control of the test specimens was excellent and well within the specified tolerances. The tension specimens preparation procedures were determined to be very satisfactory. An initial concern was the possibility of bond failure between the epoxy and the steel loading platens during a test. None occurred. All tension test failures occurred in the concrete test specimen.

The friction reduction methods used to minimize the constraint of the specimens at their interface with the steel loading platens was thought to be very good. This conclusion was reached based on the observed failure modes and fracture planes in the specimens for each test. Another basis for the conclusion was a comparison of limit stress and strain values with those reported in the literature for some of the control tests included in the test program.

Replication of the limit stress from test to test was excellent for a given load path when using specimens from the same batch for all compression tests. Replication of the limit stress for a given load path when using specimens from different batches was quite good. This was an indication of good quality control in the manufacture of the test specimens.

Replication of the limit stress for tension tests and limit strains for all tests was somewhat less consistent than the limit stress replication for the compression tests. This situation is not unique for this test program. Similar observations have been made relative to test data reported in the literature.

The load cell calibration procedure was found to be excellent. Replication of the calibration functions from loading to loading was excellent. The nonlinear output from some of the load cells did cause some inconvenience during data reduction and during testing on some load paths.

The extensometer calibration procedures were generally found to be satisfactory. Some difficulty occurred relative to replication of the extensometer output during calibration. This resulted in a more tedious and time consuming procedure than for load cell calibration. Alternate calibration procedures have been considered for future testing programs.

The data recording system utilizing a graphical display of stress versus strain data during a test is considered to have definite advantages compared to alternate digital data aquisition systems. Using this system, point in time data may be obtained while the specimen is creeping at a high rate. The investigator is immediately aware of trends in data from one load path to another as well as the replication of the data from test to test.

RECOMMENDATIONS

Several recommendations for future research which could utilize the existing triaxial testing capability with minor modifications of the testing apparatus are included in this section.

A test program similar to the present one which would investigate the effect on the limit surface location between a set of standard tests and an alternate set of tests that reach the same point in stress space by alternate stress paths. The standard tests would be used to obtain an initial definition of the limit surface. The effect of several parameters such as concrete strength or additional cycles of inelastic deformation could be included. The stress-strain response could be monitored for all tests conducted.

A test program with primary emphasis on multiaxial testing, including one principal stress in tension or tests involving biaxial tension, could be included.

The effect on stress-strain response of test specimens consisting of reinforced concrete cubes could be considered. Tests with varying amounts of reinforcement or with a fixed amount of reinforcement with tests along different load paths could be considered.

With some modification of the existing loading system, an investigation of strain softening would be feasible in the existing loading frame. The primary modification would be the installation of a loading ram which is not hydraulic on one of the loading axis.

APPENDIX A

STRESS-STRAIN PLOTS FOR STANDARD COMPRESSION TESTS

All stress and strain data are plotted for the various paths described as standard compression tests. Figure A-1 gives the results for the first path, Figure A-2 for the second path, etc. Since two experiments were performed for each path, each figure has a part (a) and a part (b) which differentiates these two sets of data.

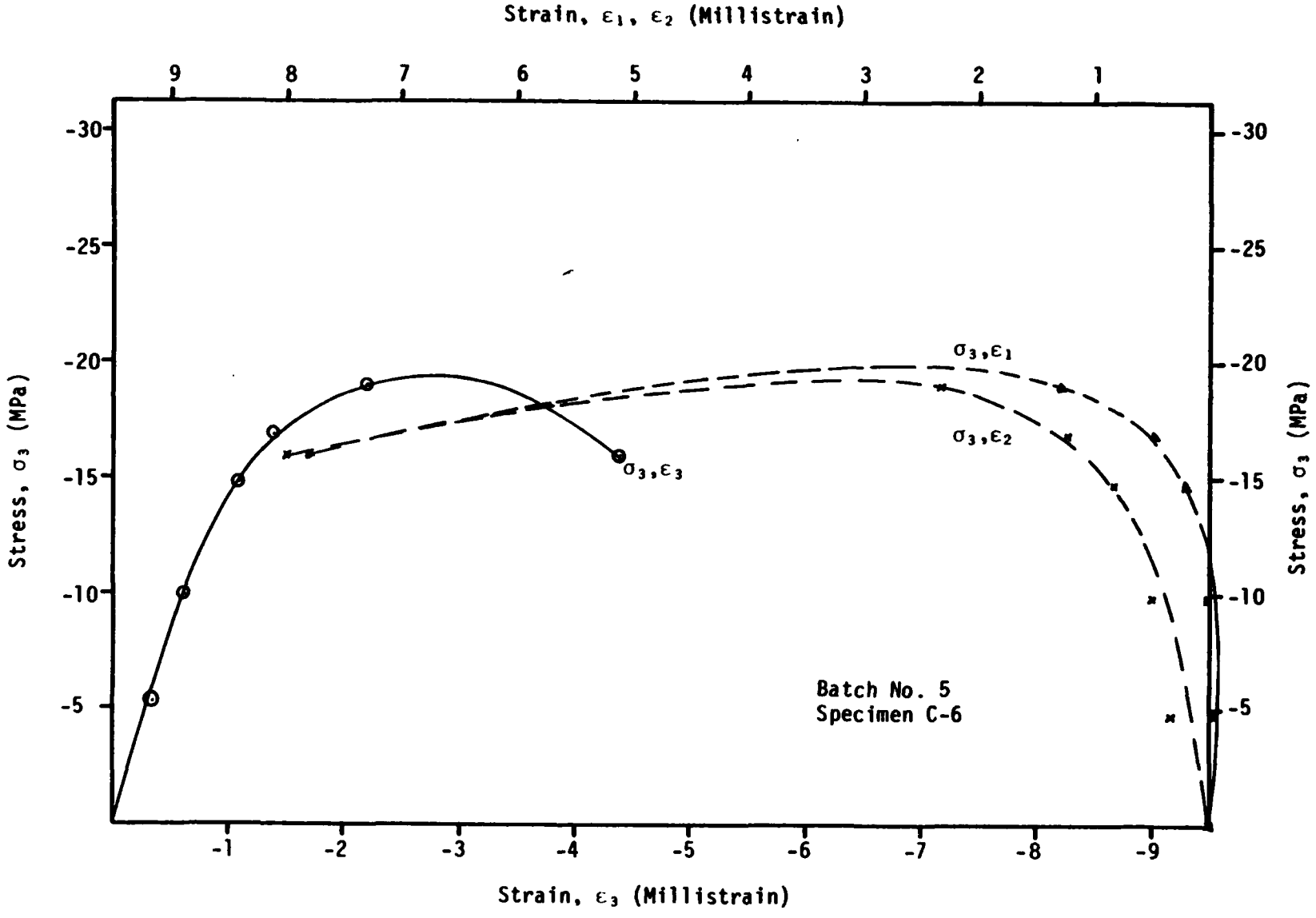

(a)

Figure A1. Load Path 1 of standard compression tests.

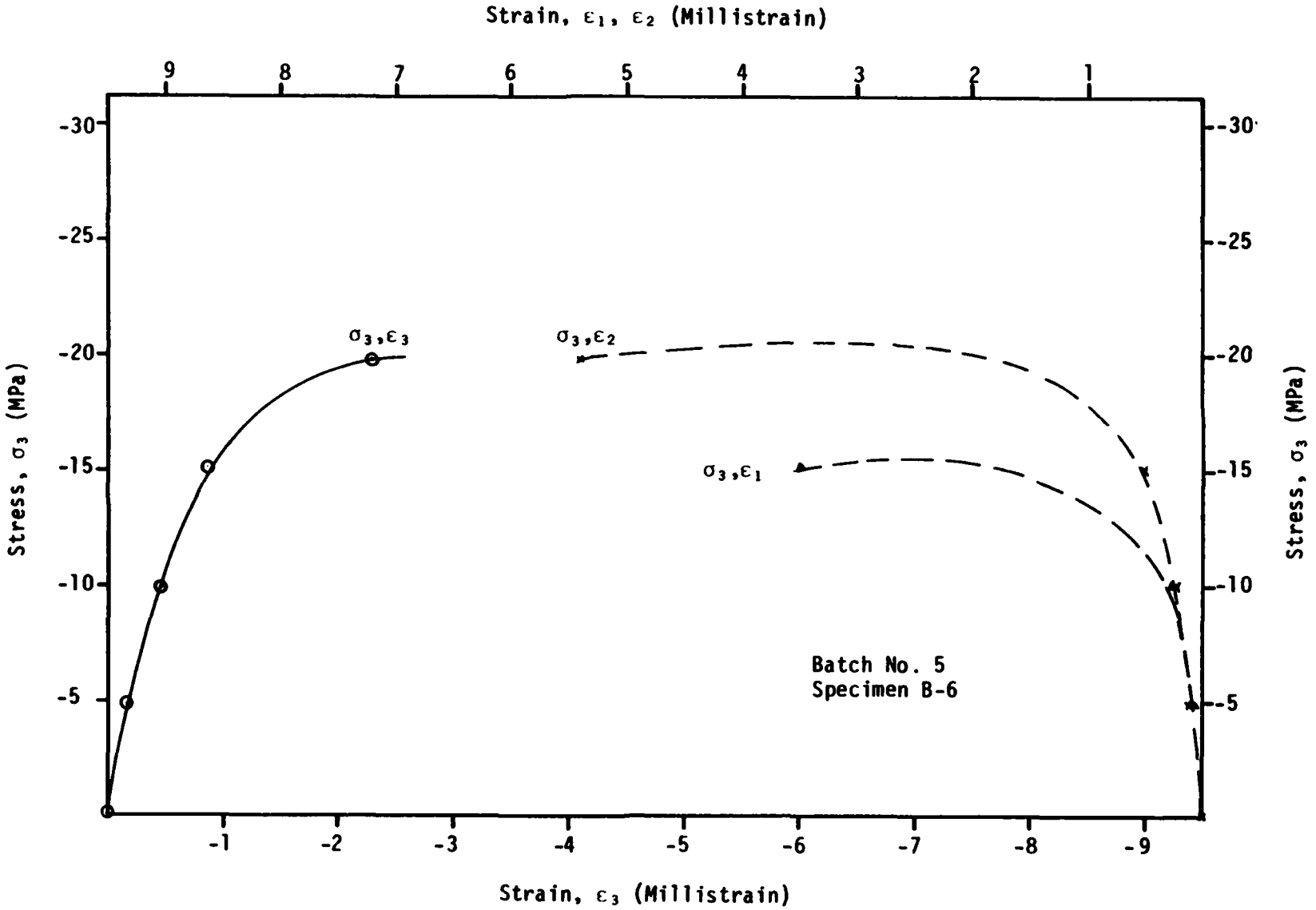

(b)

Figure A1. Continued.

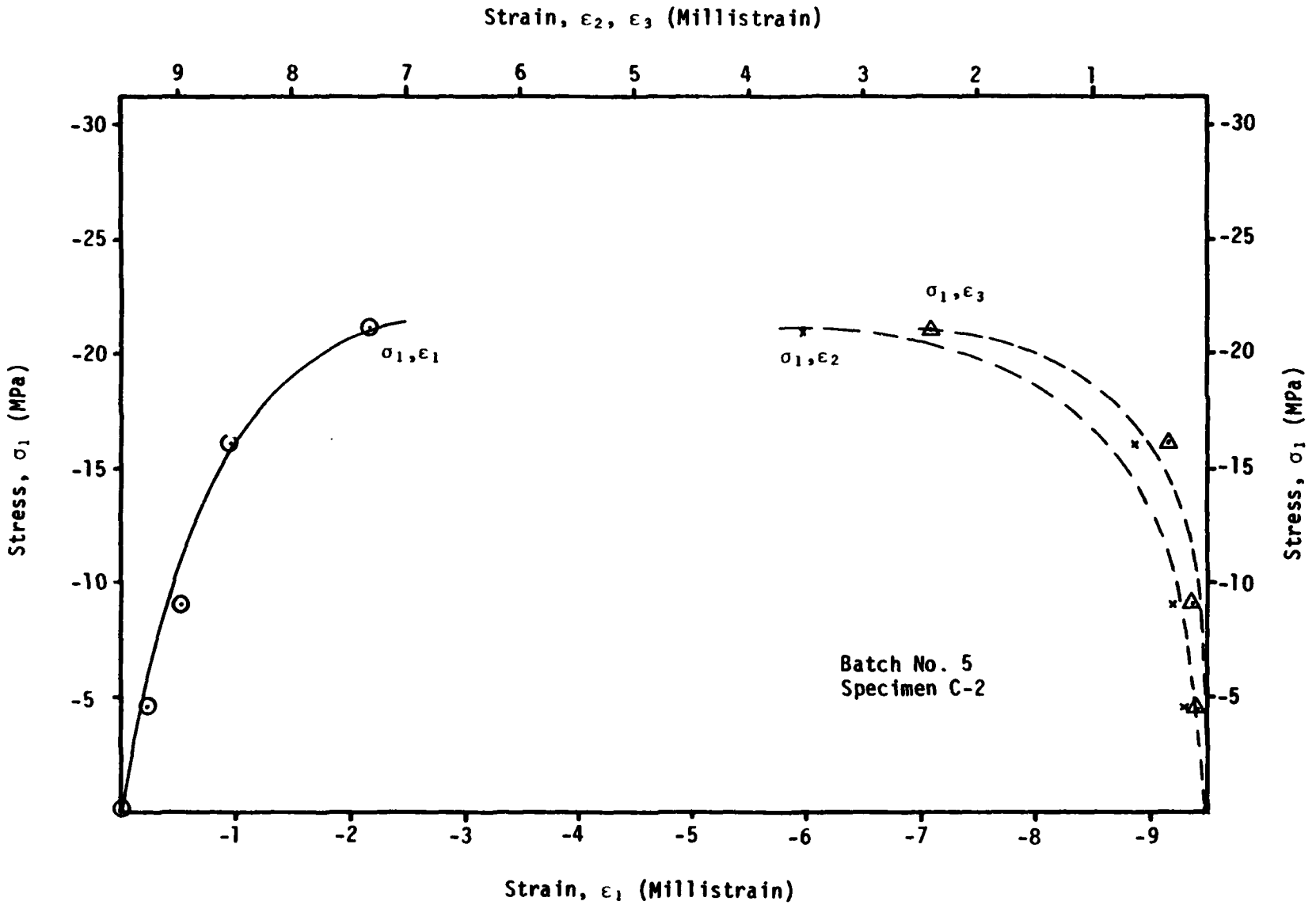

(a)

Figure A2. Load Path 2 of standard compression tests.

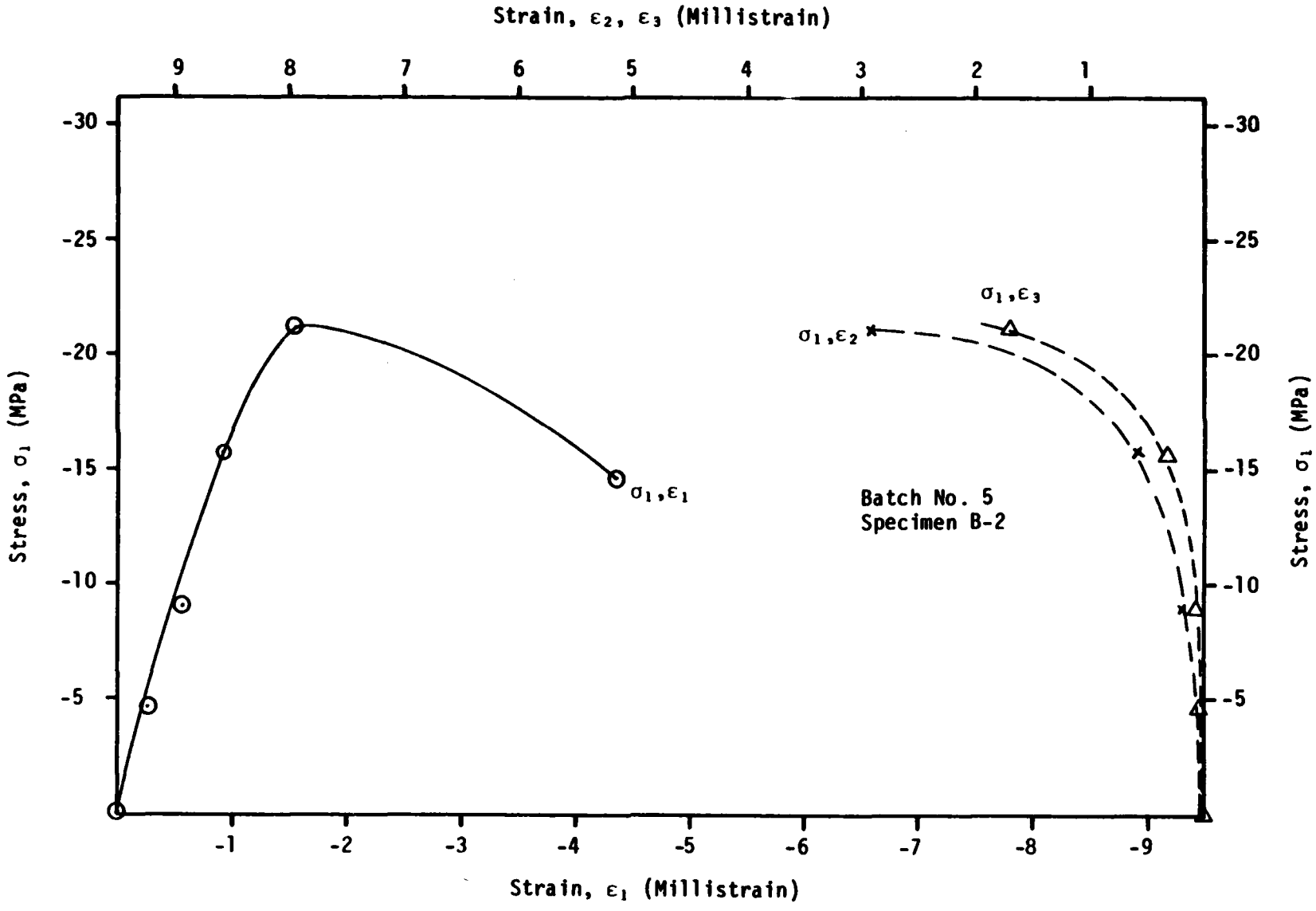

(b)

Figure A2. Continued.

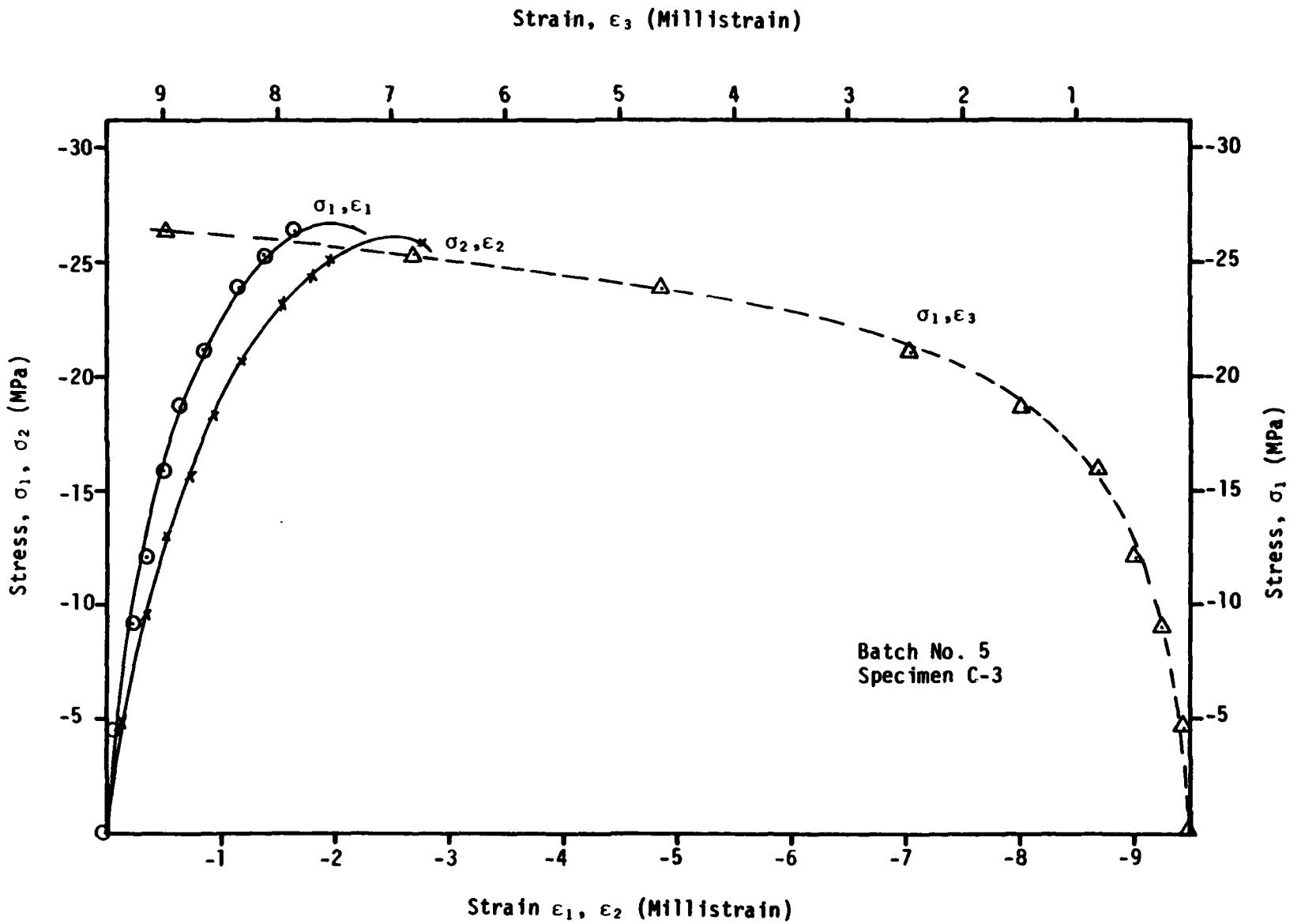

(a)

Figure A3. Load Path 3 of standard compression tests.

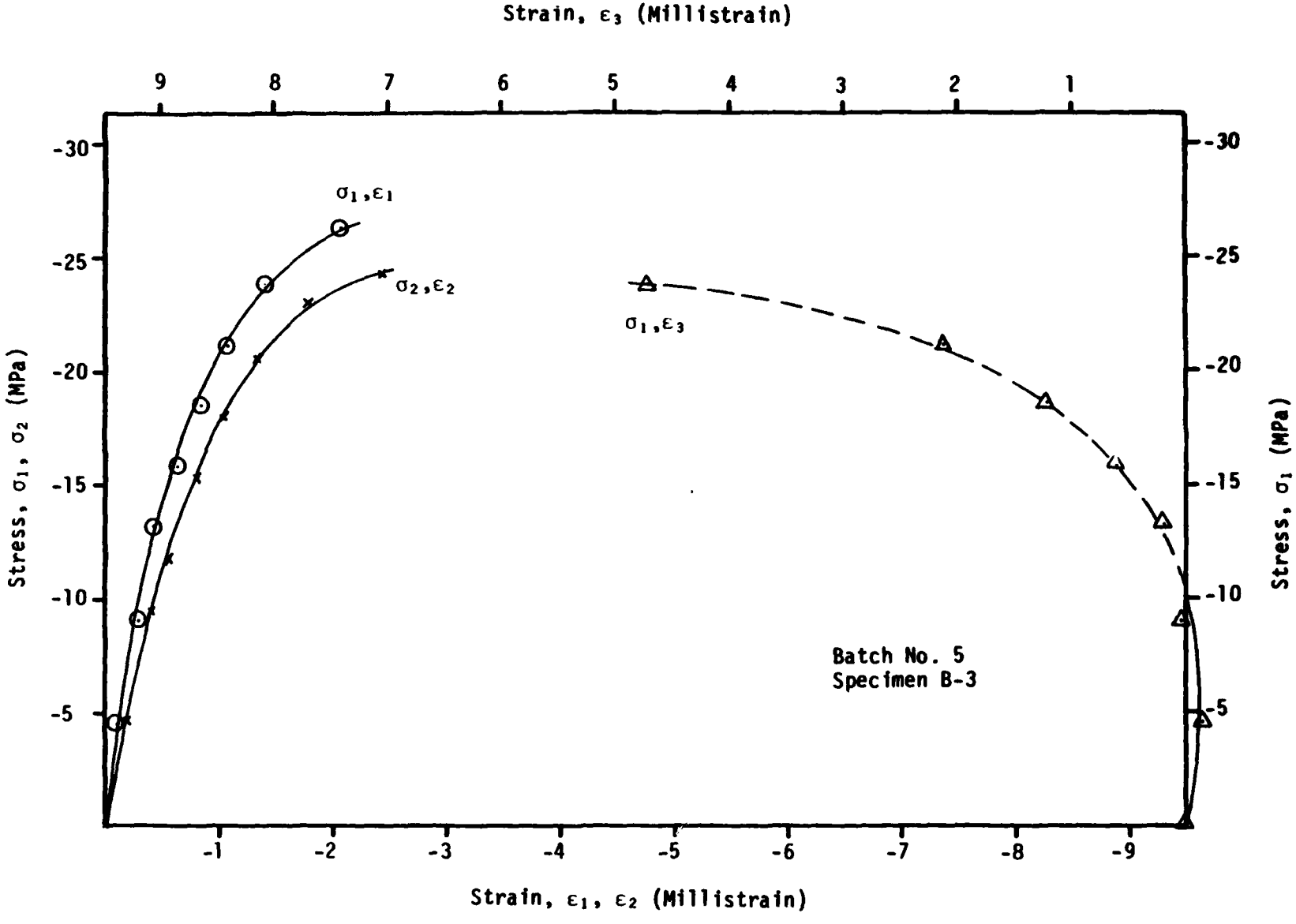

(b)

Figure A3. Continued.

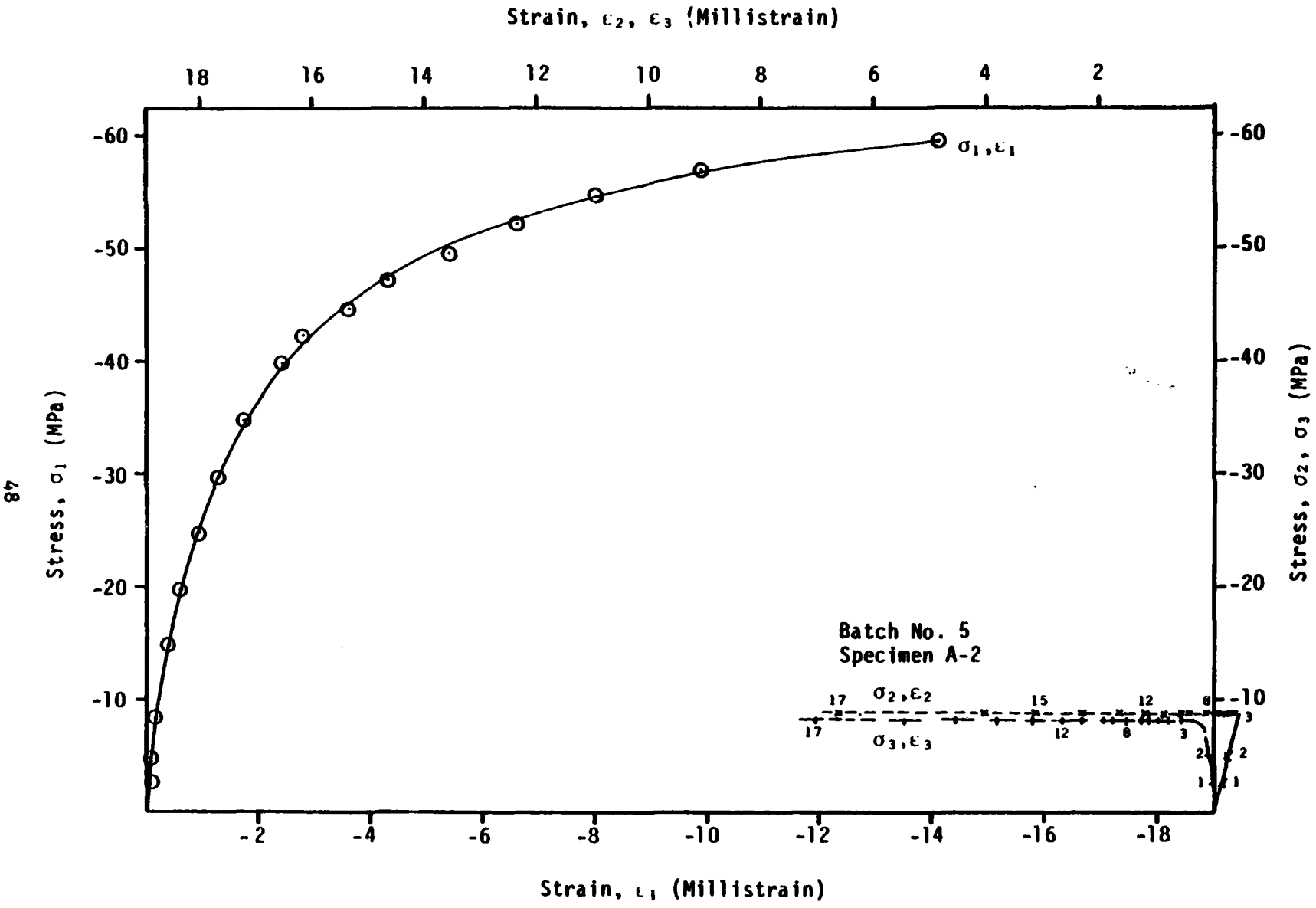

(a)

Figure A4. Load Path 4 of standard compression tests.

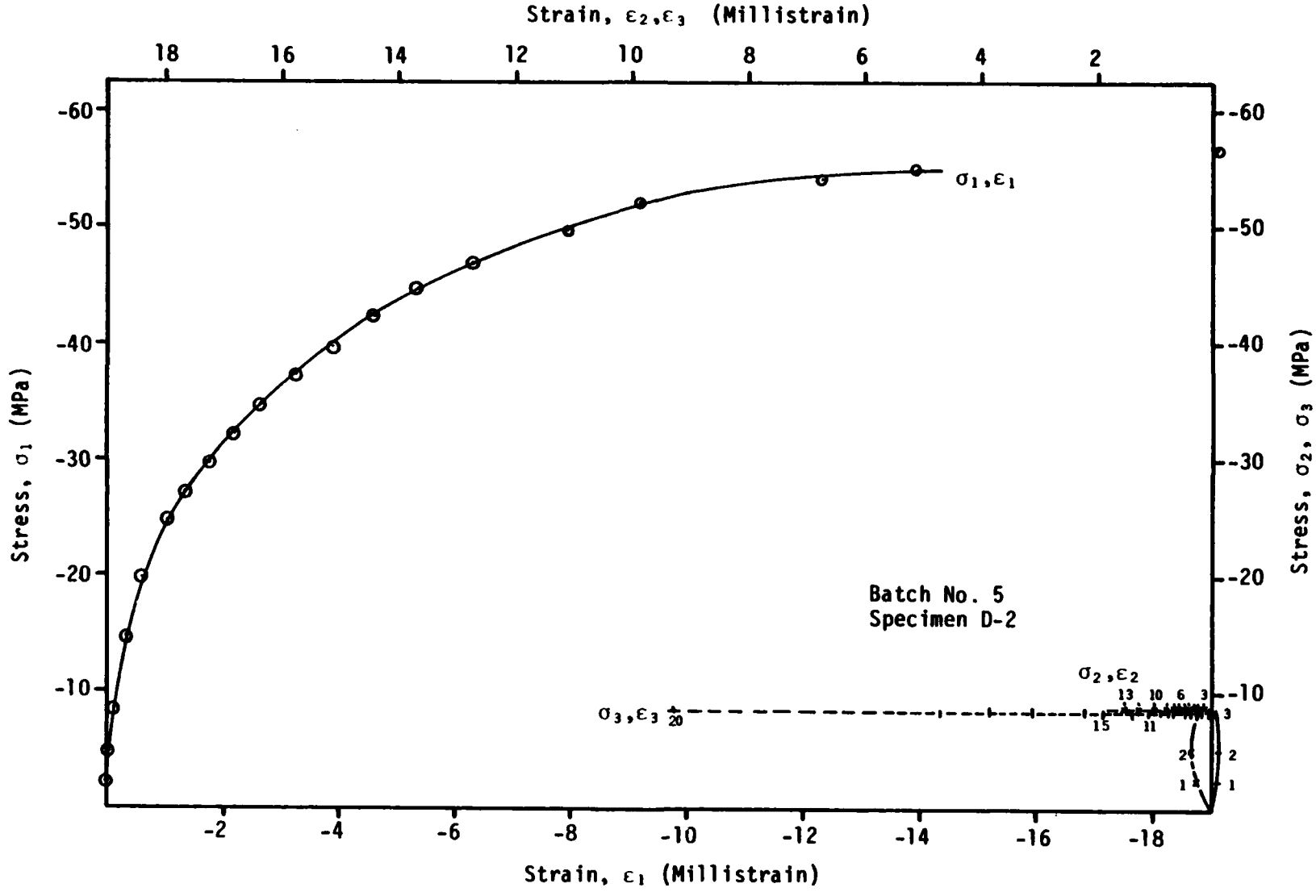

(b)

Figure A4. Continued.

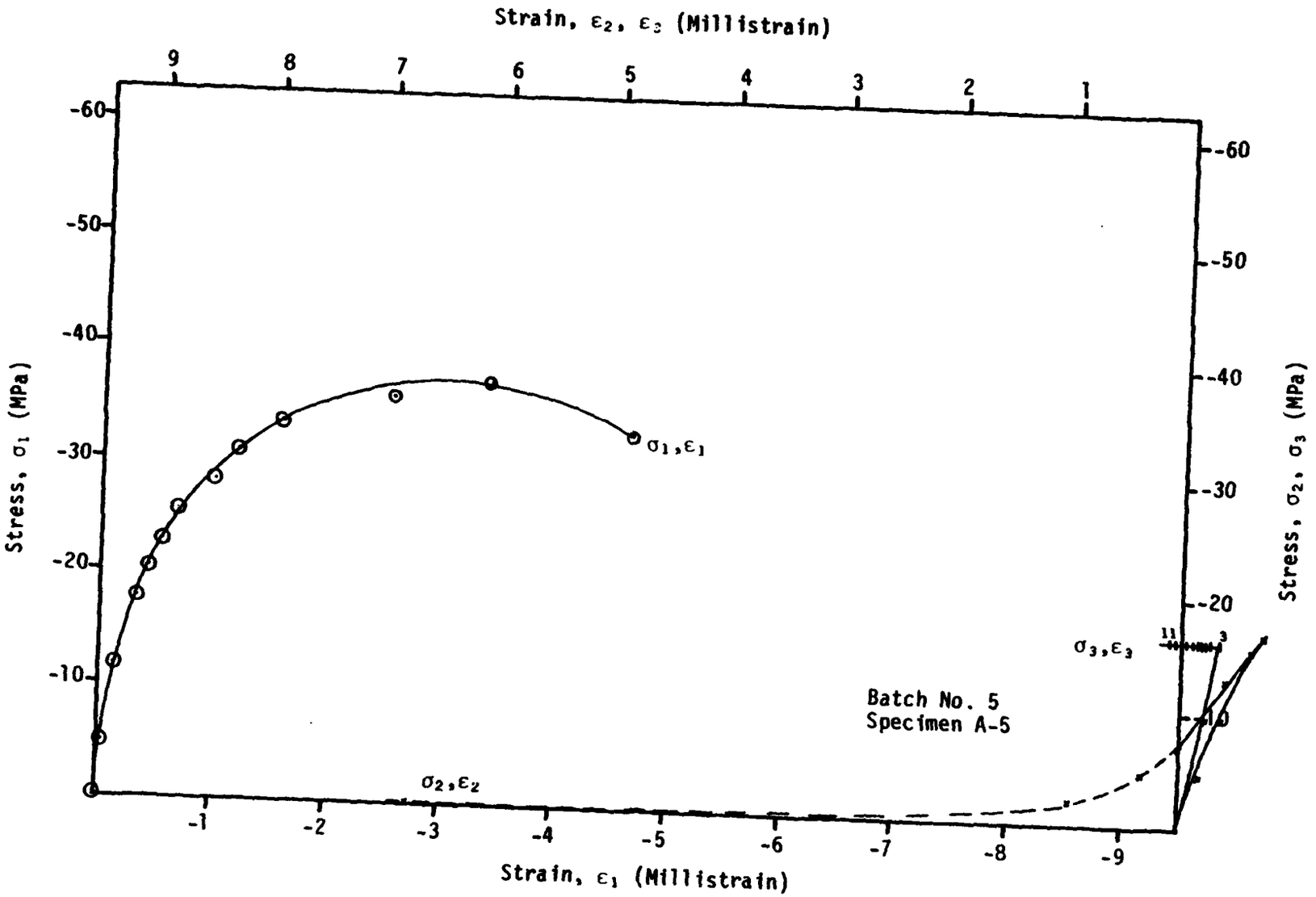

(a)

Figure A5. Load Path 5 of standard compression tests.

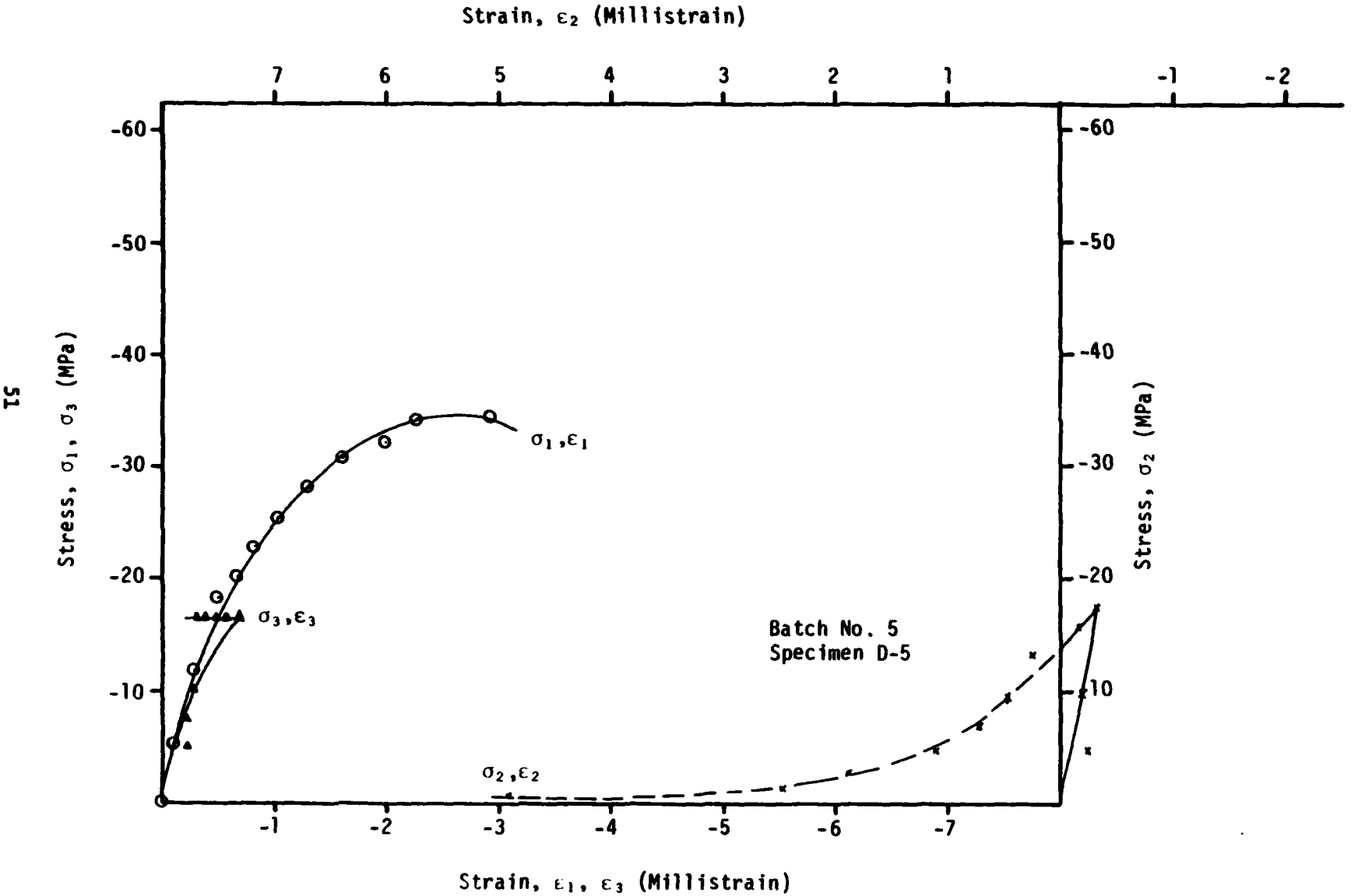

(b)

Figure A5. Continued.

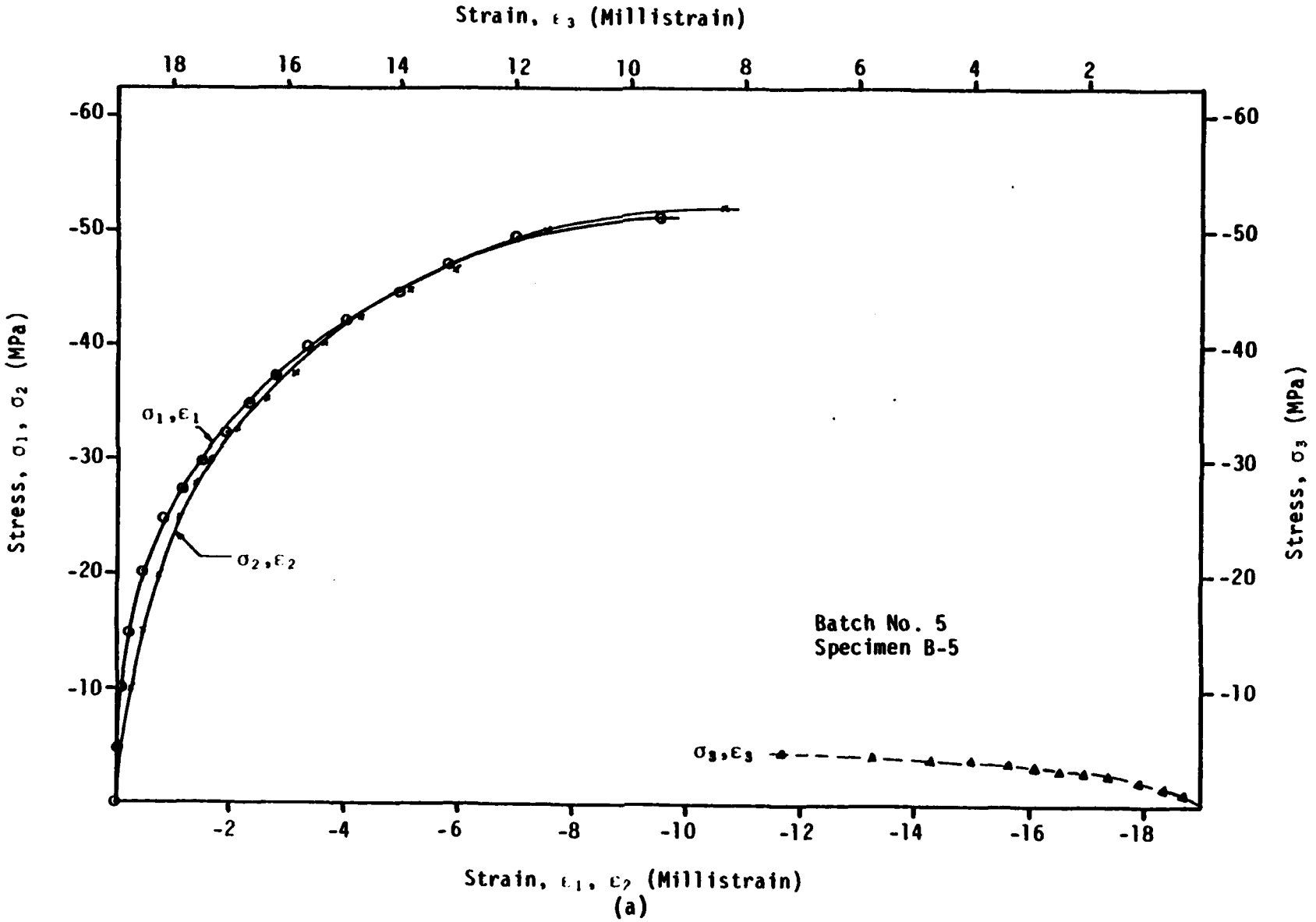

(a)

Figure A6. Load Path 6 of standard compression tests.

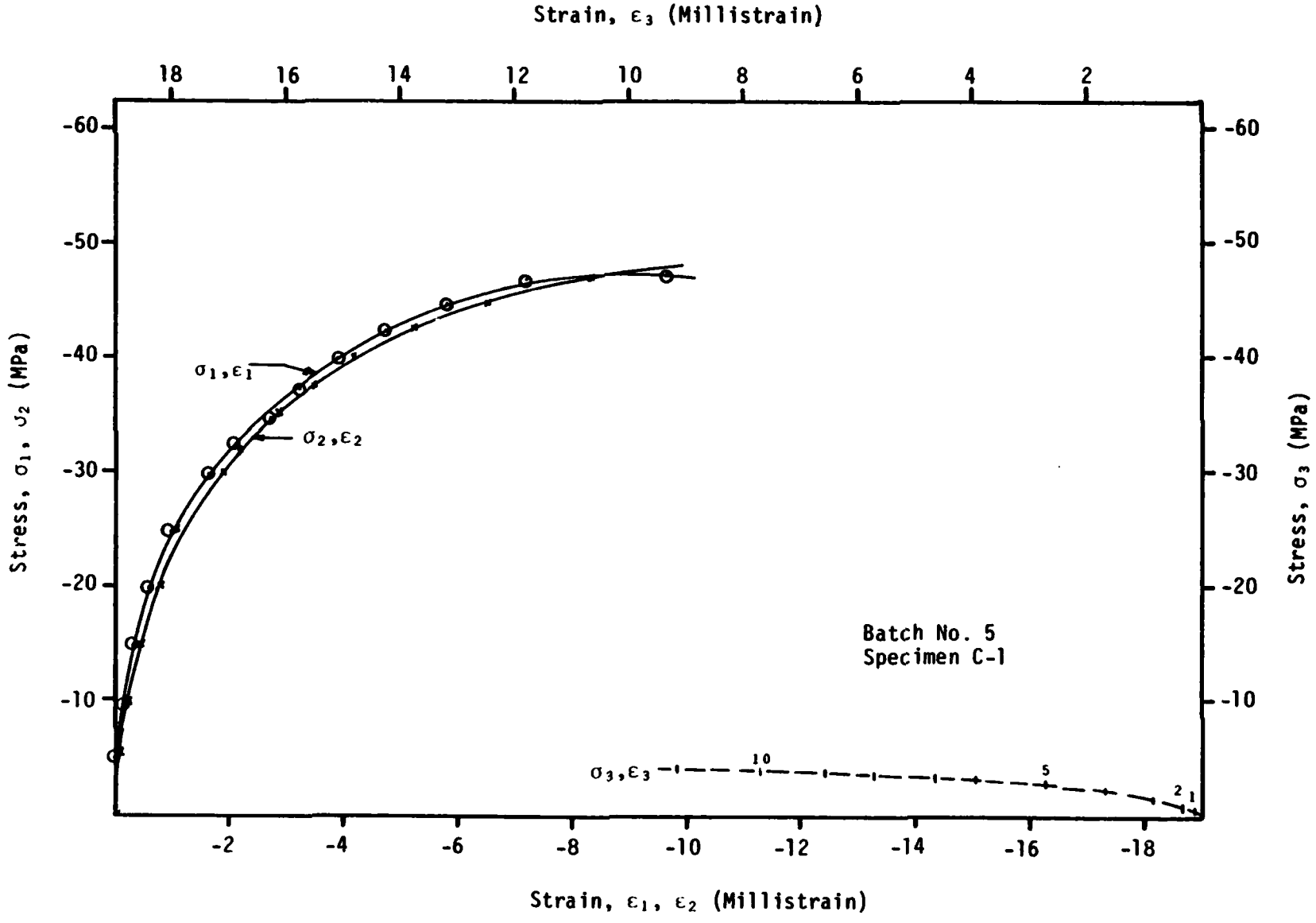

(b)

Figure A6. Continued.

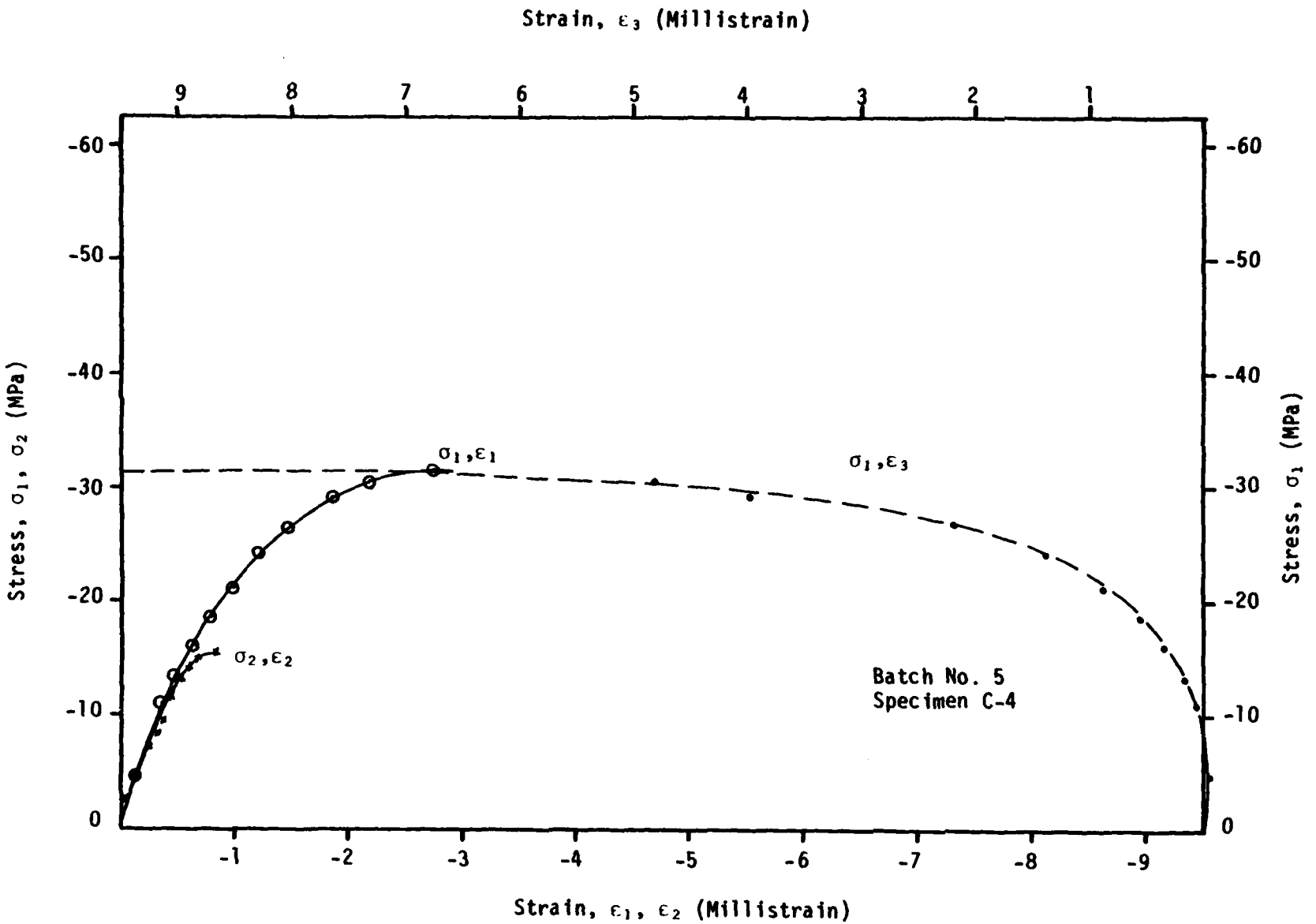

(a)

Figure A7. Load Path 7 of standard compression tests.

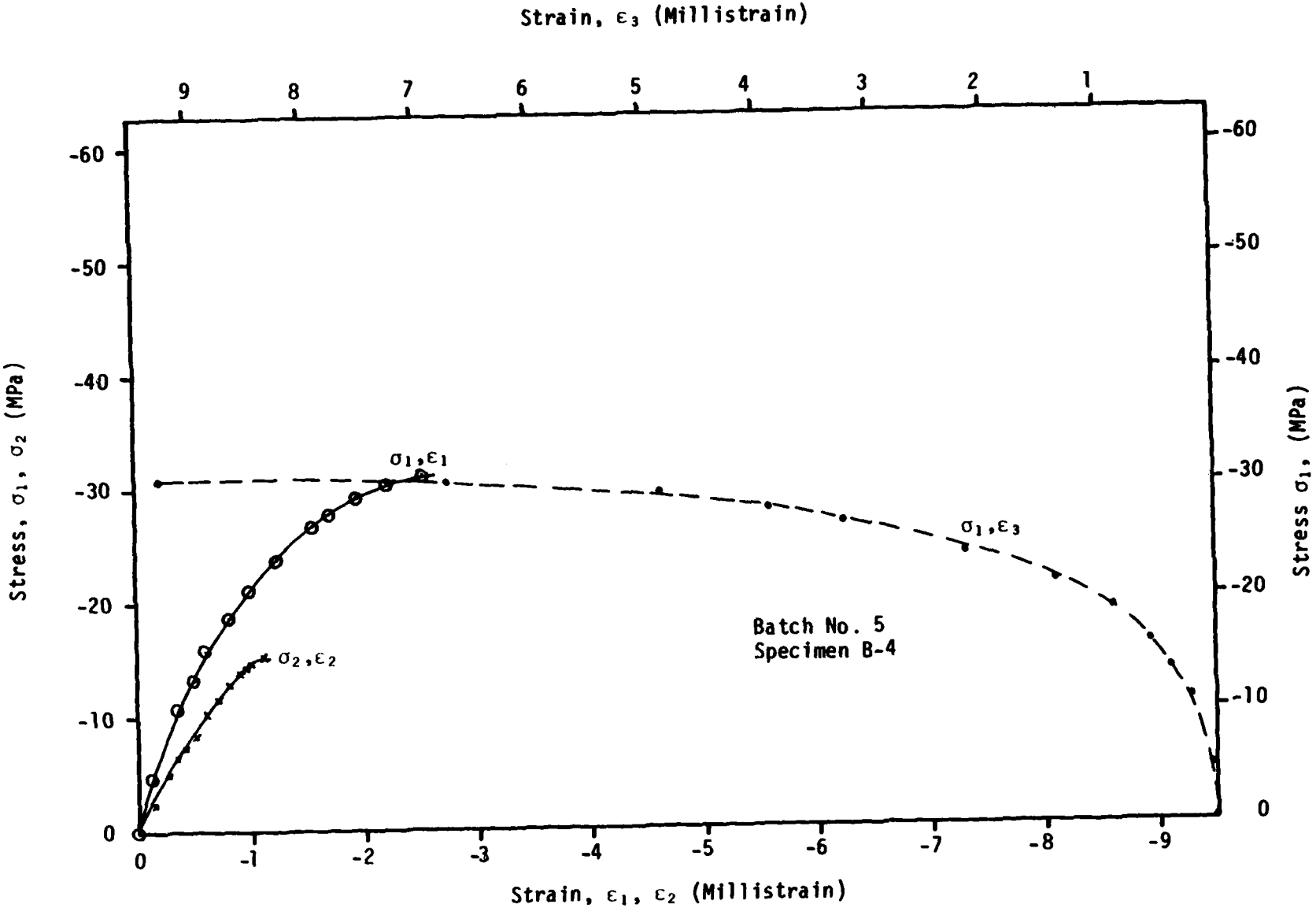

(b)

Figure A7. Continued.

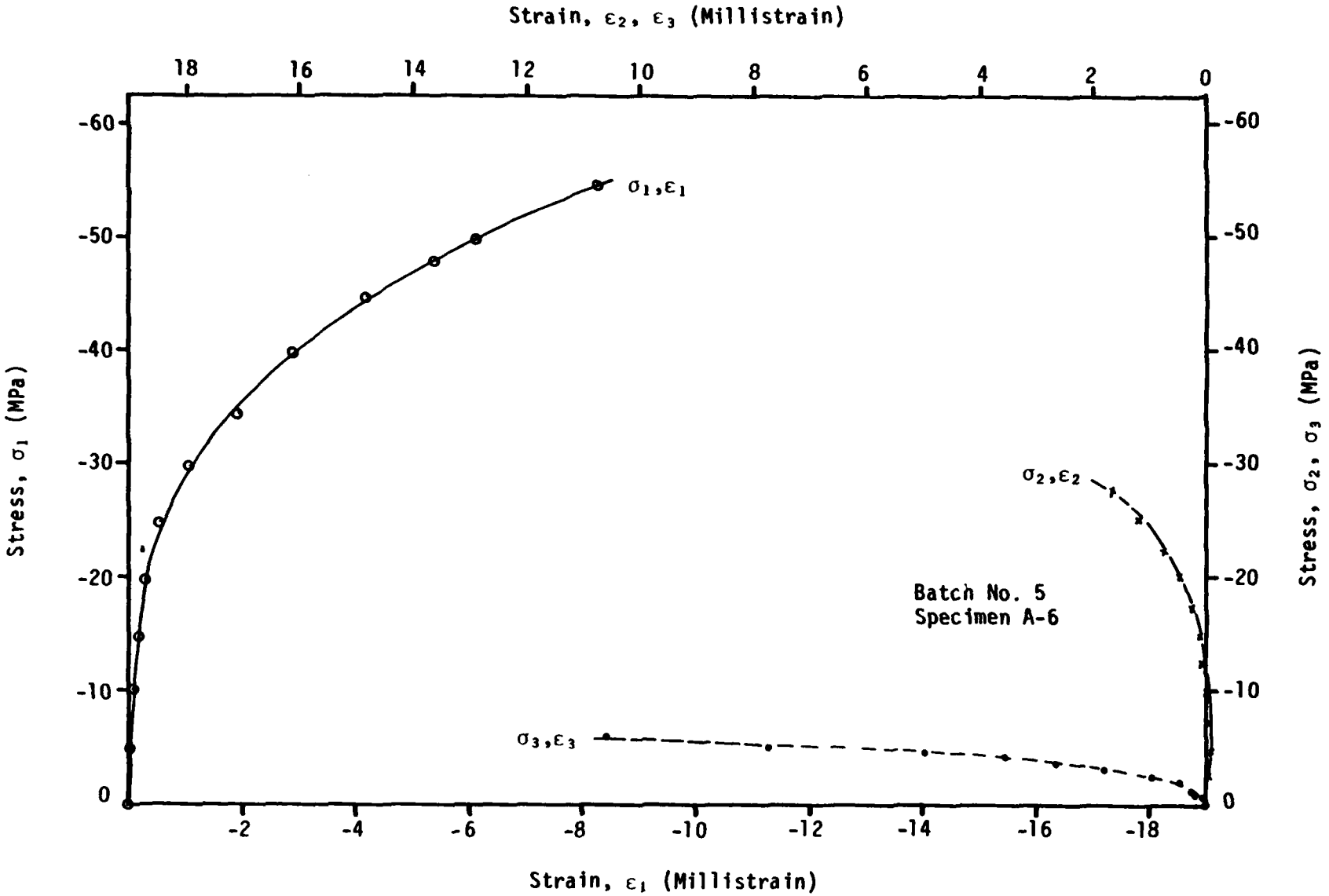

(a)

Figure A8. Load Path 8 of standard compression tests.

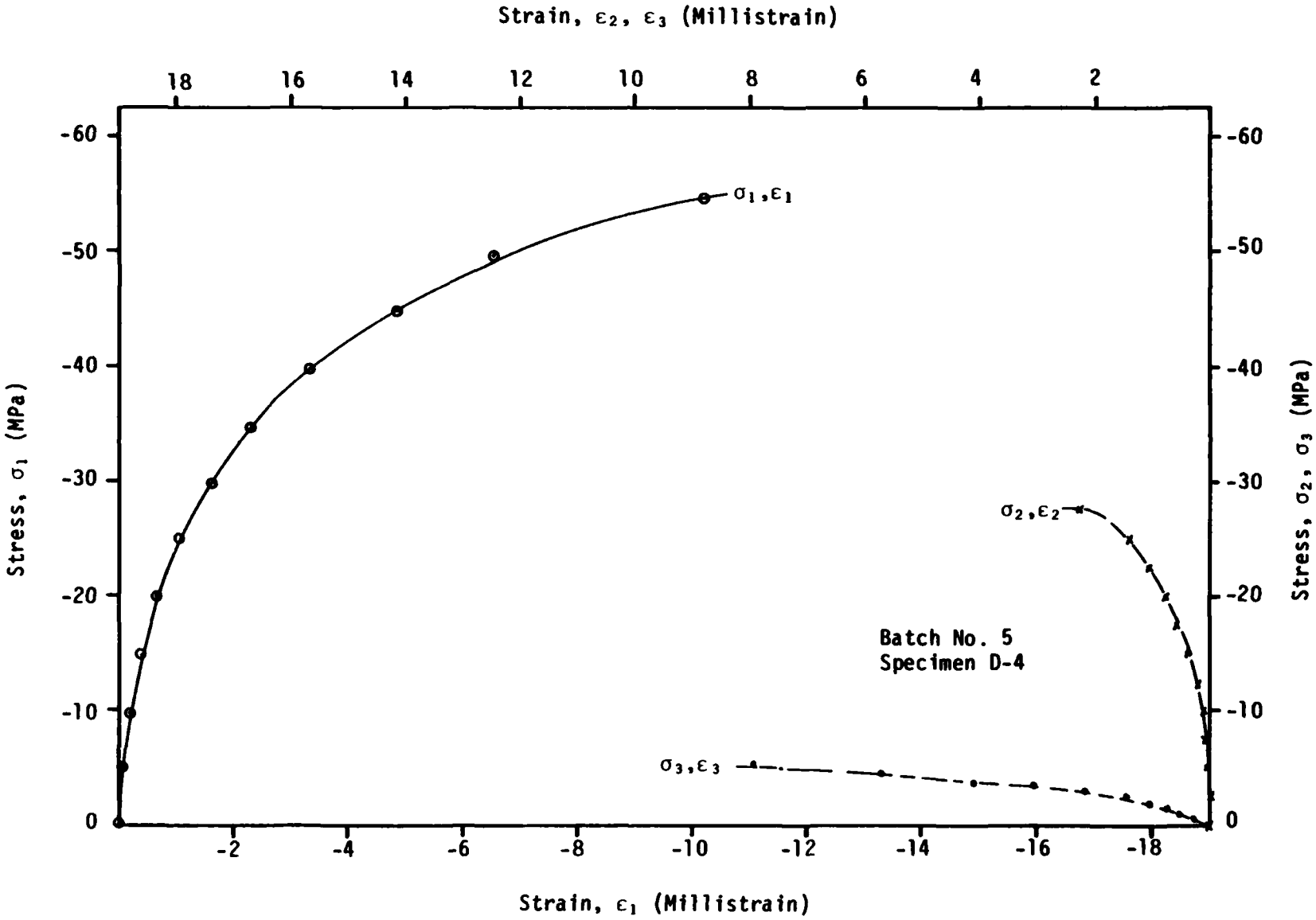

(b)

Figure A8. Continued.

APPENDIX B

STRESS-STRAIN PLOTS FOR NONSTANDARD COMPRESSION TESTS

All stress and strain data are plotted for the various paths described as nonstandard compression tests. Figure B-1 shows the results for the first path, Figure B-2 for the second path, etc. Since three experiments were performed for each path, each figure has part (a), (b) and (c) which differentiates these three sets of data.

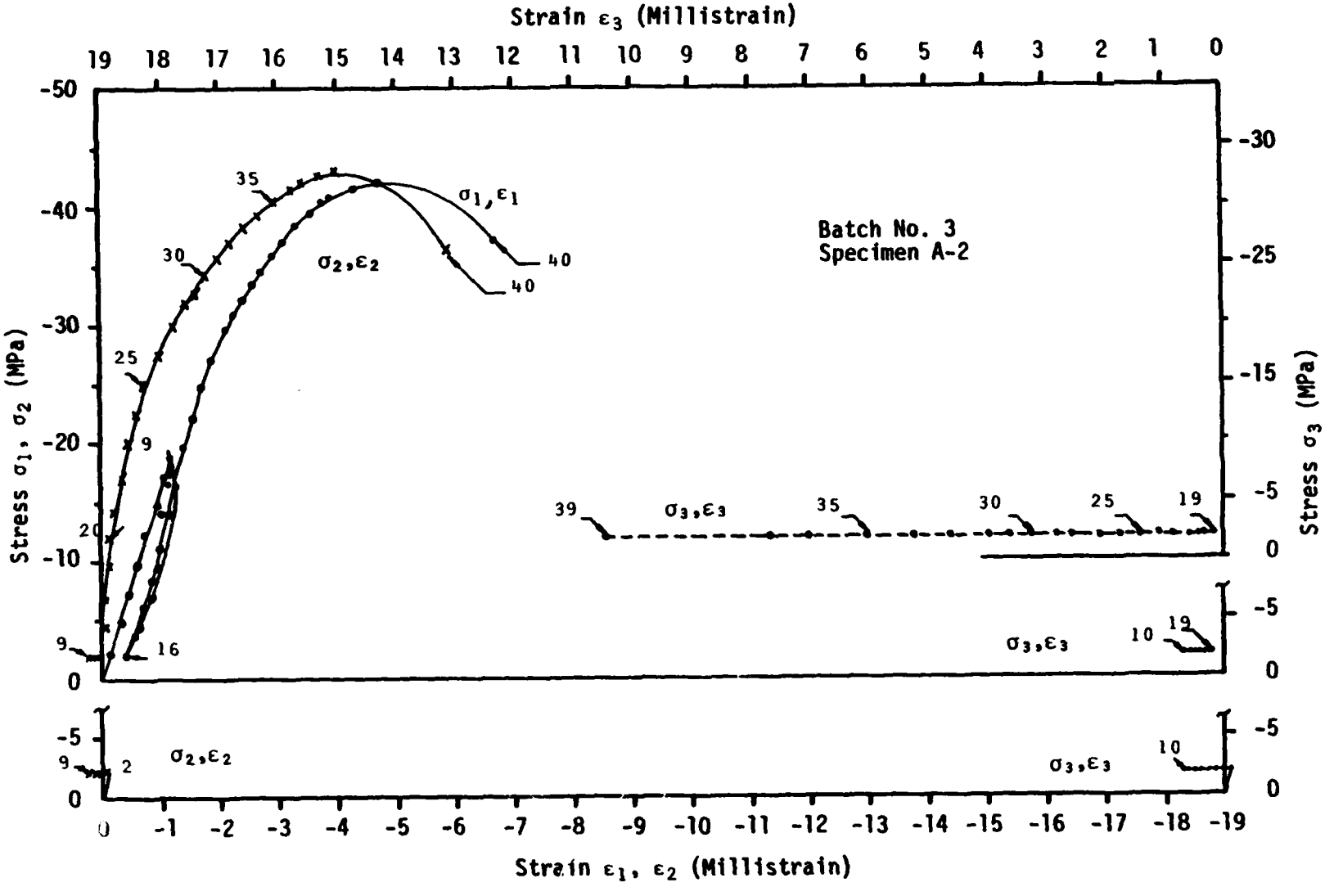

(a)

Figure B1. Load path 1 of nonstandard compression tests.

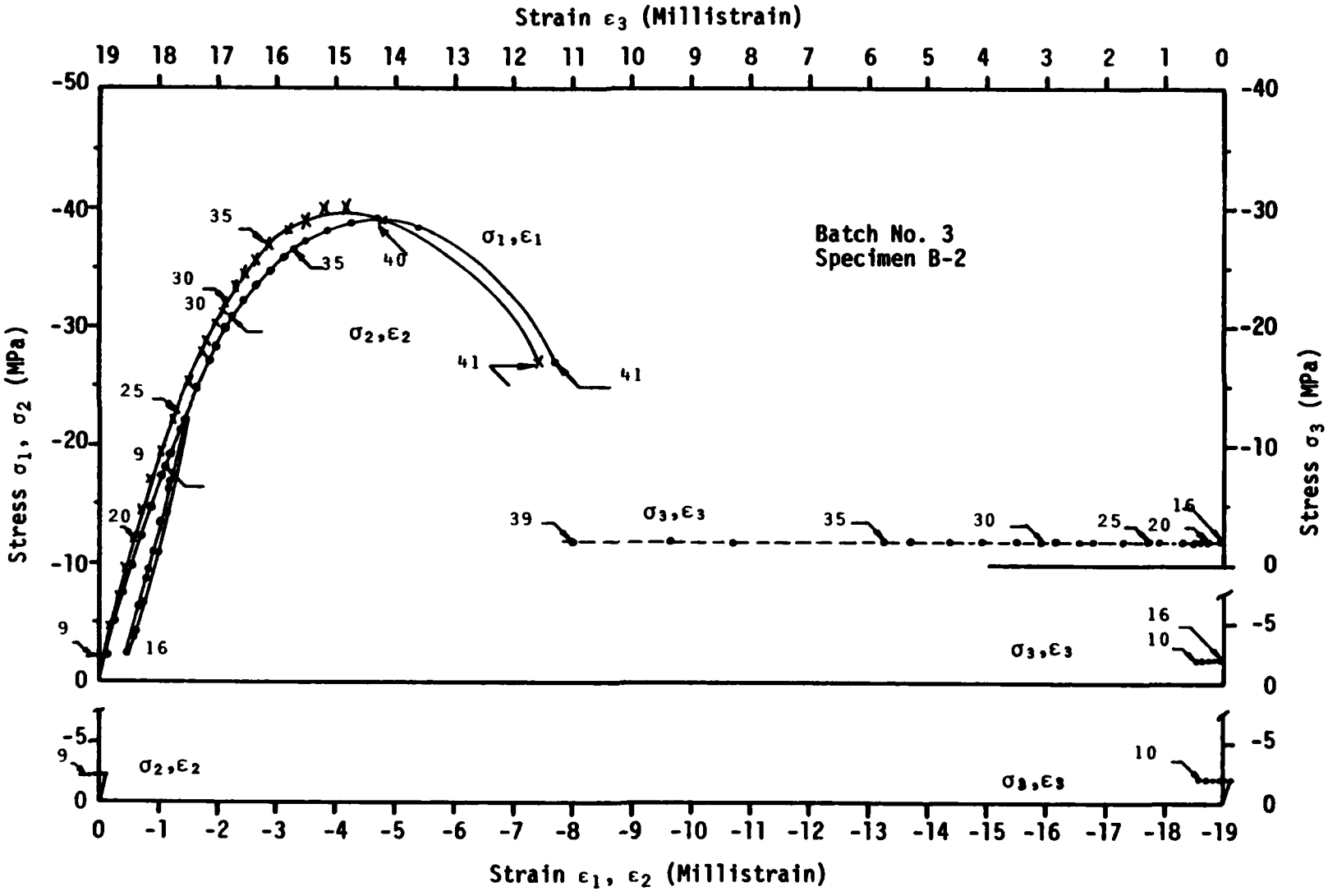

(b)

Figure B1. Continued.

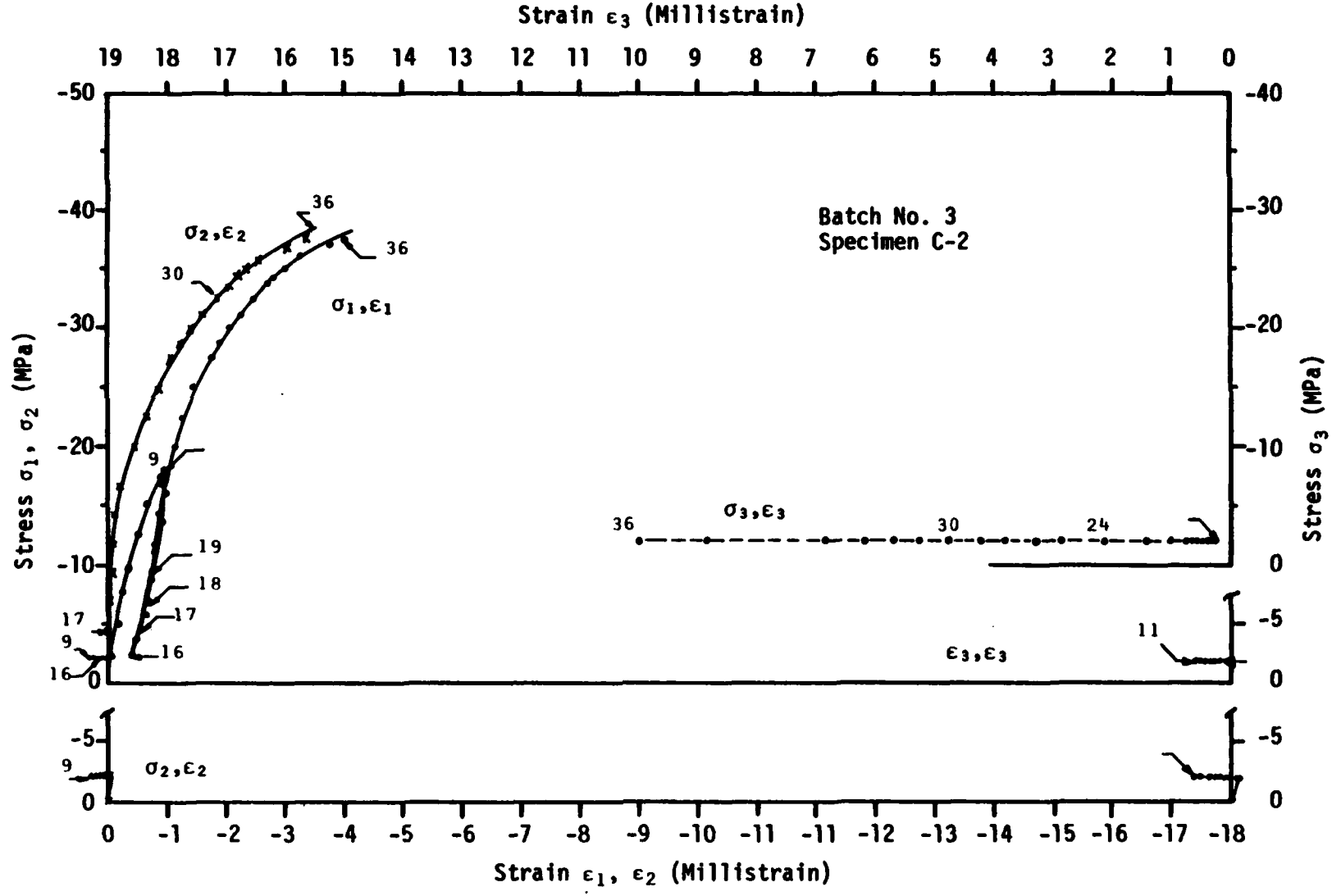

(c)

Figure B1. Continued.

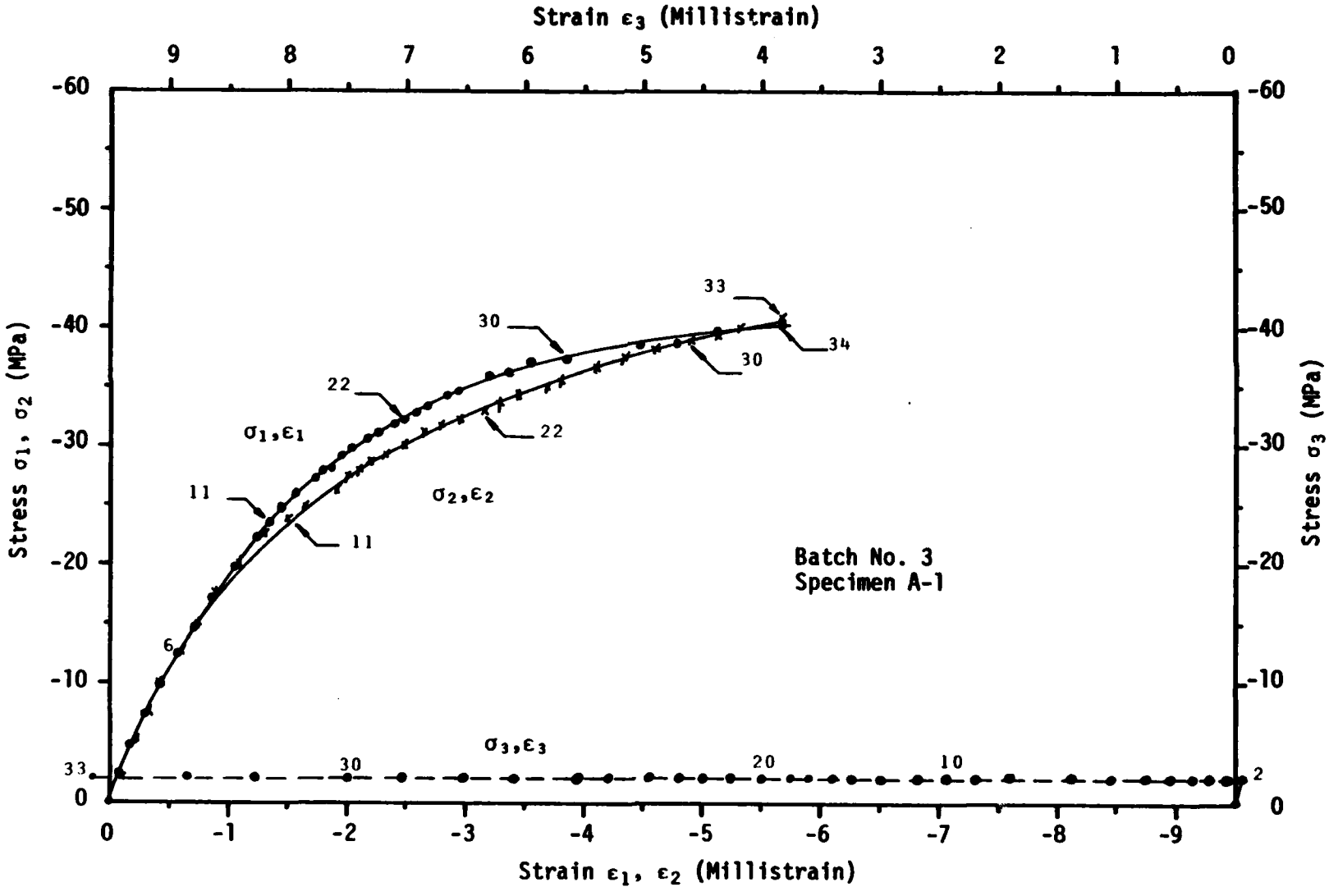

(a)

Figure B2. Load path 2 of nonstandard compression tests.

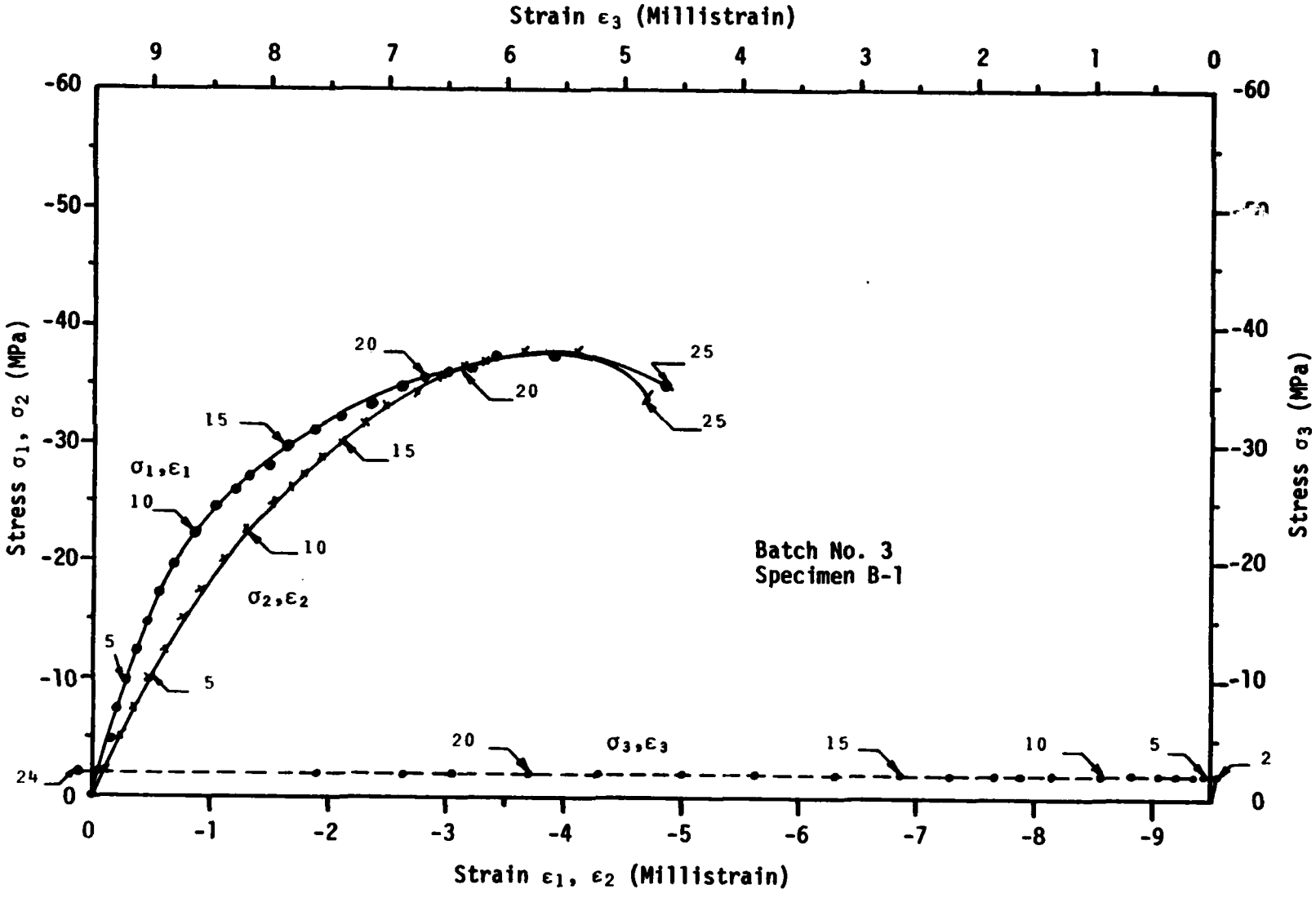

(b)

Figure B2. Continued.

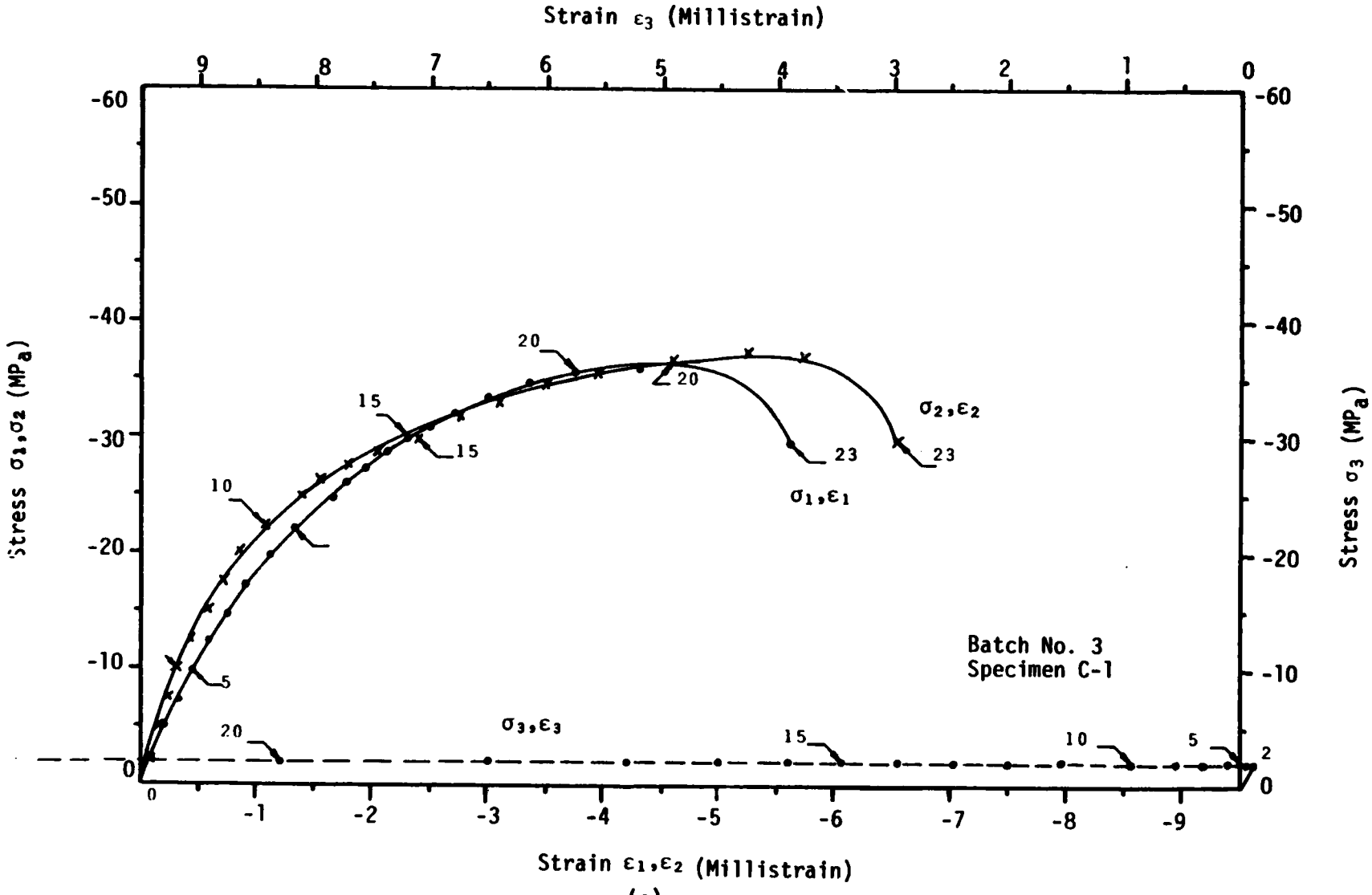

(c)

Figure B2. Continued.

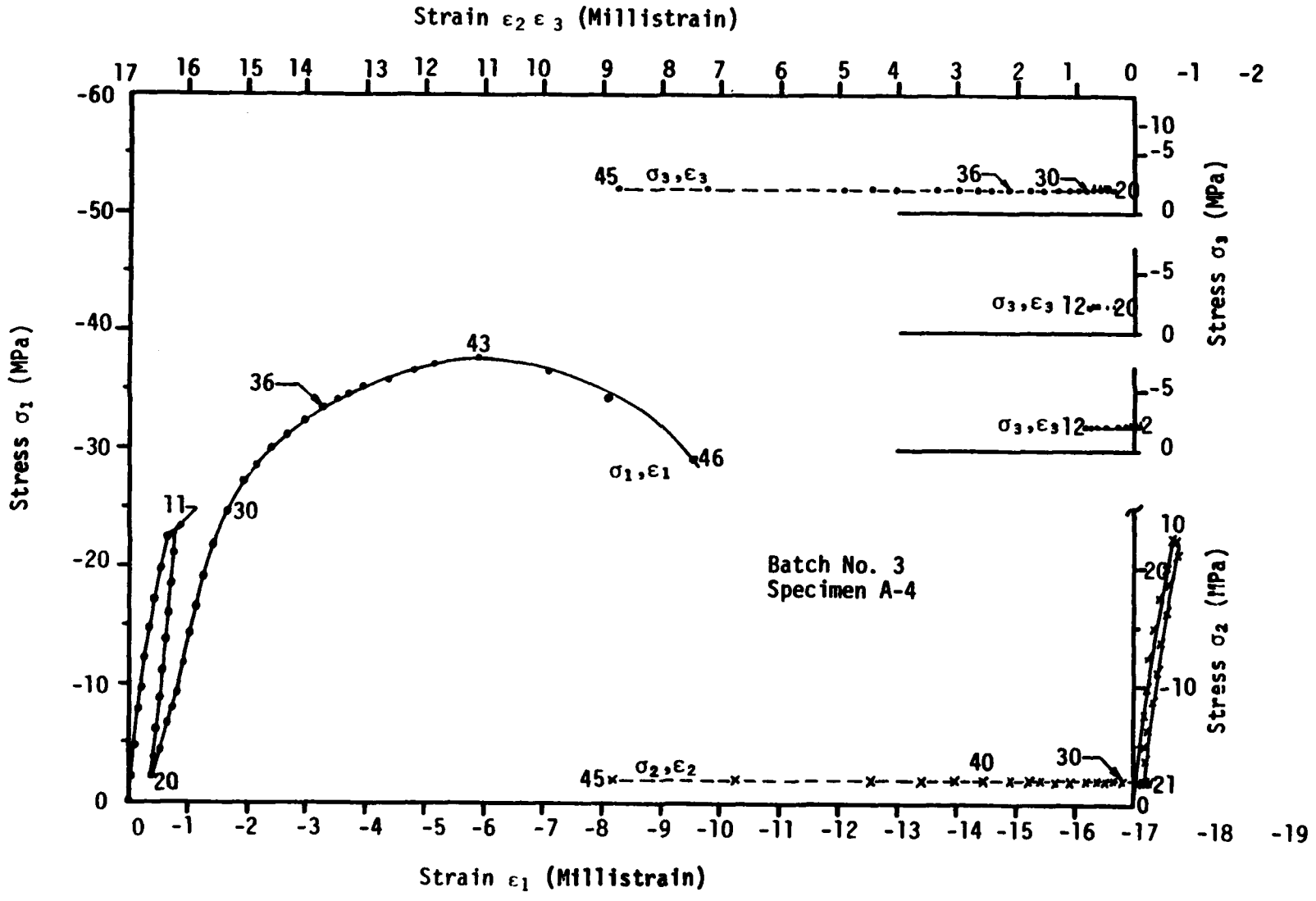

(a)

Figure B3. Load path 3 of nonstandard compression paths.

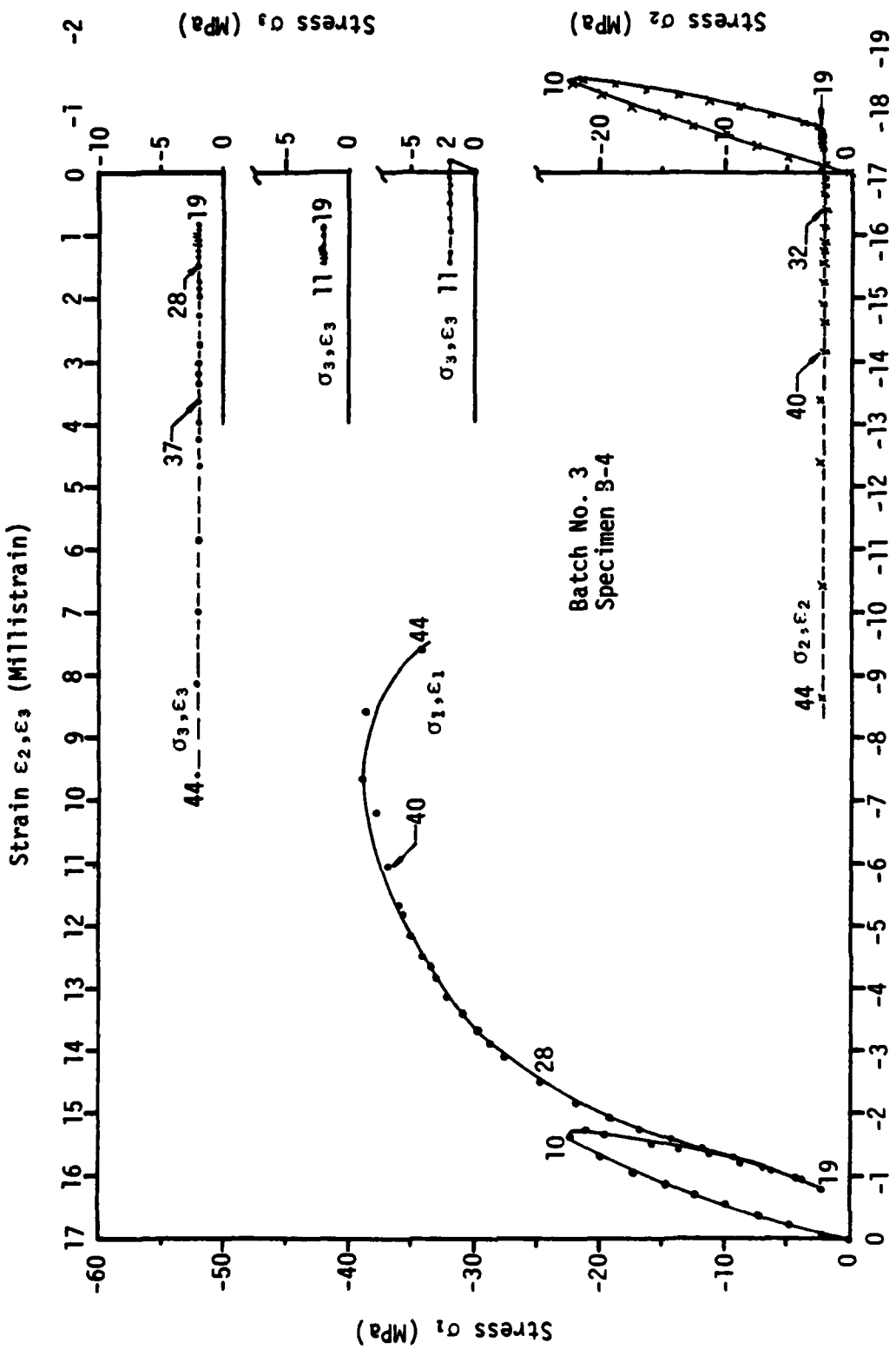

(b)

Figure B3. Continued.

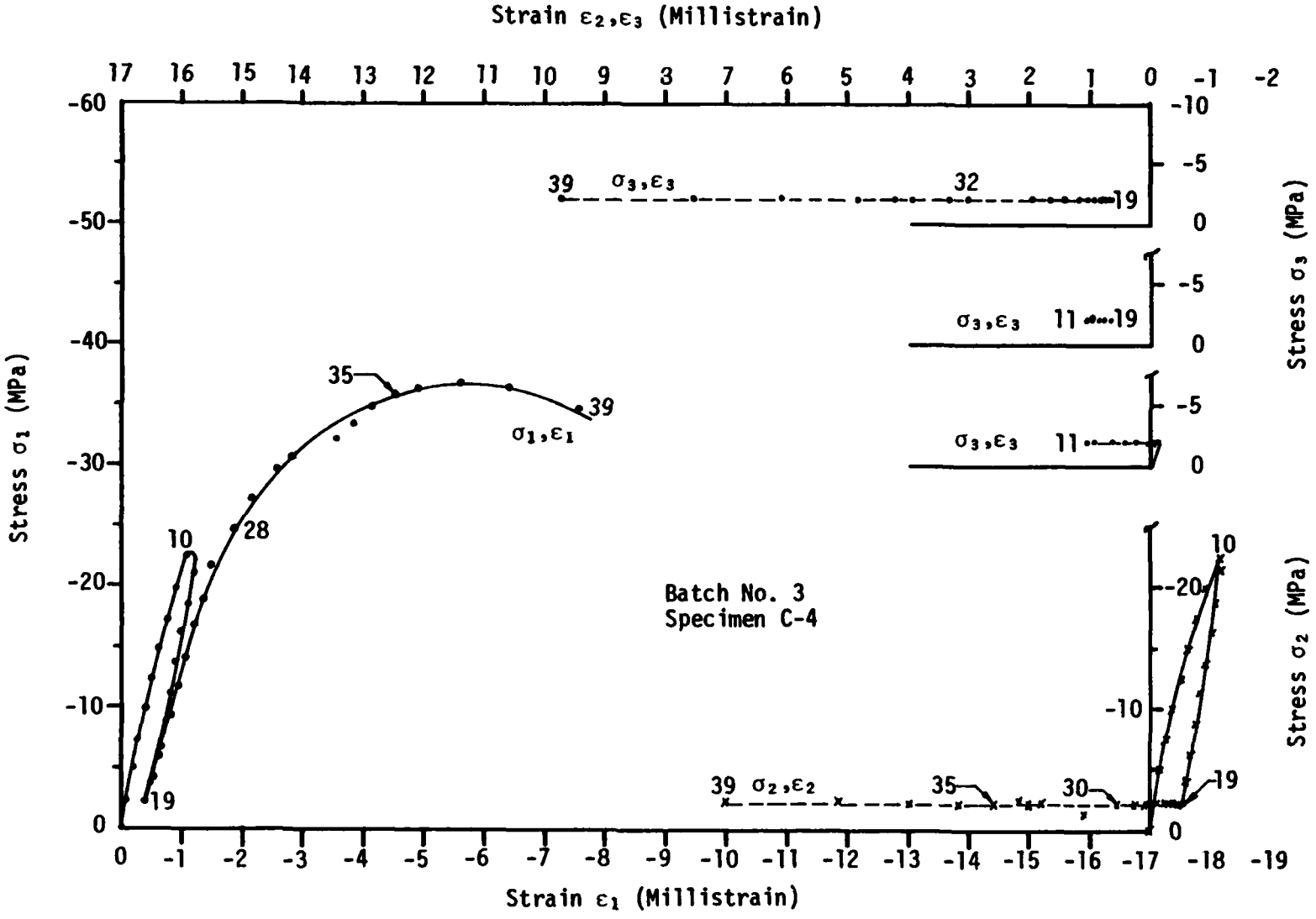

(c)

Figure B3. Continued

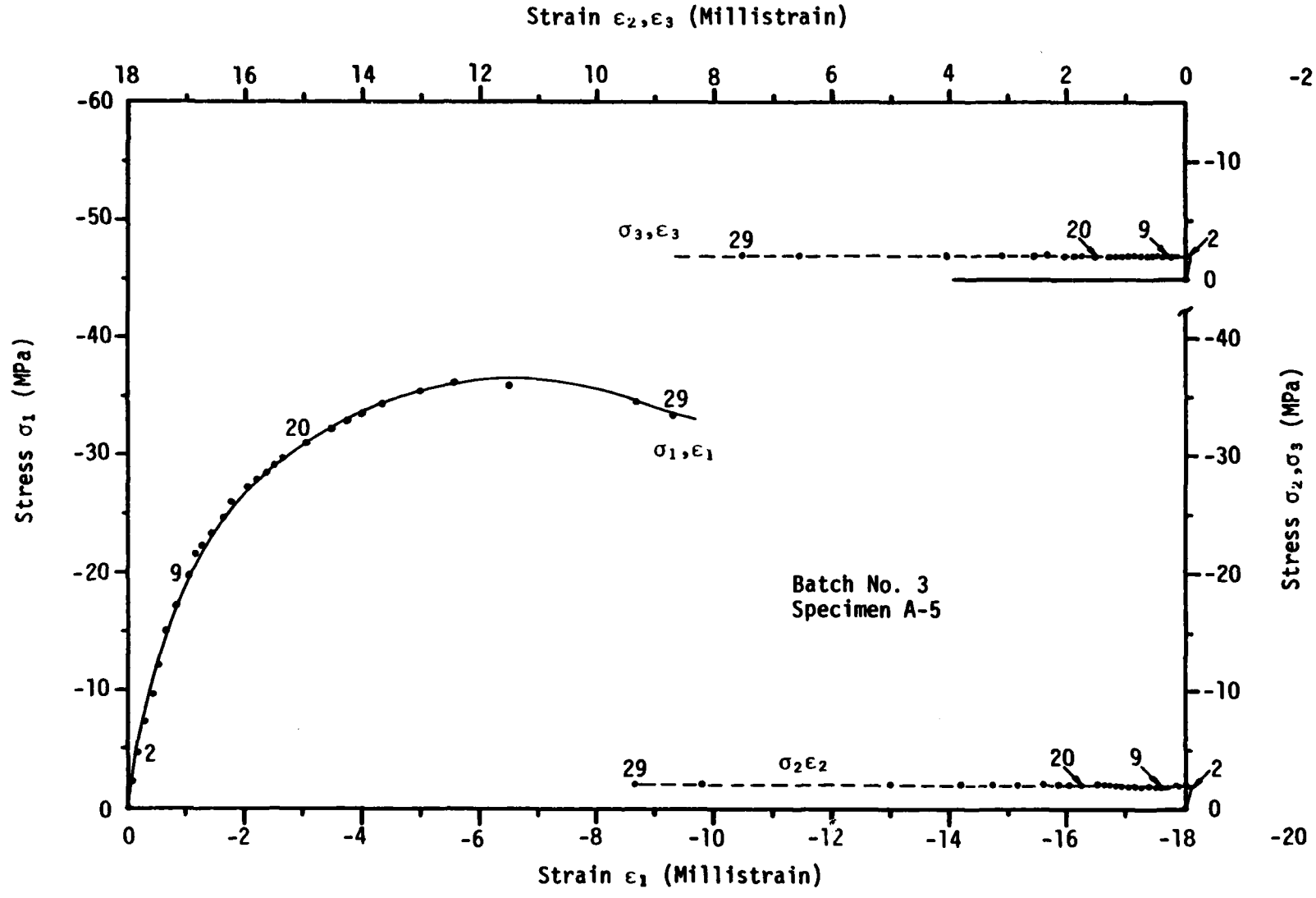

(a)

Figure B4. Load path 4 for nonstandard compression tests.

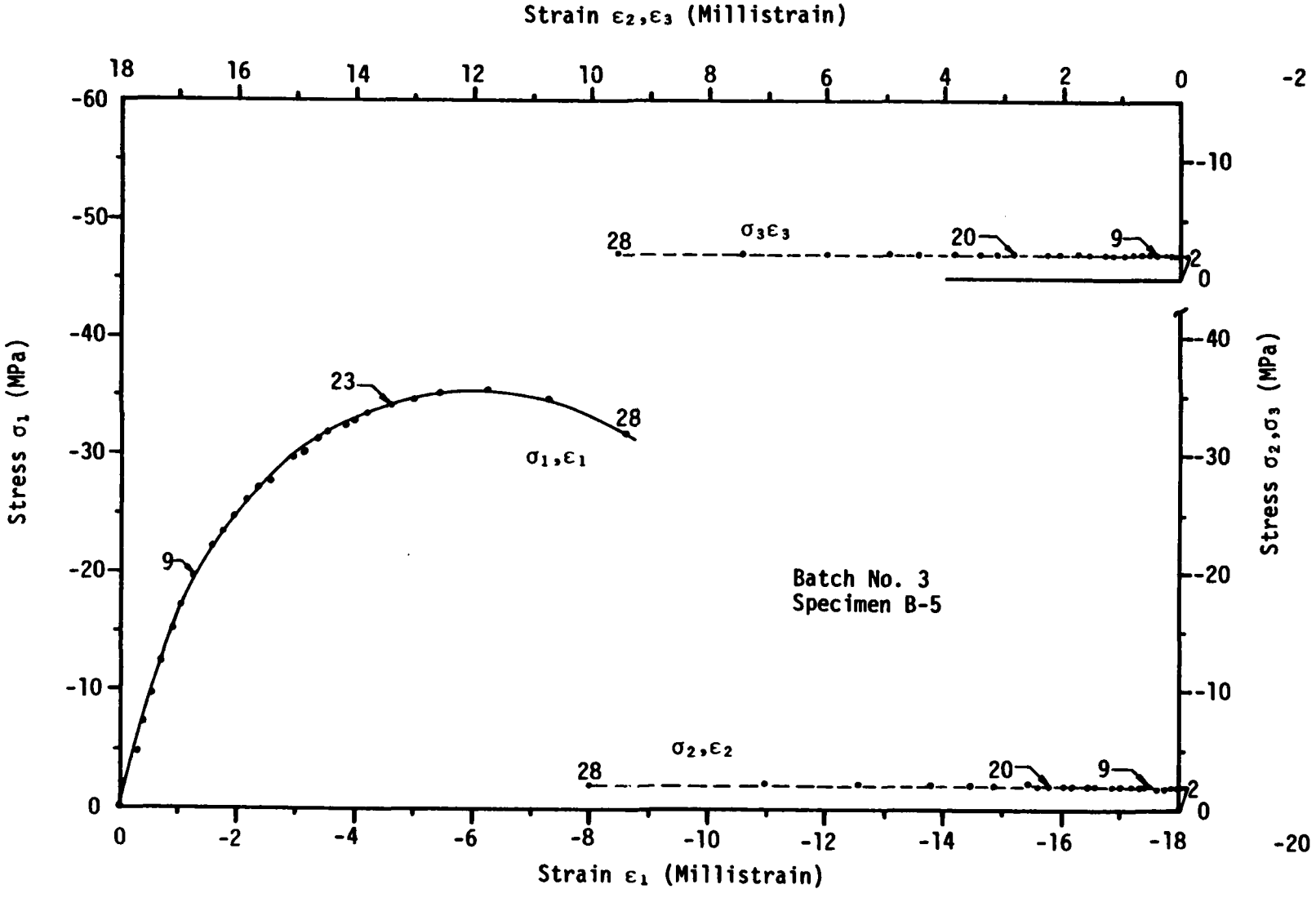

(b)

Figure B4. Continued.

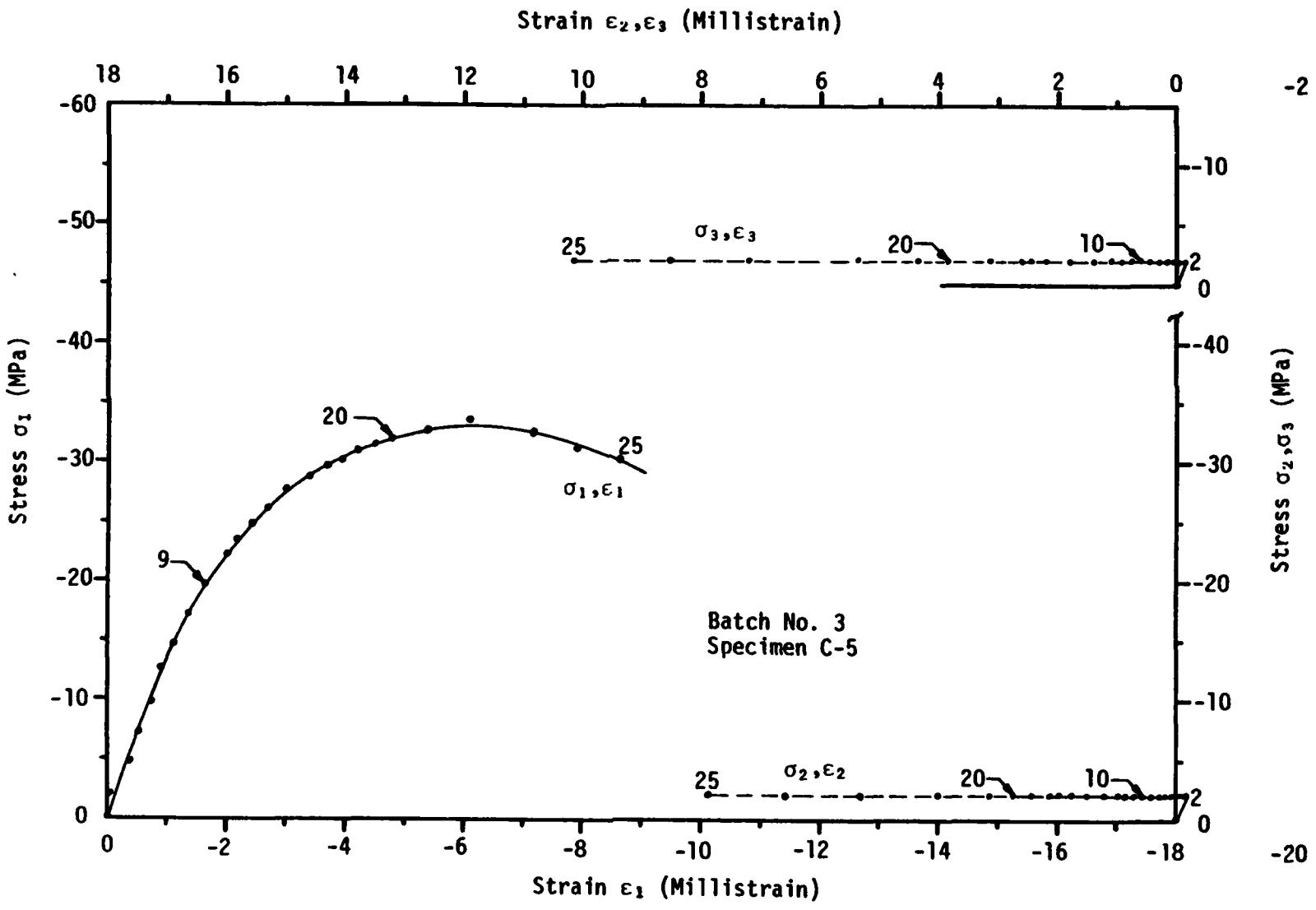

(c)

Figure D4. Continued.

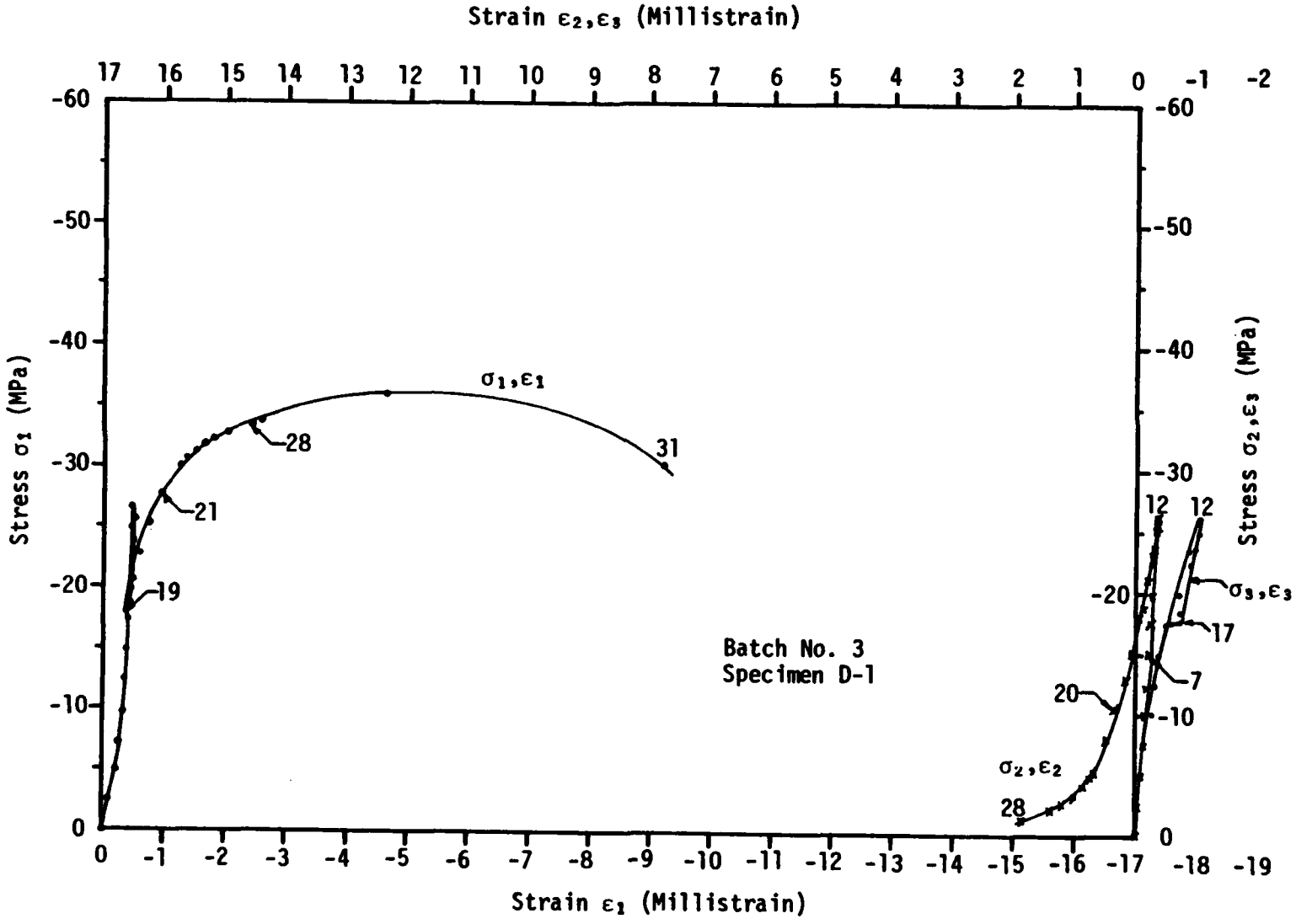

(a)

Figure B5. Load path 5 of nonstandard compression tests.

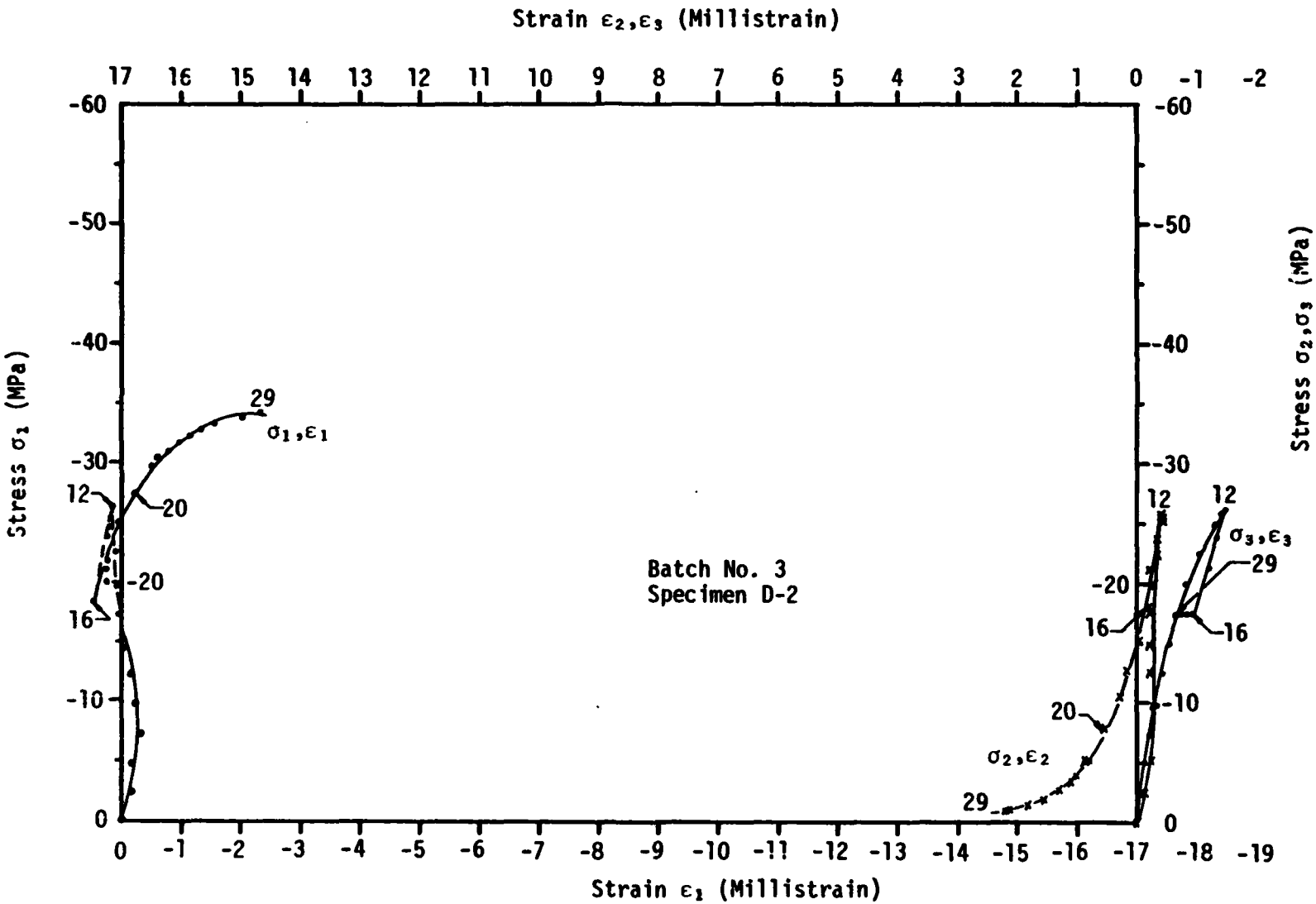

(b)

Figure 35. Continued.

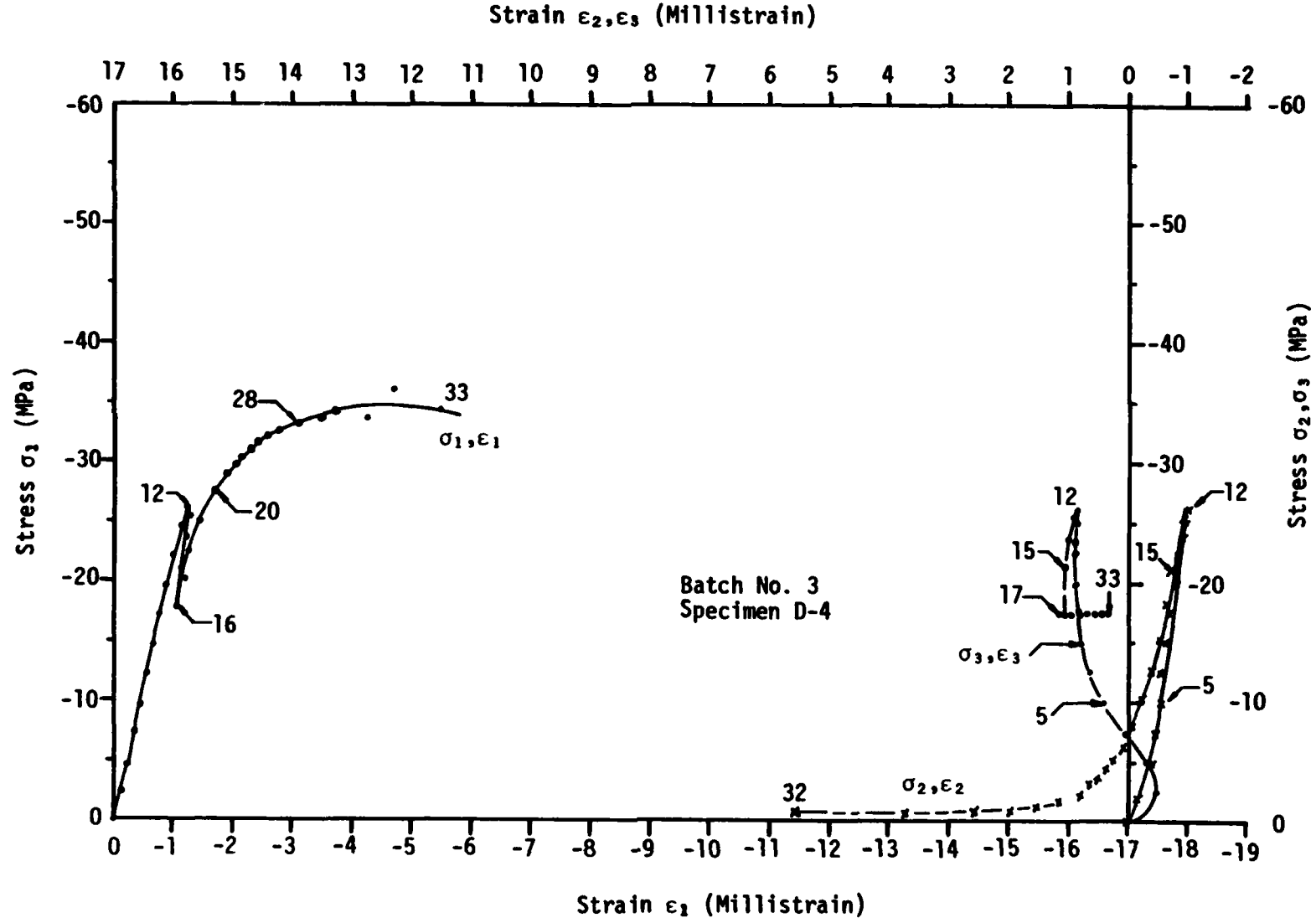

(c)

Figure B5. Continued.

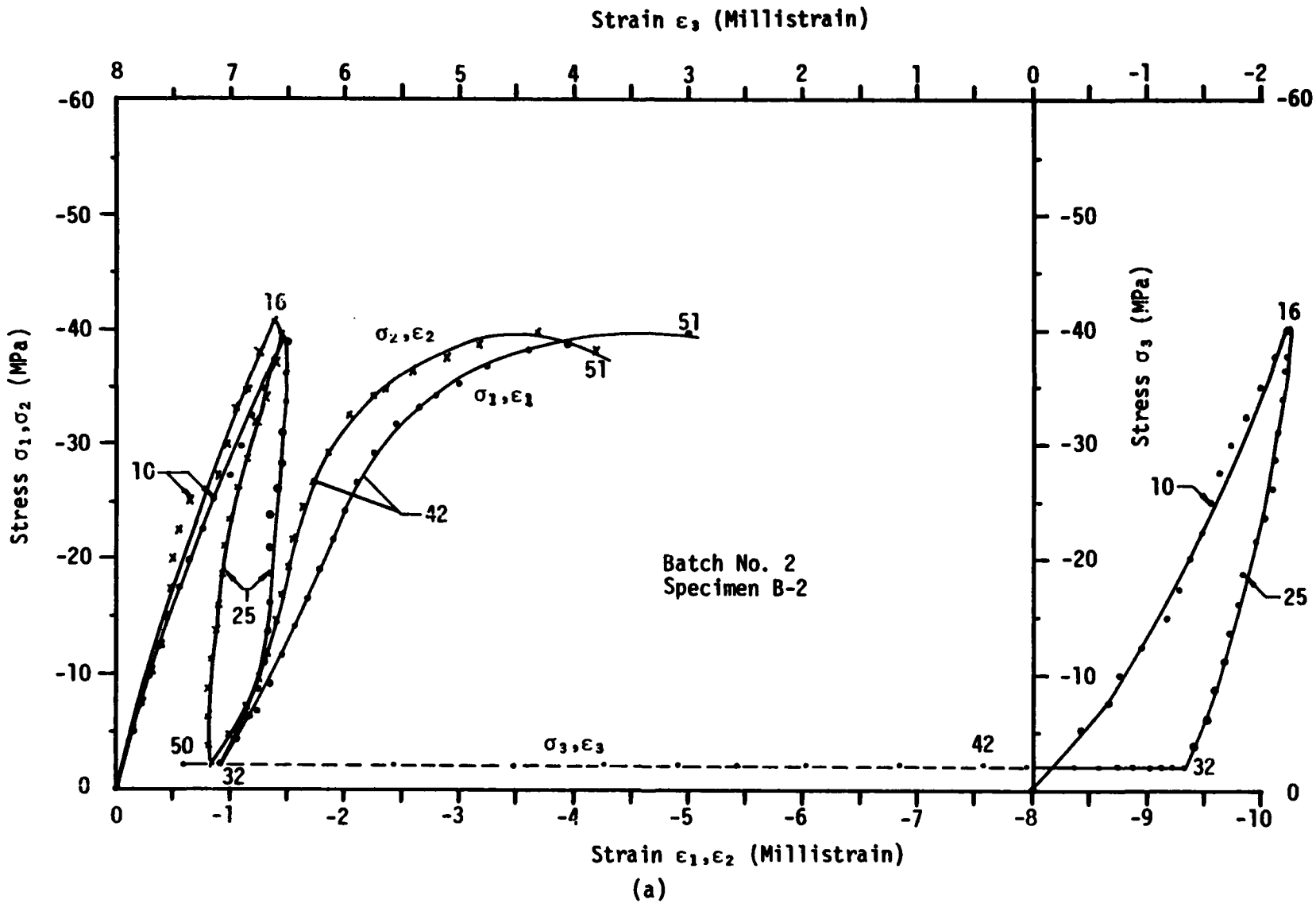

(a)

Figure B6. Load path 6 of nonstandard stress paths.

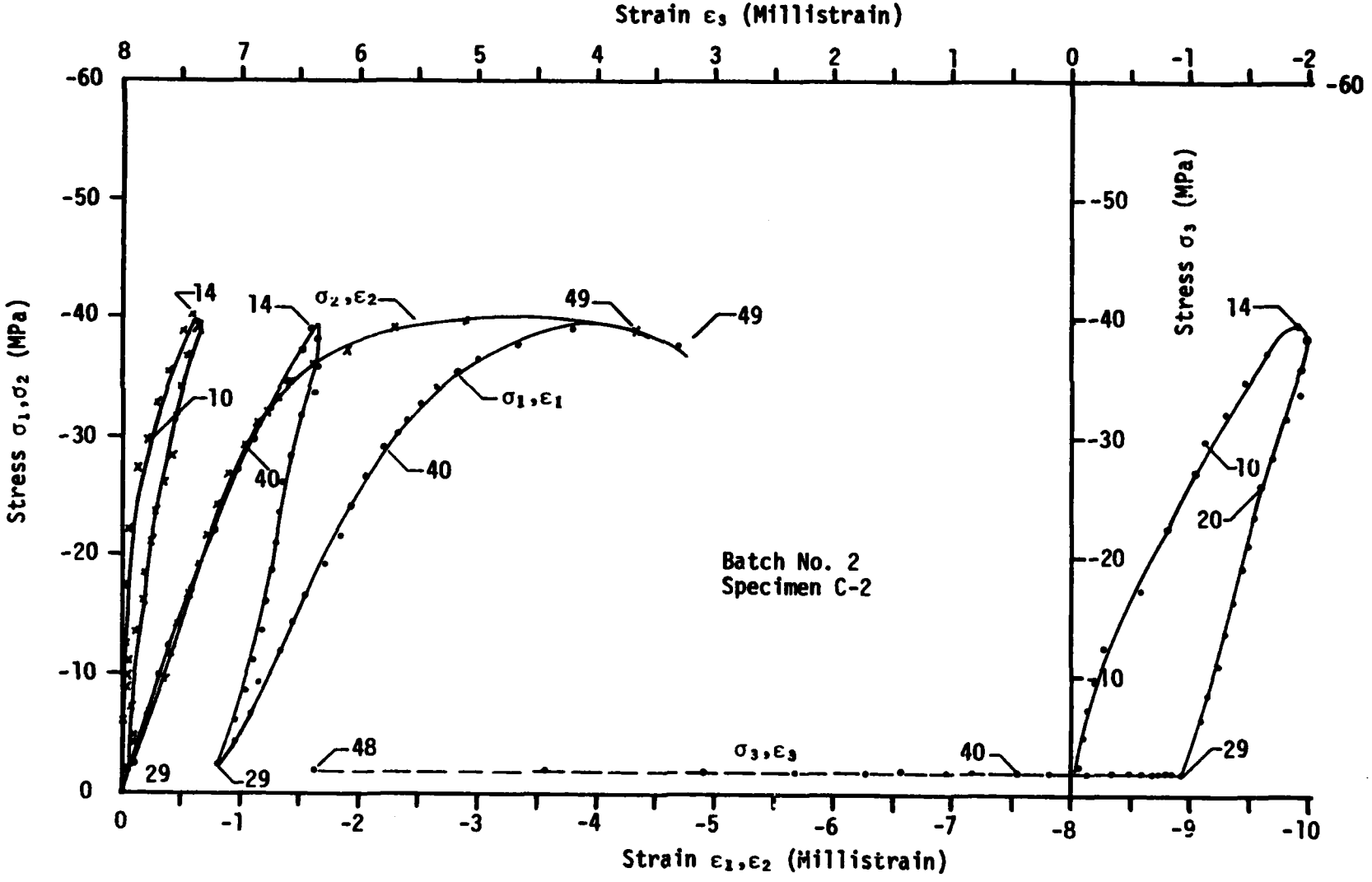

(b)

Figure B6. Continued.

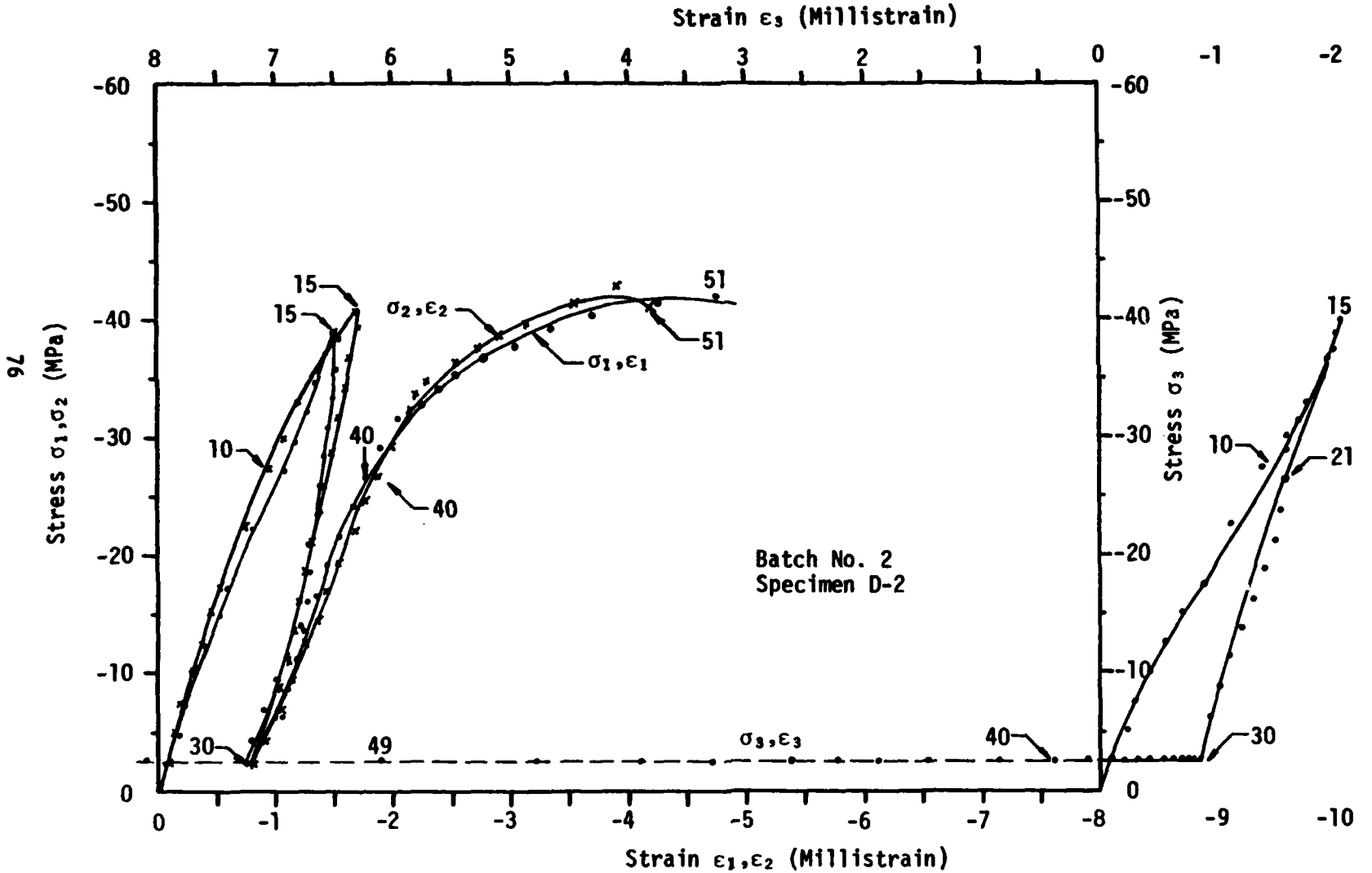

(c)

Figure B6. Continued.

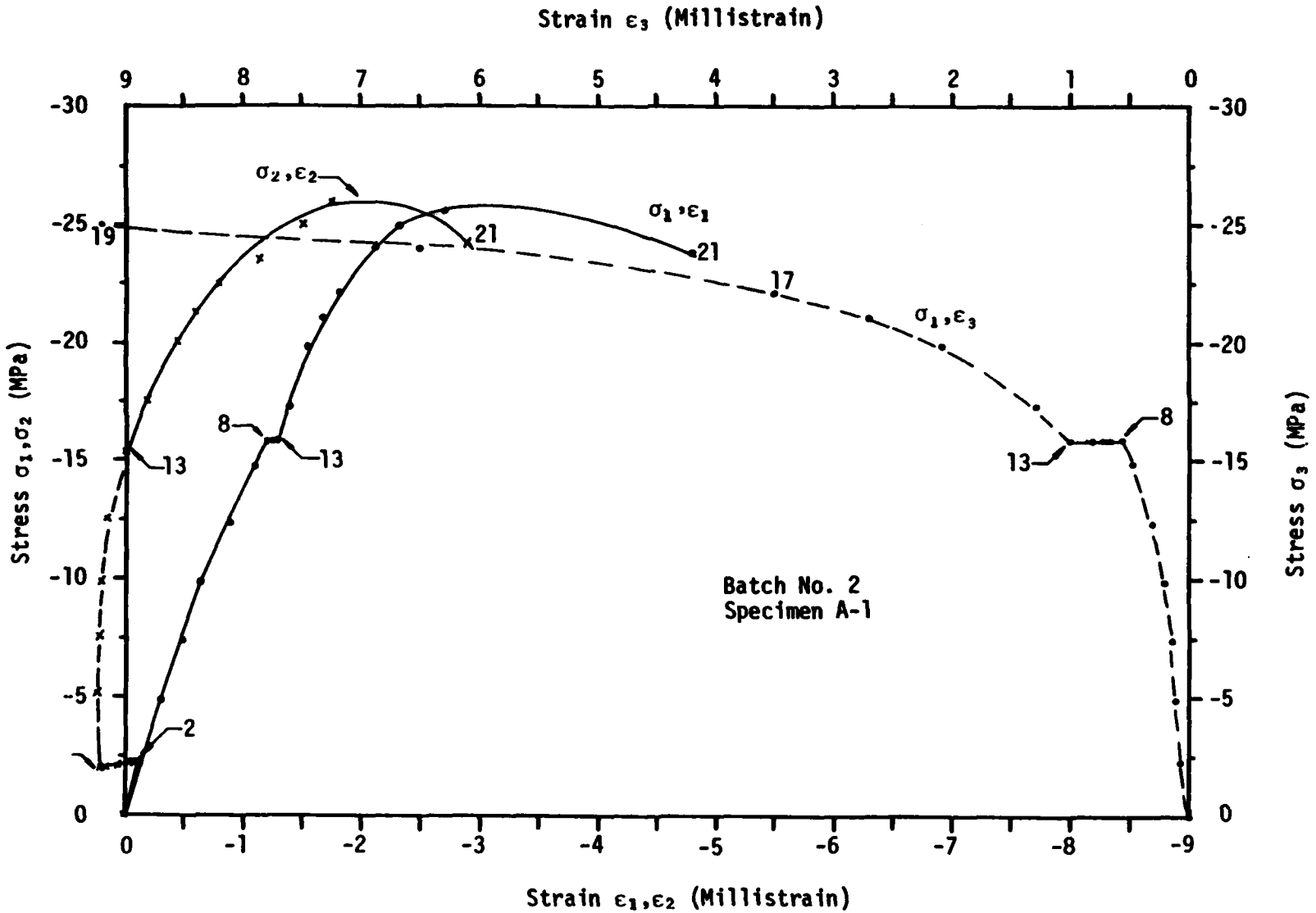

(a)

Figure B7. Load path 7 of nonstandard compression tests.

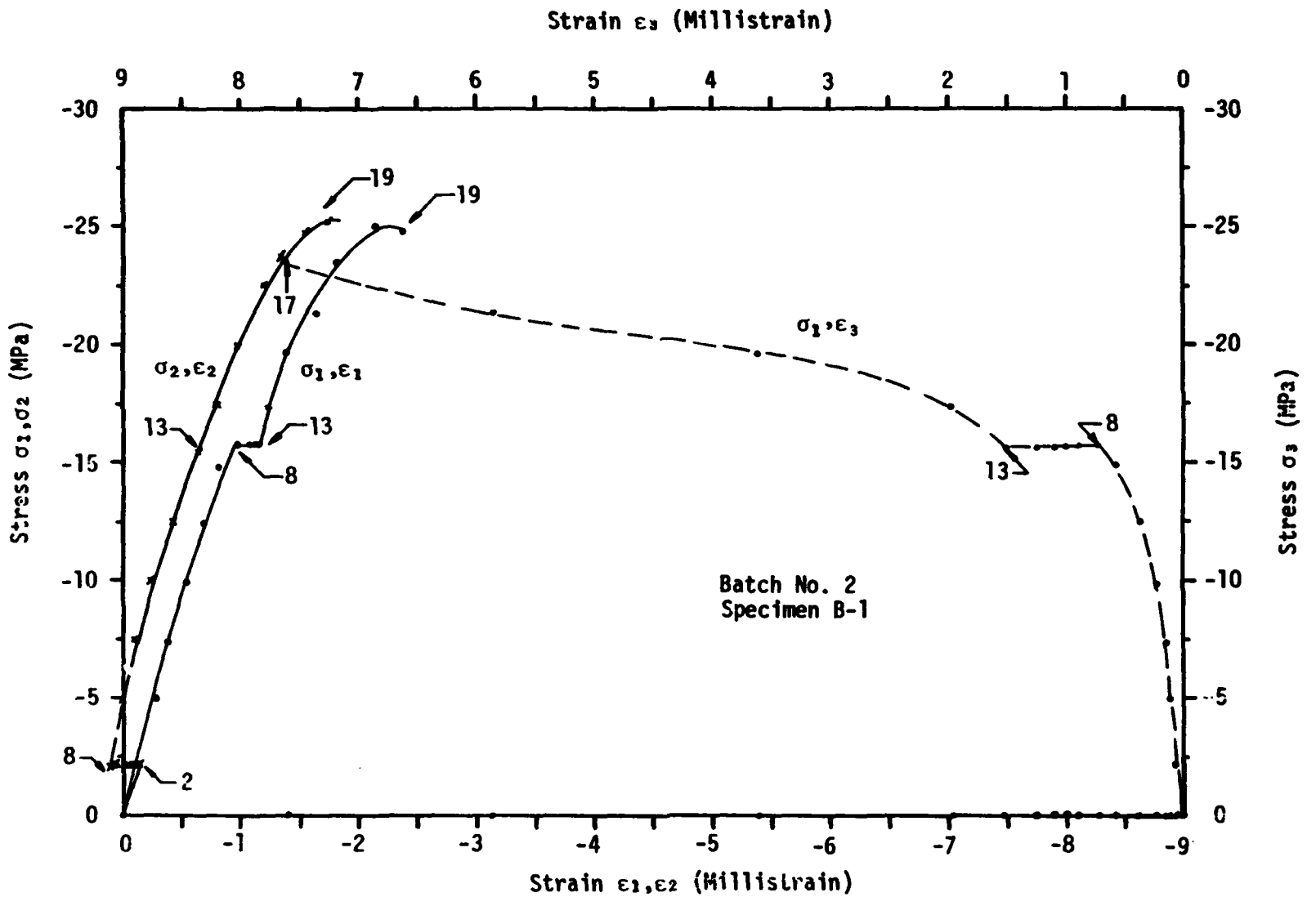

(b)

Figure B7. Continued.

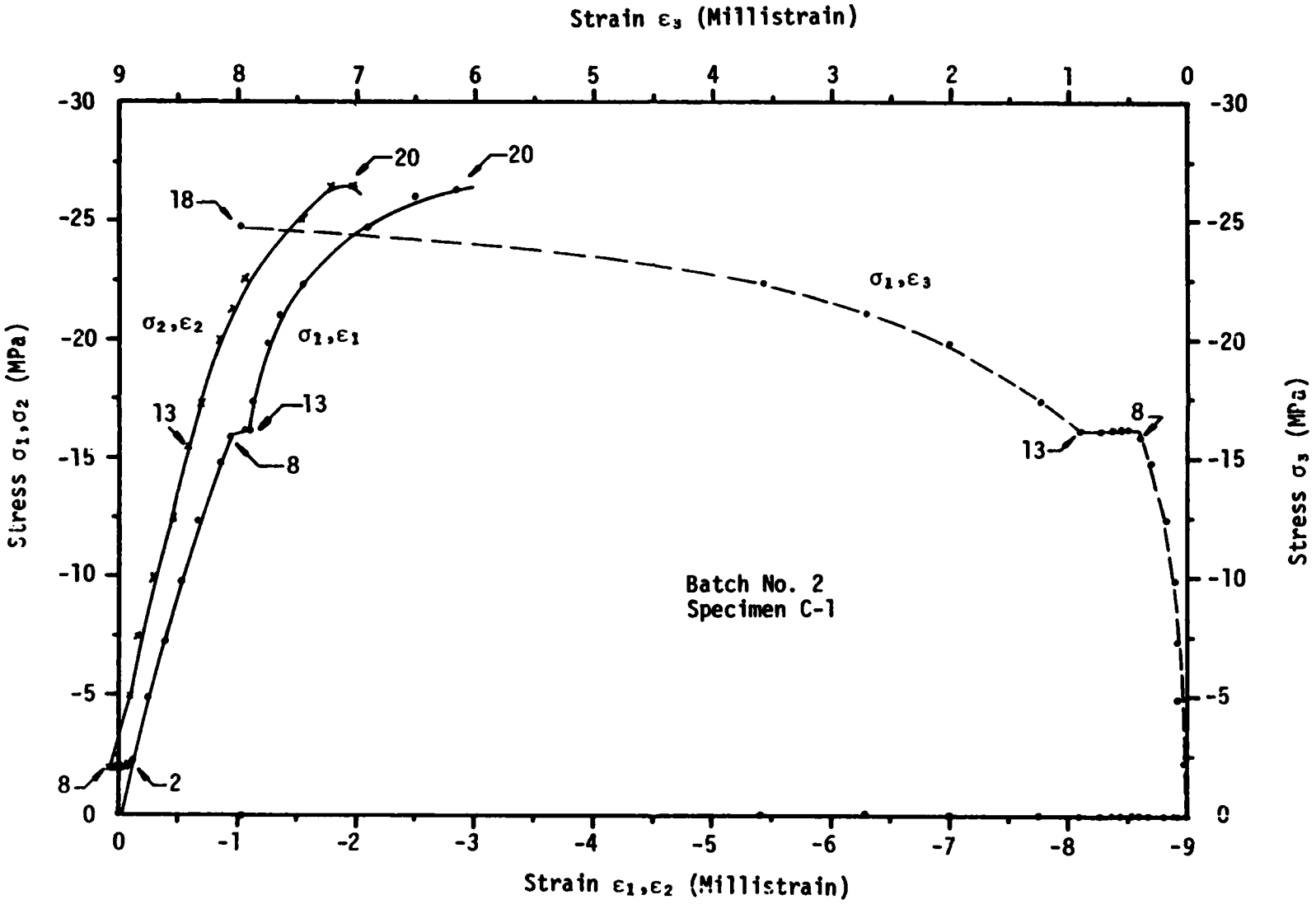

(c)

Figure B7. Continued.

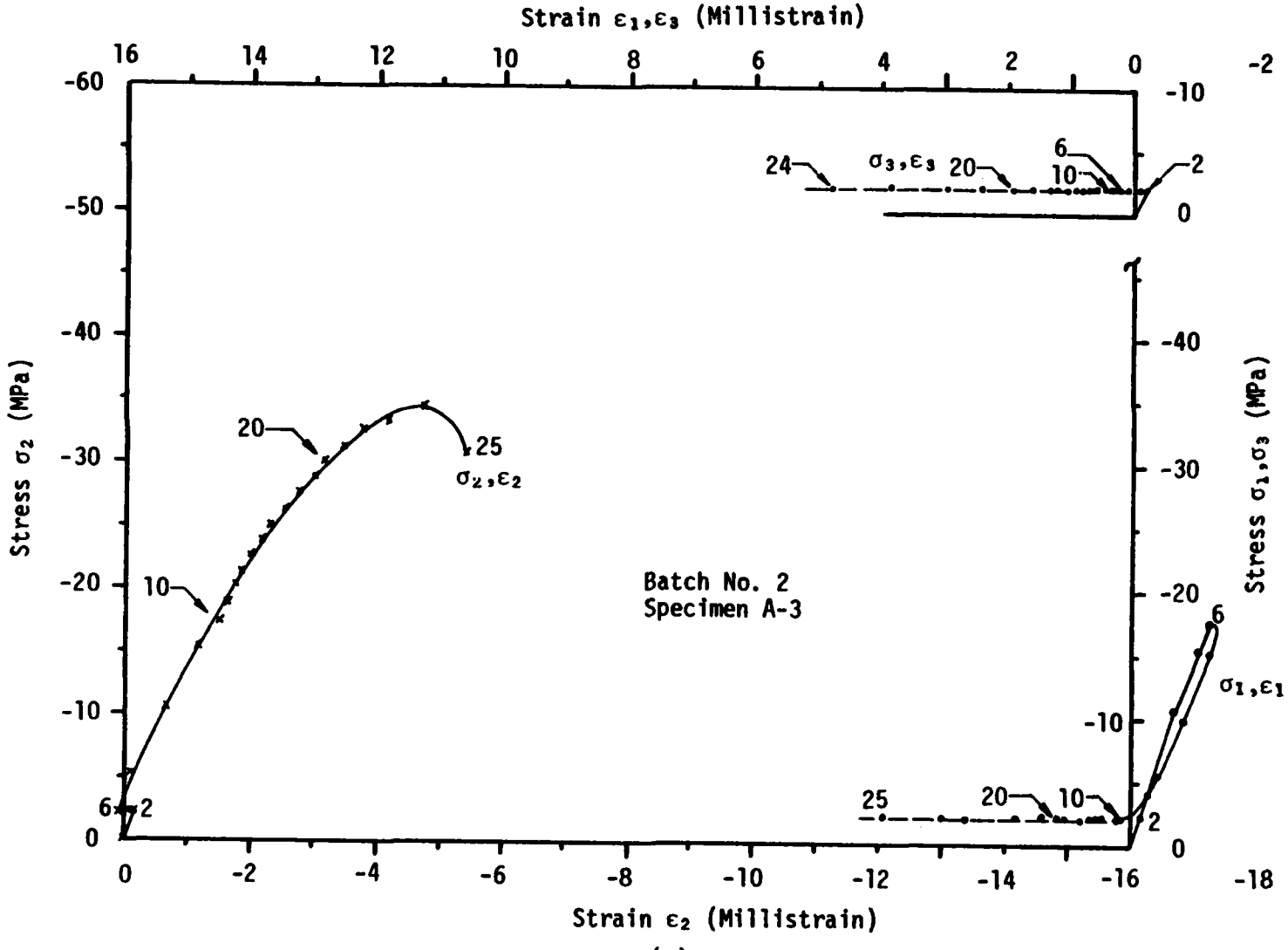

(a)

Figure 88. Load path 8 of nonstandard compression tests.

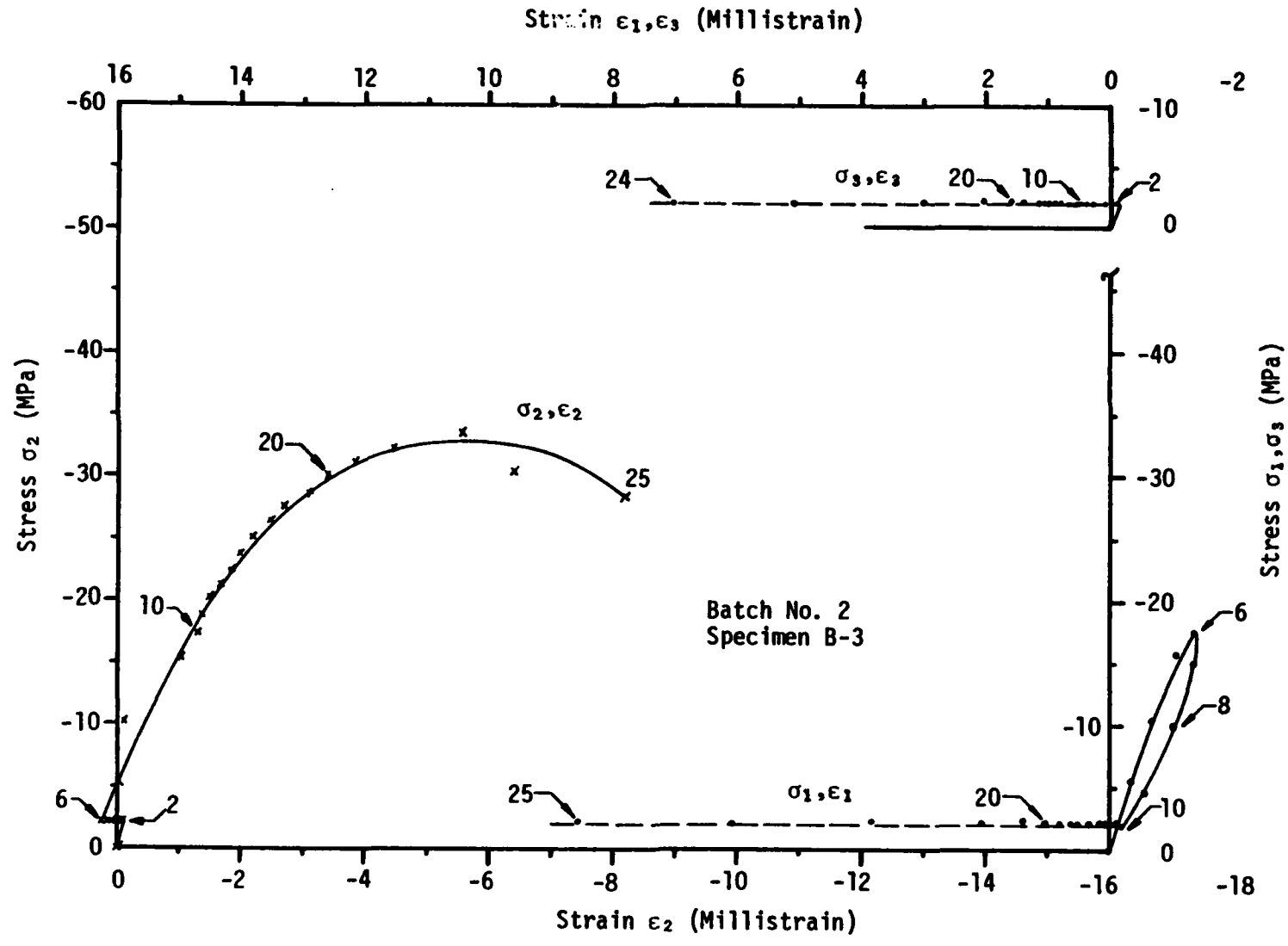

(b)

Figure B8. Continued.

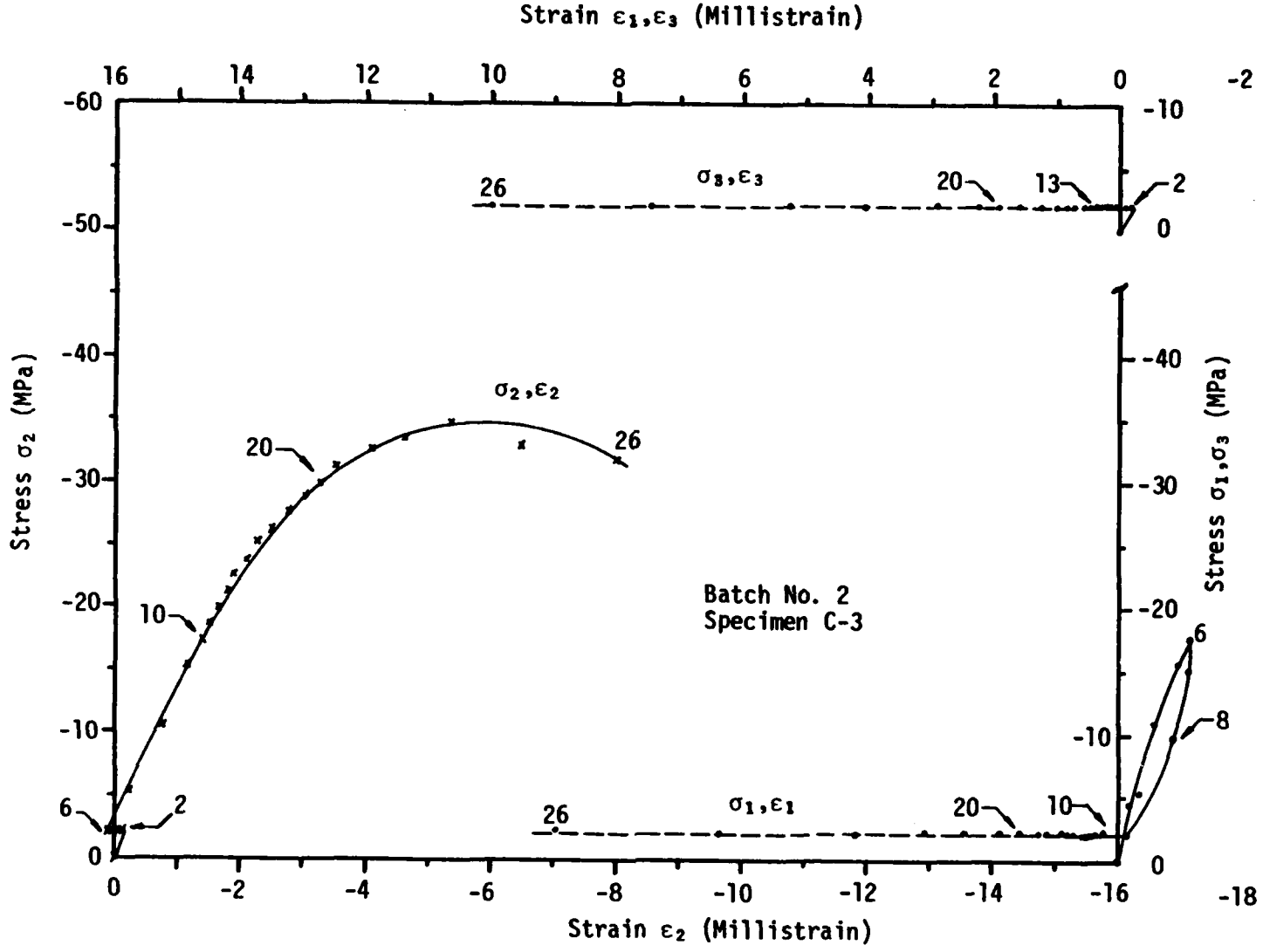

(c)

Figure B8. Continued.

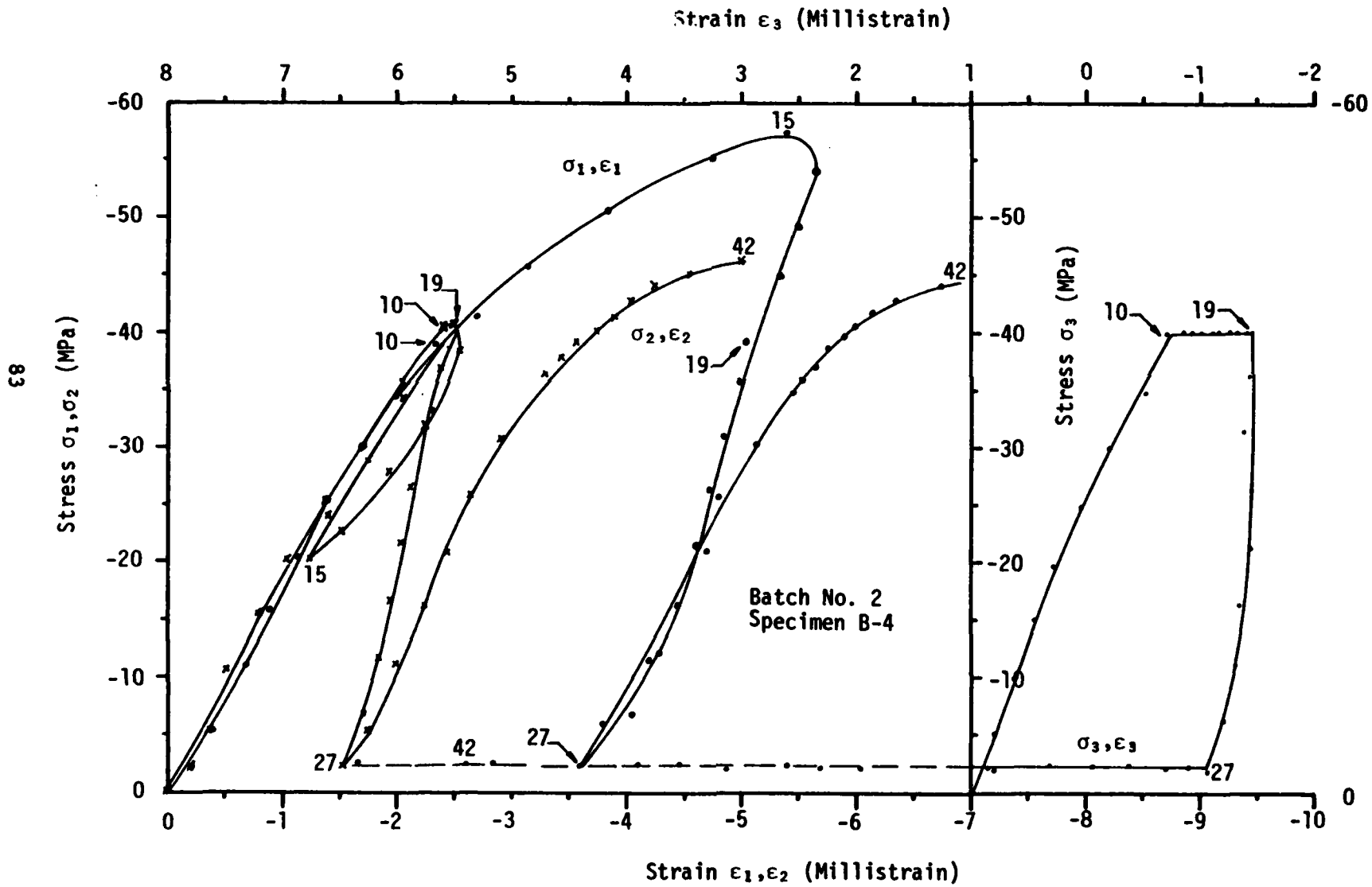

(a)

Figure B9. Load path 9 of nonstandard compression tests.

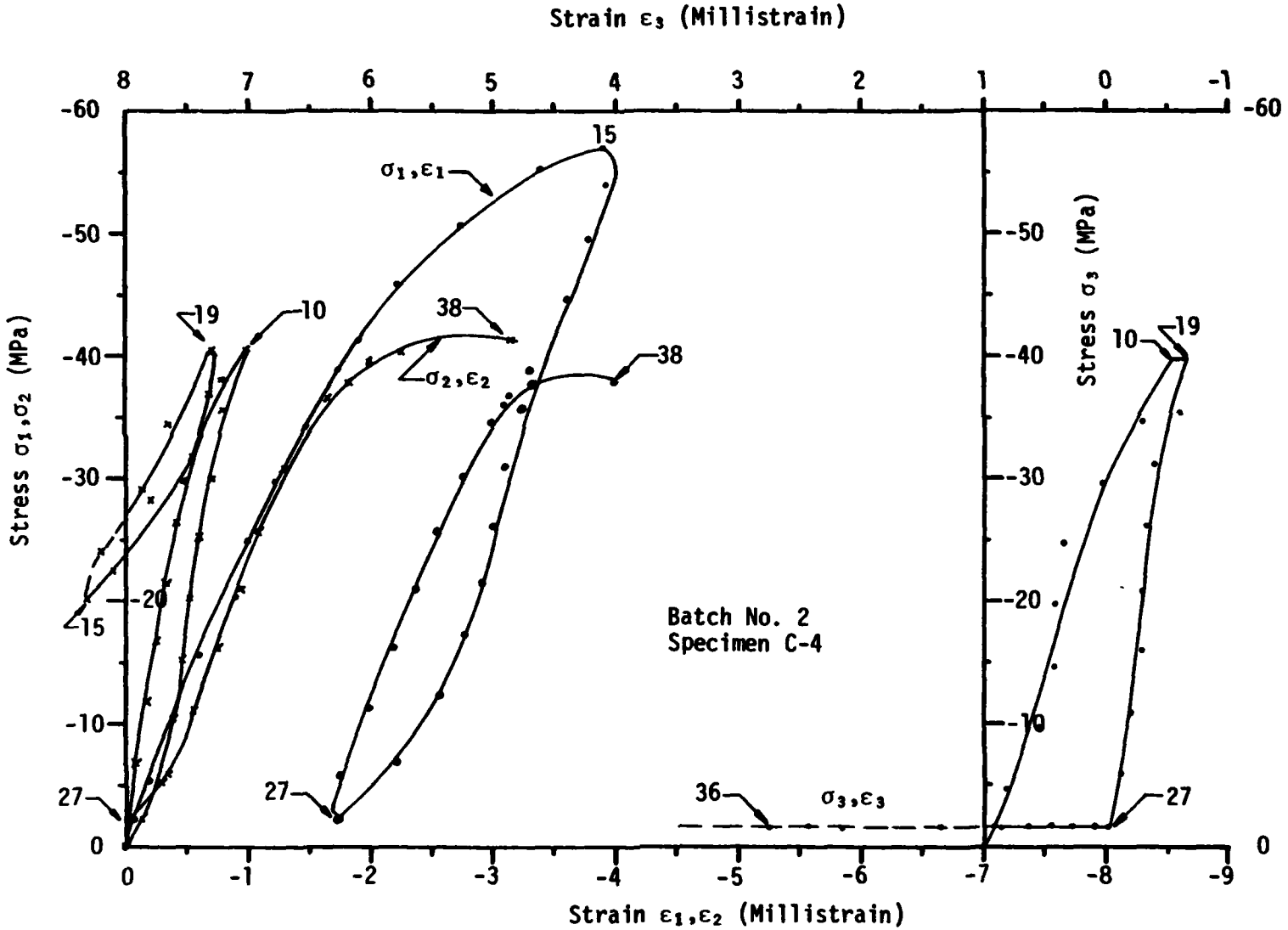

(b)

Figure B9. Continued.

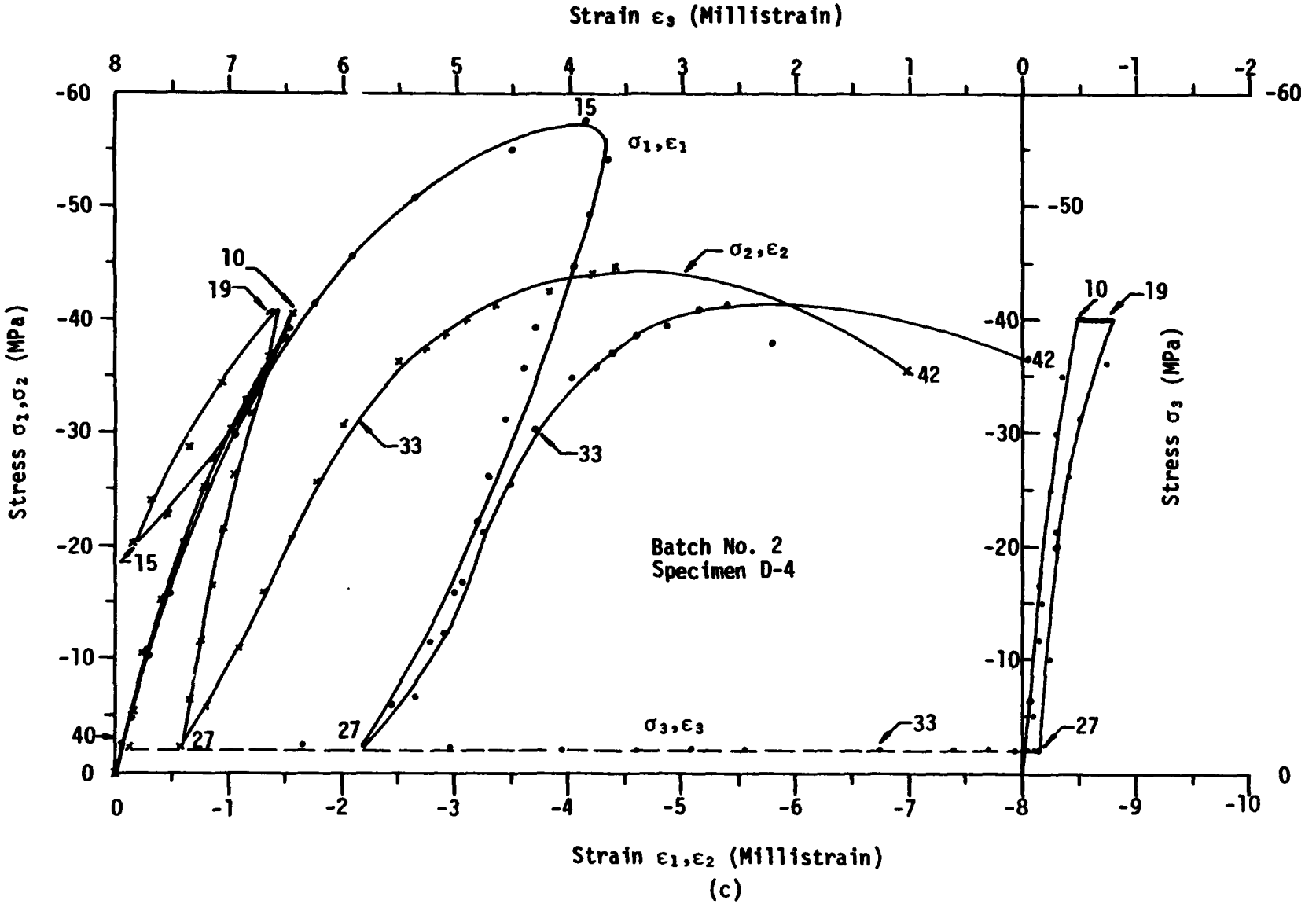

(c)

Figure D9. Continued.

APPENDIX C

STRESS-STRAIN PLOTS FOR TENSION TESTS

All stress and strain data are plotted for the various paths described as tension tests. Figure C-1 shows the results for the first path, Figure C-2 for the second path, etc. Since three experiments were performed for each path, each figure has part (a), (b) and (c) which differentiates these three sets of data.

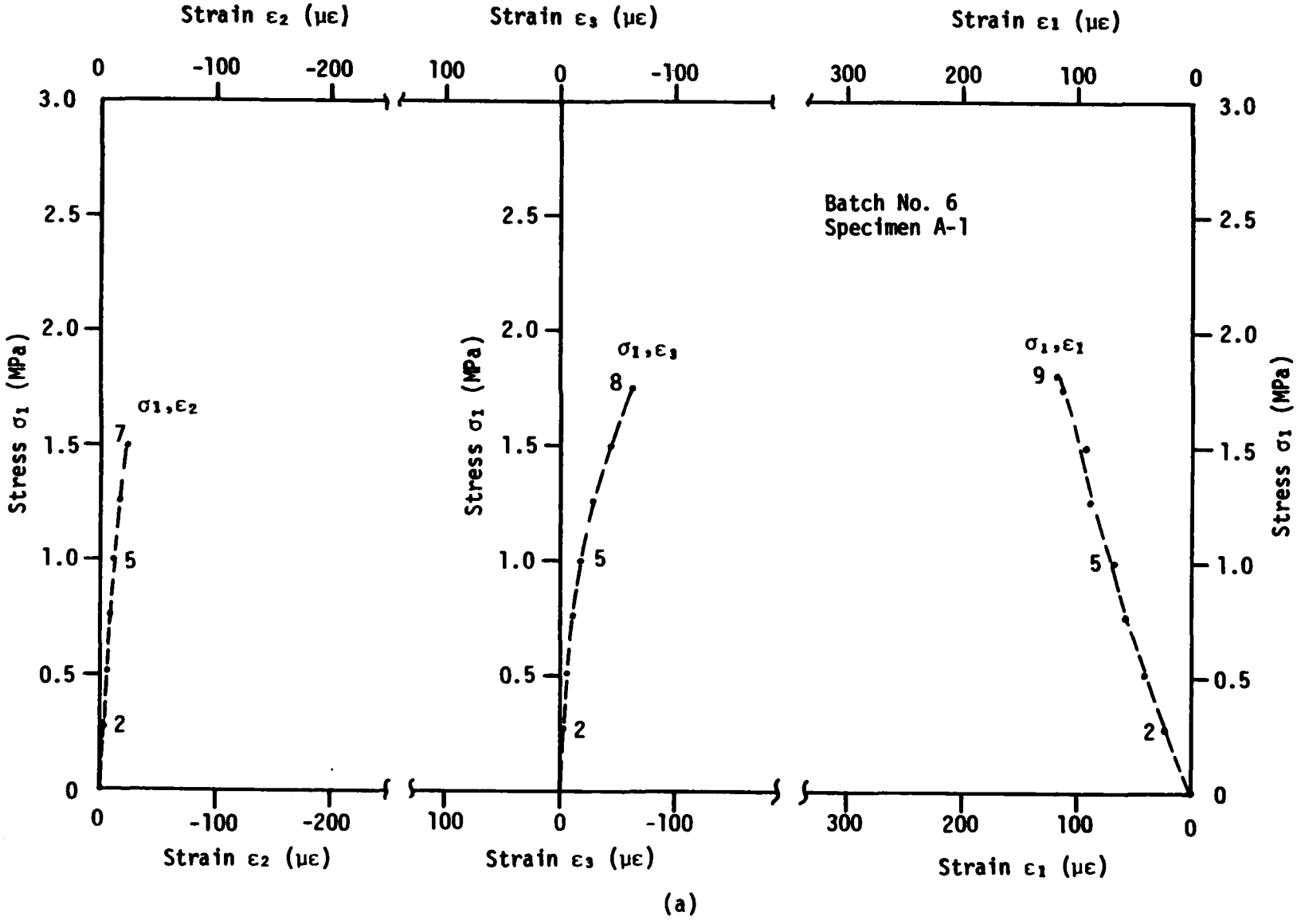

Figure C1. Load path 1 of stress paths involving tension.

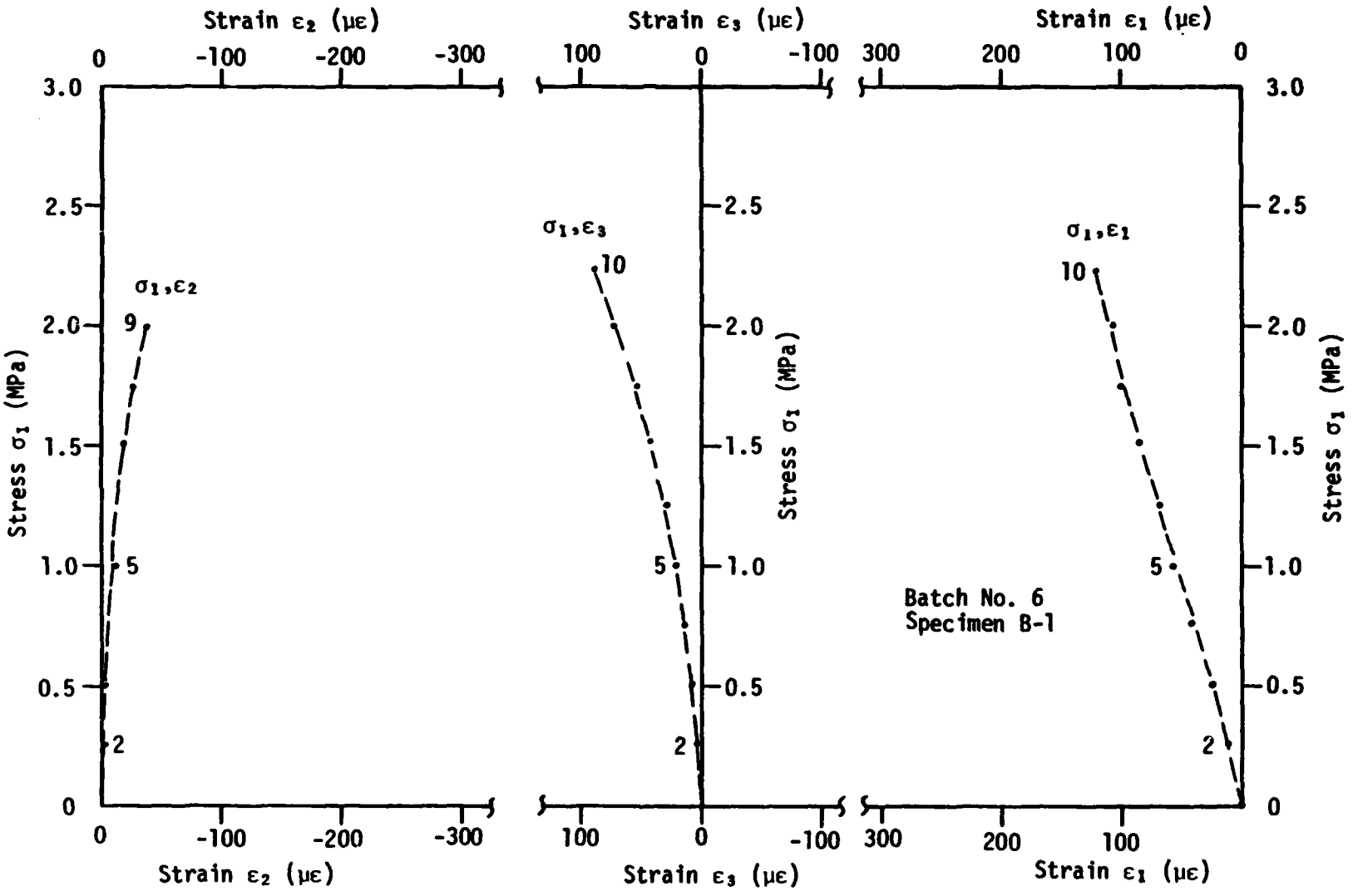

(b)

Figure C1. Continued.

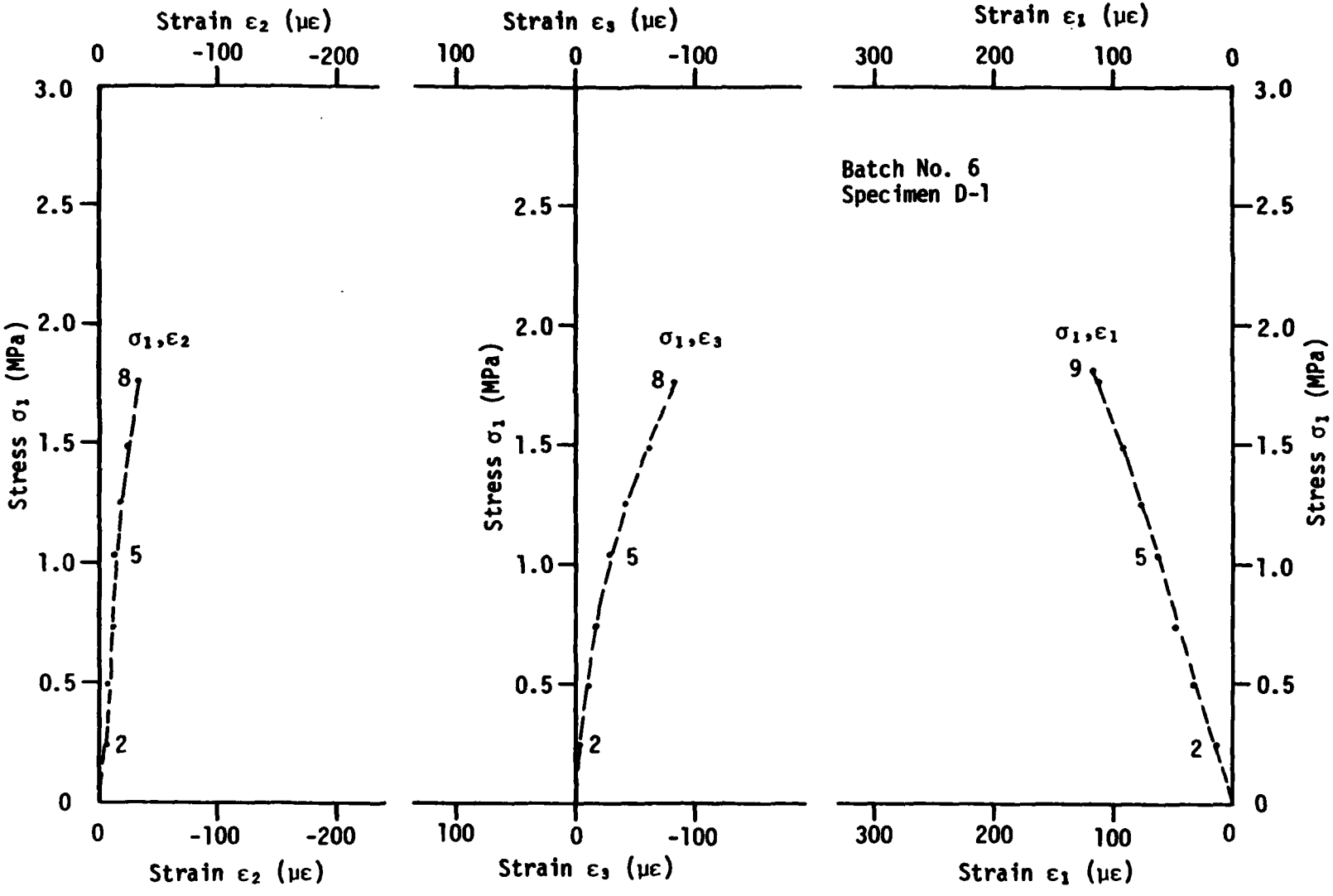

(c)

Figure C1. Continued.

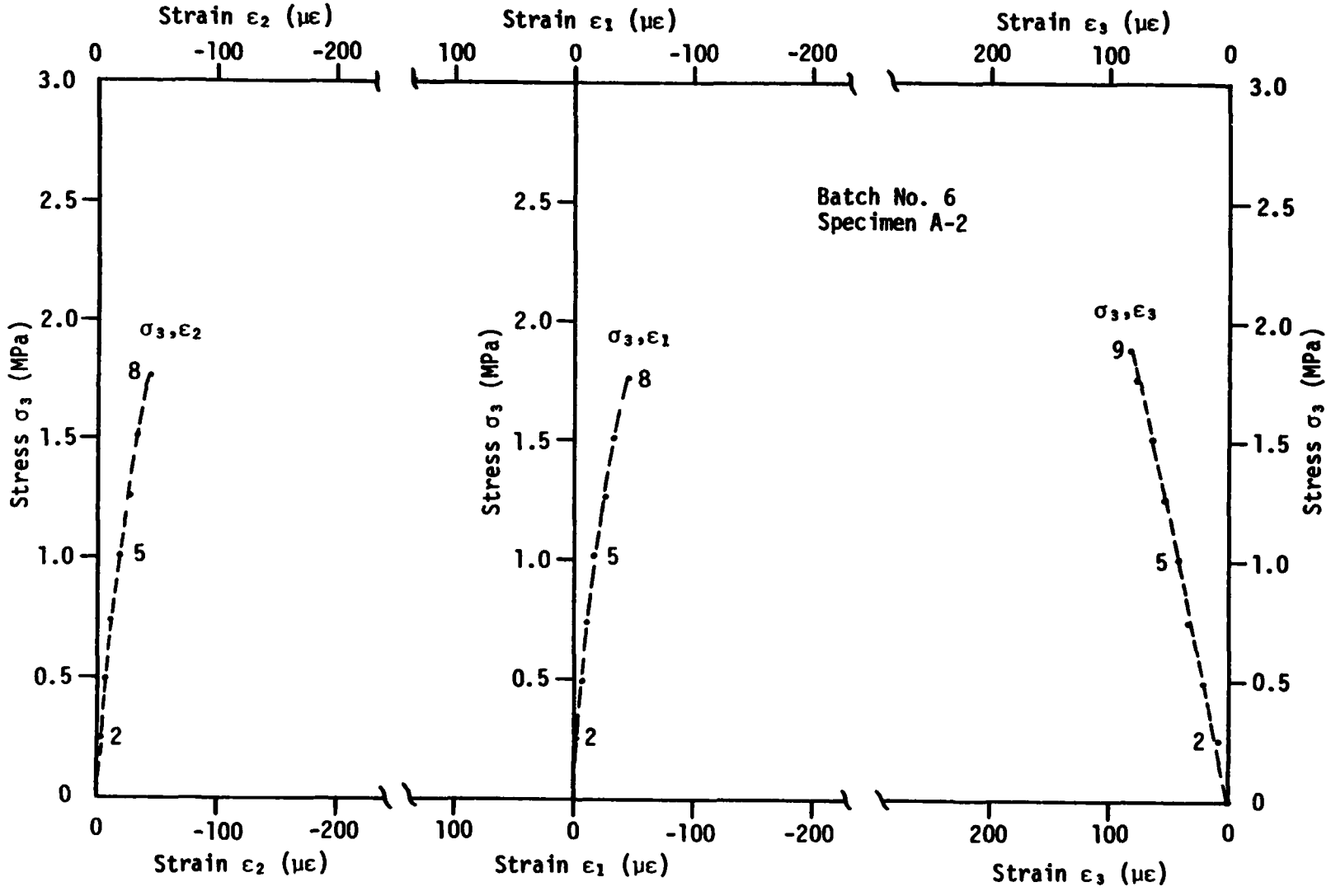

(a)

Figure C2. Load path 2 of stress paths involving tension.

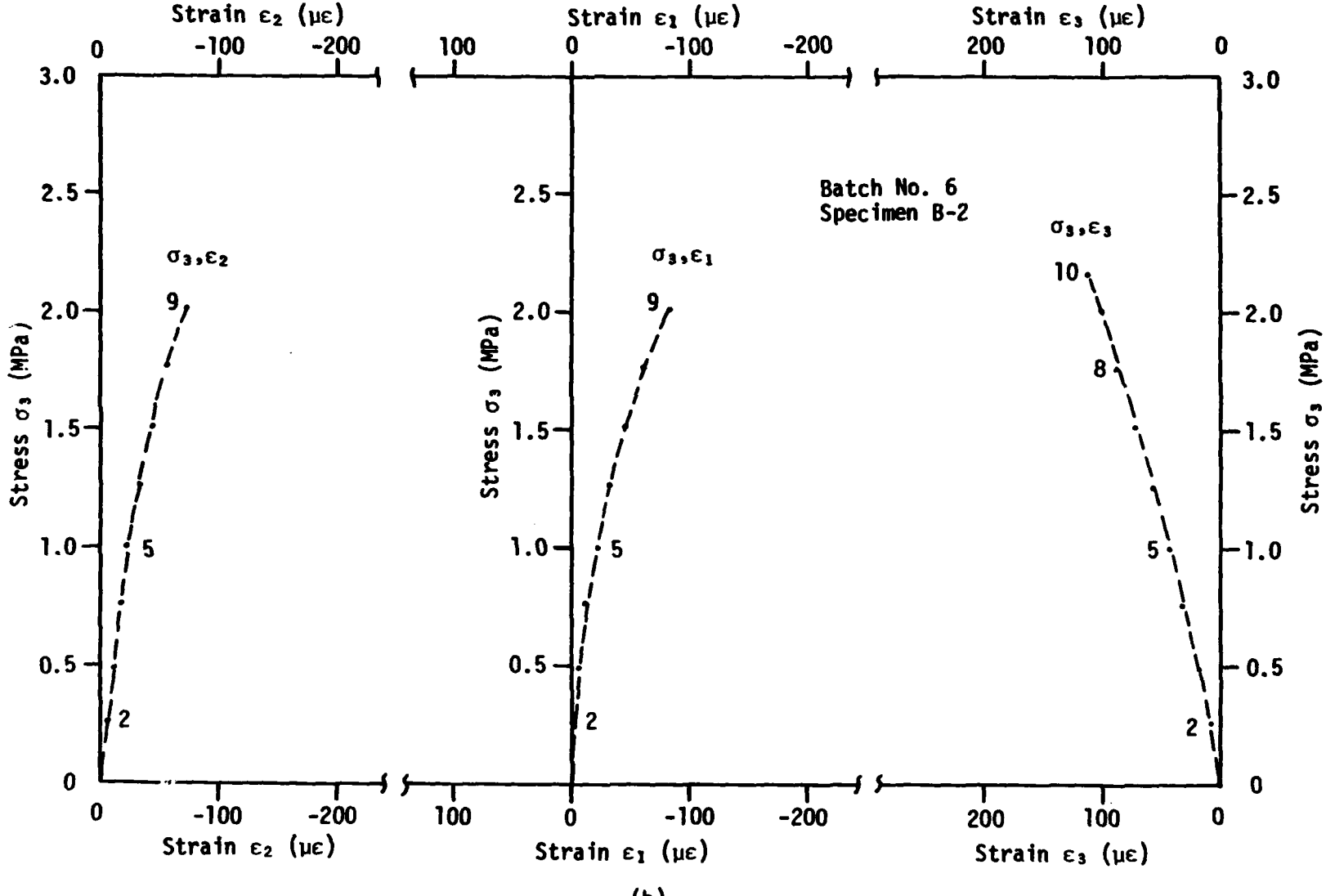

(b)

Figure C2. Continued.

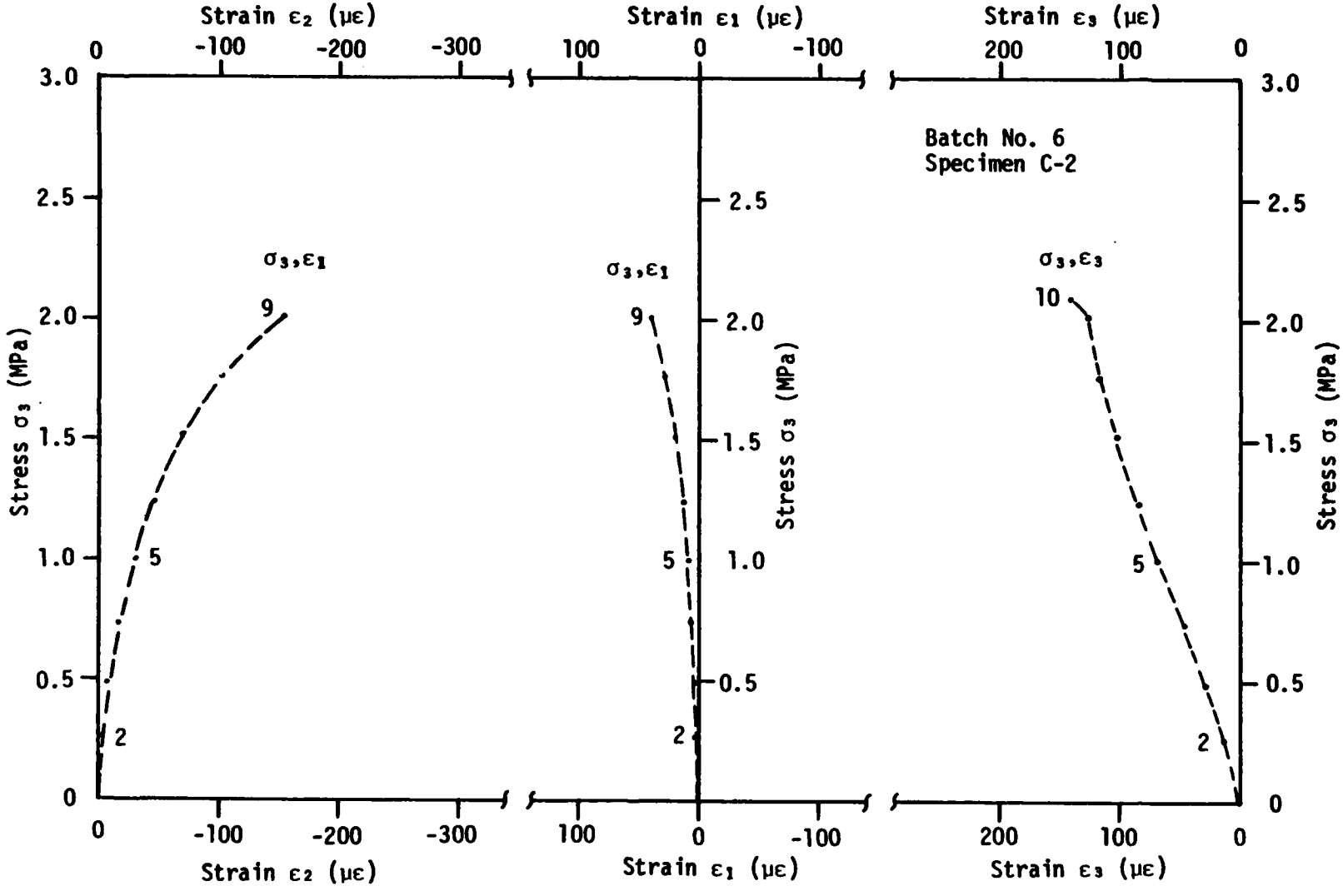

(c)

Figure C2. Continued.

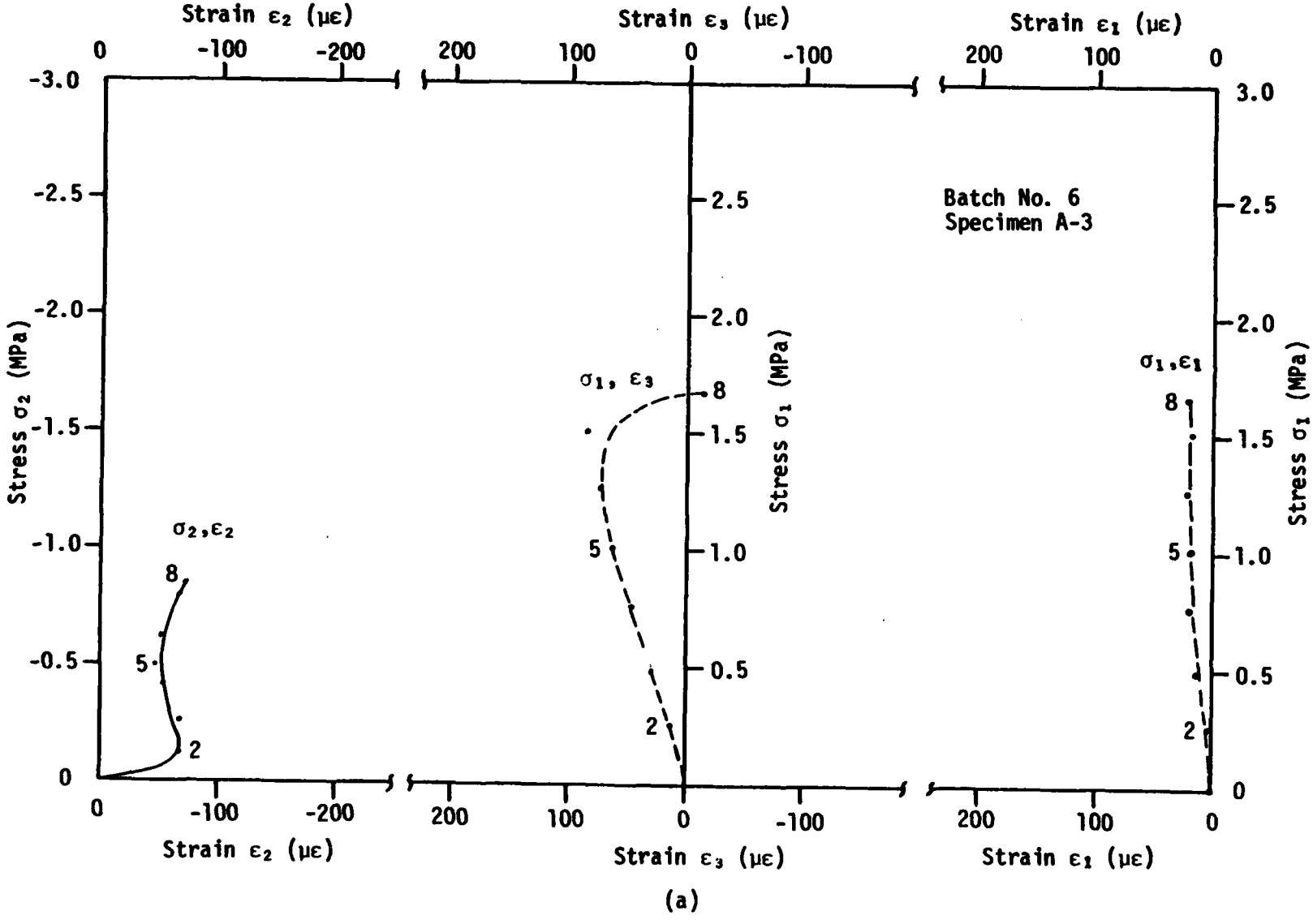

Figure C3. Load path 3 of stress paths involving tension.

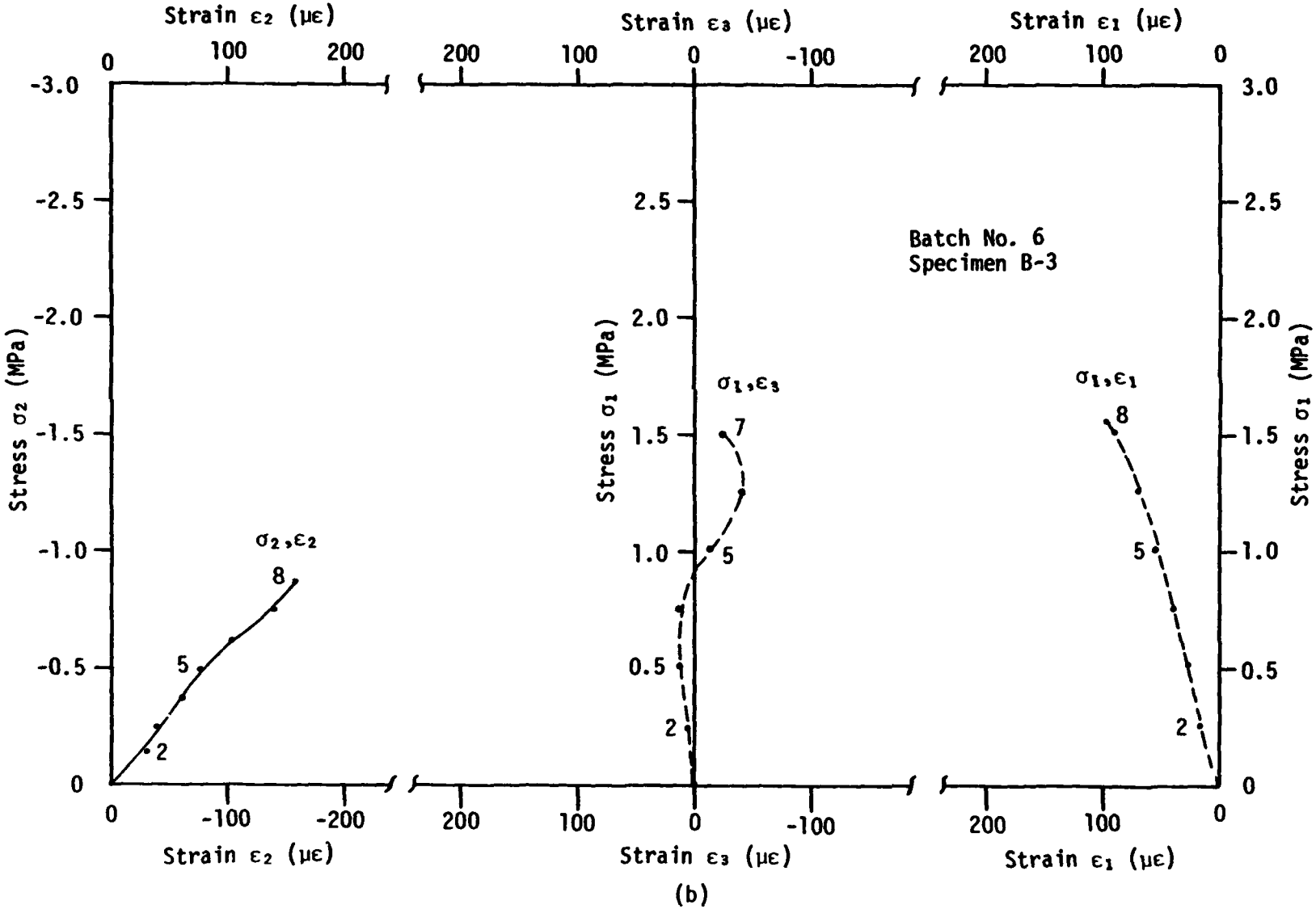

(b)

Figure C3. Continued.

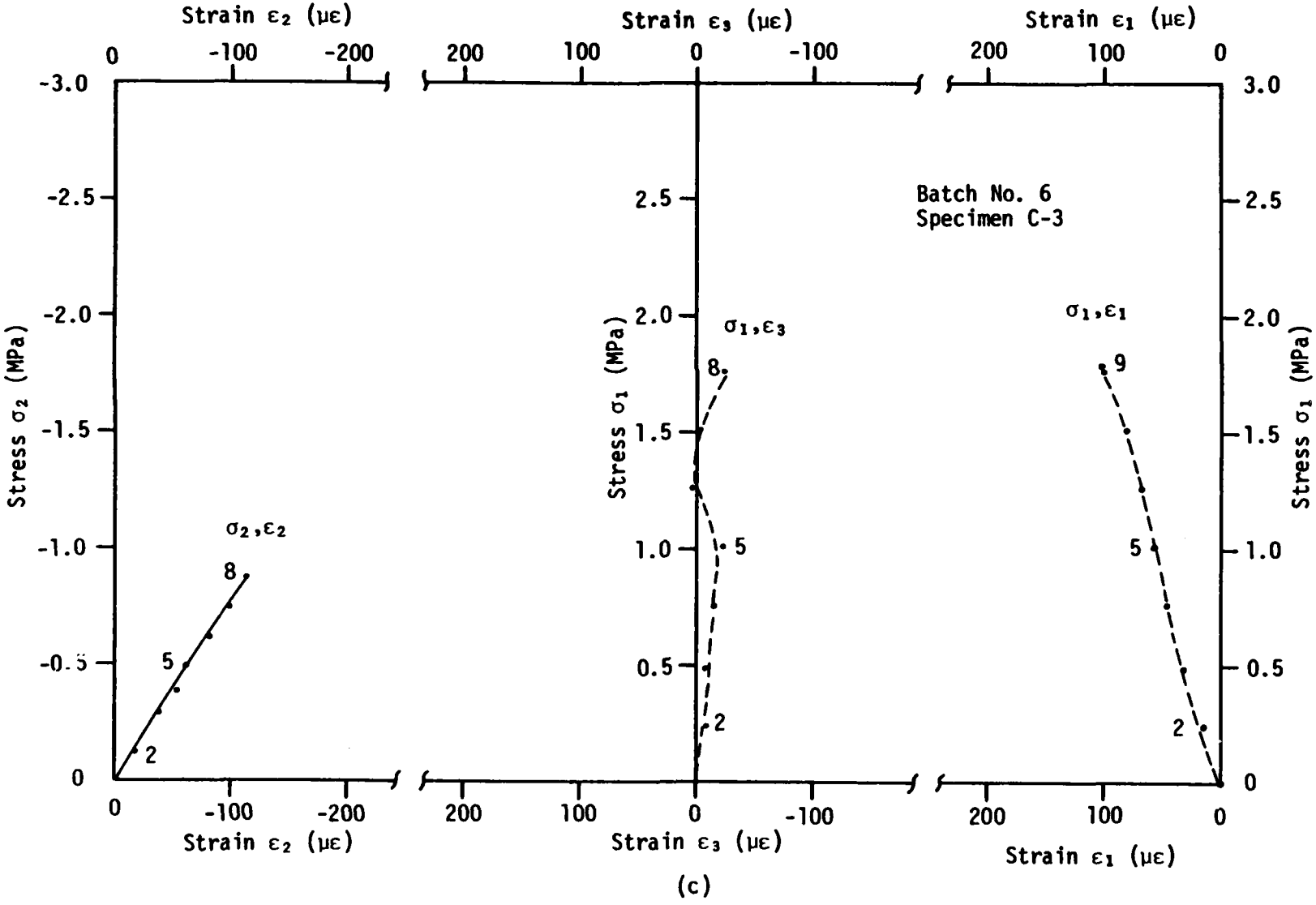

(c)

Figure C3. Continued.

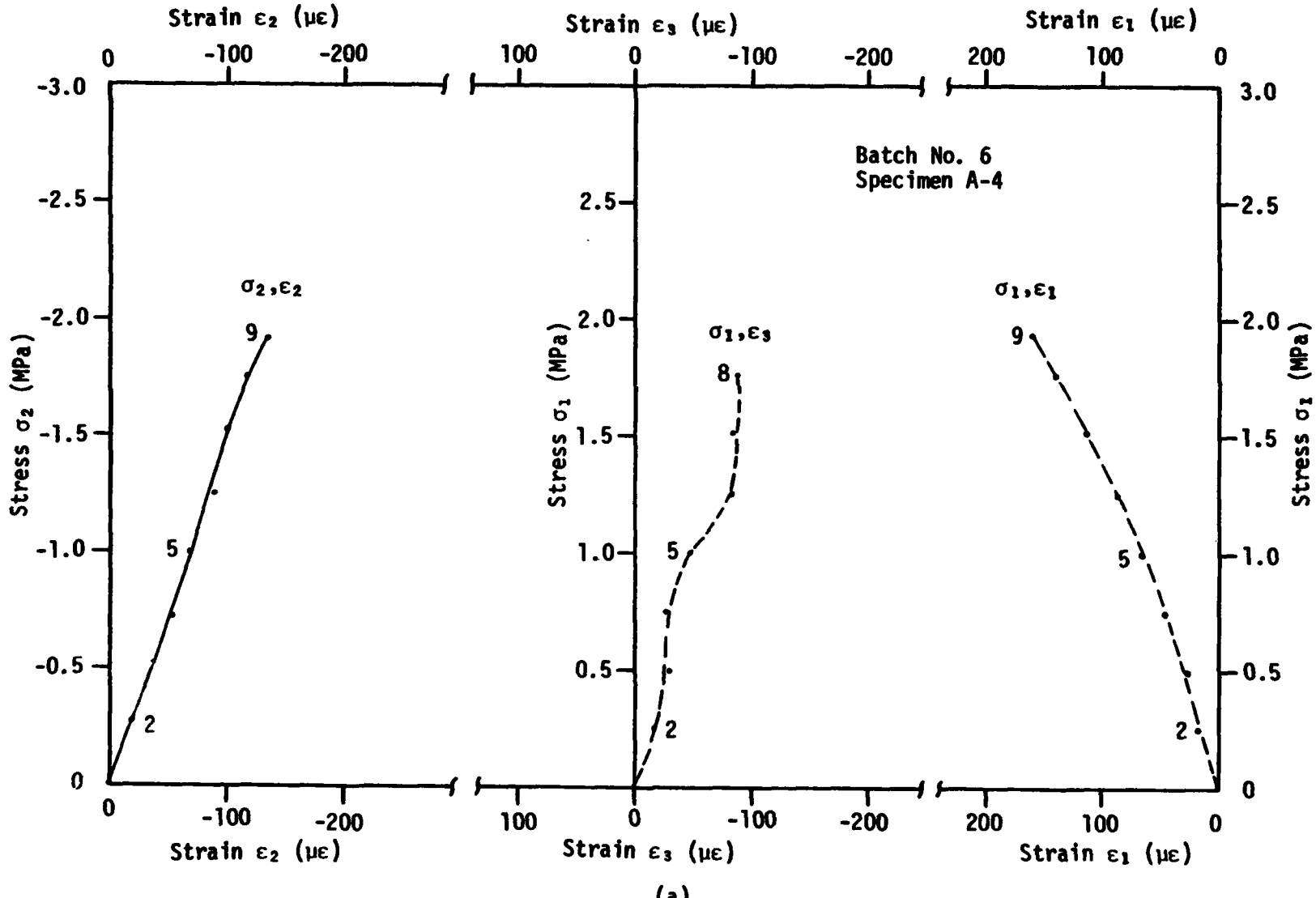

Figure C4. Load path 4 of stress paths involving tension.

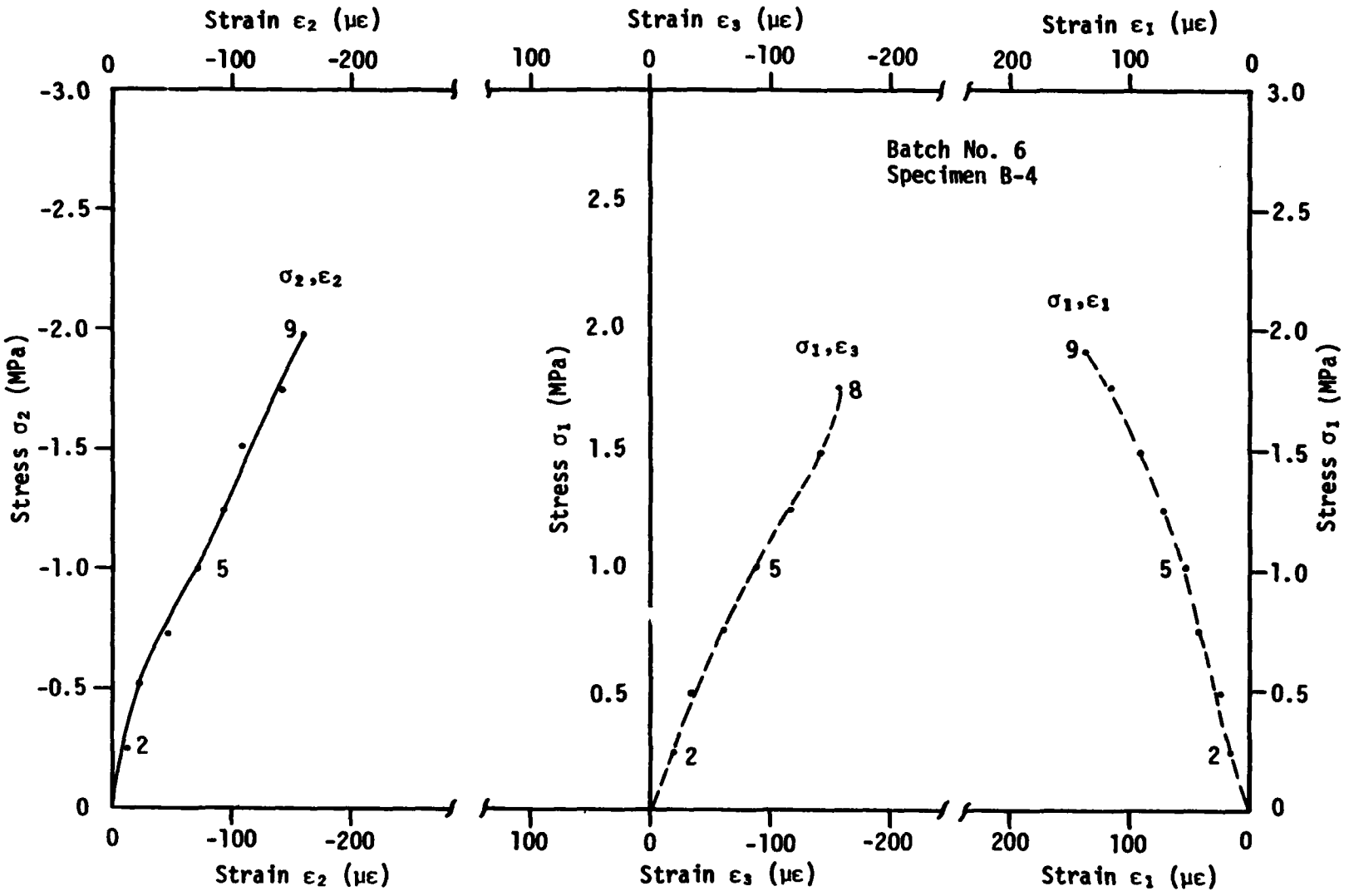

(b)

Figure C4. Continued.

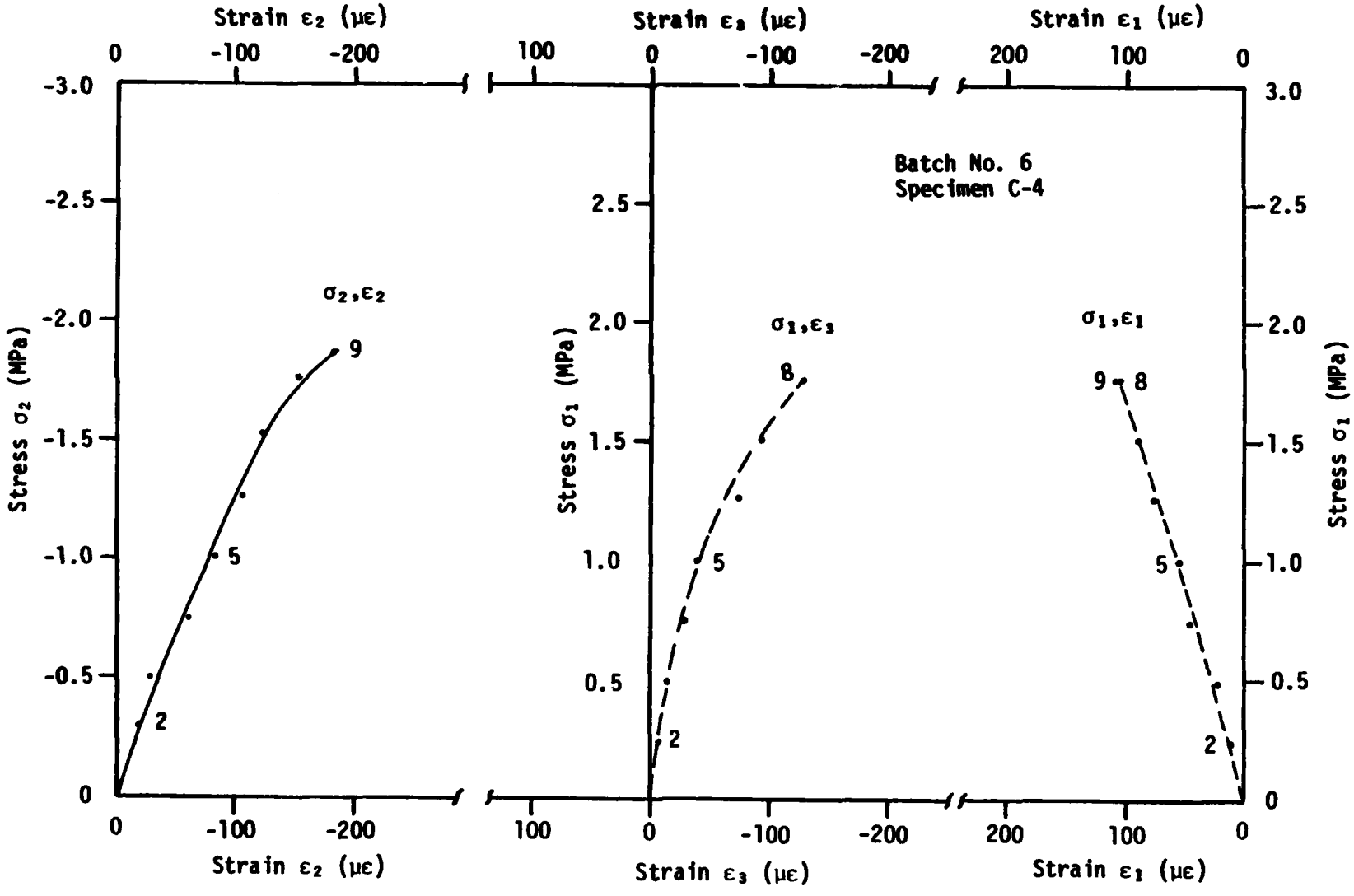

(c)

Figure C4. Continued.

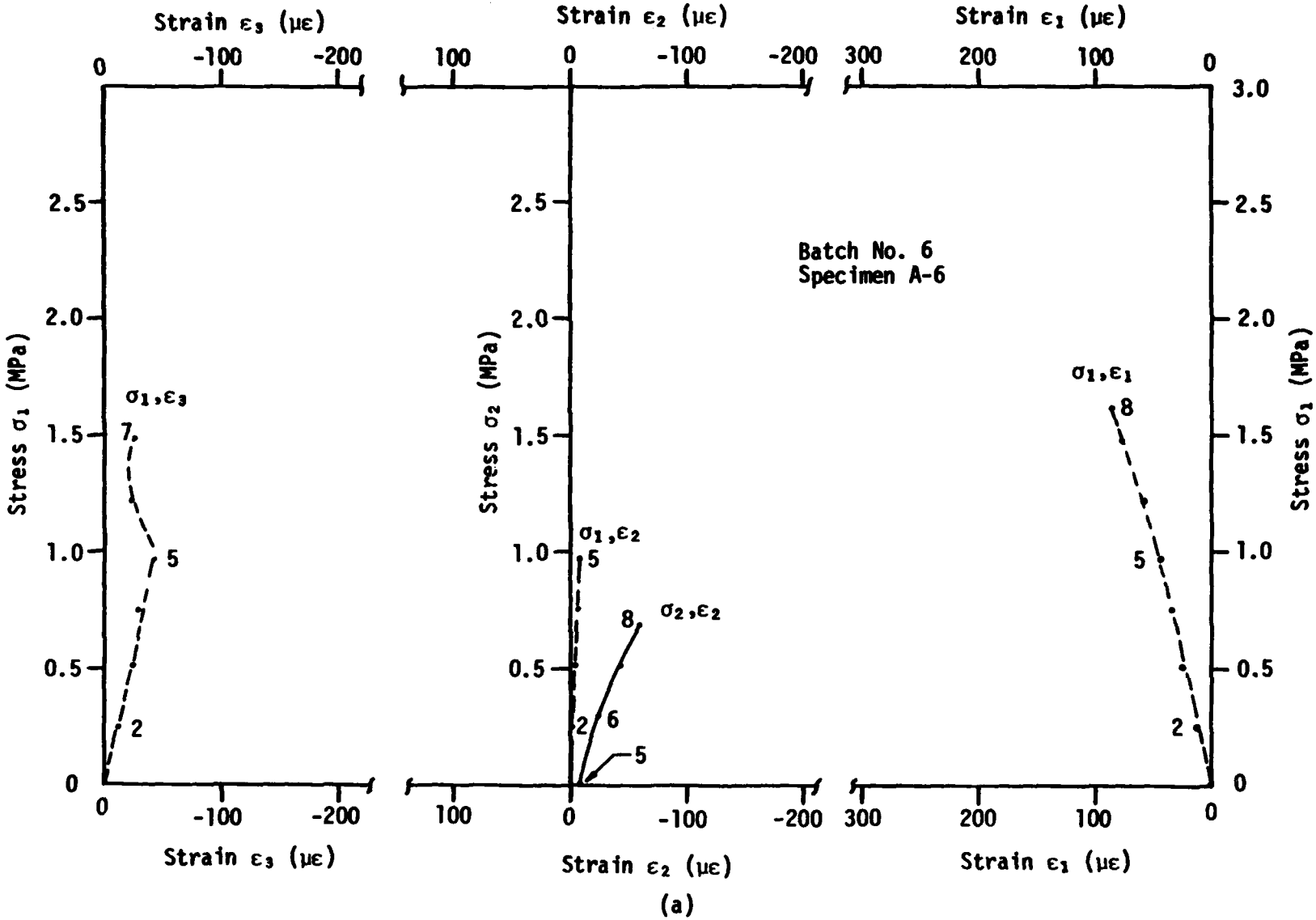

(a)

Figure C5. Load path 5 of stress paths involving tension.

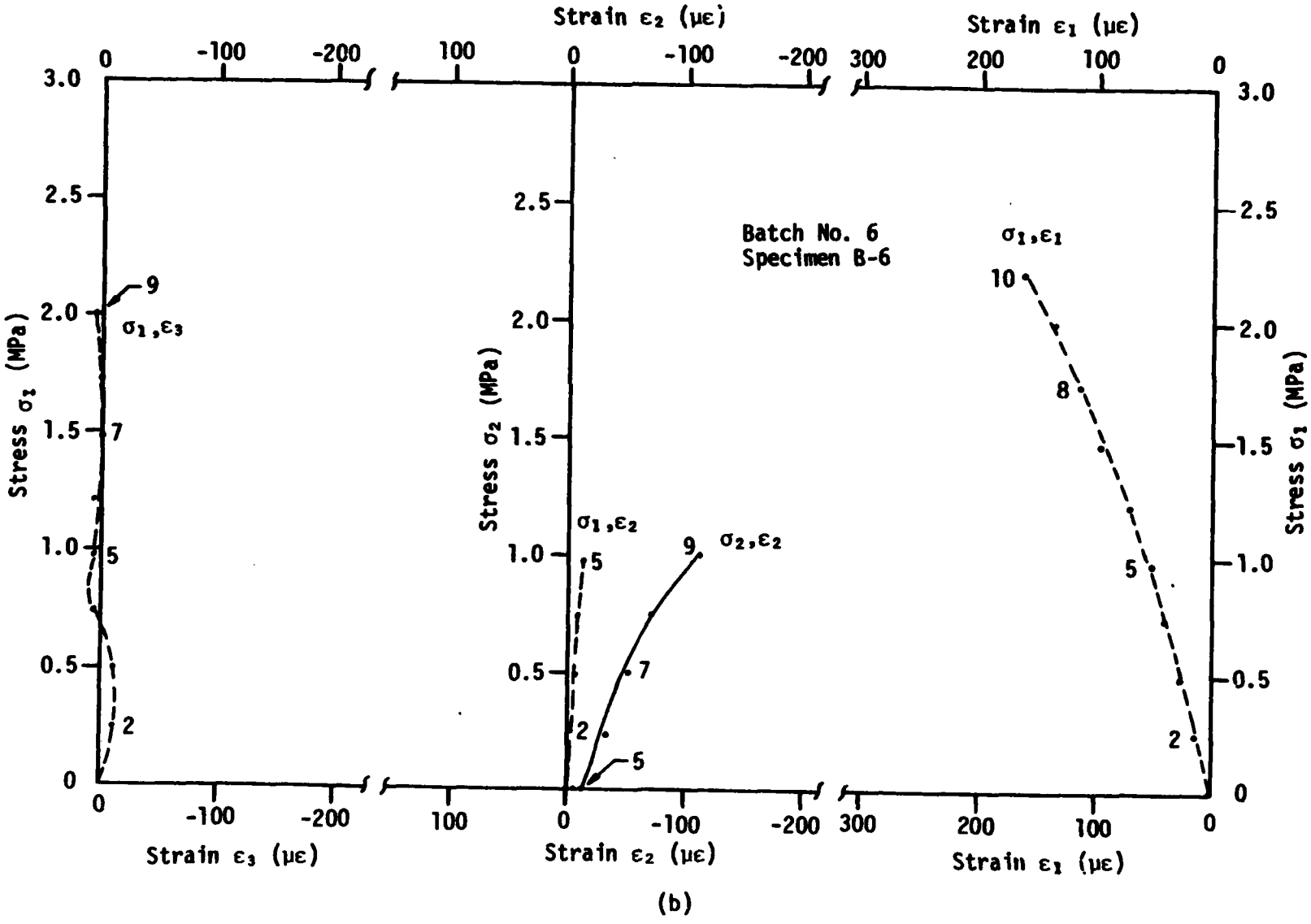

(b)

Figure C5. Continued.

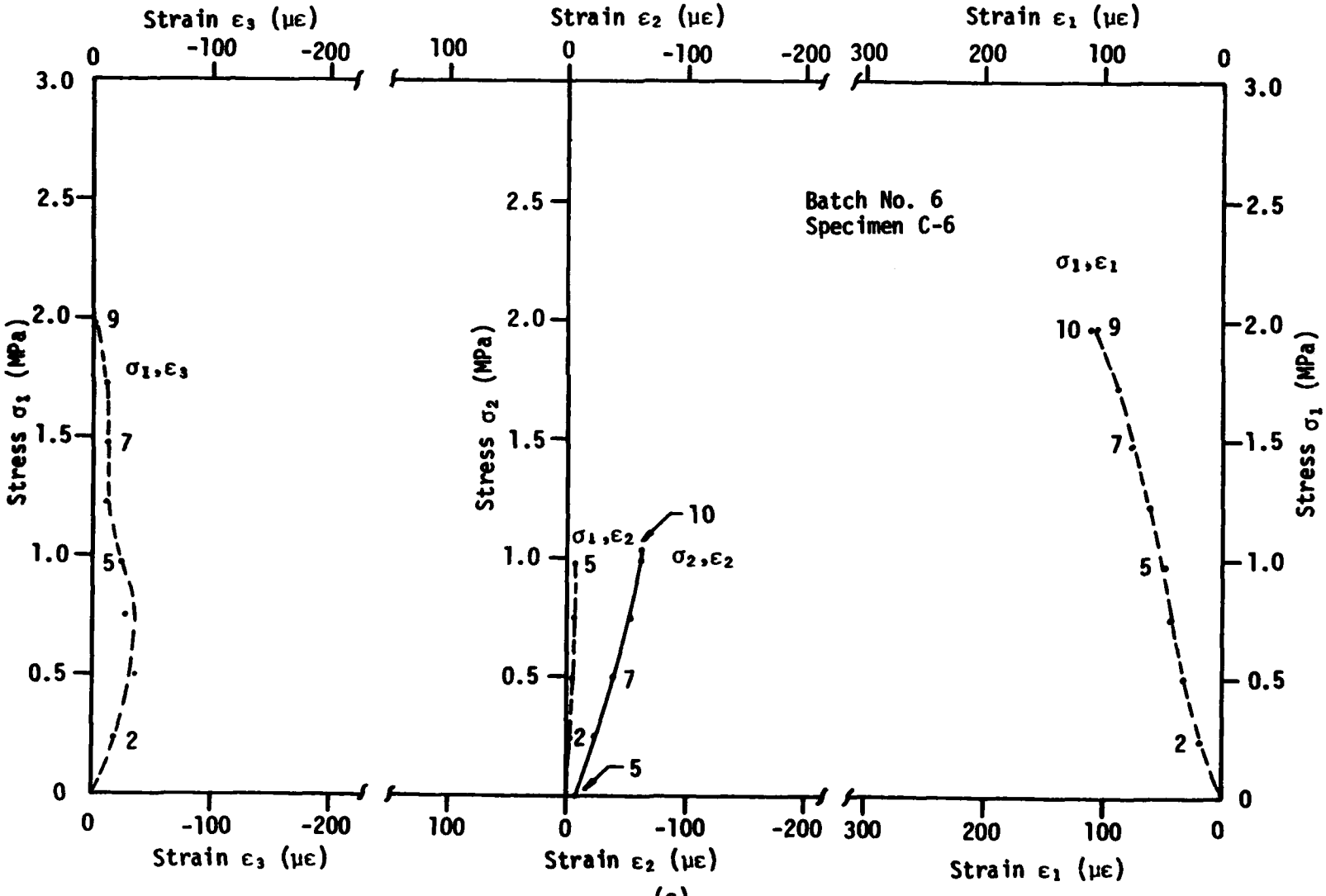

(c)

Figure C5. Continued.

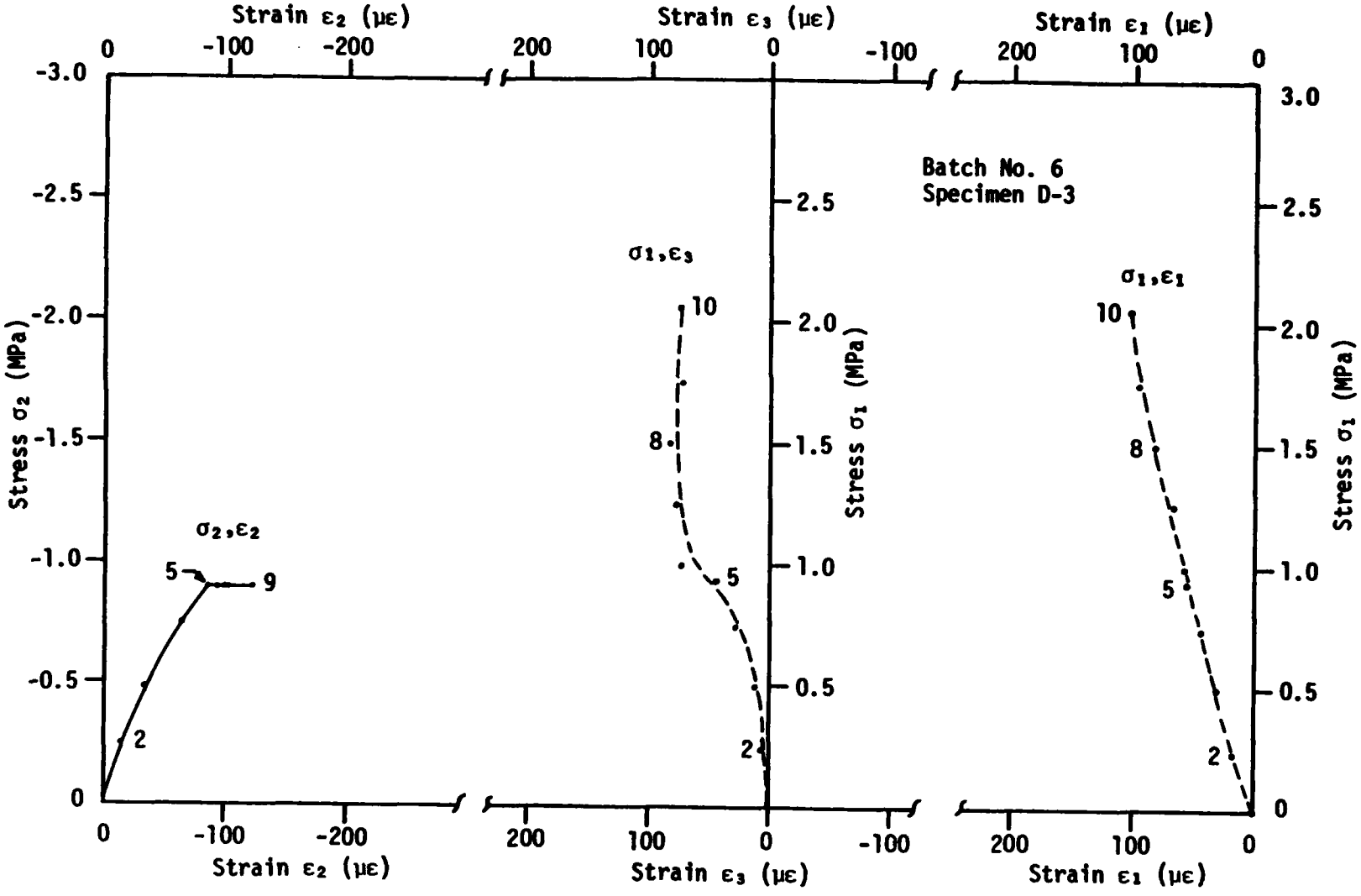

(a)

Figure C6. Load path 6 of stress paths involving tension.

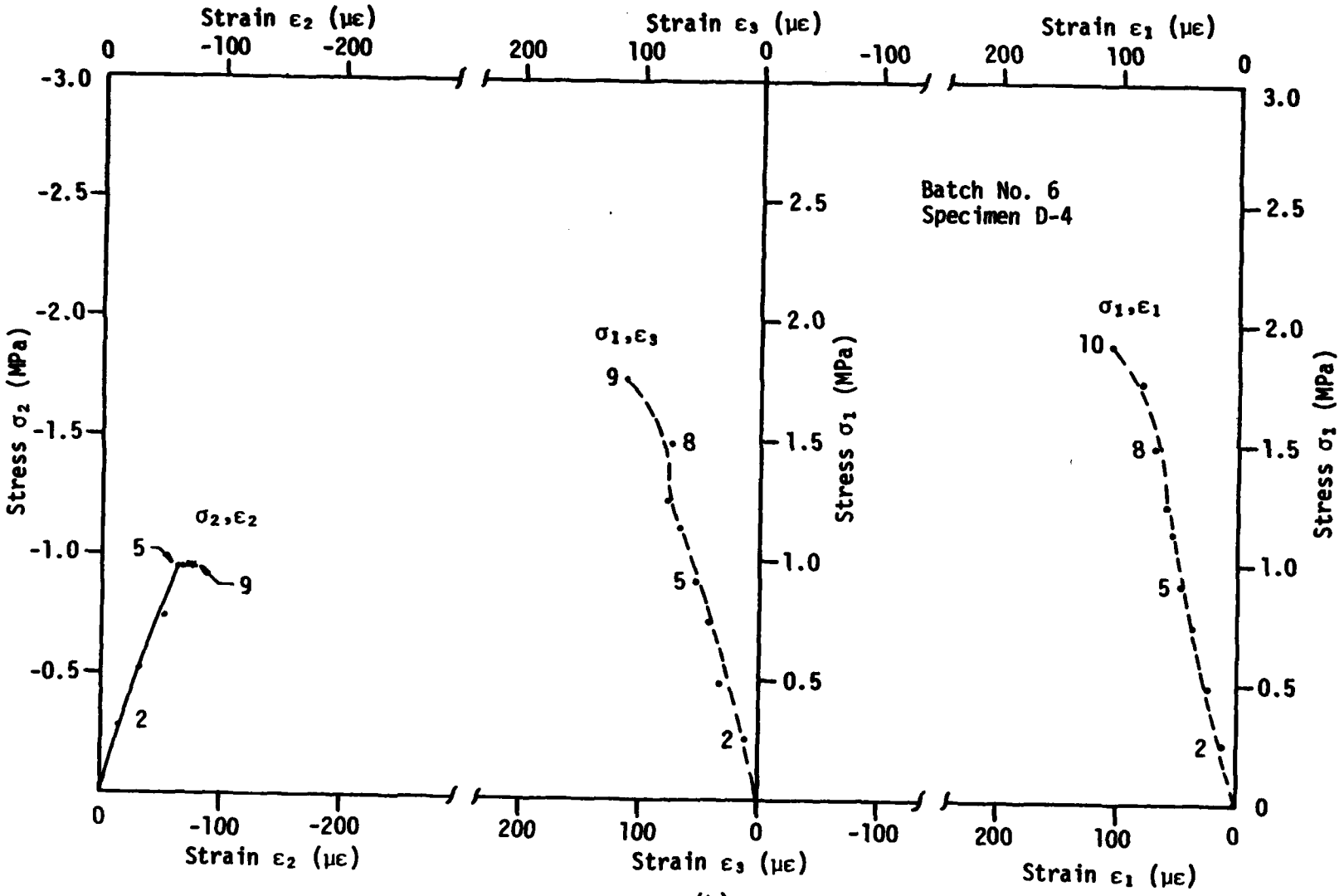

(b)

Figure C6. Continued.

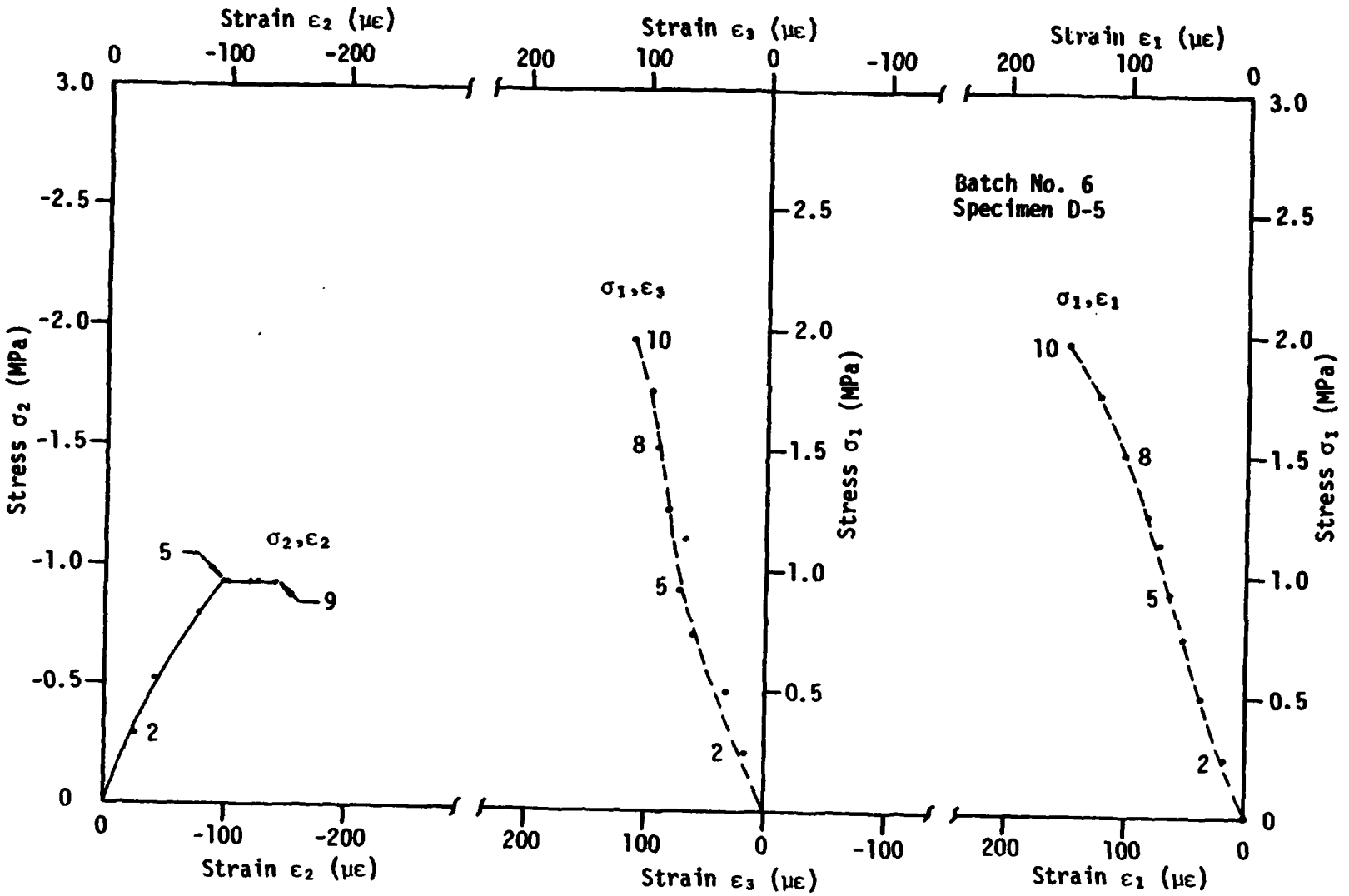

(c)

Figure C6. Continued.

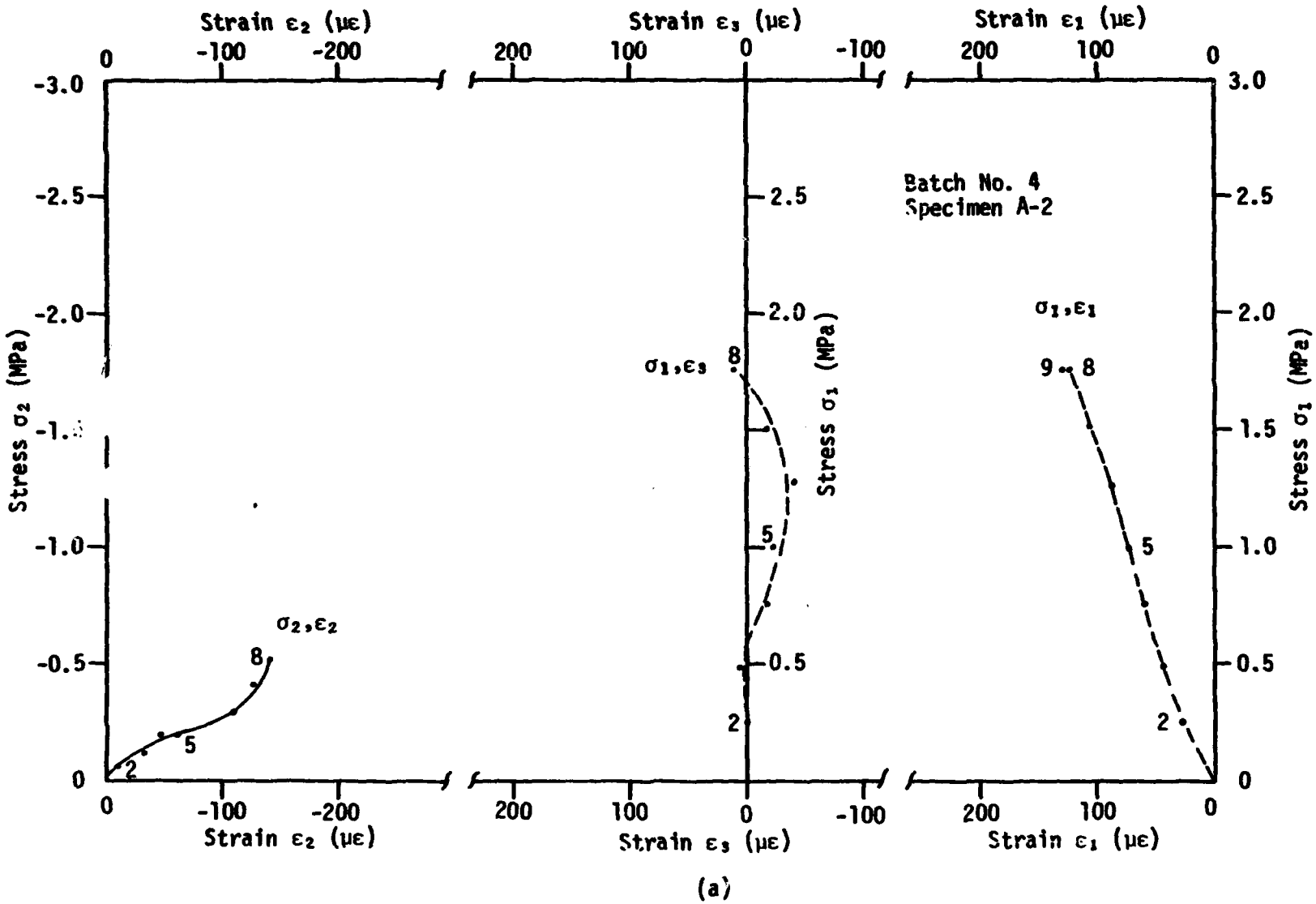

Figure C7. Load path 7 of stress paths involving tension.

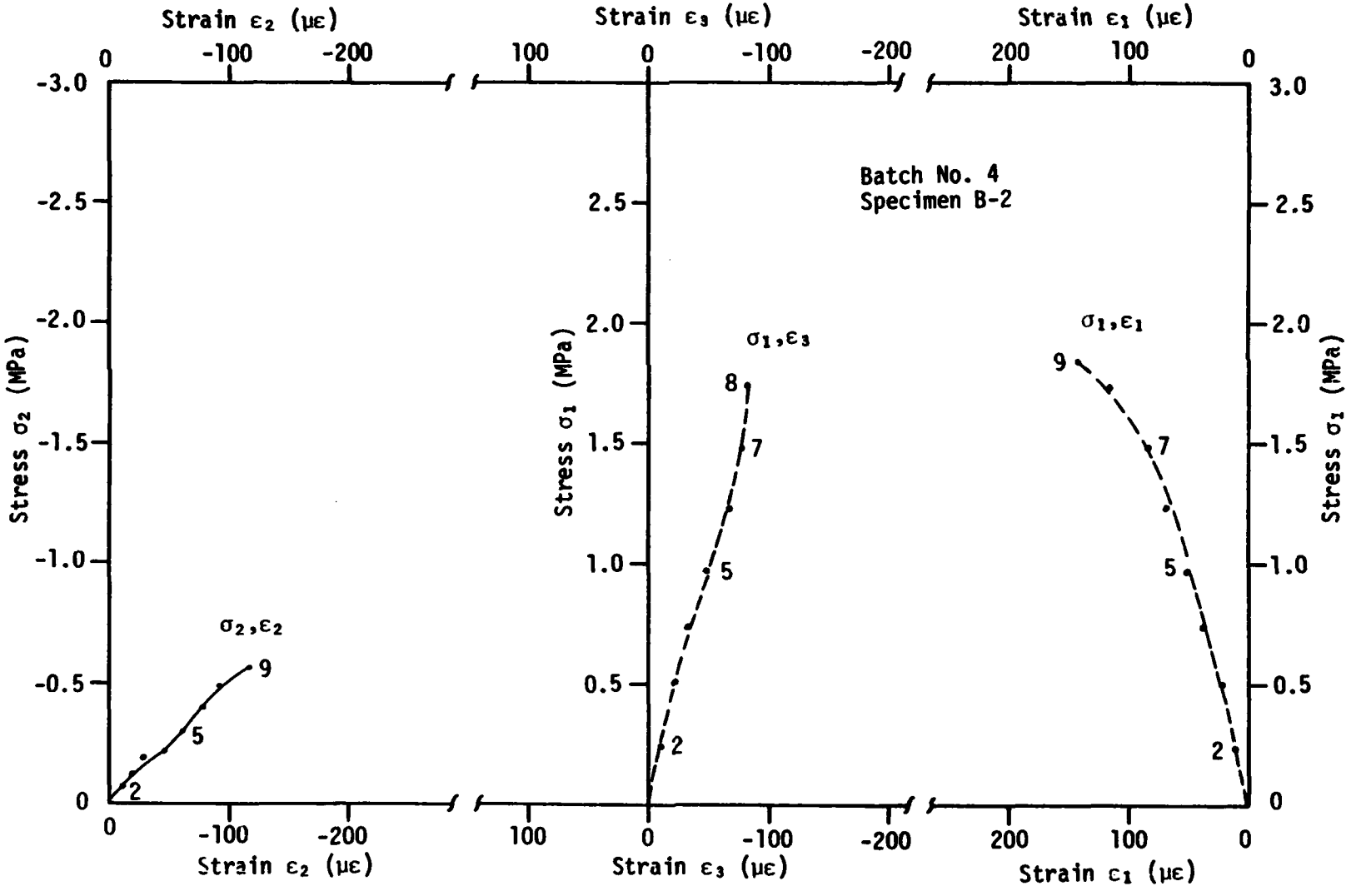

(b)

Figure C7. Continued.

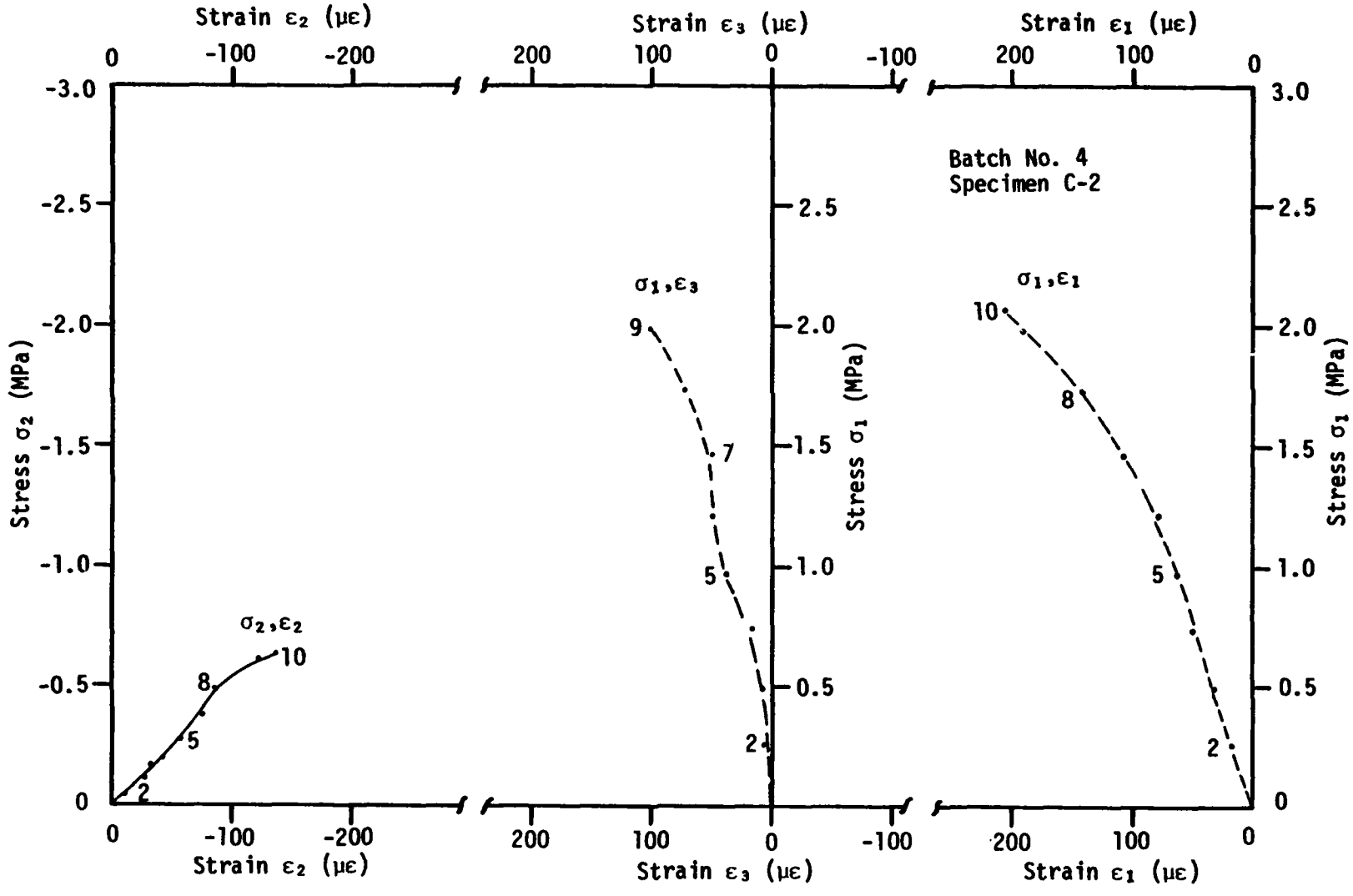

(c)

Figure C7. Continued.

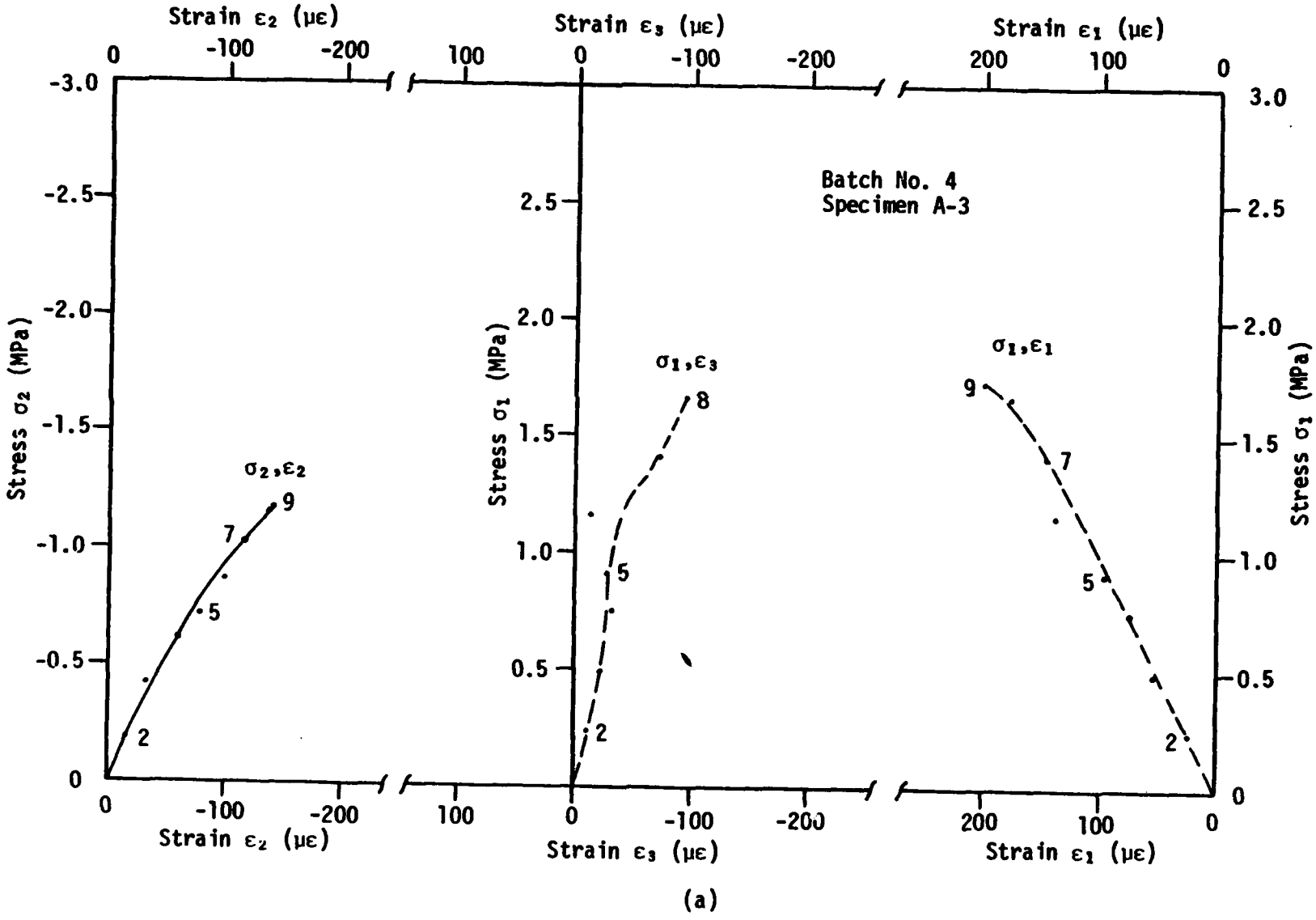

Figure C8. Load path 8 of stress paths involving tension.

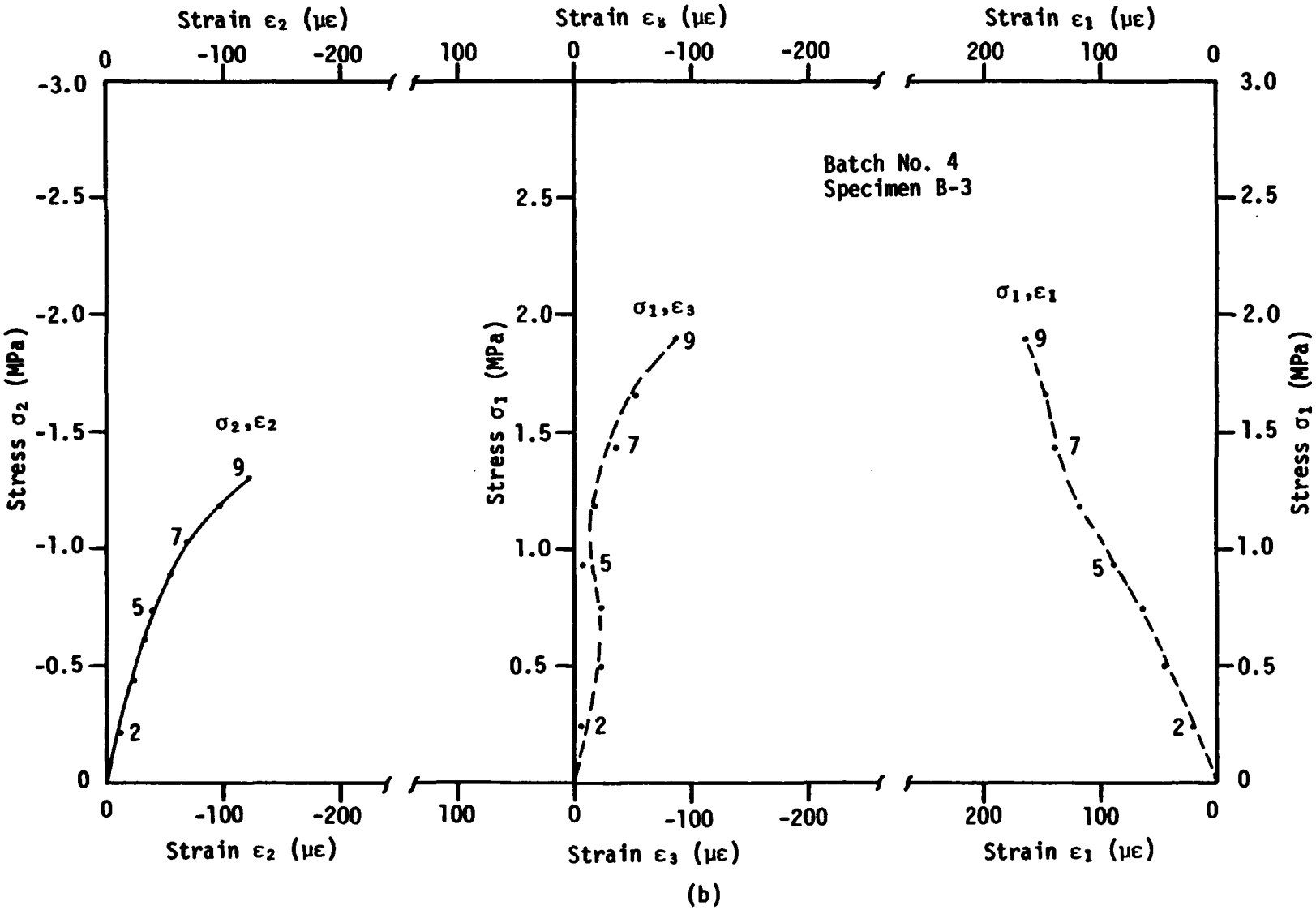

(b)

Figure C8. Continued.

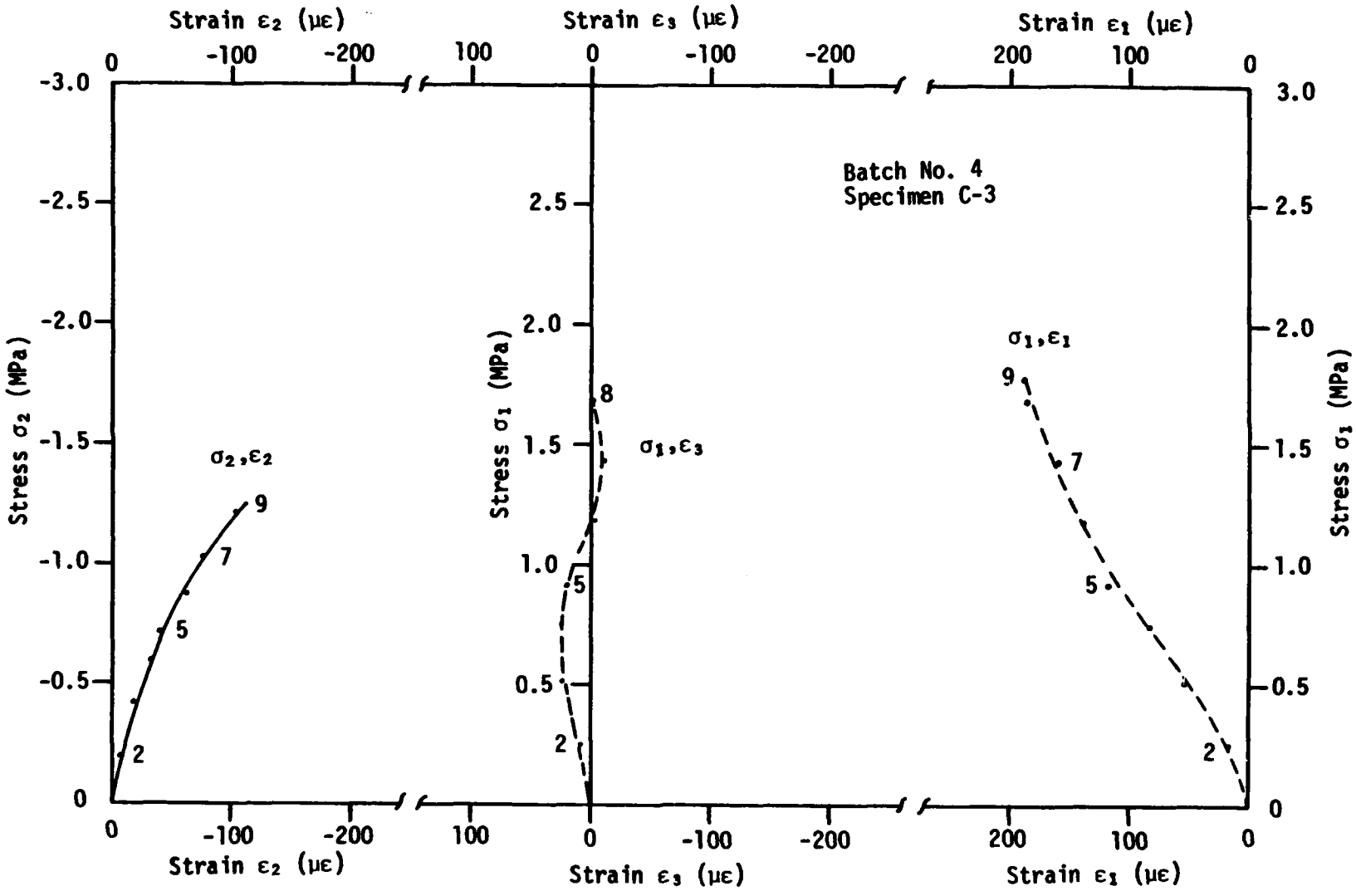

(c)

Figure C8. Continued.

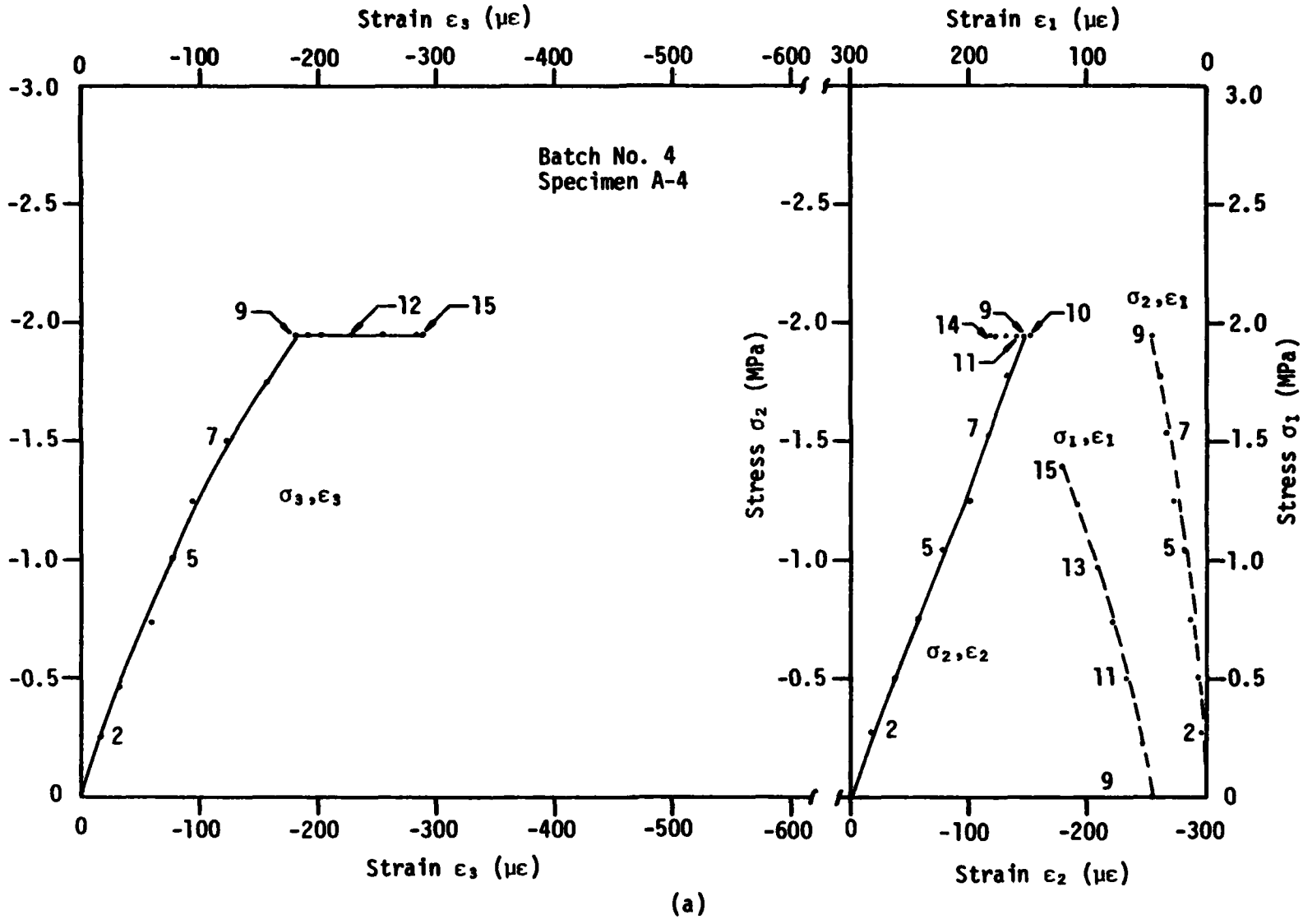

(a)

Figure C9. Load path 9 of stress paths involving tension.

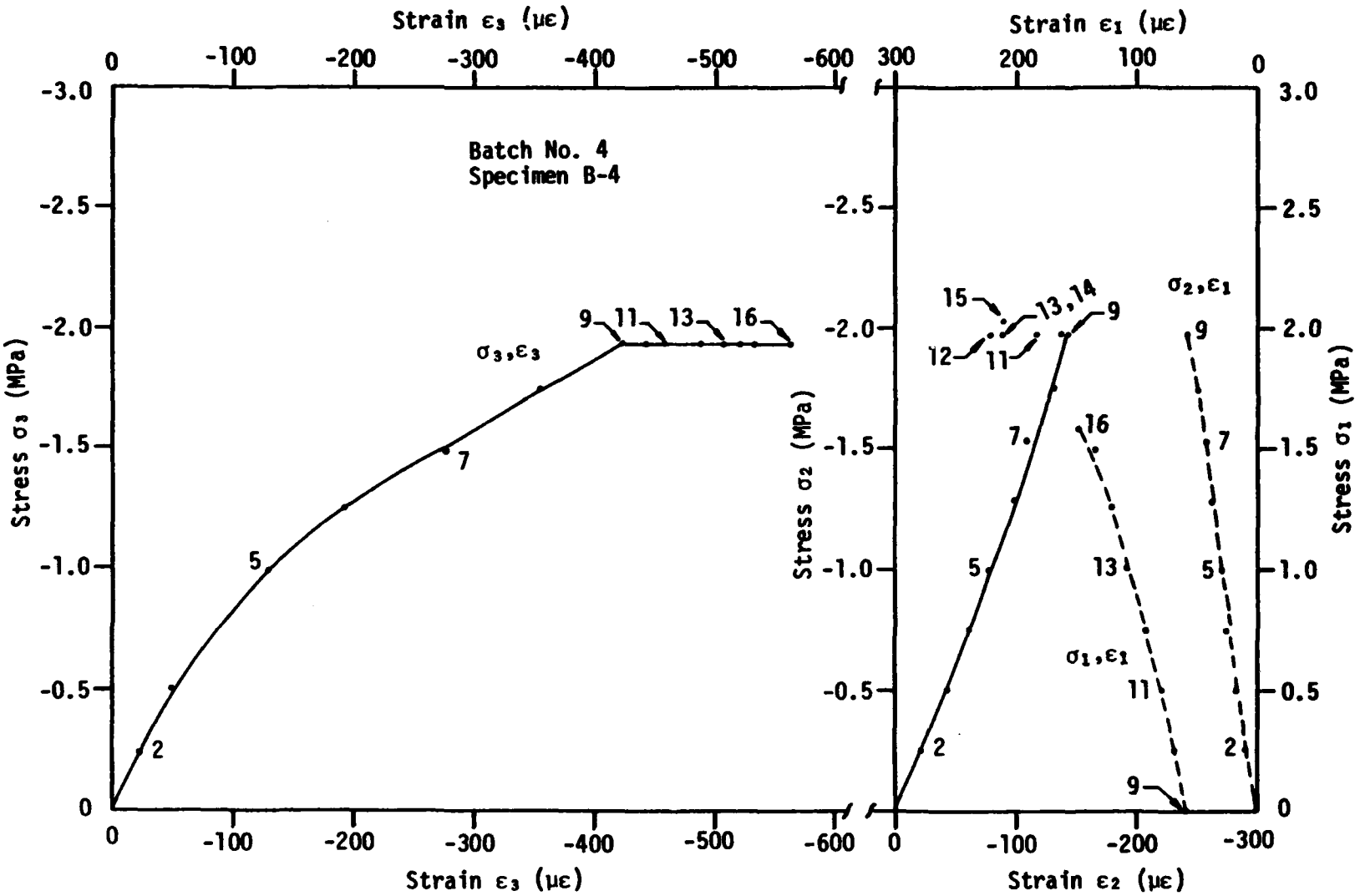

(b)

Figure C9. Continued.

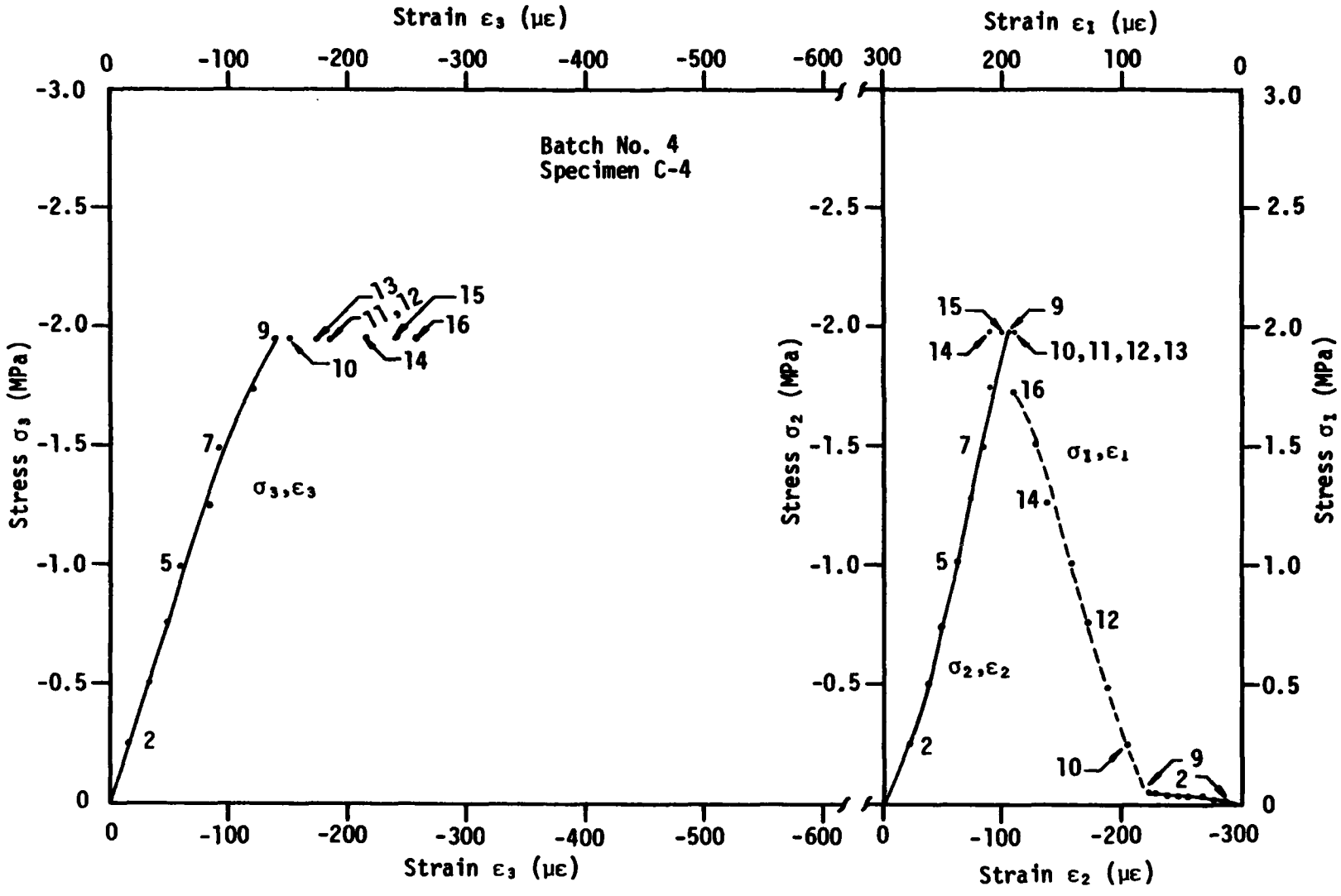

(c)

Figure C9. Continued.

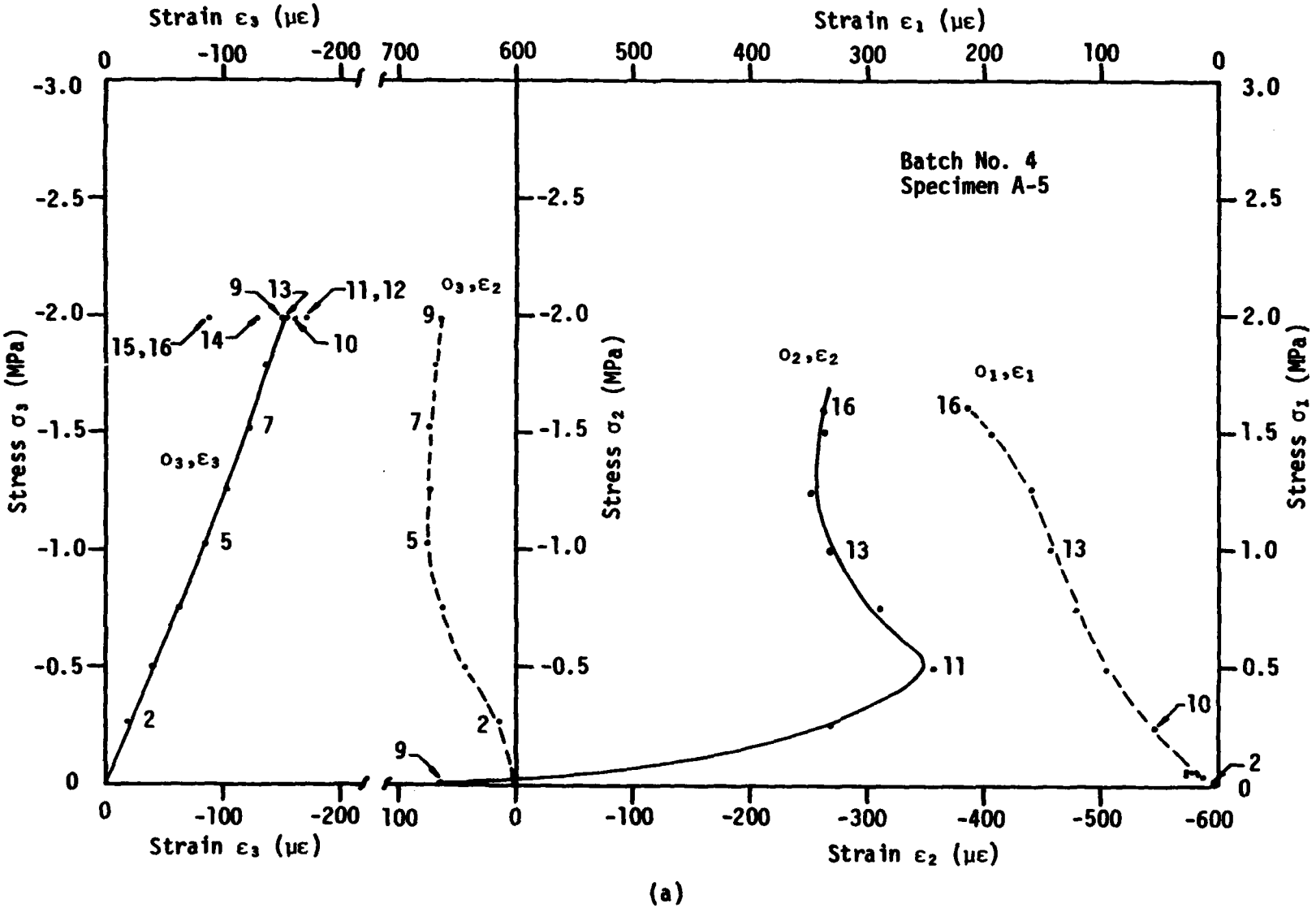

(a)

Figure C10. Stress path 10 of stress paths involving tension.

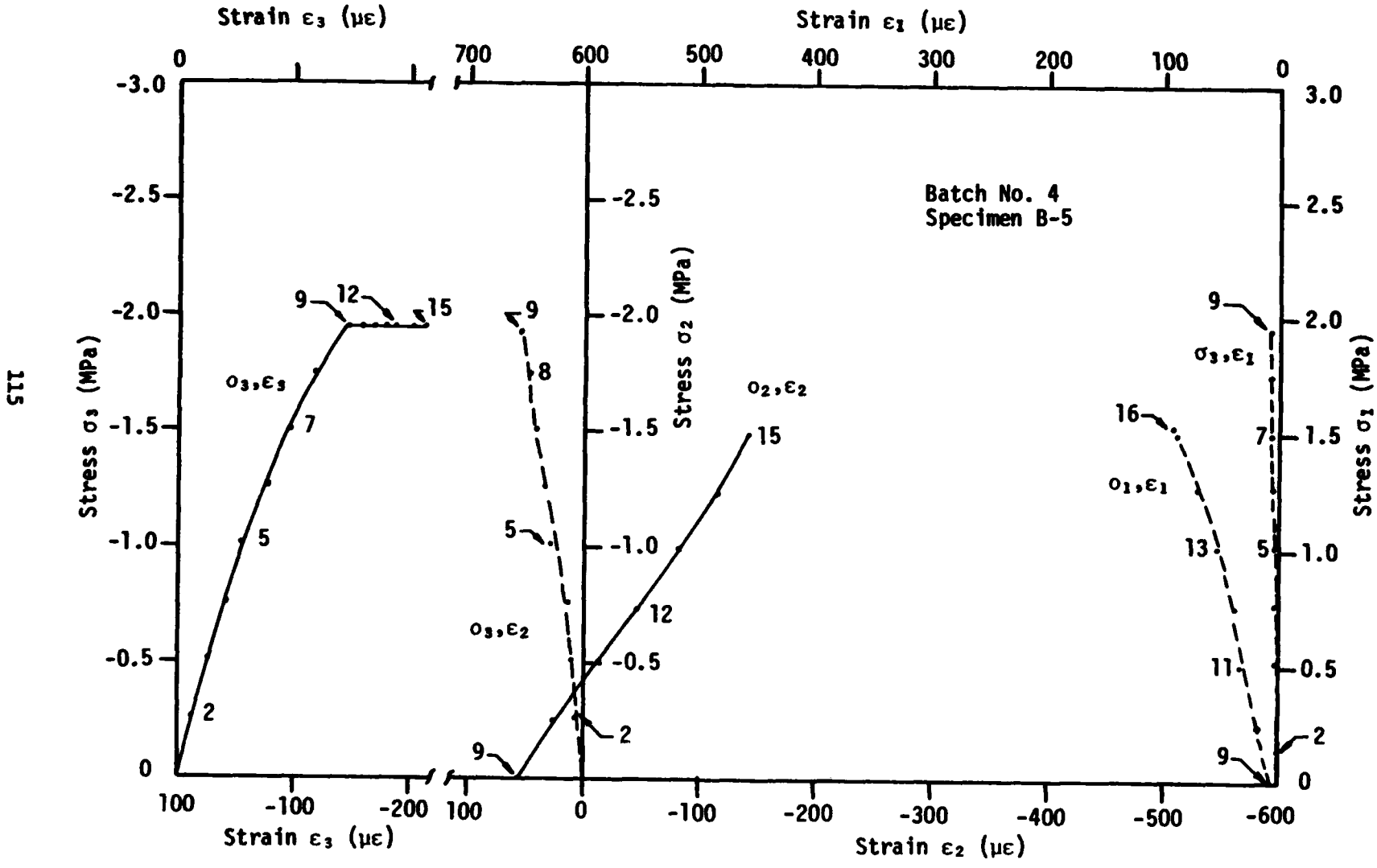

(b)

Figure C10. Continued.

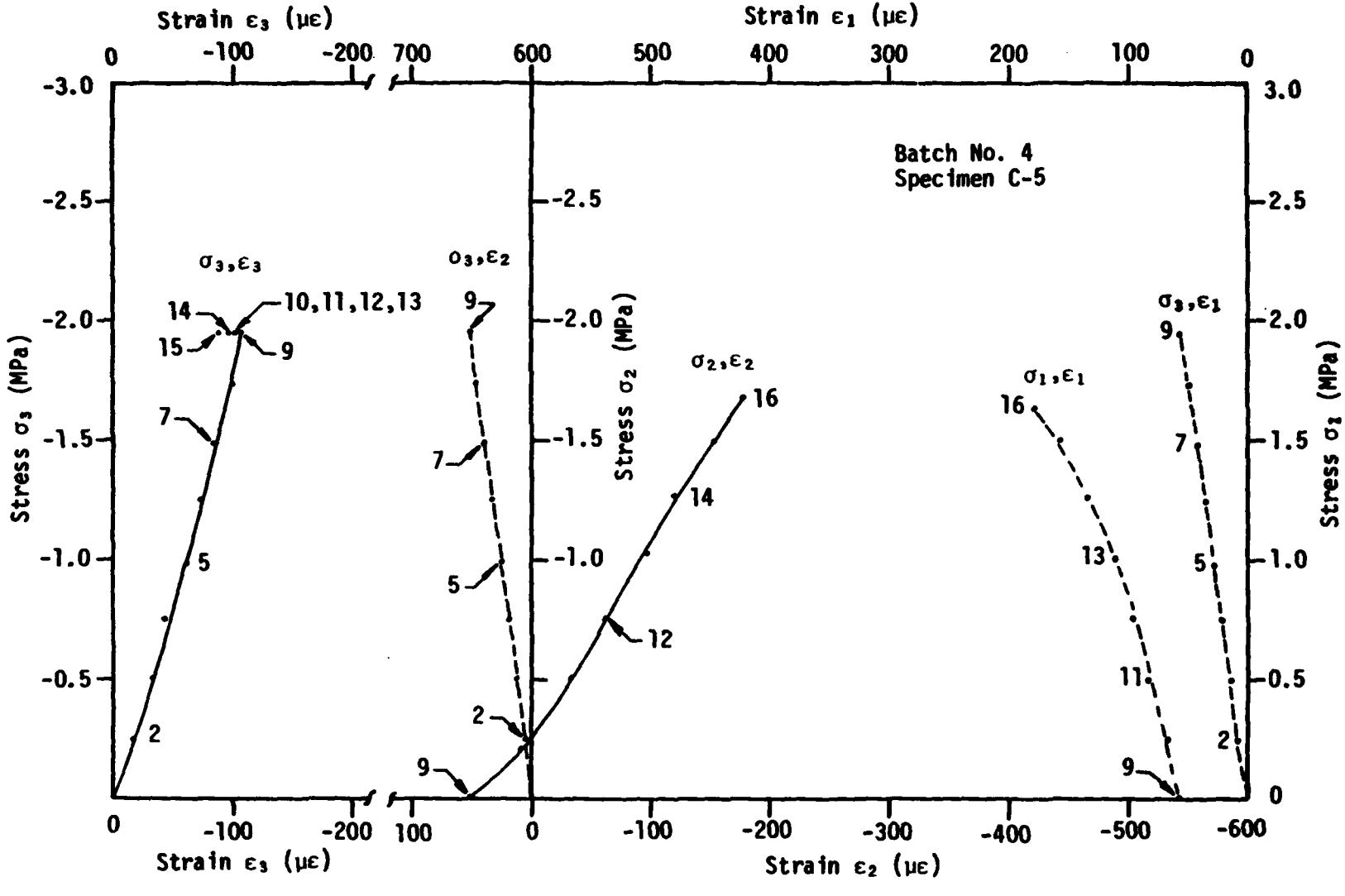

(c)

Figure C10. Continued.

APPENDIX D

CONCRETE CYLINDER TESTS

G. Krishnamoorthy
Professor of Civil Engineering and Engineering Mechanics
San Diego State University
April 1982

Load-deformation plots are shown for conventional cylindrical specimens that were provided by NMERI to San Diego State University. These specimens were made from the same batches used by New Mexico State University. The results serve as a link between experiments on a cubical specimen and traditional experiments on cylindrical specimens.

CONCRETE CYLINDER TESTING

TEST APPARATUS : 300,000 lb. capacity screw-actuated
Riehle machine

DATA ACQUISITION SYSTEM : Two 250 mil LVDT's
Two 50 mil LVDT's
Load Cell and LVDT amplifier and signal
Conditioning module
Averaging module
Two HP X-Y recorders

LOADING RATE : Machine running idle, 0.05 inch/min (ASTM:C39)

FORCE-DEFLECTION PLOTS : Two force-deflection curves were obtained for each specimen. In one, the side LVDT's (250 mil) were averaged and used as the abscissa (Figs 2 thru 25), while in the other the front and back LVDT's (50 mil) were averaged (Figs 26 thru 48).

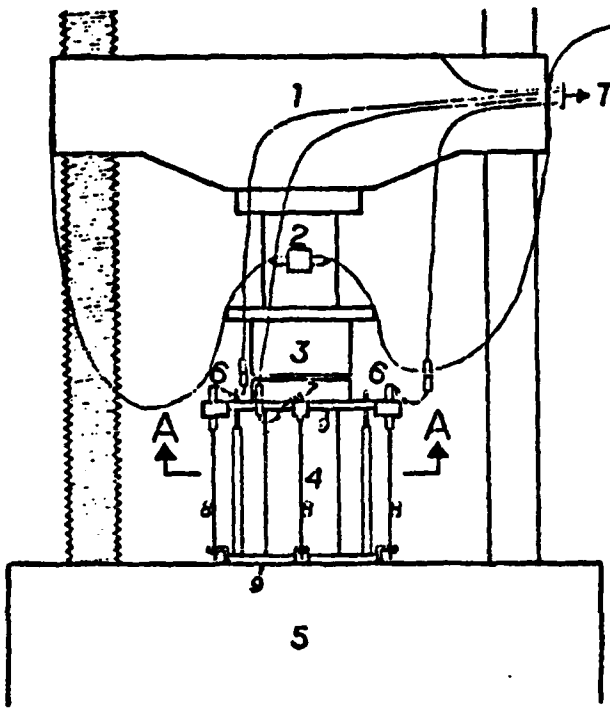

1 - moving cross head

2 - load cell

3 - spherical head

4 - concrete cylinder

5 - fixed base

6 - .250 inch LVDT

7 - .050 inch LVDT

8 - LVDT rod

9 - 1/2" steel plate

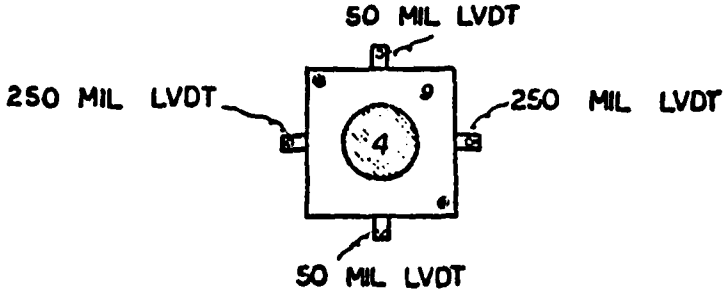

SECTION A-A

FIGURE 1 - TEST SET-UP

SUMMARY OF TEST RESULTS

BATCH NO.	SPECIMEN NO.	TYPE OF LOADING	STRENGTH PSI	INITIAL MODULUS LB/IN^2 10^{+6}
3/31/81	1	MONOTONIC	3837.4	1.78
	2	"	3806.5	1.66
	3	CYCLIC	3492.6	1.96
	4	"	3607.5	1.80
	MEAN		3686.0	1.80
	ST. DEV.		164.3	.12
3/26/81	1	MONOTONIC	3741.9	1.86
	2	"	3741.9	1.75
	3	CYCLIC	4007.6	2.01
	4	"	3961.2	1.86
	MEAN		3863.2	1.87
	ST. DEV.		141.3	.11
3/30/81	1	MONOTONIC	3724.2	2.23
	2	"	3618.1	1.88
	3	CYCLIC	3791.0	2.08
	4	"	3873.5	2.04
	MEAN		3751.7	2.06
	ST. DEV.		108.0	.14
3/27/81	1	MONOTONIC	2991.4 *	1.99
	2	"	3695.2	2.10
	3	"	3522.6	1.90
	4	CYCLIC	3744.6	1.71
	MEAN		3654.1	1.93
	ST. DEV.		116.6	.17

NOTE: No's with (*) not included in calculating the mean and standard deviation.

BATCH NO.	SPECIMEN NO.	TYPE OF LOADING	STRENGTH PSI	INITIAL MODULUS LB/IN^2 10^{+6}
4/1/81	1	MONOTONIC	3455.8	1.93
	2	"	3538.2	2.07
	3	CYCLIC	3512.4	2.21
	4	"	3264.8	1.81
	MEAN		3442.8	2.01
	ST. DEV.		123.6	.17
4/2/81	1	MONOTONIC	3507.4	2.22
	2	"	4007.5	2.34
	3	"	3450.5	2.01
	4	"	3857.9	3.19*
	MEAN		3705.8	2.19
	ST. DEV.		270.0	.17

NOTE: No's with (*) not included in calculating the mean and standard deviation.

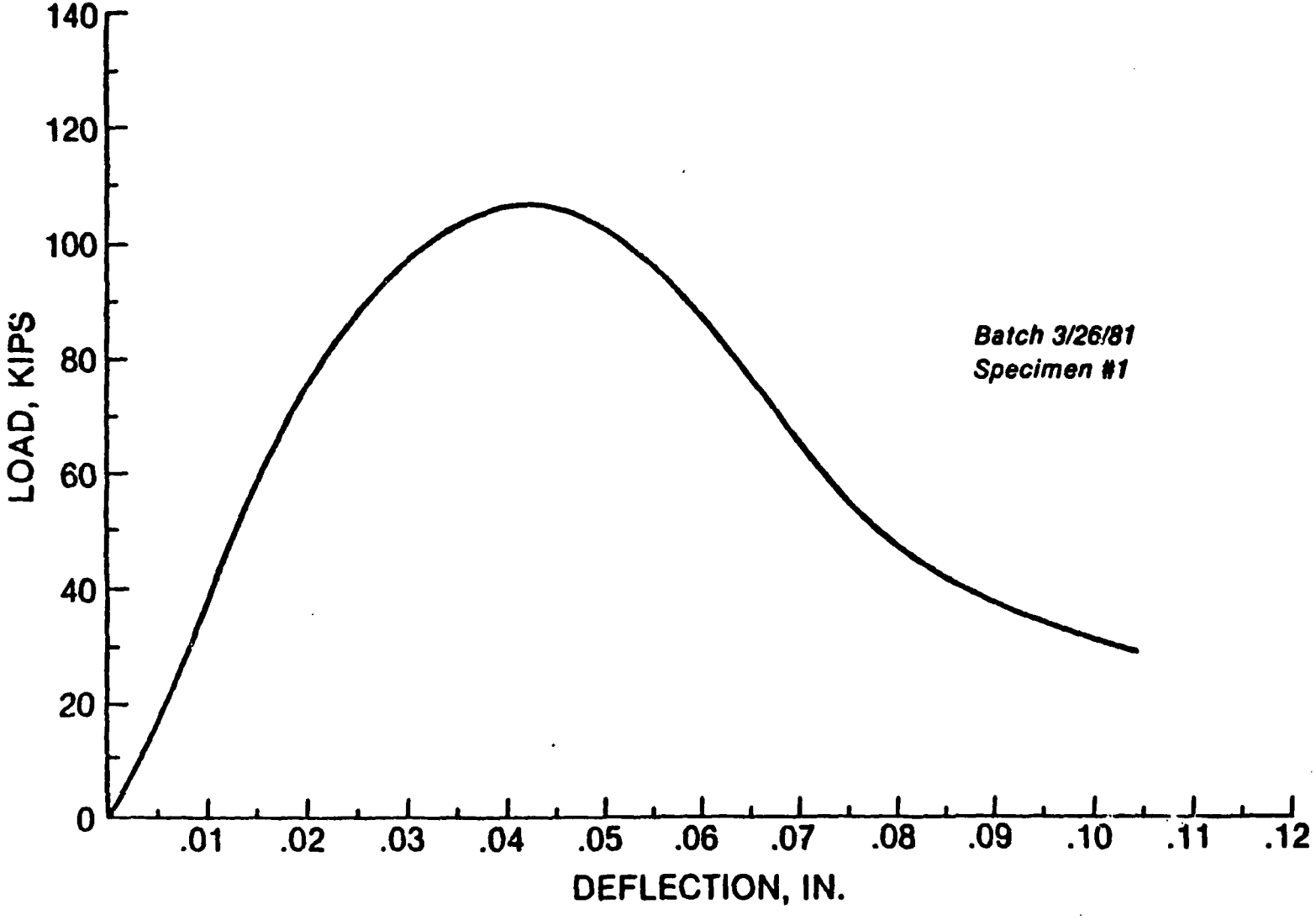
140
120
100
80
60
40
20
0
LOAD, KIPS
.01
.02
.03
.04
.05
.06
.07
.08
.09
.10
.11
.12
DEFLECTION, IN.
Batch 3/26/81
Specimen #1

FIGURE 2

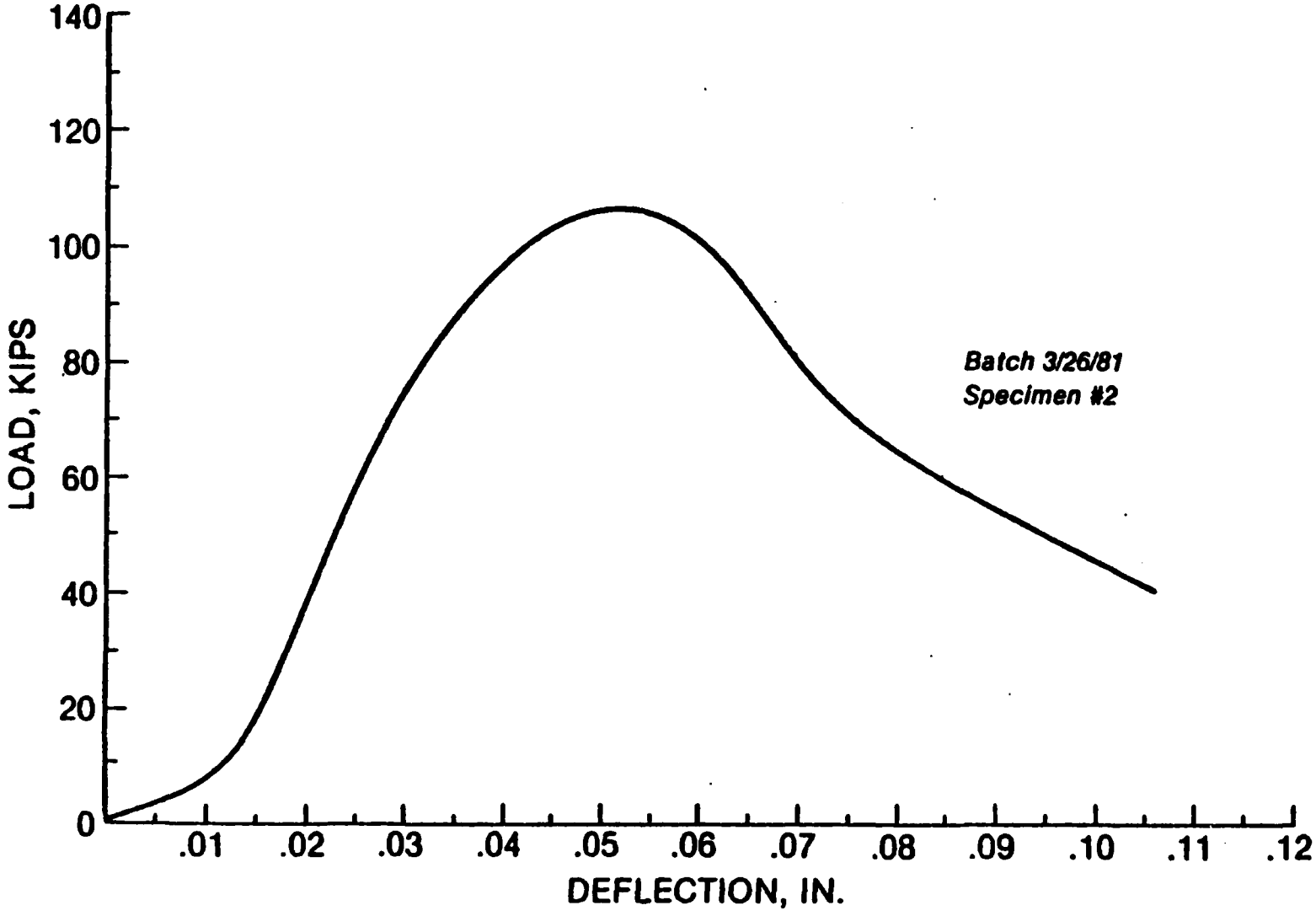
140
120
100
80
60
40
20
0
LOAD, KIPS
.01
.02
.03
.04
.05
.06
.07
.08
.09
.10
.11
.12
DEFLECTION, IN.
Batch 3/26/81
Specimen #2

FIGURE 3

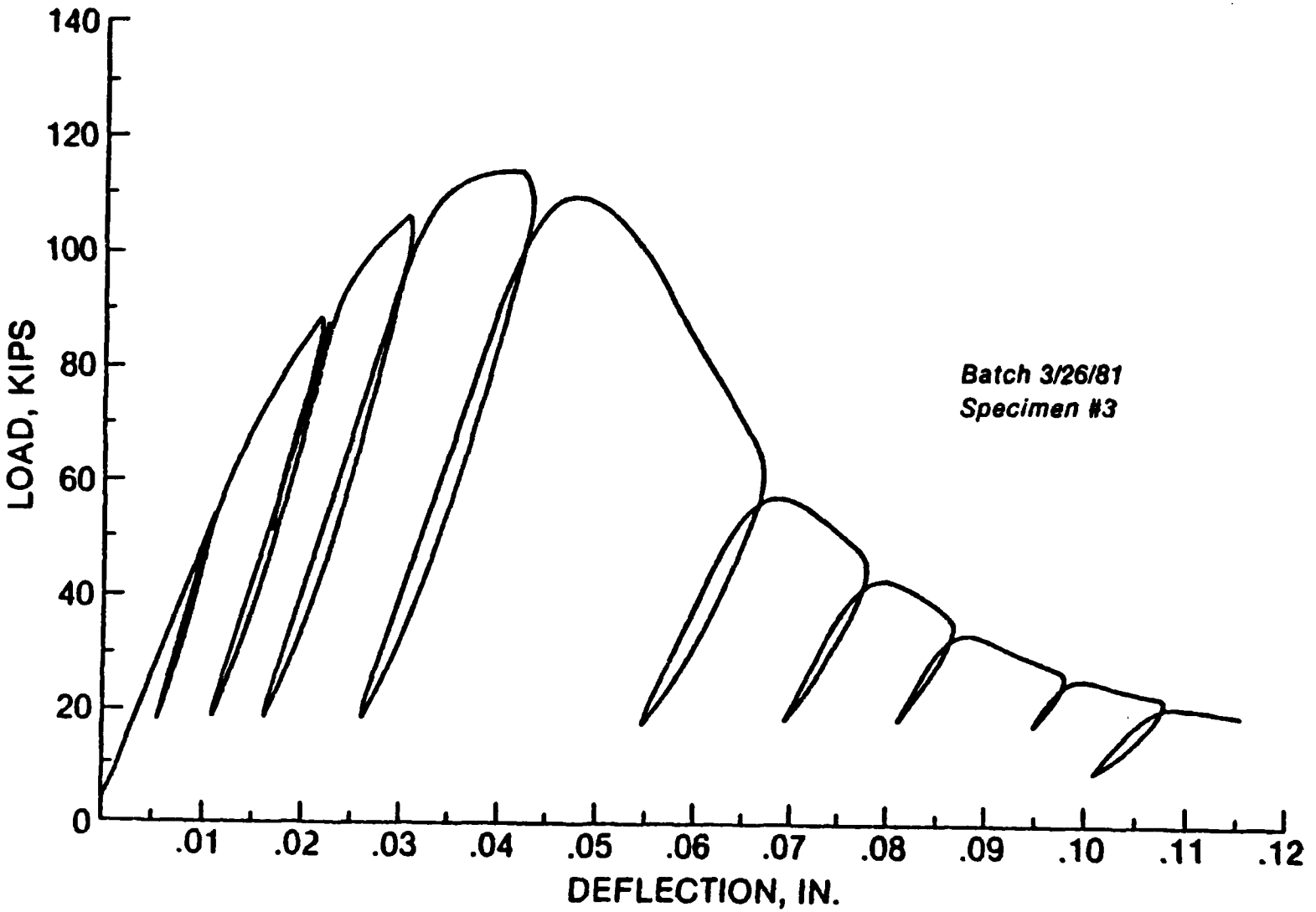
140
120
100
80
60
40
20
0
LOAD, KIPS
.01
.02
.03
.04
.05
.06
.07
.08
.09
.10
.11
.12
DEFLECTION, IN.
Batch 3/26/81
Specimen #3

Figure 4

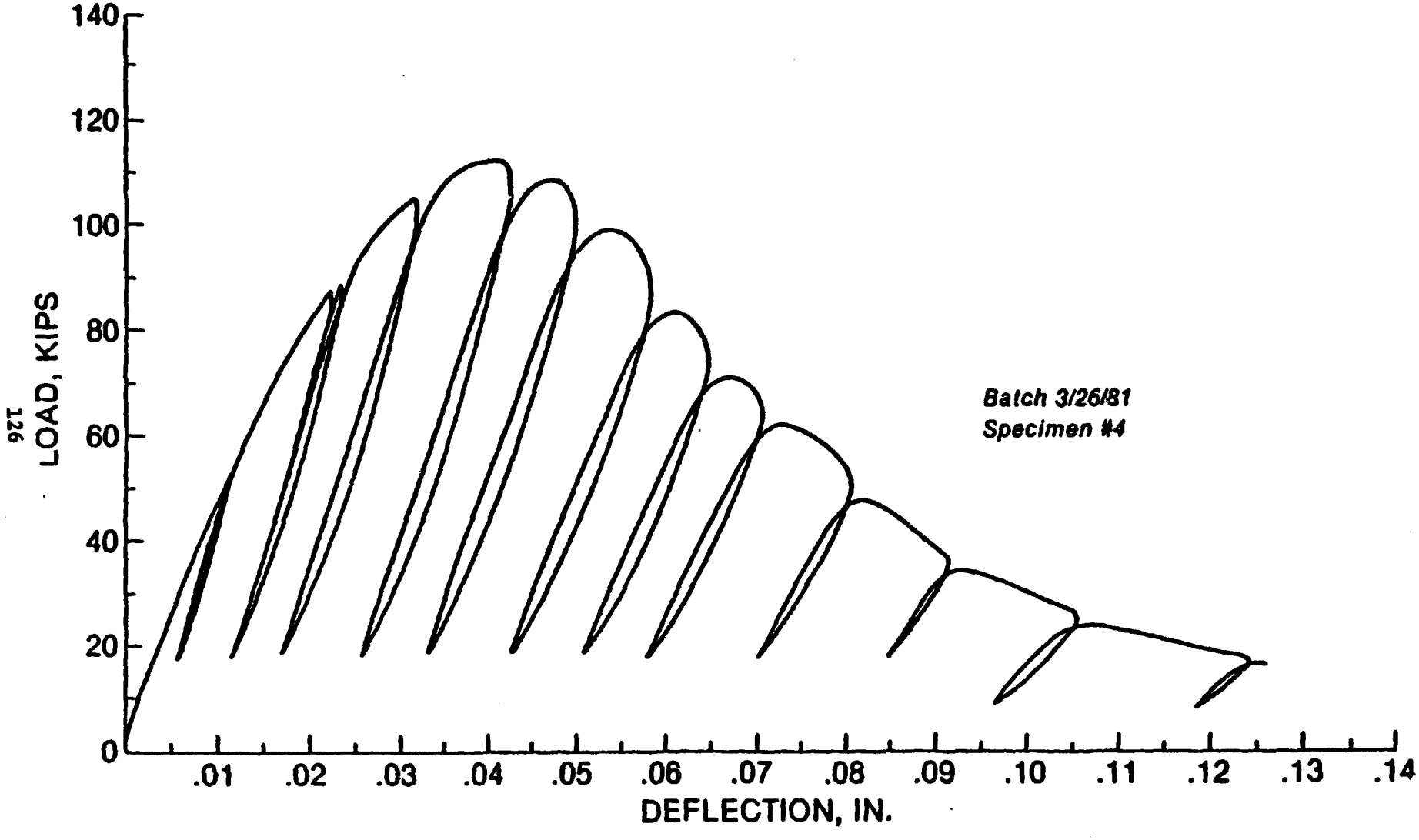
140
120
100
80
60
40
20
0
LOAD, KIPS
126
.01
.02
.03
.04
.05
.06
.07
.08
.09
.10
.11
.12
.13
.14
DEFLECTION, IN.
Batch 3/26/81
Specimen #4

Figure 5

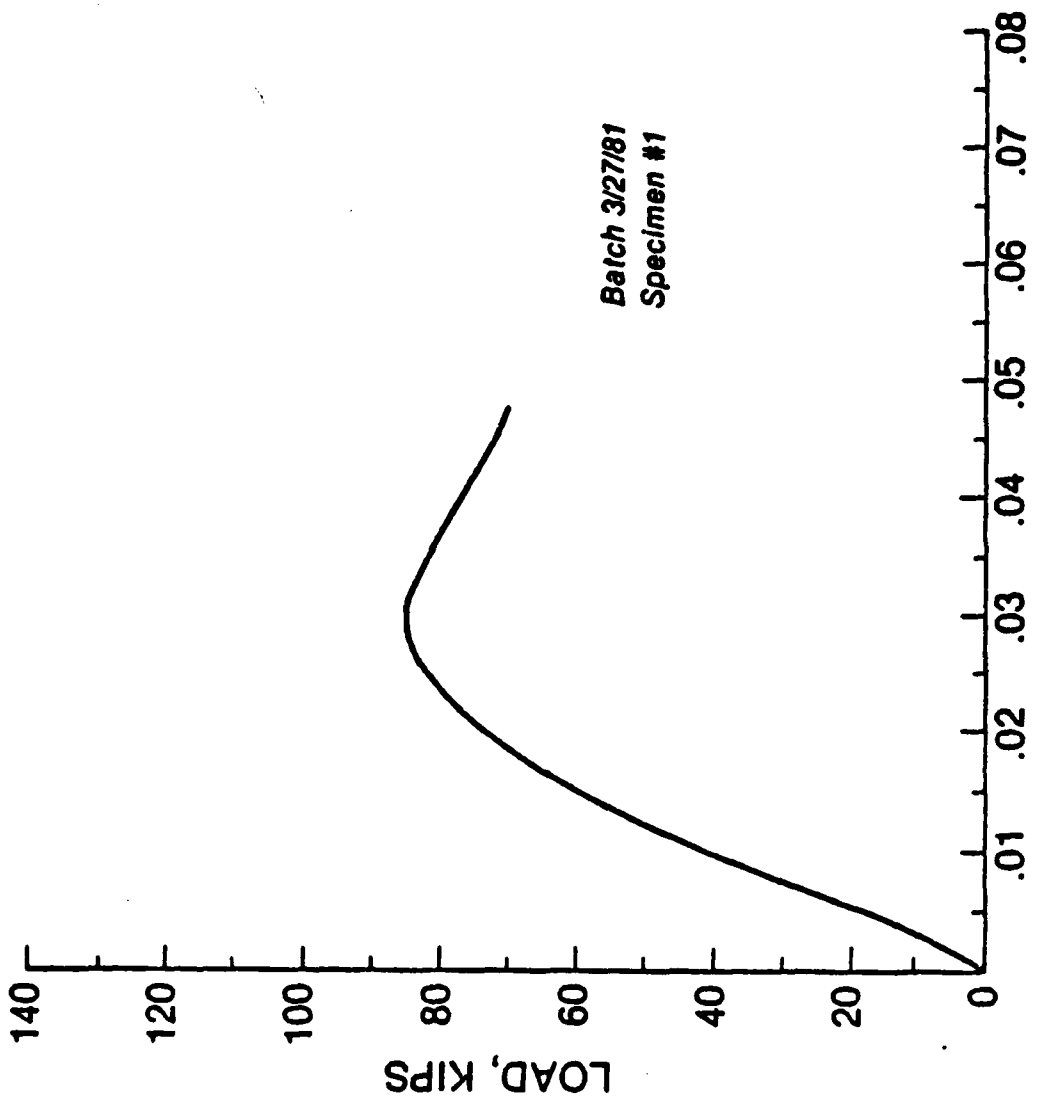
LOAD, KIPS
140
120
100
80
60
40
20
0
.01
.02
.03
.04
.05
.06
.07
.08
DEFLECTION, IN.
Batch 3/27/81
Specimen #1

Figure 6

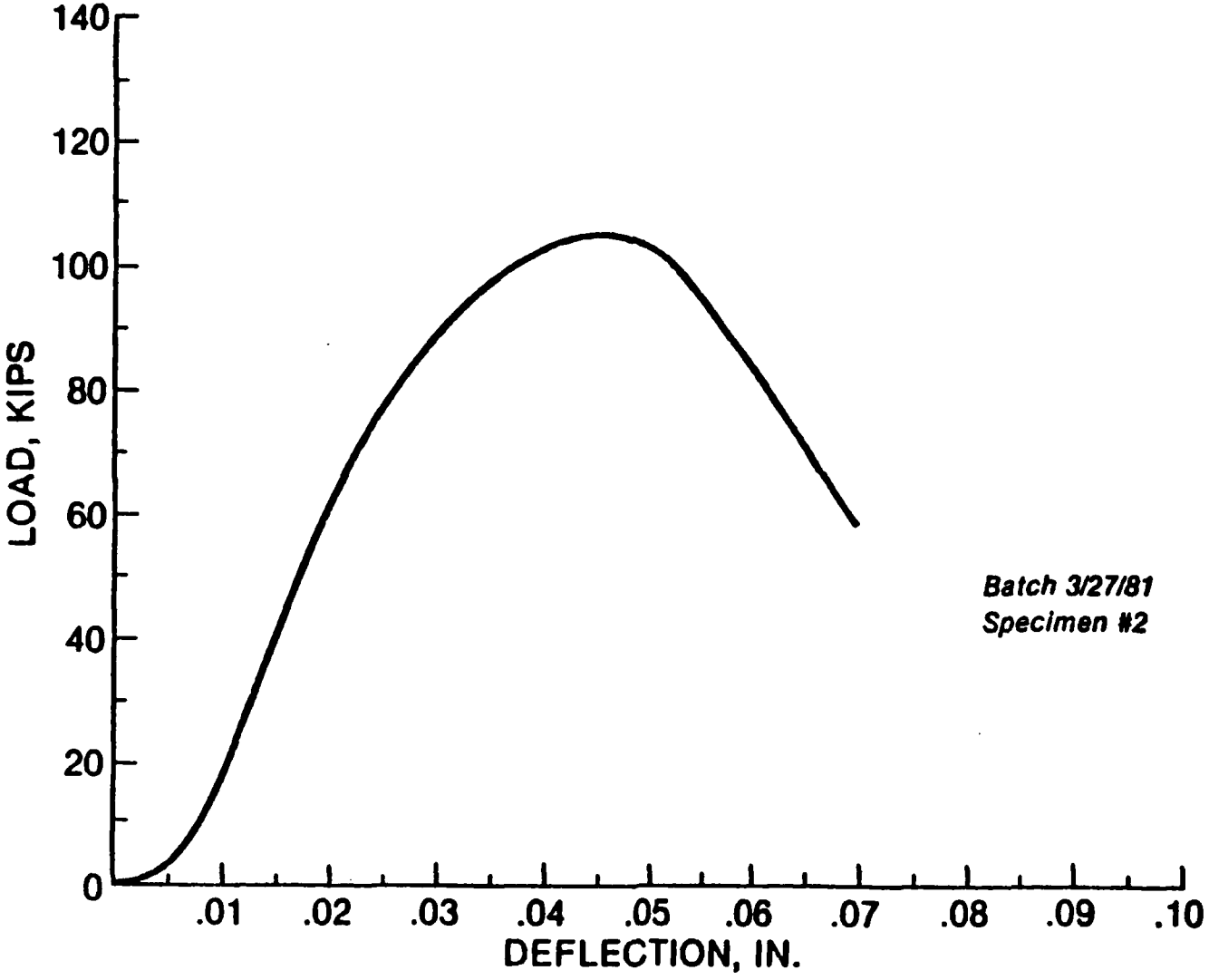
140
120
100
80
60
40
20
0
LOAD, KIPS
.01
.02
.03
.04
.05
.06
.07
.08
.09
.10
DEFLECTION, IN.
Batch 3/27/81
Specimen #2

Figure 7

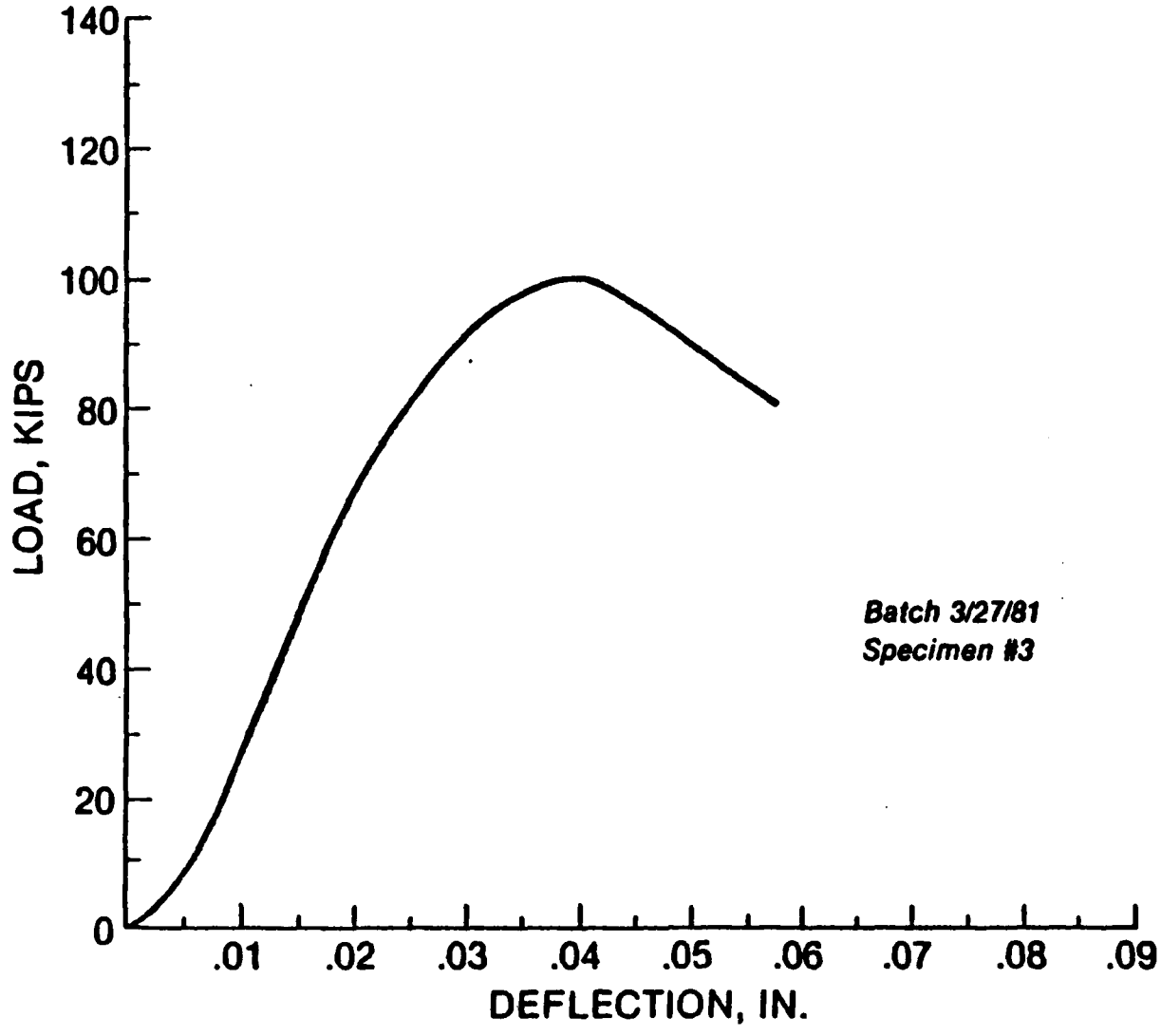
140
120
100
80
60
40
20
0
LOAD, KIPS
.01
.02
.03
.04
.05
.06
.07
.08
.09
DEFLECTION, IN.
Batch 3/27/81
Specimen #3

Figure 8

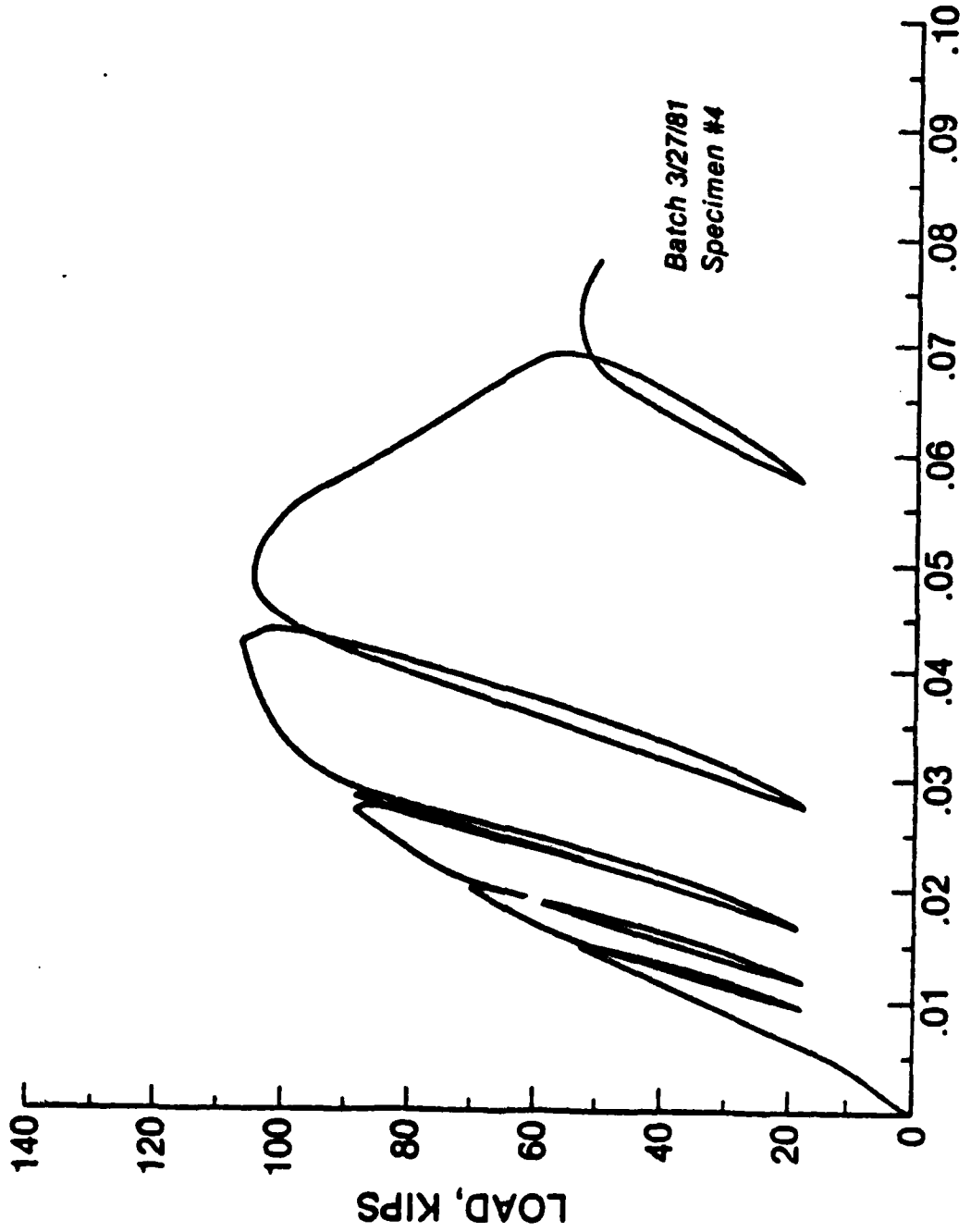
LOAD, KIPS
140
120
100
80
60
40
20
0
.01
.02
.03
.04
.05
.06
.07
.08
.09
.10
DEFLECTION, IN.
Batch 3/27/81
Specimen #4

Figure 9

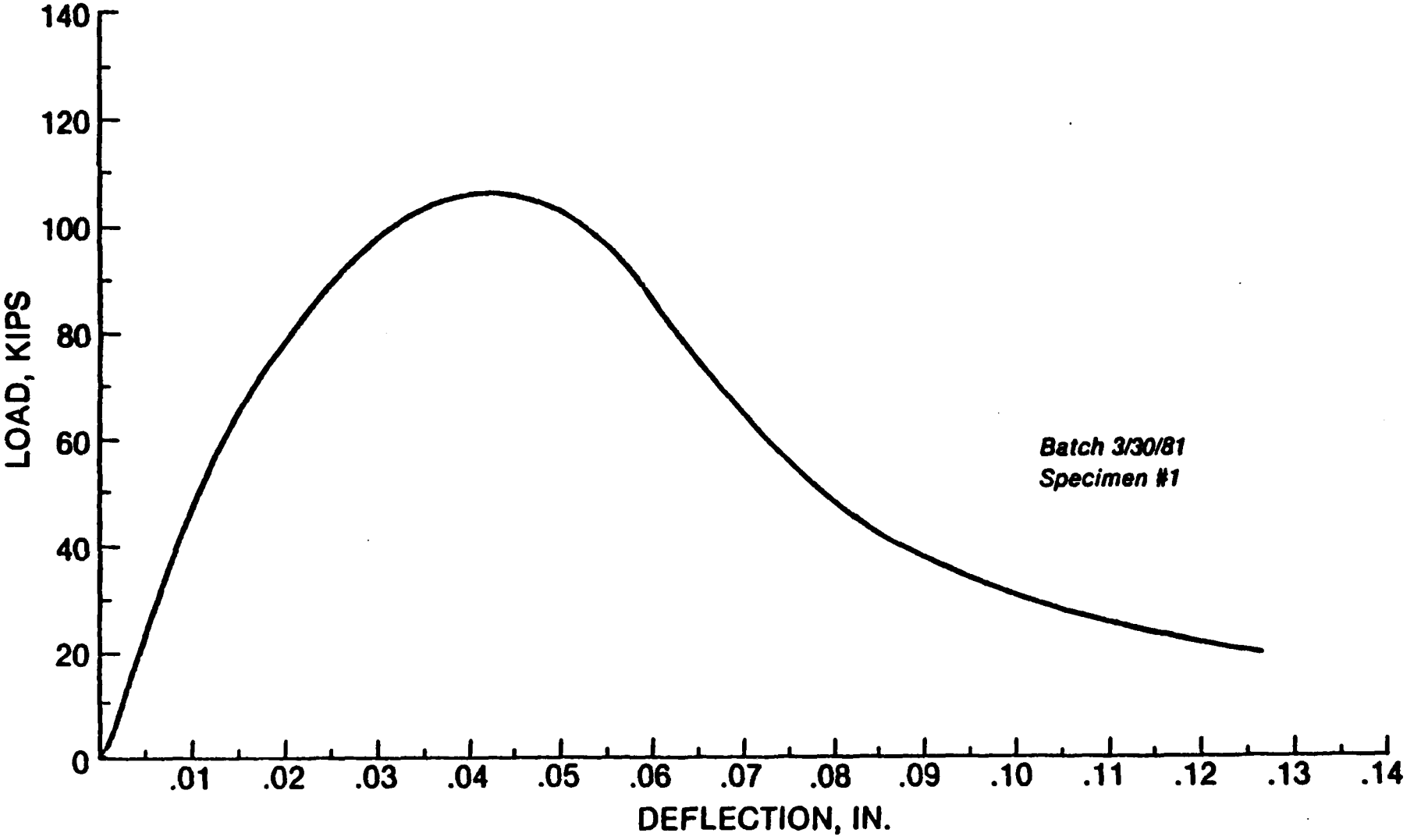
140
120
100
80
60
40
20
0
LOAD, KIPS
.01
.02
.03
.04
.05
.06
.07
.08
.09
.10
.11
.12
.13
.14
DEFLECTION, IN.
Batch 3/30/81
Specimen #1

Figure 10

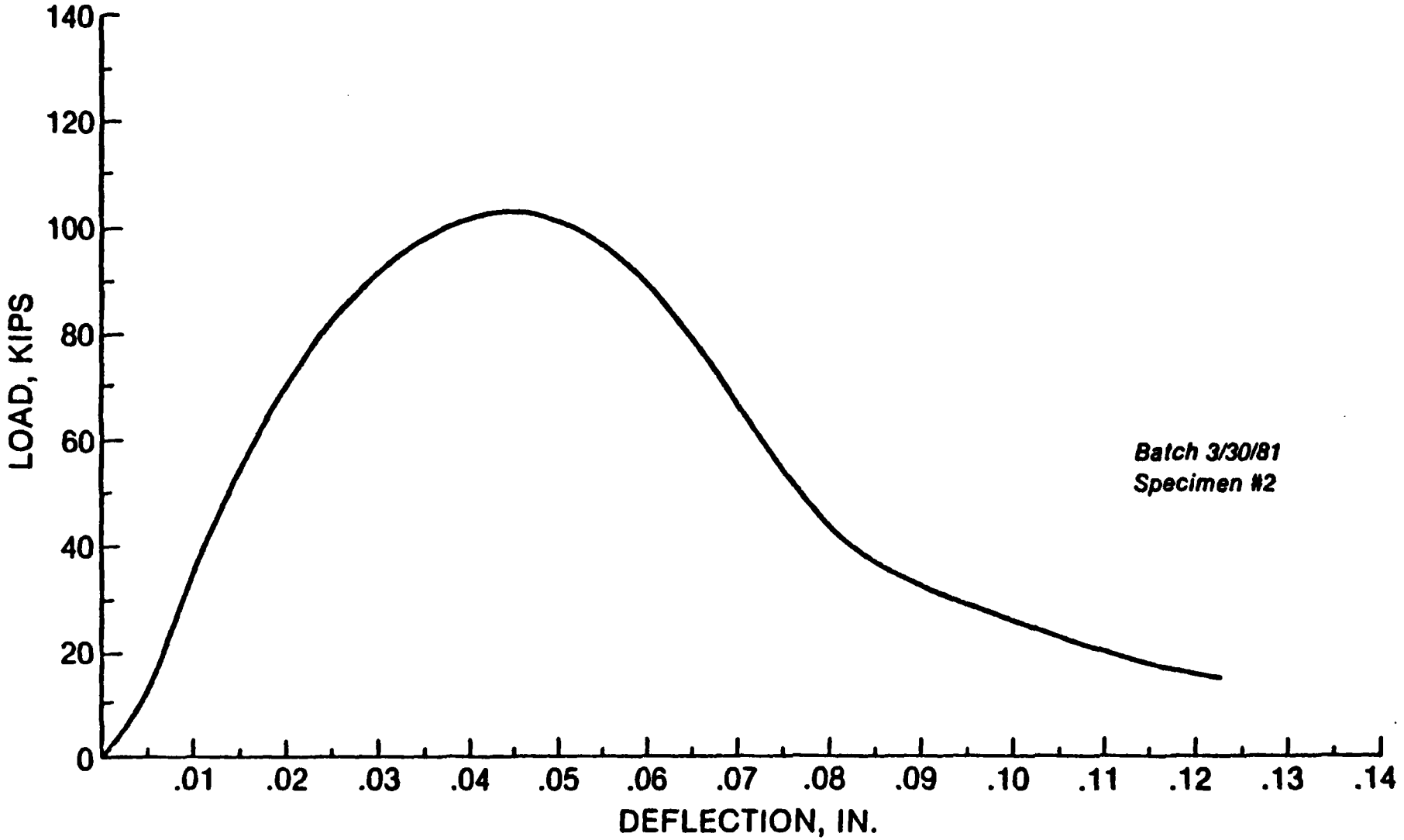
140
120
100
80
60
40
20
0
LOAD, KIPS
.01
.02
.03
.04
.05
.06
.07
.08
.09
.10
.11
.12
.13
.14
DEFLECTION, IN.
Batch 3/30/81
Specimen #2

Figure 11

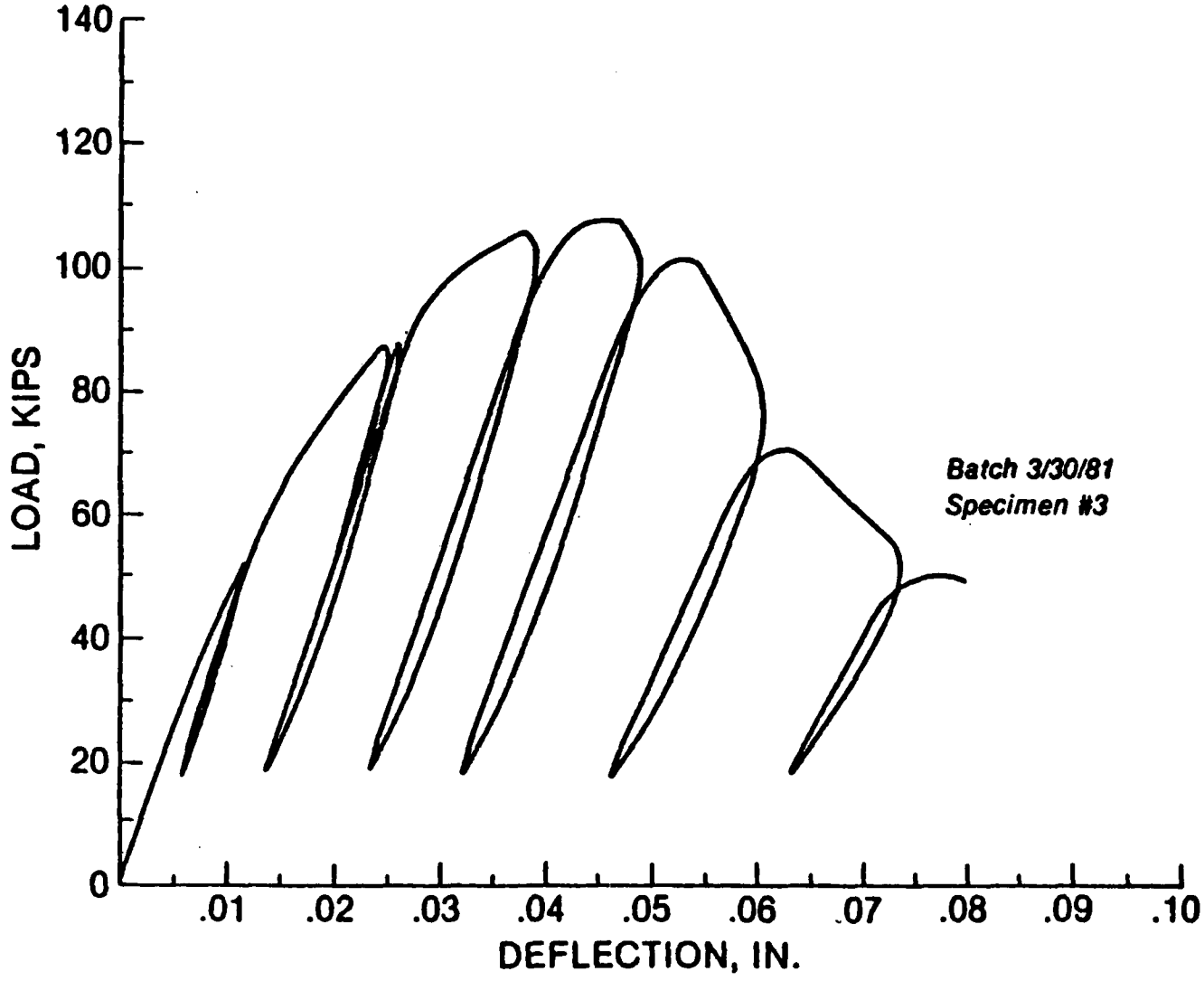
140
120
100
80
60
40
20
0
LOAD, KIPS
.01
.02
.03
.04
.05
.06
.07
.08
.09
.10
DEFLECTION, IN.
Batch 3/30/81
Specimen #3

Figure 12

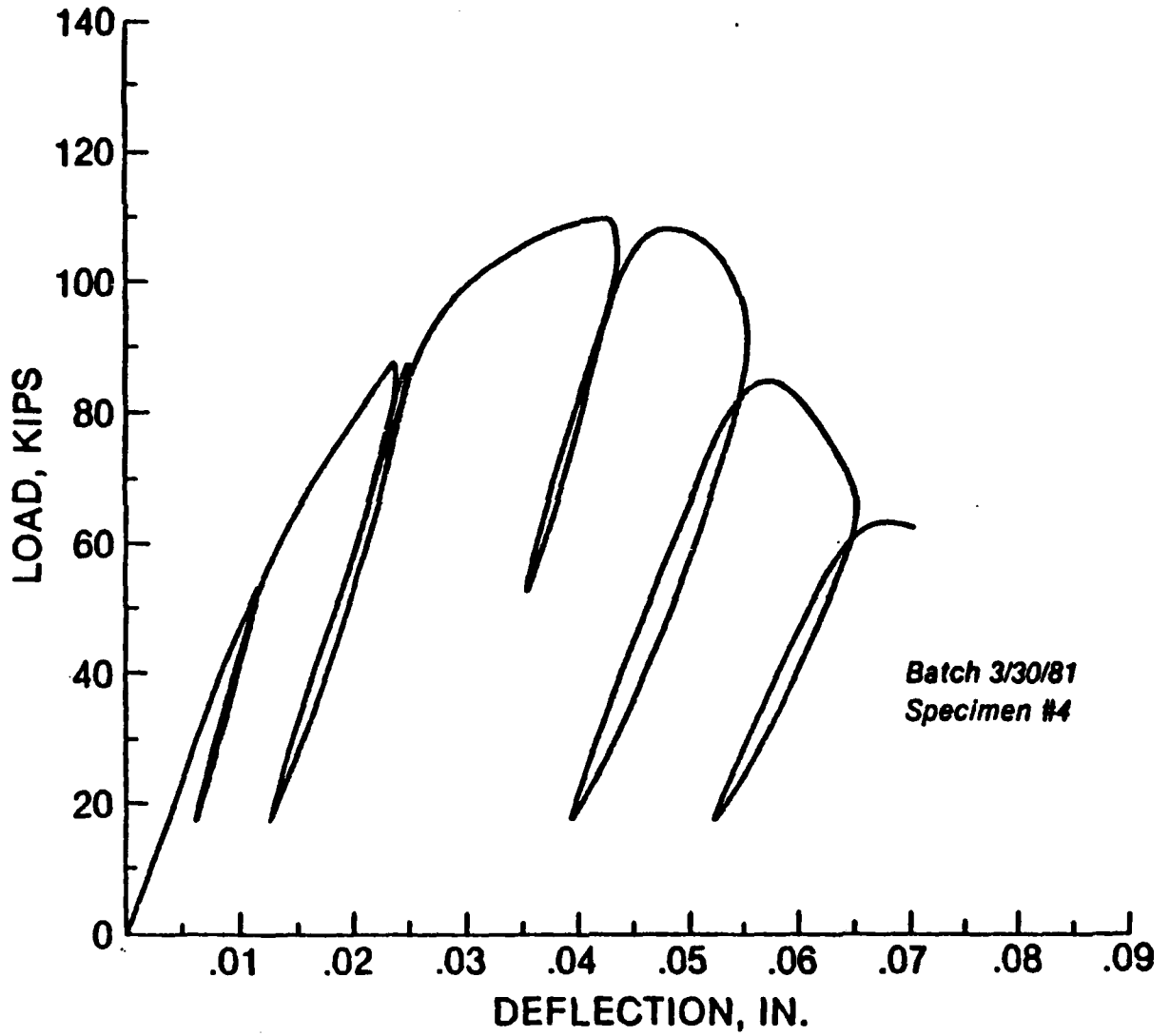
140
120
100
80
60
40
20
0
LOAD, KIPS
.01
.02
.03
.04
.05
.06
.07
.08
.09
DEFLECTION, IN.
Batch 3/30/81
Specimen #4

Figure 13

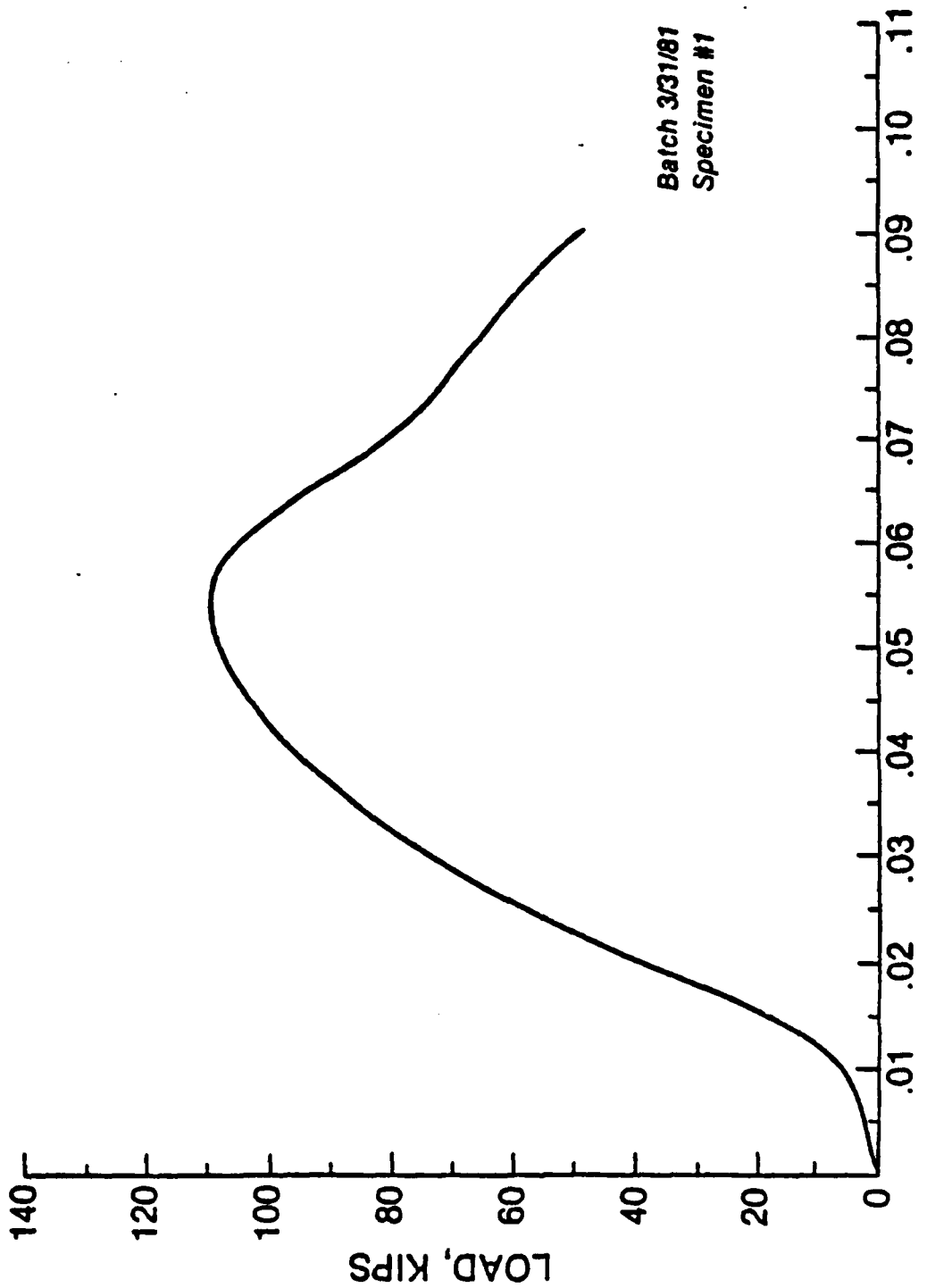
Batch 3/31/81
Specimen #1
LOAD, KIPS
140
120
100
80
60
40
20
0
.01
.02
.03
.04
.05
.06
.07
.08
.09
.10
.11
DEFLECTION, IN.

Figure 14

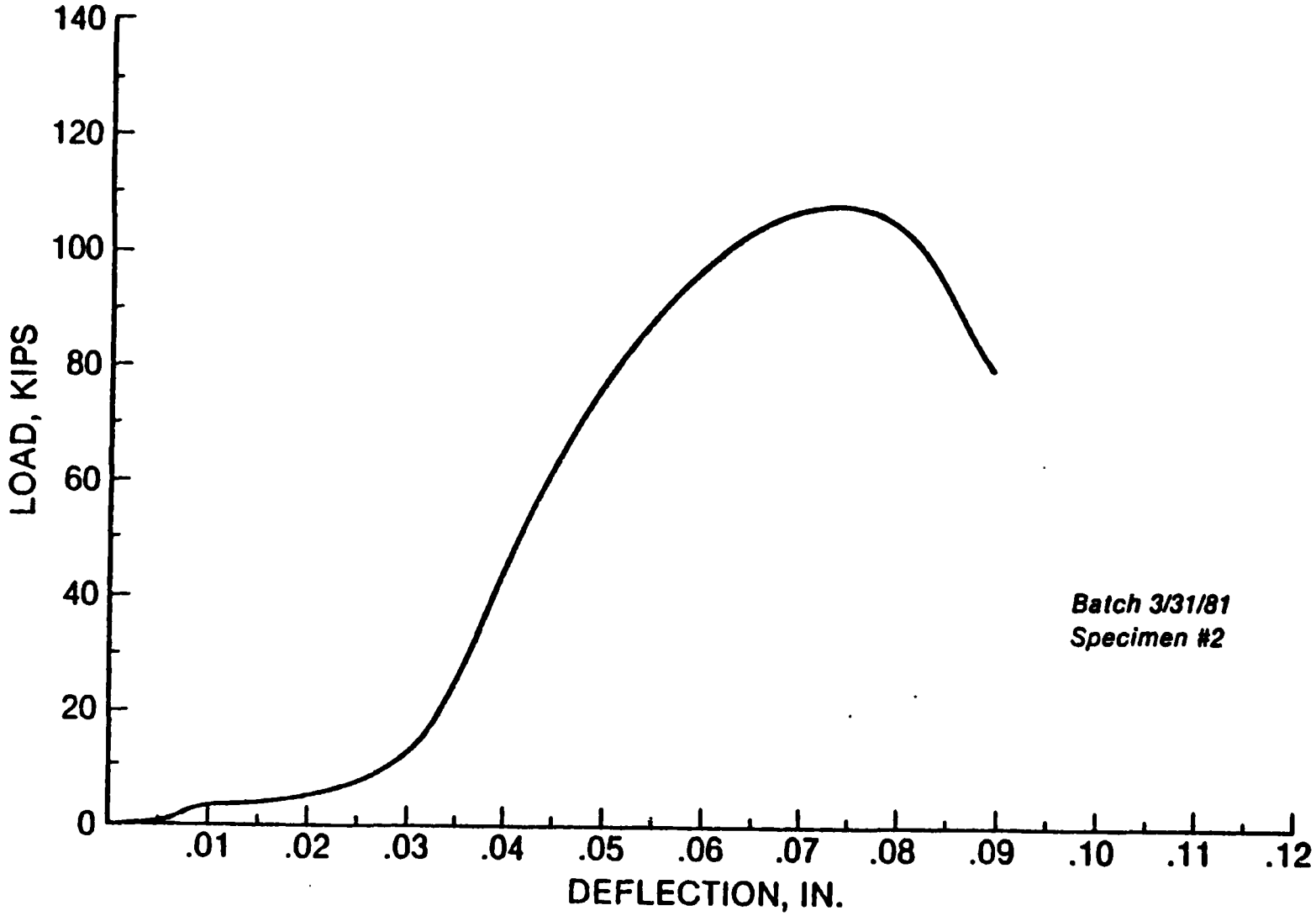
140
120
100
80
60
40
20
0
LOAD, KIPS
.01
.02
.03
.04
.05
.06
.07
.08
.09
.10
.11
.12
DEFLECTION, IN.
Batch 3/31/81
Specimen #2

Figure 15

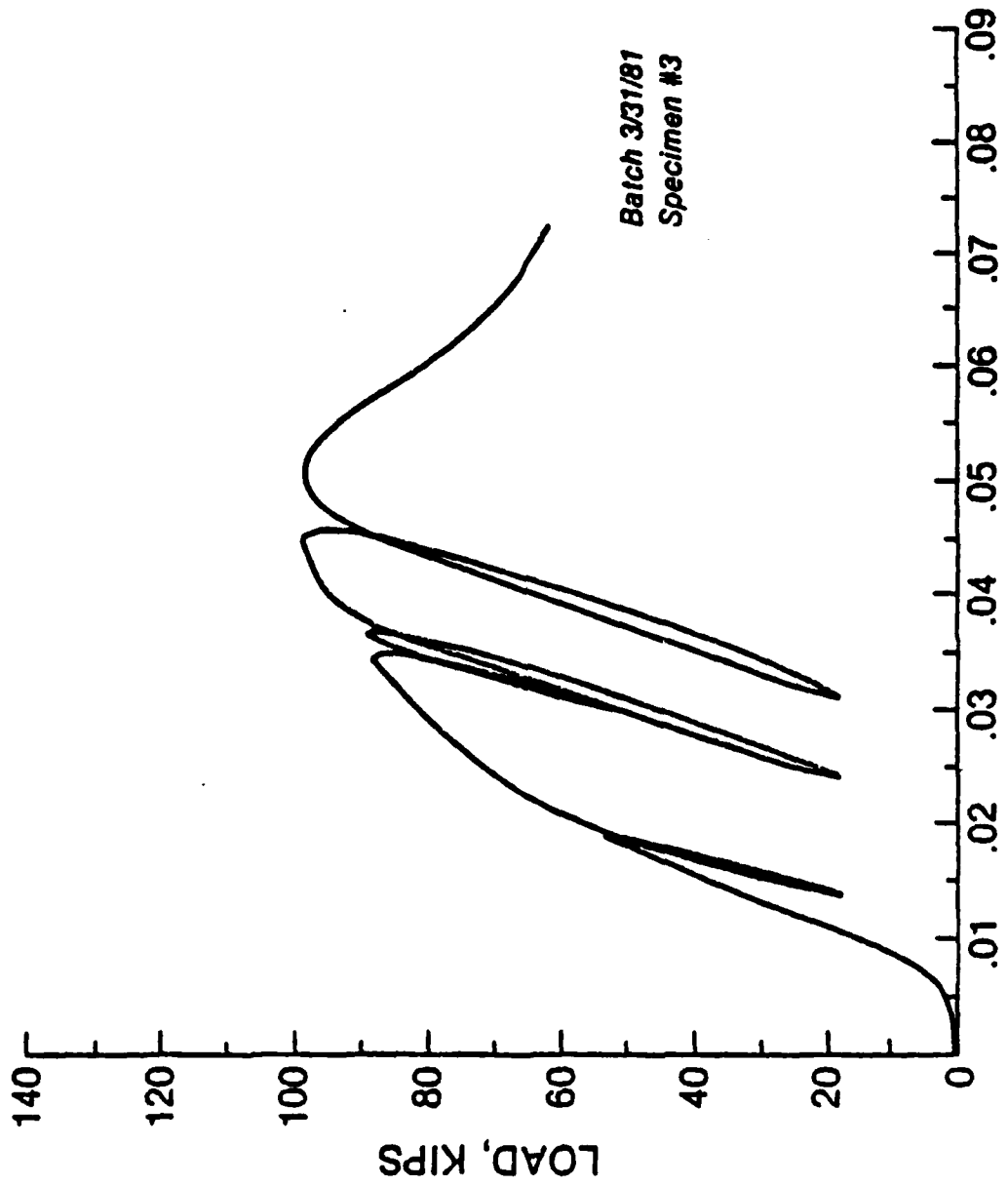
Batch 3/31/81
Specimen #3
LOAD, KIPS
0
20
40
60
80
100
120
140
DEFLECTION, IN.
.01
.02
.03
.04
.05
.06
.07
.08
.09

Figure 16

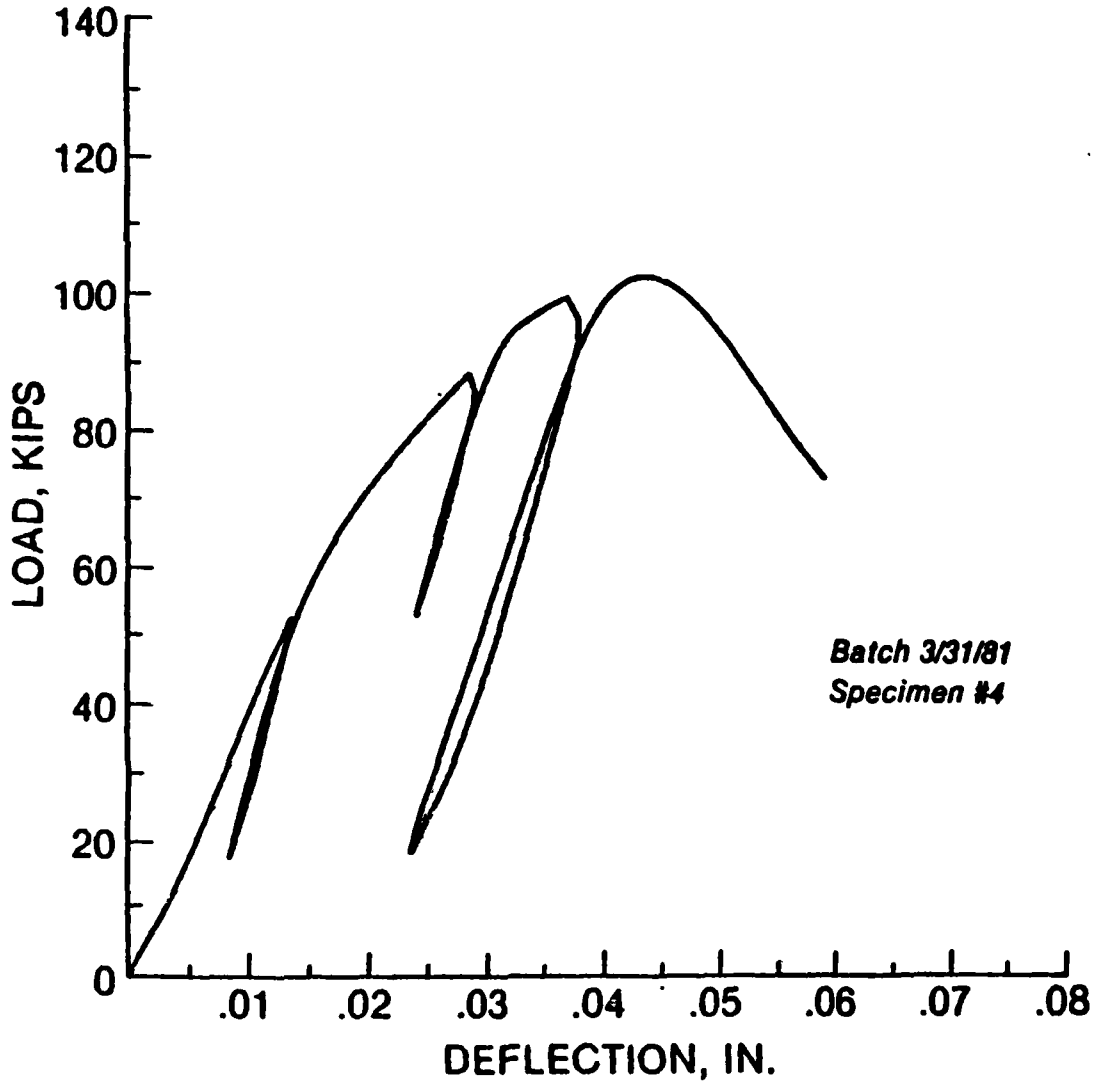
140
120
100
80
60
40
20
0
LOAD, KIPS
.01
.02
.03
.04
.05
.06
.07
.08
DEFLECTION, IN.
Batch 3/31/81
Specimen #4

Figure 17

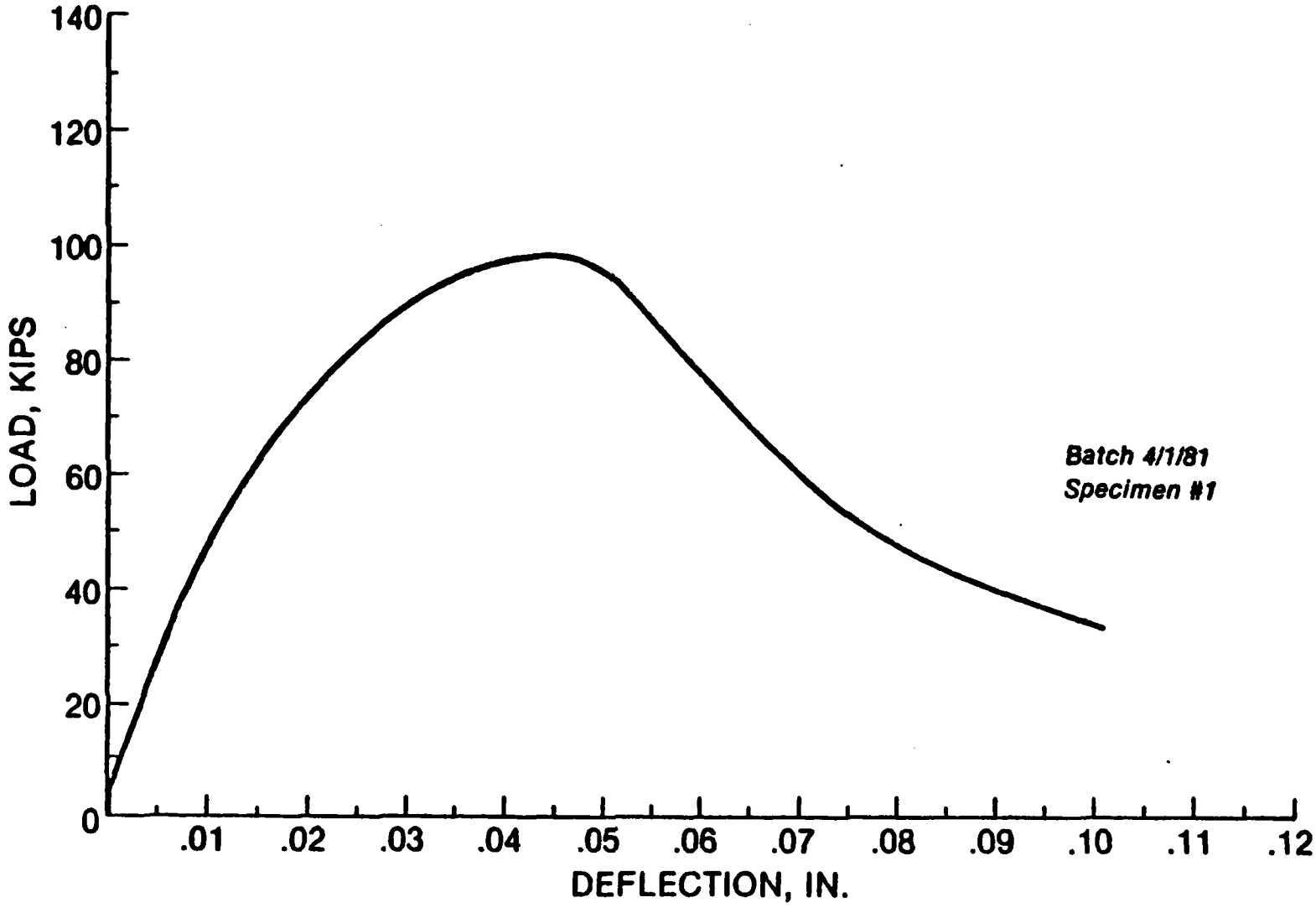
140
120
100
80
60
40
20
0
LOAD, KIPS
.01
.02
.03
.04
.05
.06
.07
.08
.09
.10
.11
.12
DEFLECTION, IN.
Batch 4/1/81
Specimen #1

Figure 18

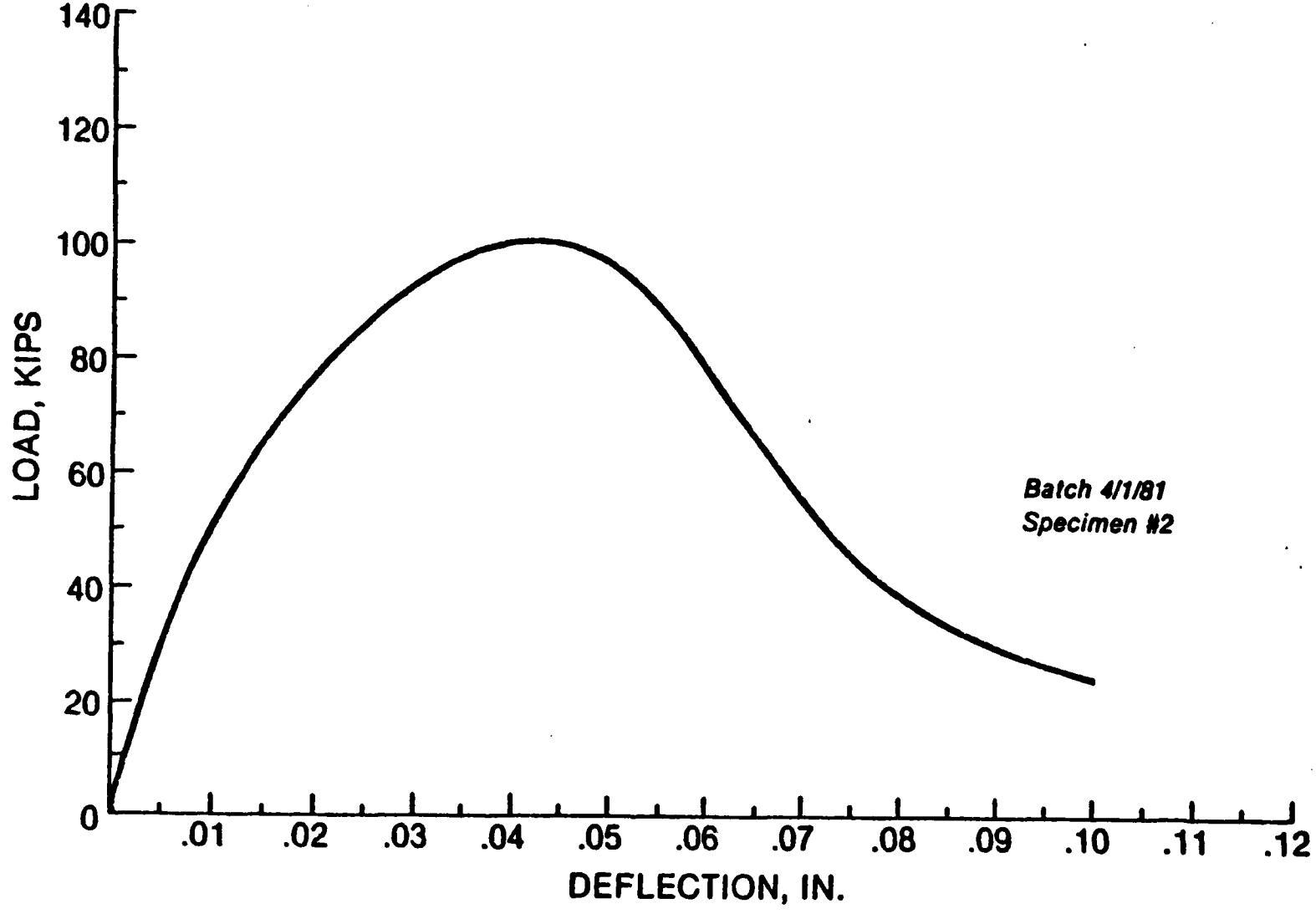
140
120
100
80
60
40
20
0
LOAD, KIPS
.01
.02
.03
.04
.05
.06
.07
.08
.09
.10
.11
.12
DEFLECTION, IN.
Batch 4/1/81
Specimen #2

Figure 19

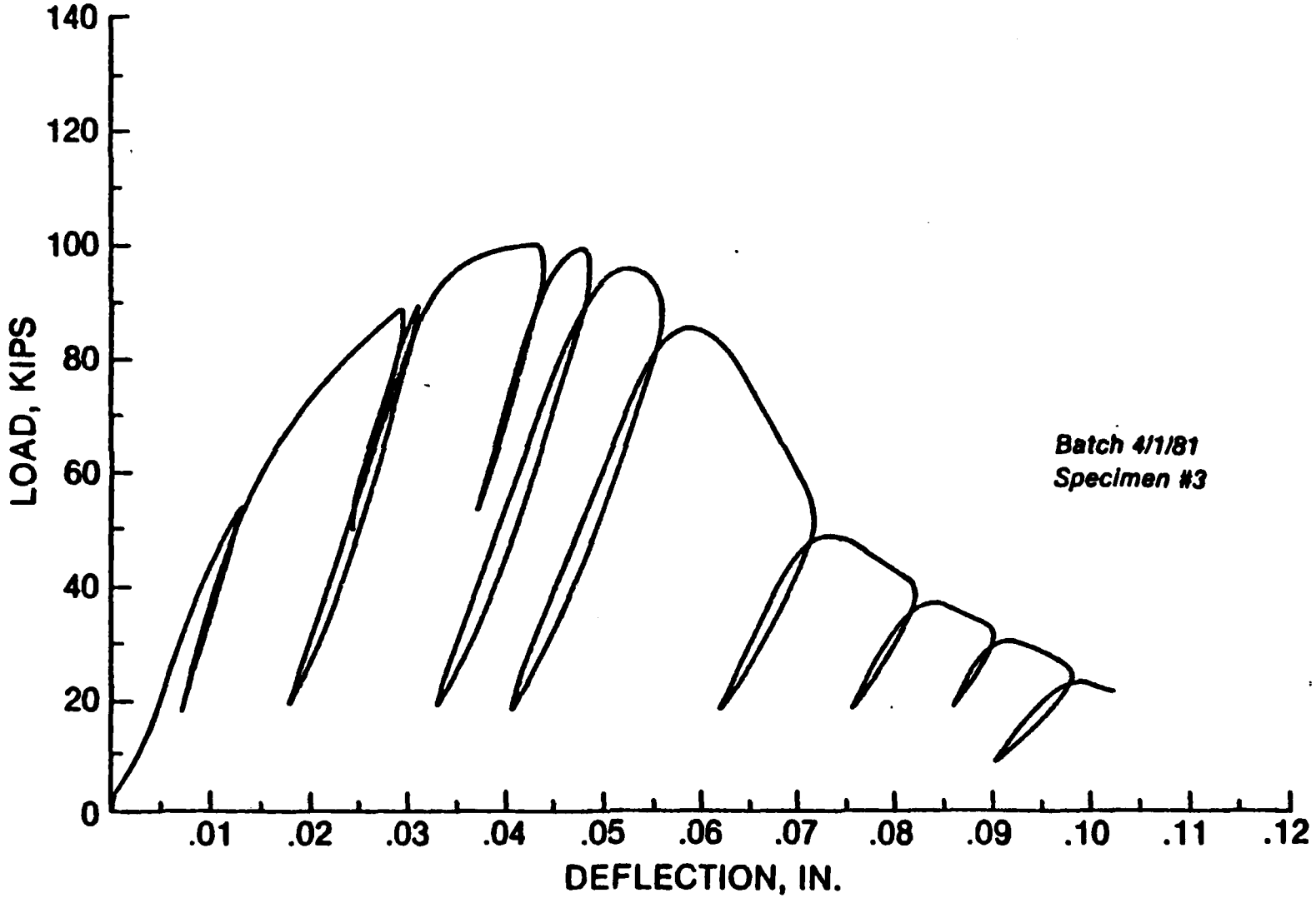
140
120
100
80
60
40
20
0
LOAD, KIPS
.01
.02
.03
.04
.05
.06
.07
.08
.09
.10
.11
.12
DEFLECTION, IN.
Batch 4/1/81
Specimen #3

Figure 20

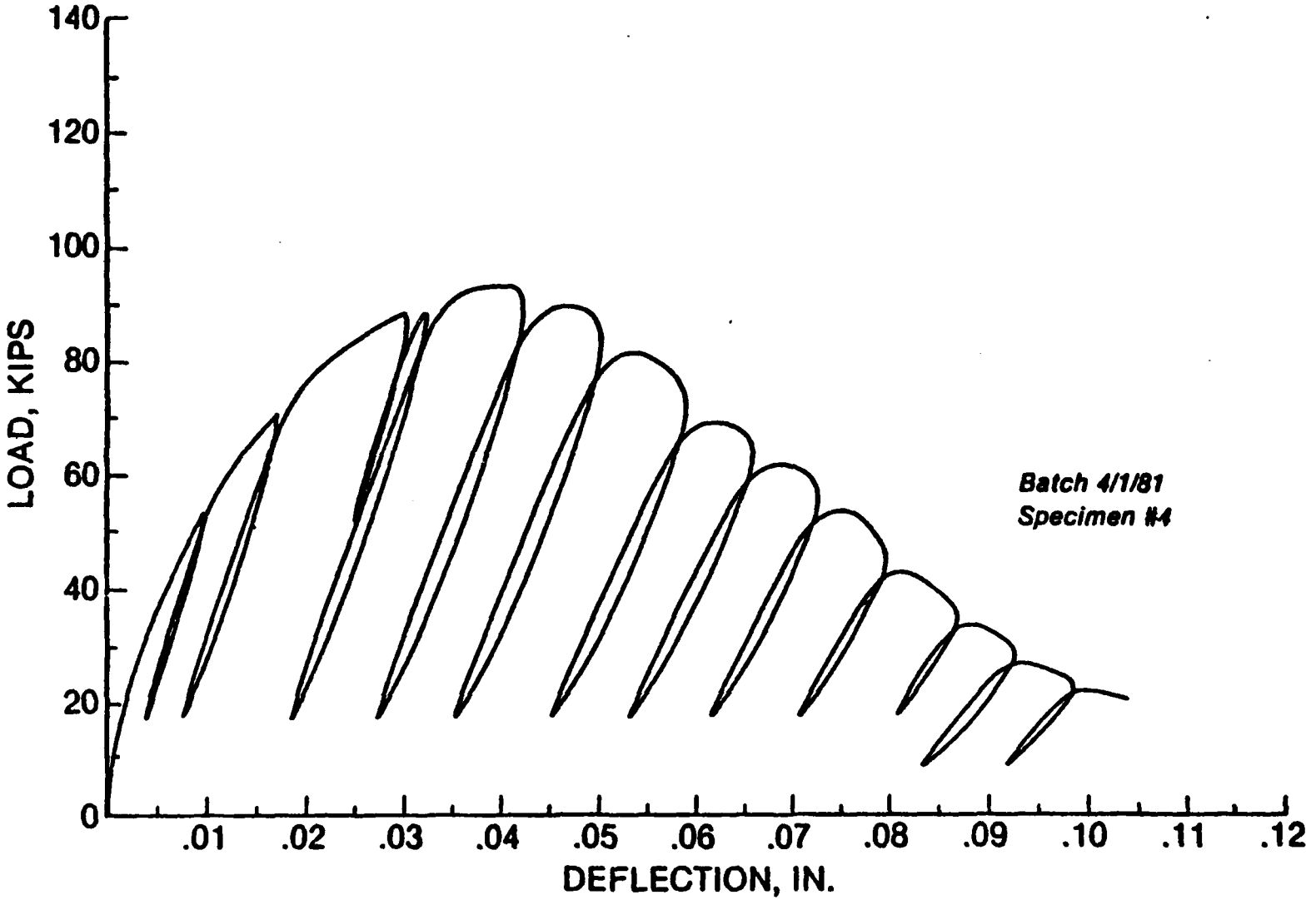
140
120
100
80
60
40
20
0
LOAD, KIPS
.01
.02
.03
.04
.05
.06
.07
.08
.09
.10
.11
.12
DEFLECTION, IN.
Batch 4/1/81
Specimen #4

Figure 21

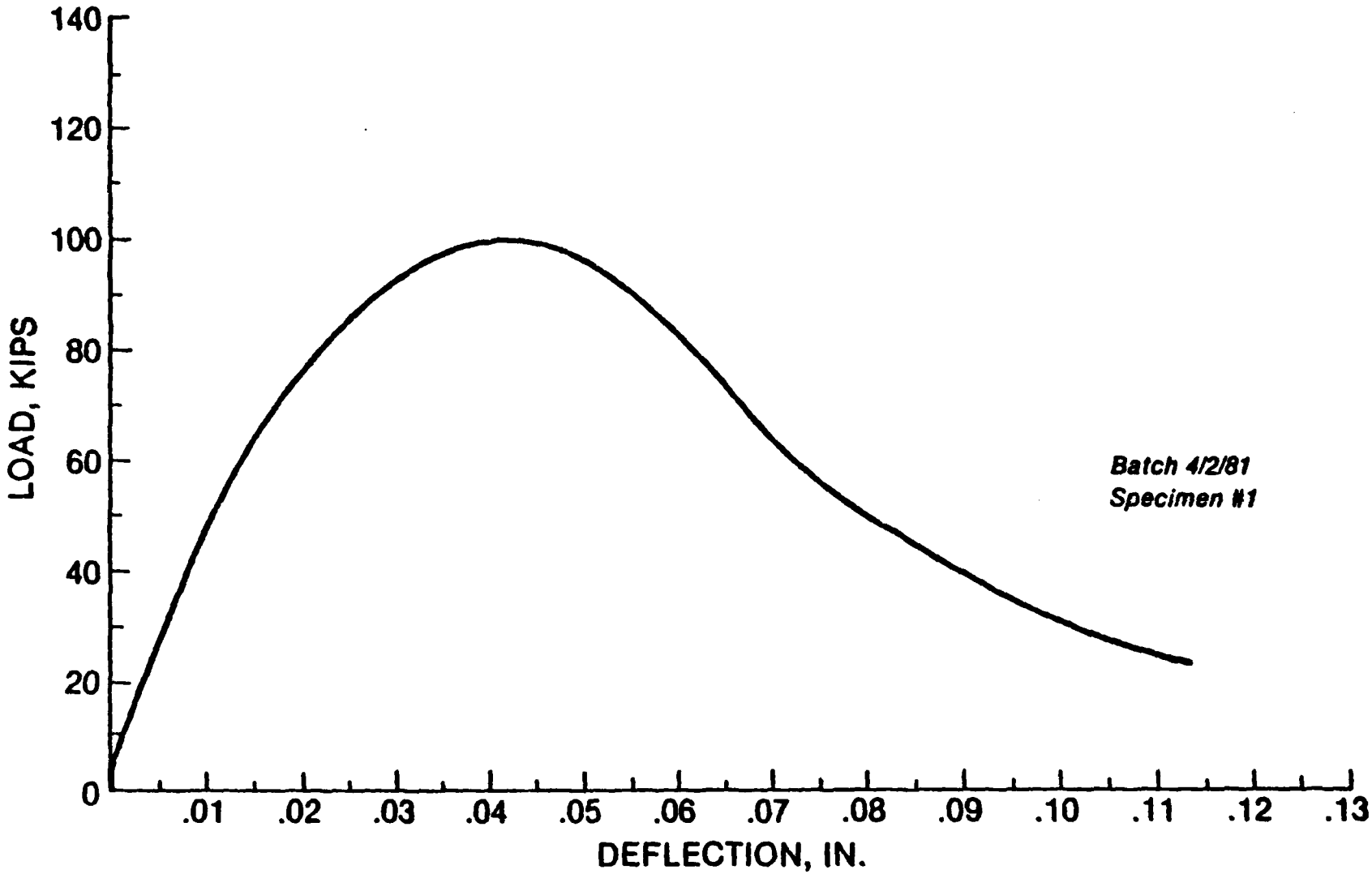
140
120
100
80
60
40
20
0
LOAD, KIPS
.01
.02
.03
.04
.05
.06
.07
.08
.09
.10
.11
.12
.13
DEFLECTION, IN.
Batch 4/2/81
Specimen #1

Figure 22

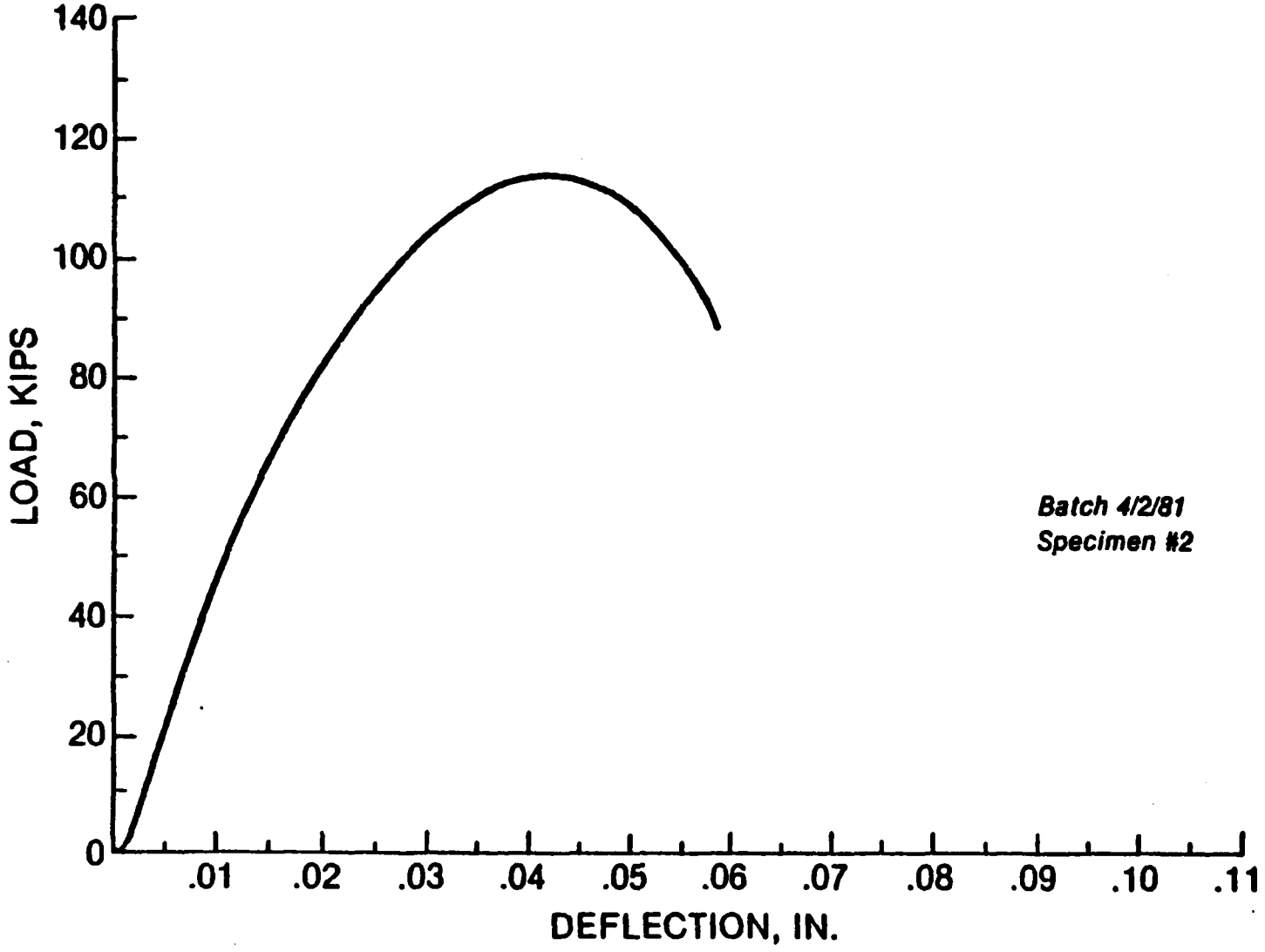
140
120
100
80
60
40
20
0
LOAD, KIPS
.01
.02
.03
.04
.05
.06
.07
.08
.09
.10
.11
DEFLECTION, IN.
Batch 4/2/81
Specimen #2

Figure 23

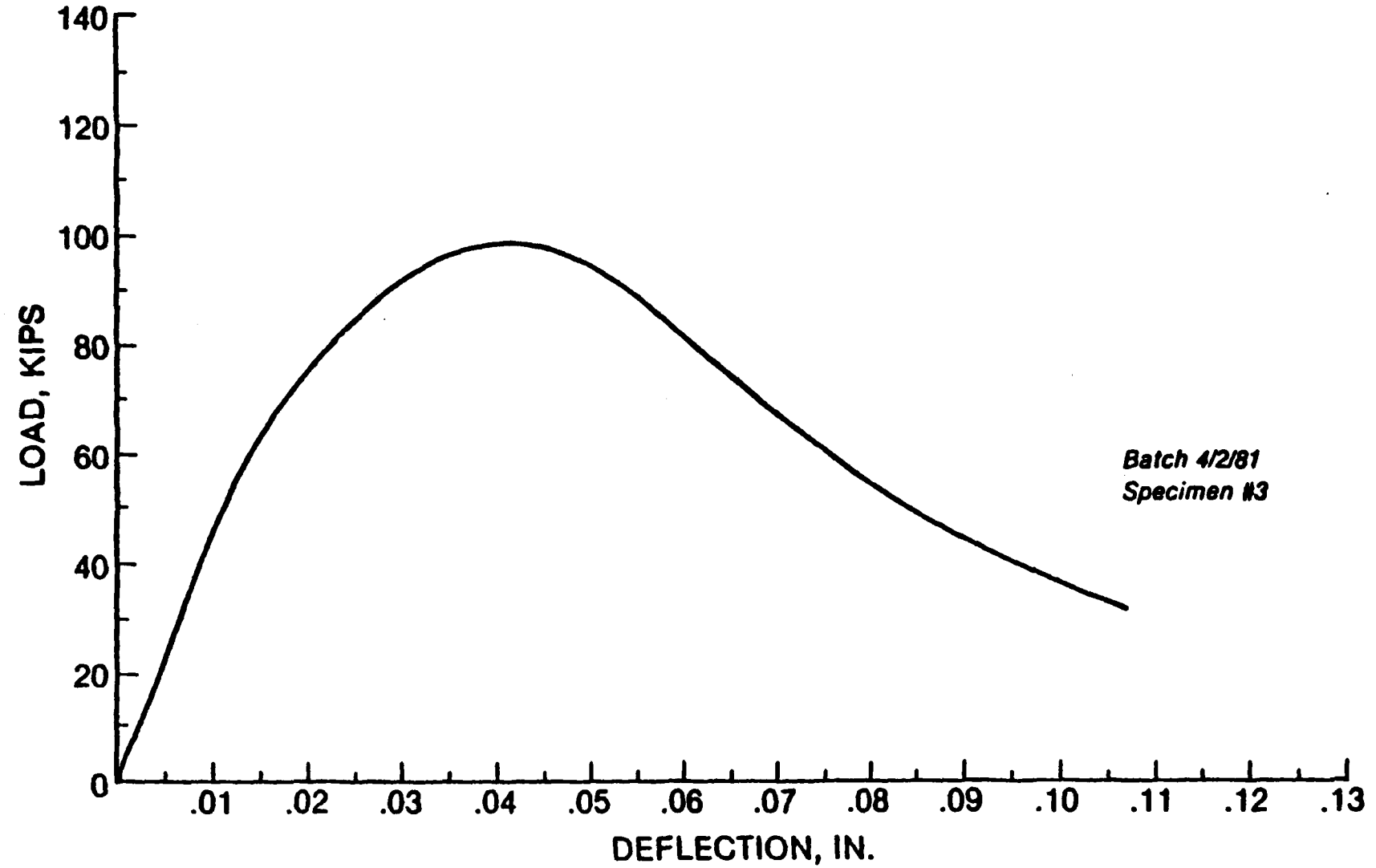
140
120
100
80
60
40
20
0
LOAD, KIPS
.01
.02
.03
.04
.05
.06
.07
.08
.09
.10
.11
.12
.13
DEFLECTION, IN.
Batch 4/2/81
Specimen #3

Figure 24

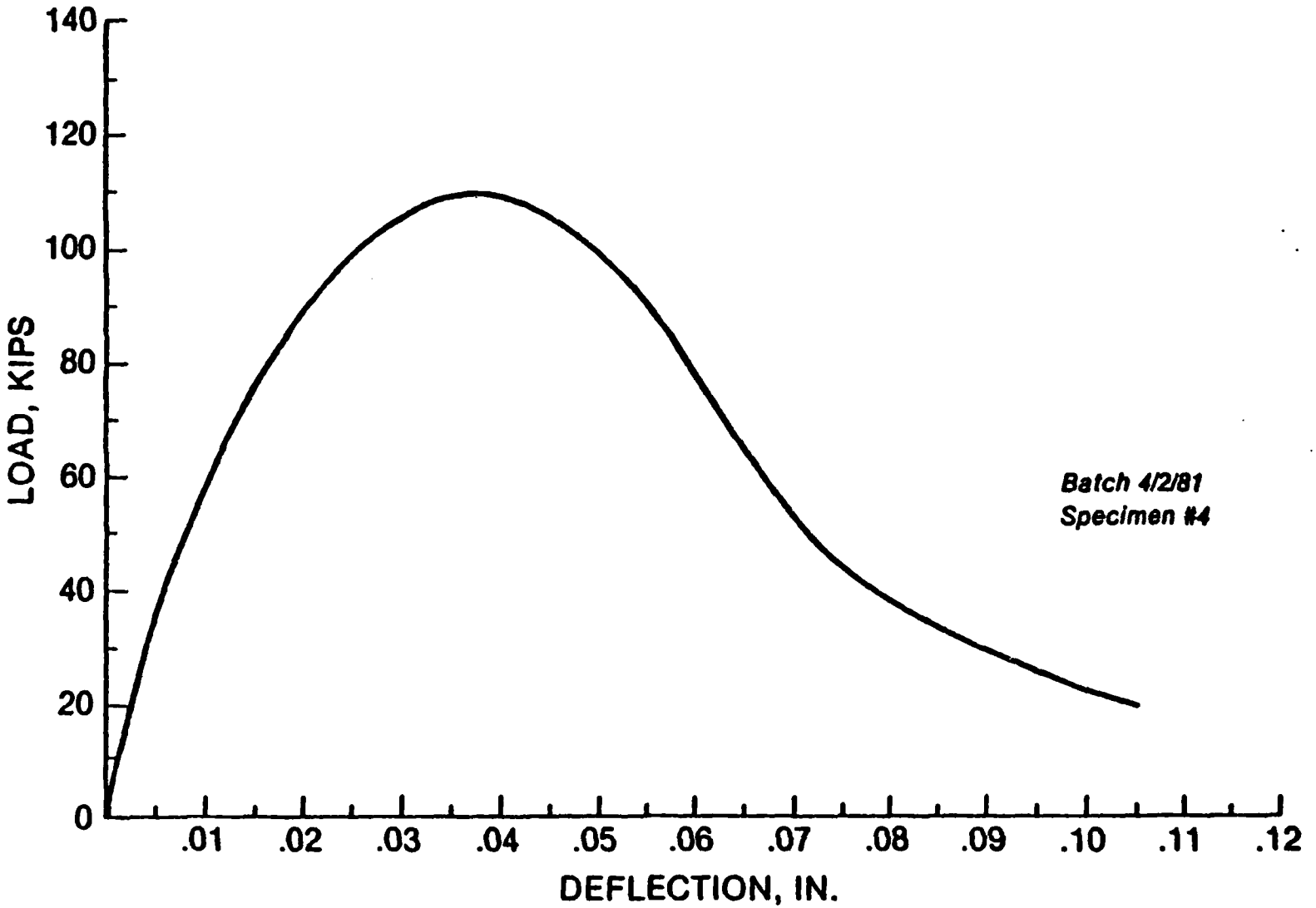
140
120
100
80
60
40
20
0
LOAD, KIPS
.01
.02
.03
.04
.05
.06
.07
.08
.09
.10
.11
.12
DEFLECTION, IN.
Batch 4/2/81
Specimen #4

Figure 25

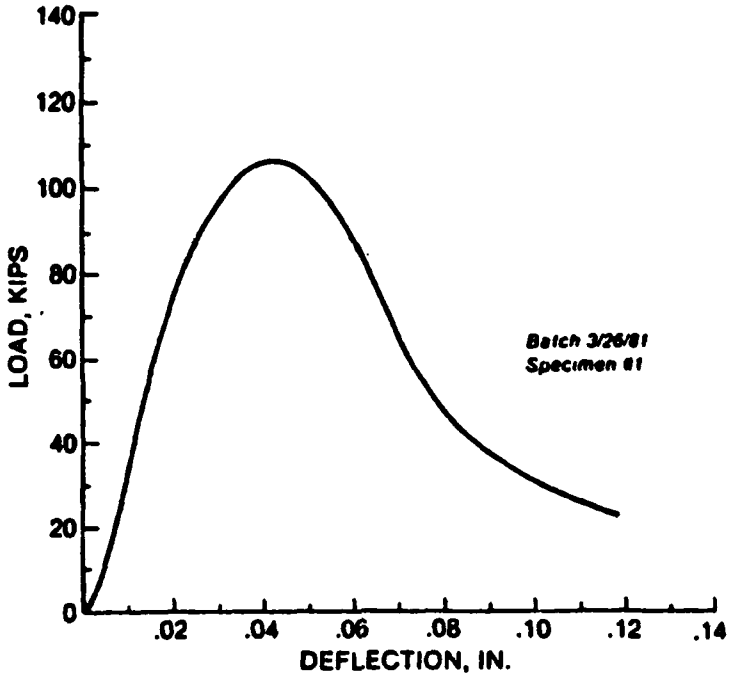

Figure 26

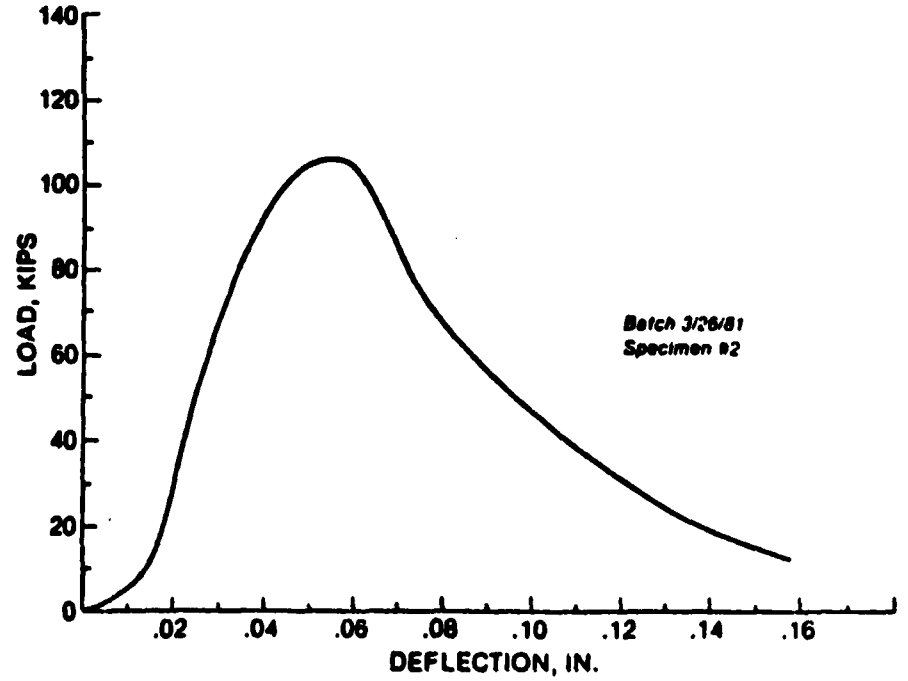

Figure 27

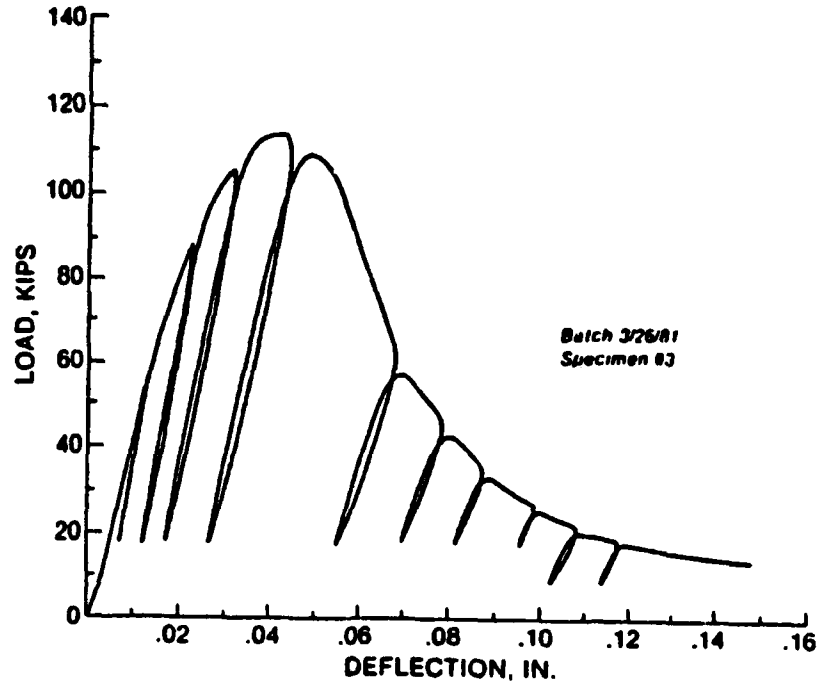

Figure 28

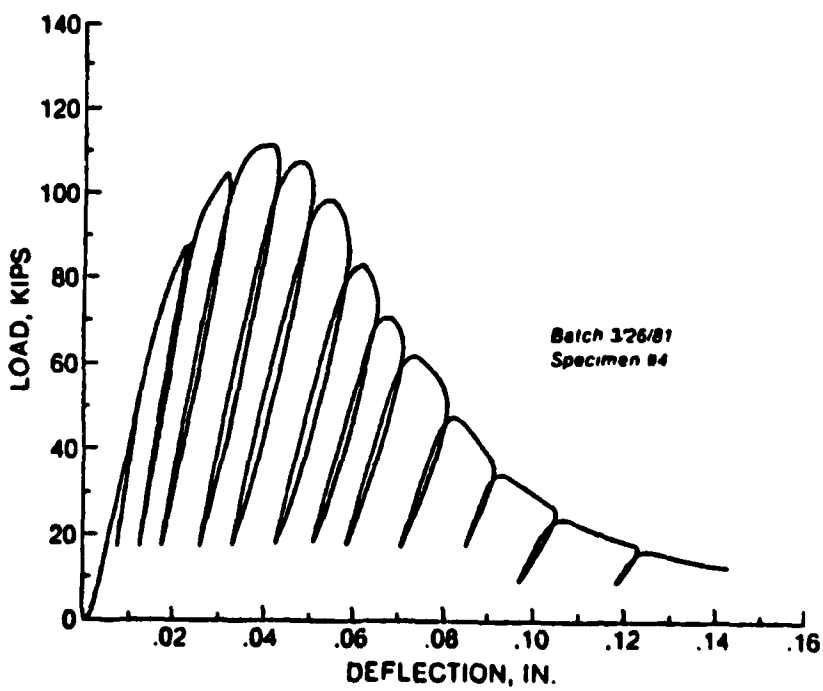

Figure 29

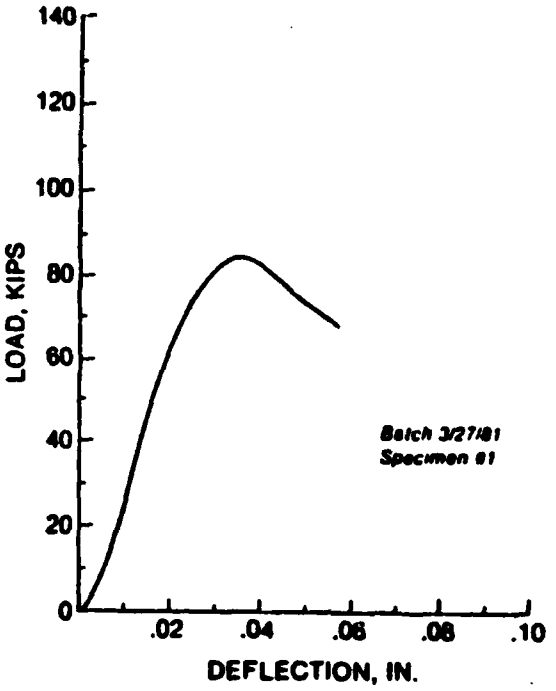

Figure 30

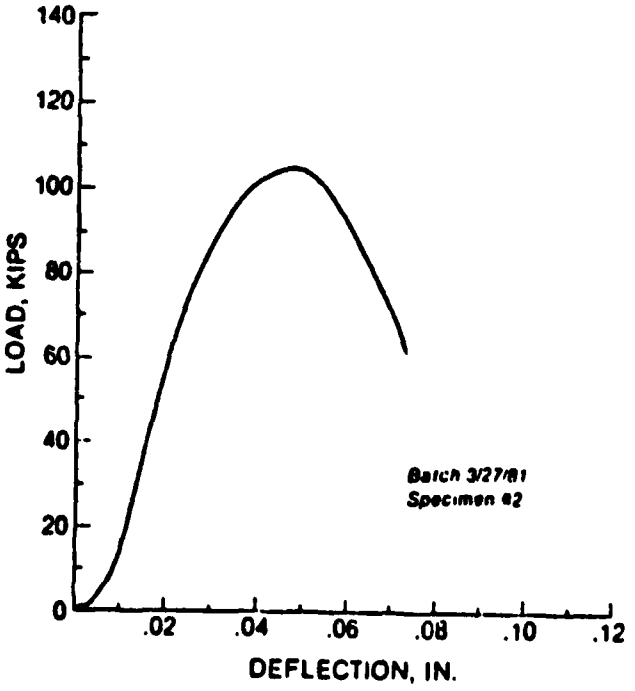

Figure 31

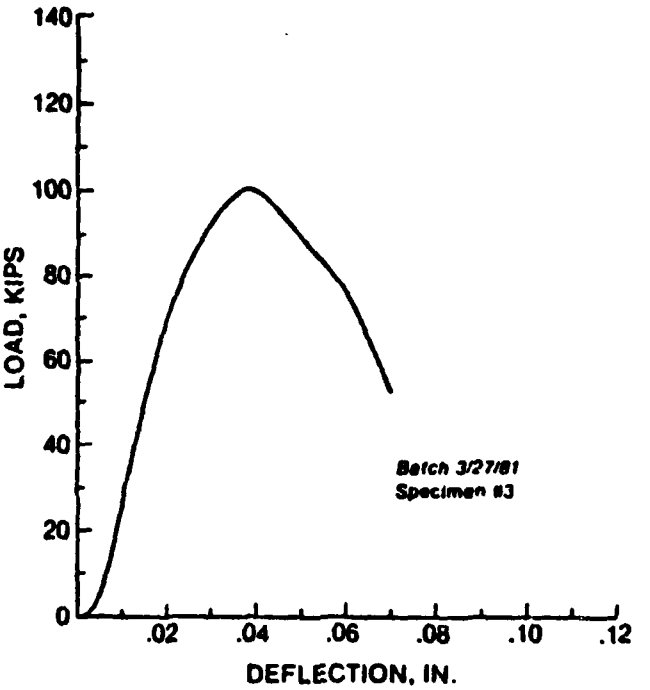

Figure 32

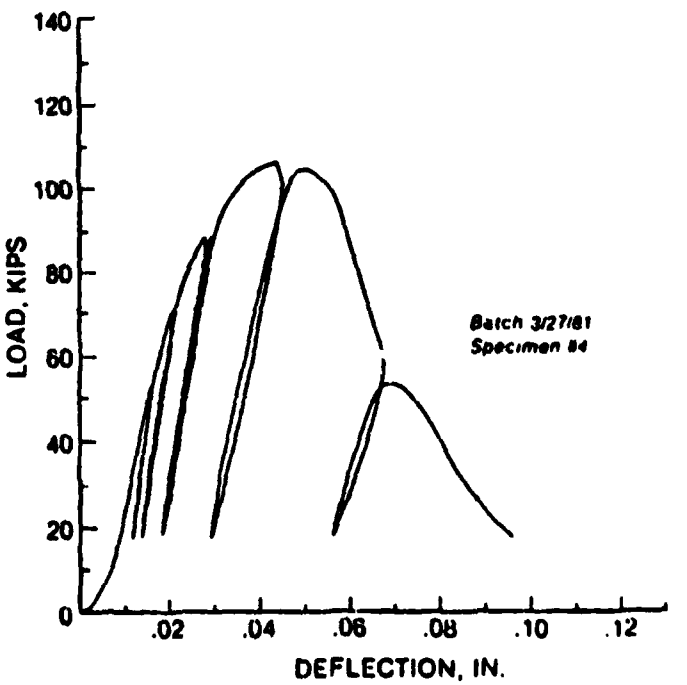

Figure 33

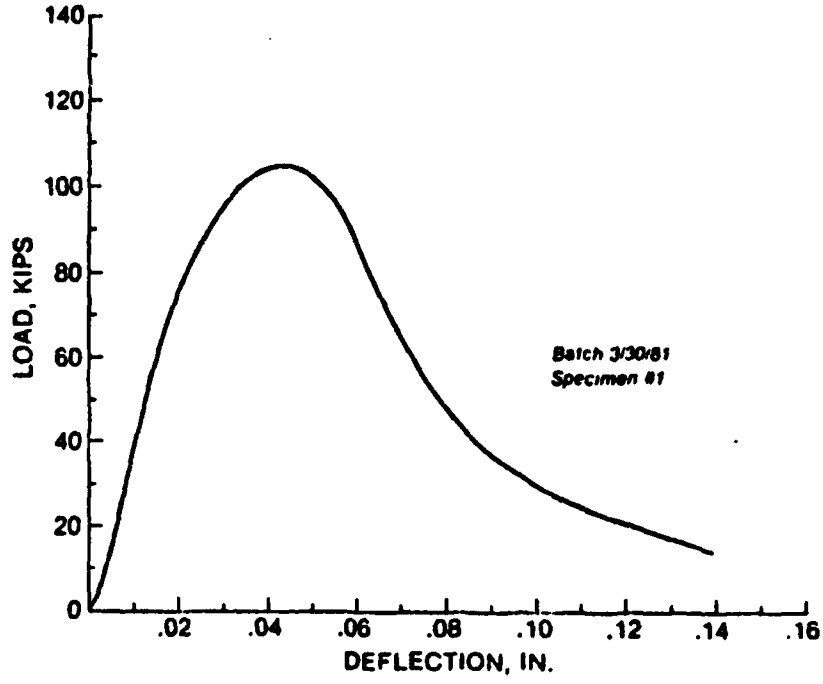

Figure 34

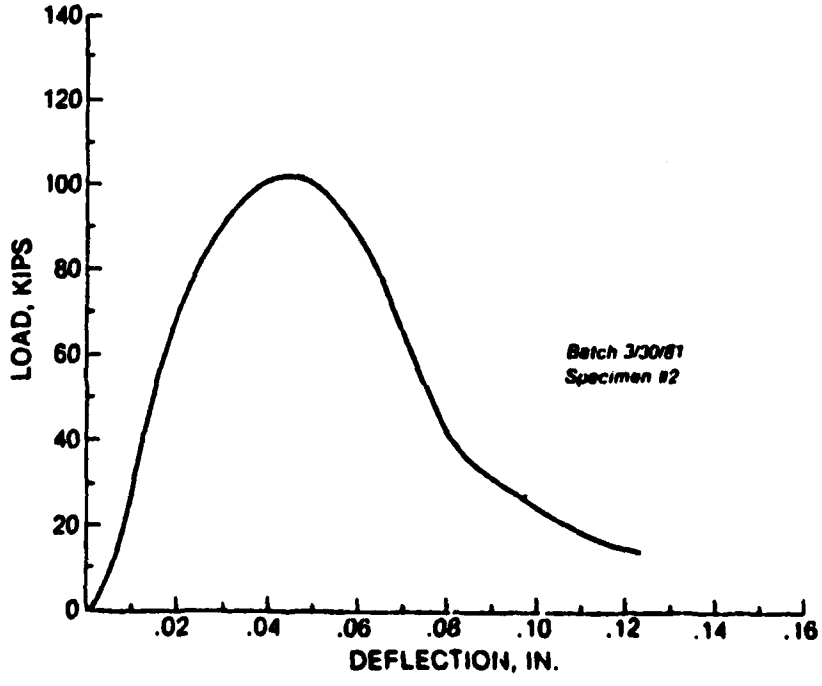

Figure 35

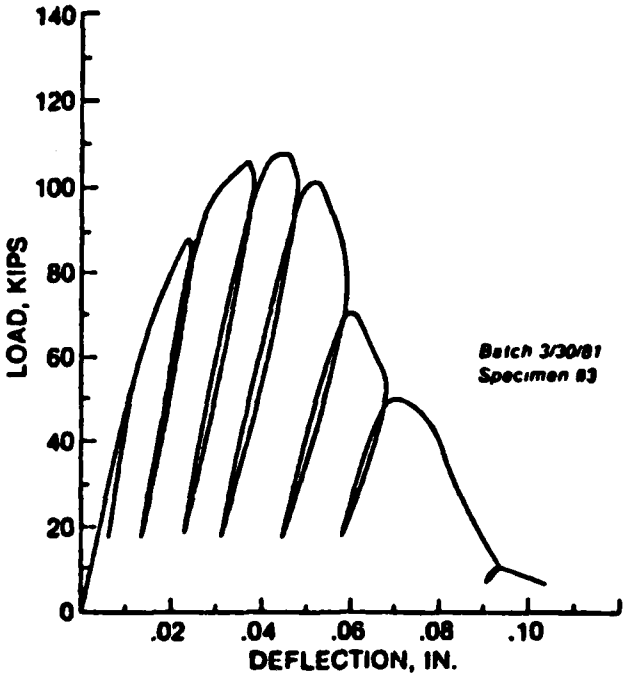

Figure 36

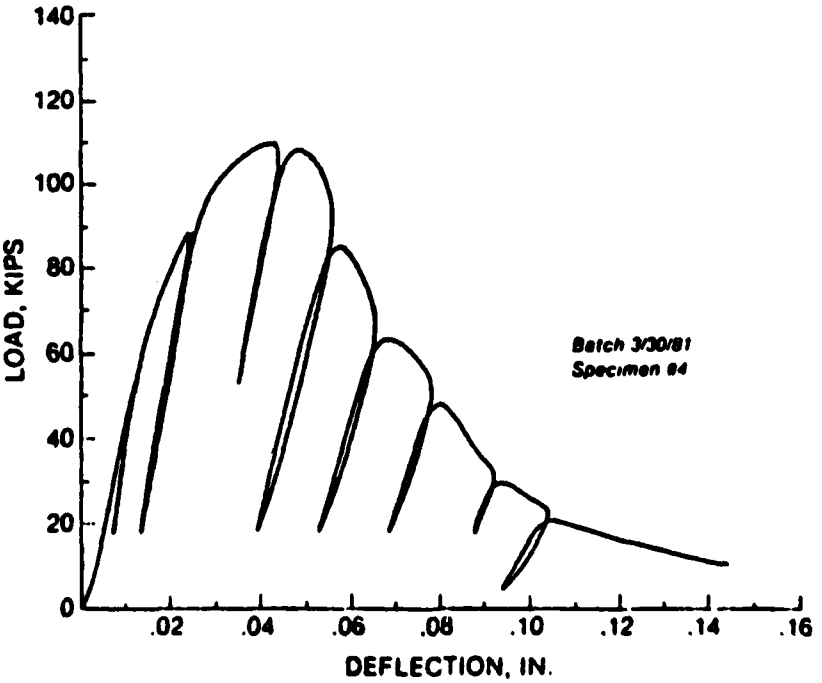

Figure 37

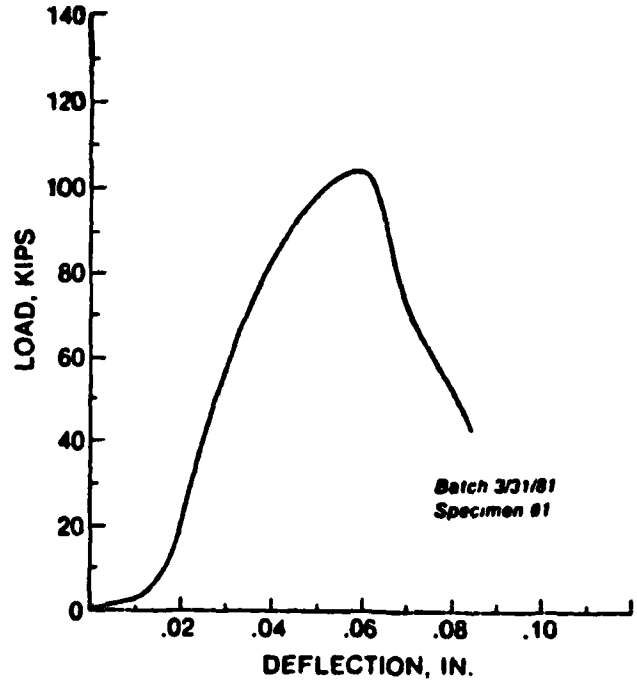

Figure 38

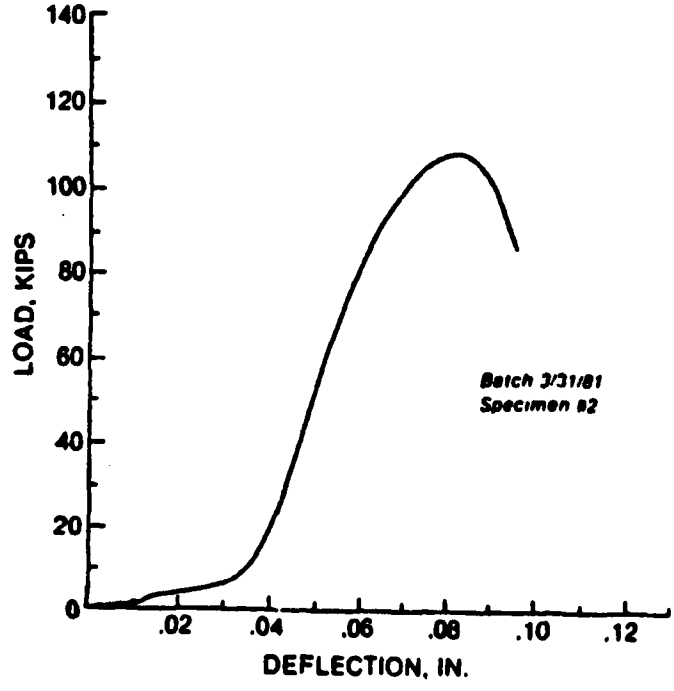

Figure 39

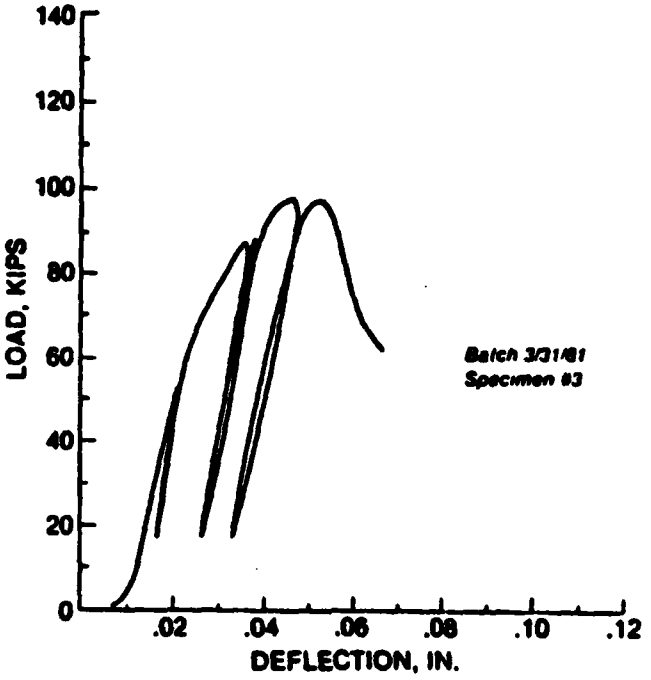

Figure 40

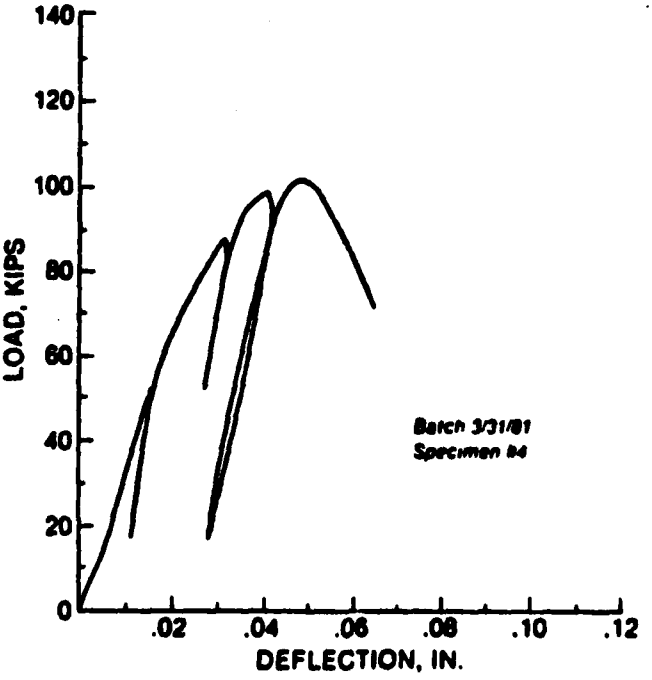

Figure 41

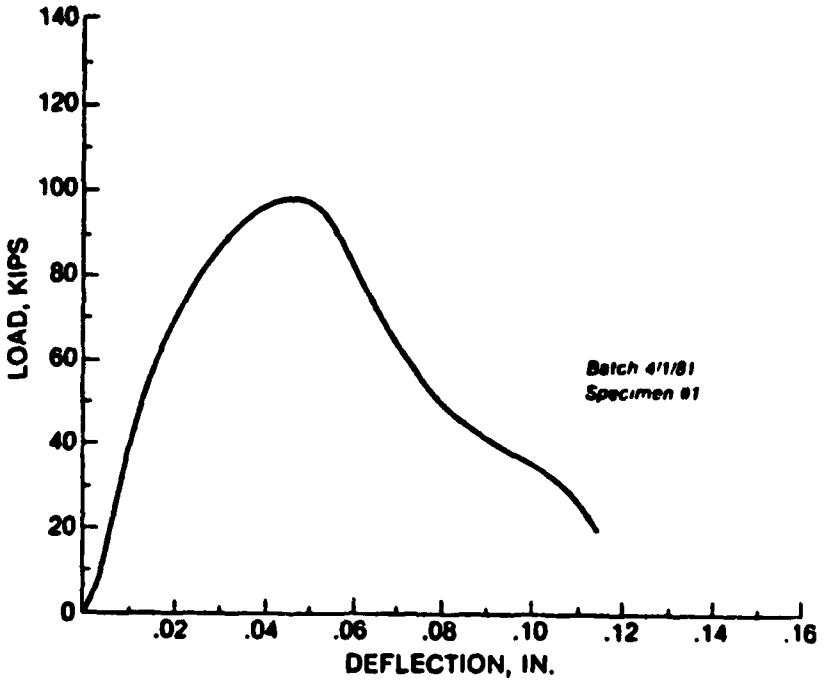

Figure 42

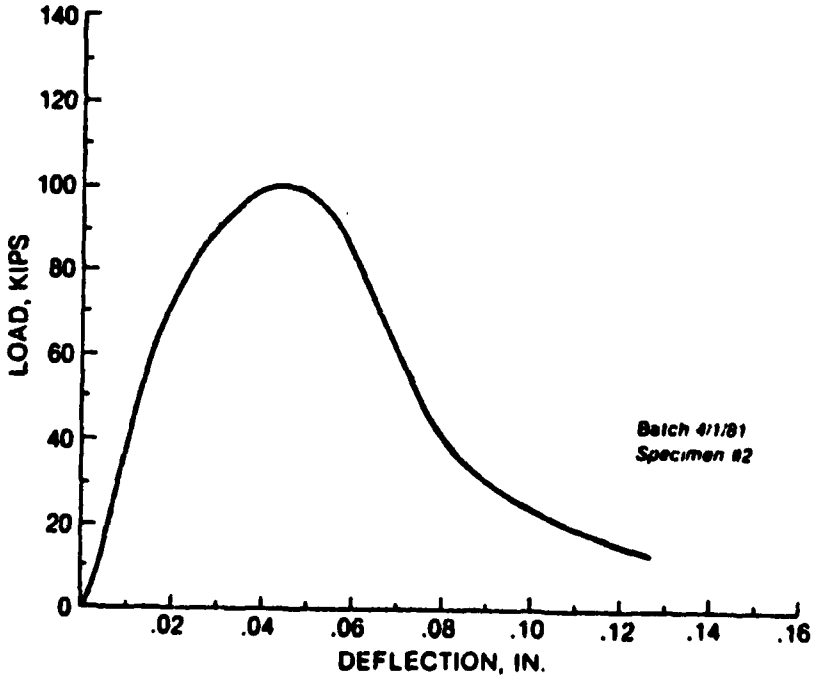

Figure 43

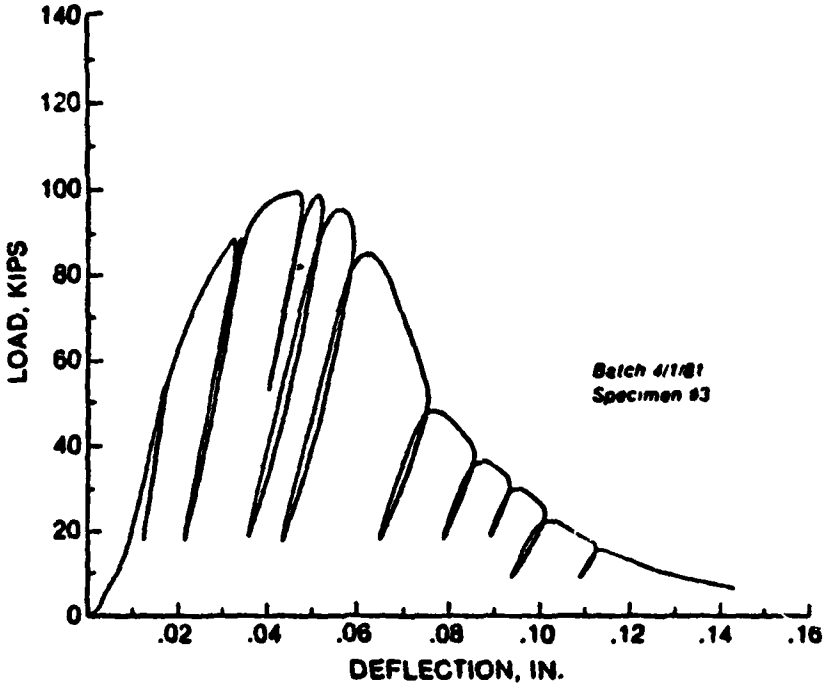

Figure 44

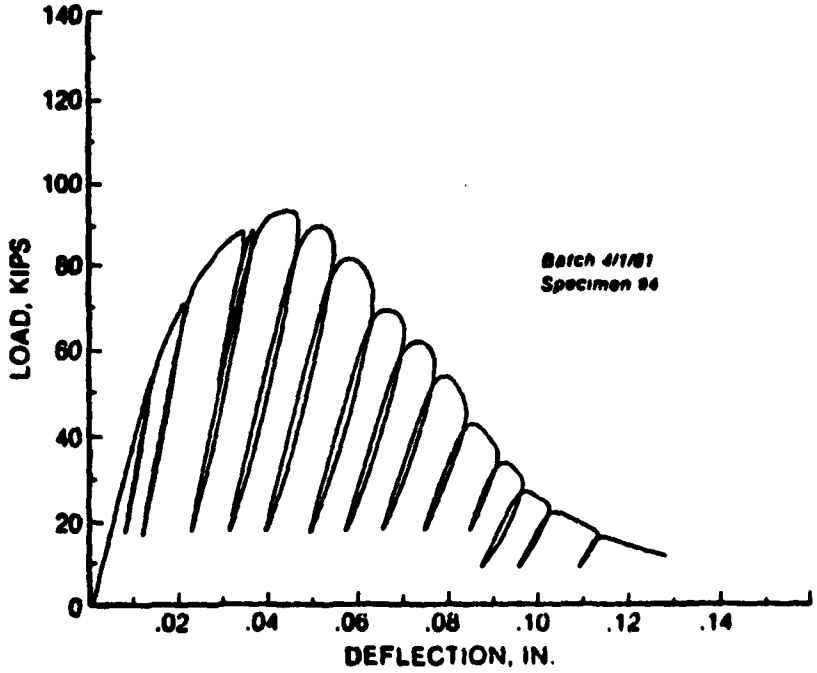

Figure 45

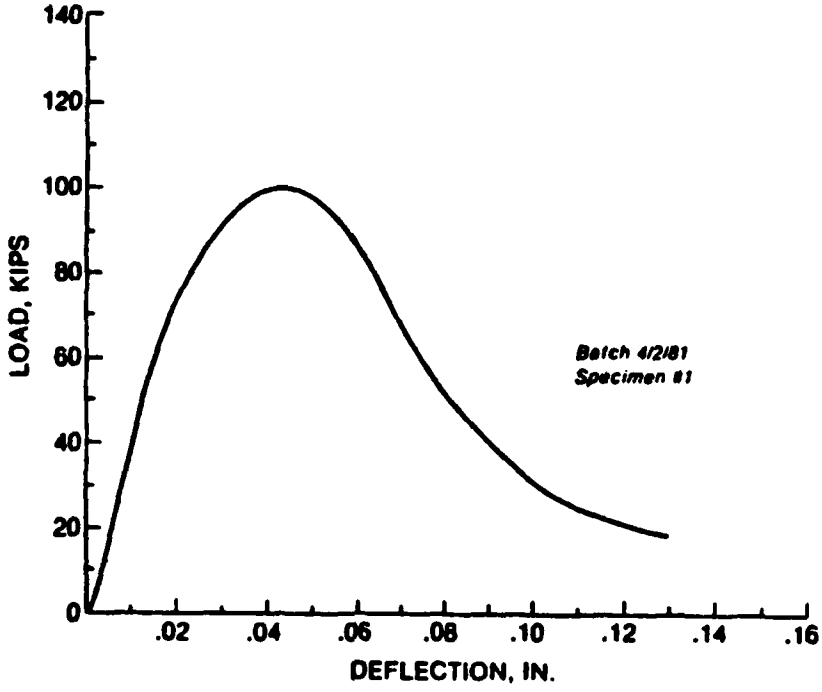

Figure 46

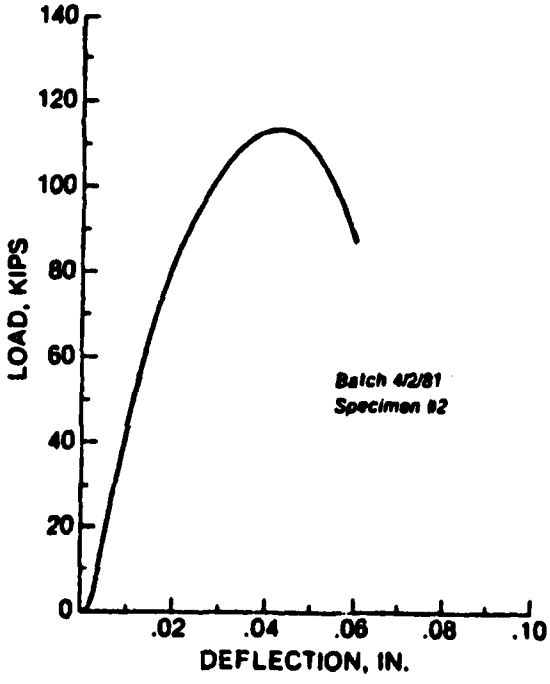

Figure 47

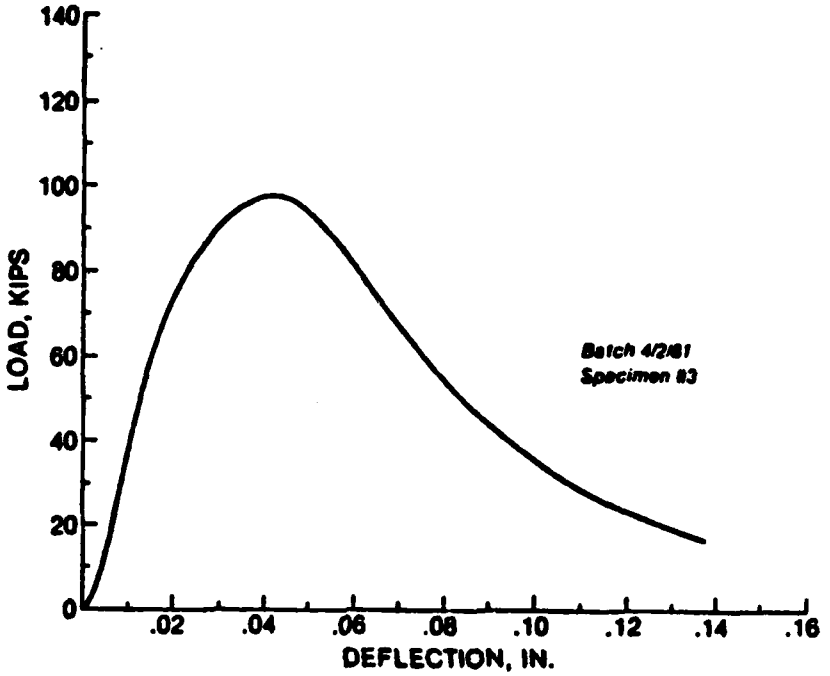
140
120
100
80
60
40
20
0
LOAD, KIPS
Batch 4/2/81
Specimen #3
.02
.04
.06
.08
.10
.12
.14
.16
DEFLECTION, IN.

Figure 48